

Investigating the effects of cannabinoid exposure on zebrafish development

by

MD Ruhul Amin

A thesis submitted in partial fulfillment of the requirements for the degree of

Doctor of Philosophy

in

Physiology, Cell and Developmental Biology

Department of Biological Sciences
University of Alberta

© MD Ruhul Amin, 2021

Abstract

Cannabis is one of the most commonly used illicit recreational drugs and is widely used for medicinal purposes. Cannabis contains three primary cannabinoids: δ^9 -Tetrahydrocannabinol (THC), Cannabidiol (CBD) and Cannabinol (CBN). The psychoactive ingredient in cannabis is THC, whereas the major non-psychoactive ingredients are CBD and CBN. In recent times, cannabis use during pregnancy has increased worldwide, and studies have reported that cannabis and many of its constituent compounds can cross the placenta (Fried, 1995; George & Vaccarino, 2015). Hence, exposure to cannabis has the potential to pose a severe risk to developing offspring. Importantly, there is a lack of information on the effects of cannabinoids on developing embryos. Therefore, in this thesis I investigated the effect of brief exposure of THC (a racemic mixture of THC), CBD and CBN during gastrulation on zebrafish development. I found that THC-, CBD- and CBN-treated embryos exhibited reduced heart rates, axial malformations and shorter trunks. These treatments also altered synaptic activity at neuromuscular junctions and reduced the number of motor neuron axonal branches. Locomotion studies show that larvae exhibited reductions in the number of escape responses to sound stimuli, but not to touch stimuli. When investigating the effects on neurons, I specifically focused on motor neurons, and reticulospinal neurons known as the Mauthner cells (M-cells) that are involved in escape response movements. Cannabinoid-treated embryos exhibited subtle alterations in M-cells morphology, which might contribute towards the escape response dynamics. An examination of free-swimming activity showed an alteration in the swimming output of cannabinoid-treated embryos. Because locomotion was altered, I also examined muscle fiber development. The fluorescent labelling and transmission electron microscopy images showed that skeletal muscle fibers were largely intact, but the red and white muscle fibers were

slightly disorganized. I also observed significant changes in the pattern of expression of nicotinic acetylcholine receptors at neuromuscular junctions.

Since cannabinoid-treated embryos exhibited a reduced response to sound, scanning electron microscopy analysis of CBN exposure showed a defective hair cell development along the lateral line. The pharmacological block of cannabinoid receptor 2 (CB₂R) with AM630 or JTE907 prevented many of the CBN-induced developmental defects, while the block of cannabinoid receptor 1 (CB₁R) with AM251 or CP945598 had little or no effect indicating that CBN-induced developmental defects are mainly CB₂R-mediated. Next, I sought to examine the effect of stereoselectivity on zebrafish embryo development because THC has four stereoisomers. (-) trans δ^9 THC (referred as (-) THC afterwards) is one of those isomers and predominantly present in natural cannabis. I found that (-) THC affects the gross morphology, heart rate, MN branching and locomotion similar to other cannabinoids. Most importantly, (-) THC (>0.5 mg/L)-treated zebrafish did not survive past 15 days of development. Since embryos treated with (-) THC did not rise in the water column or swim, I investigated swimbladder development and found that the (-) THC treatment negatively impacted swimbladder development in a sonic hedgehog-dependent manner. In support of this, RNAseq analysis revealed downregulation of hedgehog genes, including *ptch2*, *smo*, *gli1* and *gili2b*. In addition, more than 1000 and 1400 genes were downregulated and upregulated respectively in (-) THC-treated embryos.

I asked whether the brief exposure of cannabinoids had persistent effects into later life stages. Therefore, I reared the exposed embryos to adulthood and carried out open field, novel object approach and shoaling tests. Both (-) THC and CBD-treated adult zebrafish exhibited anxiety-like behavior compared to controls. Finally, I found that brief exposure to (-) THC and

CBD has a transgenerational impact because F1 embryos collected from (-) THC and CBD parents exhibited reduced locomotion, alterations in primary MN branching and changes in the expression of the neuronal marker genes, including *c-fos* and *bdnf*. Together, these findings indicate that zebrafish exposed to cannabinoids during gastrulation exhibit changes in various aspects of development (including, neuronal, muscle and swimbladder development) that may impact embryonic locomotion; a number of these changes are associated with alteration in gene expression. In addition, these brief exposures to cannabinoids had a persistent effect in adult and into the next generation.

Preface

This thesis is an original work of Md Ruhul Amin. All the experiments were conducted according to the research ethics approval from University of Alberta Research Ethics Board, Project name “Synaptic maturation in the fish embryos”, AUP00000816.

Results presented in chapter 3, and parts of the discussion (8.1) have been published as Kazi T. Ahmed, Md Ruhul Amin, Parv Shah & Declan W. Ali ; 2018; ‘Motor neuron development in zebrafish is altered by brief (5-hr) exposures to THC (tetrahydrocannabinol) or CBD (cannabidiol) during gastrulation’, Scientific Reports volume 8, Article number: 10518. I was responsible for concept formation, data collection, analysis and manuscript writing. Kazi Ahmed assisted me in training for electrophysiology and behavioral experiments and manuscript writing. Parv Shah (undergraduate student) also assisted me in some experimental aspects. Dr. Declan W Ali was the supervisory author. He was involved with concept formation and analysis and manuscript composition.

Results presented in chapter 4, and parts of the discussion have been published as Md Ruhul Amin, Kazi T. Ahmed & Declan W. Ali ; 2020; ‘Early Exposure to THC Alters M-Cell Development in Zebrafish Embryos’, Biomedicines. 2020 Jan; 8(1): 5. I was responsible for concept formation, data collection, analysis and manuscript writing. Kazi Ahmed assisted me in the collection of data for qPCR experiments. Dr. Declan W Ali was the supervisory author. He was involved with concept formation and analysis and manuscript composition.

Results presented in chapter 5, and parts of the discussion will be submitted as independent articles.

Results presented in chapter 6, and parts of the discussion have been submitted as Md Ruhul Amin, Kazi T. Ahmed & Declan W. Ali; ‘Cannabinoid receptor 2 (CB₂R) mediates cannabinol (CBN) induced developmental defects in zebrafish’, iScience. I was responsible for concept formation, data collection, analysis and manuscript writing. Kazi Ahmed assisted me in training electrophysiology and was also involved in manuscript writing. Dr. Declan W Ali was the supervisory author. He was involved with concept formation and analysis and manuscript composition.

Results presented in chapter 7, and parts of the discussion will be submitted as independent articles.

Acknowledgement

At first, I would like to express my sincere gratitude and respect to my supervisor Dr. Declan Ali. He has given me the opportunity to explore science independently and to think critically. This work could not have been done without his continuous guidance and support. Apart from his time and ideas, his rapport and kindness have made things easier for me in my academic and personal life.

I am immensely grateful to my co-supervisor Dr. John Chang. His continuous guidance, encouragements and assistance helped me a lot throughout my PhD program. I would like to express my gratitude to my other committee member Dr. Keith Tierney for his feedbacks and suggestions throughout my graduate study.

Special thanks to Dr. Trevor Hamilton, for their suggestions, collaborations and help I have received during this time. I would like to thank Dr. Ted Allison and all the members from his lab, for their suggestions, collaborations and help I have received. I must acknowledge that I was fortunate to have friends and lab mates like Kazi, Sufian, Hae-won, Lakhan who helped me a lot in many ways.

I would like to gratefully acknowledge the Assistance from Troy (MBSU) for his assistance and guidance during this period. It would have been difficult without your guidance. I also, would like to thank Arlene from Microscope Facility, Biological Science for being amazing all the time. Lastly, I would like to thank Carole from aquatic facility.

Table of Contents

Chapter 1	1
Introduction and Literature Review	1
1.1 Introduction	1
1.2 Endocannabinoid system	4
1.2.1 Cannabinoid receptors activation and signalling	4
1.2.2 Ligands	11
1.3 Exposure to cannabinoids during development	21
1.3.1 Effect of acute cannabinoid exposure in animal studies	21
1.3.2 Effect of chronic exposure of cannabinoids in animal studies	23
1.4 Zebrafish as a model organism	24
1.4.1 ECS in Zebrafish	26
1.4.2 Muscle structure of zebrafish	28
1.4.3 Zebrafish motor neurons	29
1.4.4 Hair cell development in zebrafish	31
1.4.5 Swimbladder development in zebrafish	35
1.5 Research Objectives and hypothesis	36
Chapter 2	63
Materials and methods	63
2.1 Animal care and exposure to THC, CBD and CBN	63
2.2 Embryo imaging and morphological observations	65
2.3 Immunohistochemistry	66
2.4 Electrophysiology	68
2.4.1 Analysis of mEPCs	69
2.5 Locomotion in embryos and larva	69
2.5.1 Locomotory response to sound and touch	70
	viii

2.5.2 Spontaneous coiling activity (Locomotion at 1 dpf)	70
2.5.3 Escape Response in 2 dpf Embryos	71
2.5.4 Escape response to touch using ethovision (Locomotion at 2 dpf)	71
2.5.5 Free Swimming (Locomotion at 3-6 dpf)	72
2.6 Behavioral experiments in adults	73
2.6.1 Open field (OF) test	73
2.6.2 Novel object approach (NOA) test	74
2.6.3 Shoaling test	74
2.7 Transmission Electron Microscopy (TEM)	75
2.8 Scanning Electron Microscopy (SEM)	75
2.9 RT-qPCR Subunits	76
2.10 RNAseq library preparation and data analysis	77
2.11 Statistics	78
Chapter 3	79
Motor neuron development in zebrafish is altered by brief (5.5-h) exposure to THC (tetrahydrocannabinol) or CBD (cannabidiol) during gastrulation	79
3.1 Results	79
3.1.1 Gross Morphology	79
3.1.2 Electrophysiology	81
3.1.3 Motor neuron immunolabelling	83
3.1.4 nAChR labeling	84
3.1.5 Locomotion	85
Chapter 4	106
Early Exposure to THC Alters M-Cell Development in Zebrafish Embryos	106
4.1 Results	106
4.1.1 THC exposure reduces axonal diameter of M-cell	106

4.1.2 Escape response properties were altered due to THC exposure	107
4.1.3 White and red muscle fibers appear thinner and slightly disorganized in THC treated embryos	108
4.1.4 THC does not alter nAChR subunit expression	109
4.1.5 THC exposure alters the locomotion at 5 dpf	109
Chapter 5	123
Transgenerational effect of CBD on locomotion, motor neuron development and gene expression in zebrafish	123
5.1 Results	123
5.1.1 CBD during gastrulation affects the locomotion during development (burst activity, escape response and free swimming)	123
5.1.2 Brief exposure to CBD during gastrulation affects the locomotion in adult zebrafish.	126
5.1.3 The exposure of CBD during gastrulation in F0 generation has a persistent effect on the locomotion of F1 embryos.	127
5.1.4 F1 embryos produced from CBD-treated parents (F0 generation) exhibited altered MN branching.	129
5.1.5 Brief embryonic exposure of CBD altered the gene expression in F0 and F1 generations	130
5.1.6 Embryonic exposure of CBD affected the expression of ECS genes in F0 and F1 generations	131
Chapter 6	158
Cannabinoid receptor 2 (CB ₂ R) mediates cannabiniol (CBN)-induced developmental defects in zebrafish	158
6.1 Results	158
6.1.1 CBN affects gross morphology, heart rate, MN development, locomotion and hair cell development	159
6.1.2 CBN exposure affects kinocilia development	161

6.1.3 Blocking CB ₂ R activity rescue morphology	163
6.1.4 CBN induces alterations in MN branching via CB ₂ R	165
6.1.5 Co-exposure of CBN and CB ₂ R antagonists prevents locomotor deficits	166
6.1.6 Pharmacological blocking of CB ₂ R inhibits CBN-induced alteration of hair cell development	168
Chapter 7	199
Brief exposure to (-) THC affects embryonic and adult locomotion; the effect persisted in the offsprings	199
7.1 Results	199
7.1.1 Brief exposure to (-) THC during gastrulation is detrimental to the development of zebrafish embryos	199
7.1.2 (-) THC exposure (during gastrulation) affects the locomotion of zebrafish embryos	200
7.1.3 (-) THC exposure significantly reduced the frequency of mEPCs	202
7.1.4 The exposure to (-) THC significantly altered the MN branching	203
7.1.5 Brief exposure to (-) THC during gastrulation altered muscle fiber morphology	204
7.1.6 Blocking CB ₁ R activity inhibited (-) THC-induced mortality and morphological alteration	204
7.1.7 Brief exposure to (-) THC is lethal to zebrafish embryos, disrupts swimbladder development	205
7.1.8 Blocking cannabinoid receptor activity did not rescue normal development of swimbladder; however, activation of Shh prevented (-) THC-induced swimbladder defects	206
7.1.9 Transcriptomic changes in zebrafish embryos (F0) following brief exposure of (-) THC during gastrulation	208
7.1.10 Brief exposure to (-) THC during gastrulation has a persistent effect on the locomotion of adult zebrafish	210
7.1.11 The exposure of (-) THC during gastrulation in F0 generation has a transgenerational effect on the locomotion of F1 embryos.	211

Chapter 8	239
Discussion and conclusion	239
8.1 Overview of the findings	239
8.2 Exposure to cannabinoids (THC, CBD, CBN and (-) THC) alters gross morphology, survival, hatching, heart rate, neuronal development (MN and M-cell), muscle development and synaptic activity	242
8.3 Exposure to THC, CBD, CBN and (-) THC resulted in locomotion defects	247
8.4 CBN exposure during gastrulation affect zebrafish cilia development	252
8.5 (-) THC exposure during gastrulation affects swimbladder development and induce transcriptional changes	255
8.6 CBD and (-) THC exposure during gastrulation affect the behavior in the adult zebrafish	257
8.7 CBD and (-) THC exposure during gastrulation affect the locomotion of zebrafish offspring in the F1 generation	258
8.8 Mechanism of action of cannabinoid-induced developmental defects	261
8.8.1 Cannabinoid receptors mediated second messenger system	261
8.8.2 Reactive oxygen species (ROS)-mediated mechanism	266
8.8.3 Endocannabinoid-mediated mechanisms	267
8.8.4 Epigenetic mechanism	269
8.9 Conclusion and future directions	272
References	278
Appendices	303

List of Tables

Table 1. 1 Properties of phytocannabinoids and endocannabinoids at CB ₁ R and CB ₂ R.....	59
Table 1. 2 Structure and properties of synthetic agonists at CB ₁ R and CB ₂ R.....	60
Table 1. 3 Structure and properties of synthetic antagonists at CB ₁ R and CB ₂ R.....	61
Table 1. 4 <i>K_i</i> values for phytocannabinoids and endocannabinoids at CB ₁ R and CB ₂ R.....	62
Table 5. 1 List of primers used for RT-qPCR.....	157

List of Figures

Figure 1. 1 Chemical structure of phytocannabinoids and endocannabinoids.....	39
Figure 1. 2 Phytocannabinoids and endocannabinoids bind to cannabinoid receptors.....	41
Figure 1. 3 Endocannabinoid system (ECS).....	43
Figure 1. 4 Protein Structure of active form of CB ₁ R and CB ₂ R	45
Figure 1. 5 Superimposure of active and inactive structures of CB ₁ R (A) and CB ₂ R (B).	47
Figure 1. 6 Schematic outline of second messenger pathway activation.....	49
Figure 1. 7 Schematic of primary motor neuron branching in zebrafish.	51
Figure 1. 8 Ultrastructure of muscle organization.	53
Figure 1. 9 Schematic outline showing activation and inactivation of the Hedgehog pathway. ..	55
Figure 1. 10 Schematic outline of cannabinoid exposure	57
Figure 3. 1 Effect of THC and CBD exposure on zebrafish embryos	86
Figure 3. 2 Effect of vehicle control of THC (methanol) on morphology, survival and hatching of zebrafish embryos.	88
Figure 3. 3 Effect of vehicle control of CBD (methanol) on morphology, survival and hatching of zebrafish embryos.	90
Figure 3. 4 Effect of THC and CBD exposure on survival and hatching.	92
Figure 3. 5 Effect of THC exposures on heart rate.	94
Figure 3. 6 Miniature endplate currents (mEPCs) recorded from zebrafish white muscle	96
Figure 3. 7 Antibody labelling (anti-znp1) of axonal branches of primary motor neurons at 2 dpf	98
Figure 3. 8 Antibody labelling (anti-zn8) of axonal branches of secondary motor neurons at 2 dpf	100
Figure 3. 9 Expression of nicotinic acetylcholine receptors (nAChRs) at 2 dpf	102
Figure 3. 10 Quantification of the response rate of 5-dpf zebrafish larvae to touch and sound stimuli	104
Figure 4. 1 THC exposure reduces M-cell axonal diameter	111
Figure 4. 2 Exposure to THC during gastrulation alters escape response parameters.....	113
Figure 4. 3 Co-labeling of red muscle fibers and nAChRs using anti-F59 and Alexa 488 conjugated α -bungarotoxin, respectively	115
Figure 4. 4 Co-labeling of white muscle fibers and nAChRs using anti-F310 and Alexa 488 conjugated α -bungarotoxin, respectively	117
Figure 4. 5 The relative levels of nAChR subunits (α 1, γ and ϵ) mRNAs were analyzed by RT-qPCR.....	119

Figure 4. 6 THC exposure affects free swimming activity (locomotion) of zebrafish embryos at 5 dpf.....	121
Figure 5. 1 Effect of CBD exposure on spontaneous coiling activity in F0 embryos at 1 dpf... 133	
Figure 5. 2 Brief exposure of CBD affect the escape behavior at 2 dpf.....	135
Figure 5. 3 Effect of CBD exposure on free swimming at 3-6 dpf.....	137
Figure 5. 4 Brief exposure of CBD during gastrulation alters the locomotion in adults	139
Figure 5. 5 Treatment of CBD in F0 embryos caused an anxiety-like behavior in adult zebrafish	141
Figure 5. 6 Unexposed F1 embryos showed altered spontaneous coiling activity following CBD exposure in F0 embryos	143
Figure 5. 7 Untreated F1 embryos exhibited decreased escape behavior following brief exposure in F0 generation	145
Figure 5. 8 Untreated F1 embryos showed altered free swimming following an exposure of CBD in F0 embryos	147
Figure 5. 9 Primary MN staining of F1 embryos showed an altered branching pattern.....	149
Figure 5. 10 RT-qPCR of neuronal marker genes	151
Figure 5. 11 Gene expression of endocannabinoid system related genes (F0 embryos)	153
Figure 5. 12 Gene expression of endocannabinoid system related genes (of F1 embryos).....	155
Figure 6. 1 Effect of CBN exposure during gastrulation on zebrafish embryos.....	170
Figure 6. 2 Effect of CBN exposure on zebrafish hatching and malformation.	173
Figure 6. 3 CBN exposure affects the development of kinocilia in the otolith and along posterior lateral line (pLL).....	175
Figure 6. 4 Dose response of CB ₁ R and CB ₂ R antagonists during gastrulation.....	177
Figure 6. 5 Effect of CB ₁ R and CB ₂ R antagonists on heart rate.....	180
Figure 6. 6 Effect of CB ₁ R and CB ₂ R antagonists on survival and hatching of zebrafish embryos	181
Figure 6. 7 Effect of CB ₁ R and CB ₂ R antagonist on locomotion.....	184
Figure 6. 8 Effects of co-exposure of CBN with CB ₁ R and/or CB ₂ R antagonists at gastrulation on morphological characteristics, survival, and heart rate.....	186
Figure 6. 9 Combined exposure of CB ₂ R and CBN inhibits CBN-induced alteration of primary MN branching	189
Figure 6. 10 Reprsentative tracing of primary MN.	191
Figure 6. 11 Combined exposure of CBN with CB ₂ R antagonists exhibited significantly improved locomotion	193
Figure 6. 12 Blocking CB ₁ R and CB ₂ R activity inhibits CBN-induced alteration of kinocilia development partially and fully, respectively.....	195
Figure 6. 13 Blocking CB ₂ R activity prevented CBN mediated alteration of otolith structure..	197

Figure 7. 1 Effect of (-) THC on the development of zebrafish embryos.....	213
Figure 7. 2 Effect of (-) THC on locomotion during development of F0 embryos	215
Figure 7. 3 Effect of (-) THC on synaptic activity at NMJ.....	217
Figure 7. 4 Exposure of (-) THC severely impacted the primary and secondary MN development in F0 embryos	219
Figure 7. 5 Exposure of (-) THC altered the muscle morphology of F0 embryos.....	221
Figure 7. 6 Co-exposure of (-) THC with CB ₁ R antagonist prevented (-) THC-mediated effects	223
Figure 7. 7 (-) THC exposure is lethal to zebrafish development and alteration of swim bladder development might contribute towards the (-) THC-induced lethality.....	225
Figure 7. 8 Activation of hedgehog pathway inhibited (-) THC-mediated alteration of swimbladder.....	227
Figure 7. 9 RNAseq analysis of (-) THC treated embryos	229
Figure 7. 10 (-) THC mediated altered gene expression is linked to various biological process (BP).....	231
Figure 7. 11 (-) THC mediated altered gene expression is linked to various biological process (BP).....	233
Figure 7. 12 Adult zebrafish exhibited alteration in their behavior following a brief exposure of (-) THC in F0 embryos	235
Figure 7. 13 Untreated F1 embryos showed a persistent alteration in their locomotion following an exposure in F0 generation	237
Appendix Figure 1 Blocking CB ₂ R activity inhibited CBD-induced defects in gross morphology of zebrafish embryos.....	303
Appendix Figure 2 Blocking CB ₂ R activity inhibited CBD-induced reduction in heart rate of zebrafish embryos	305
Appendix Figure 3 Combined exposure of CB ₂ R and CBD inhibits CBD-induced alteration of primary MN branching	307
Appendix Figure 4 Combined exposure of CB ₂ R antagonists and CBD inhibits CBD-induced alteration of secondary MN branching.	309
Appendix Figure 5 Blocking TRPV1 activity inhibited CBD-induced mortality of zebrafish embryos.....	311
Appendix Figure 6 Combined exposure of TRPV1 antagonists and CBD inhibits CBD-induced alteration of primary and secondary MN branching.....	313

List of Abbreviations

ABHD4- Alpha/beta domain hydrolases 4
ABHD6- Alpha/beta domain hydrolases 6
ABHD12- Alpha/beta domain hydrolases 12
ACh- Acetylcholine
AC- Adenylate cyclase
AChR- Acetylcholine receptor
AD- Alzheimer's disease
AEA- Anandamide
AA- Arachidonic acid
aLL- Anterior lateral line
BDNF- Brain-derived neurotrophic factor
CaP- Caudal primary motor neuron
cAMP- Cyclic adenosine monophosphate
CB₁R- Cannabinoid receptor 1
CB₂R- Cannabinoid receptor 2
CB₃- Cannabinoid receptor 3
CBD- Cannabidiol
CBN-Cannabinol
CHO-Chinese hamster ovary
CNS- Central nervous system
CRIP1a-Cannabinoid interacting protein 1a
COX-2- Cyclooxygenase-2
dpf- Days post fertilization

DAGL- Diacylglycerol lipase
Dhh- Desert hedgehog
DRG- Dorsal root ganglion
ECL - Extracellular loop
ECS – Endocannabinoid system
eCB- Endocannabinoid
EAE- Experimental autoimmune encephalomyelitis
FAAH- Fatty acid amino hydrolase
Hh- Hedgehog
hpf- Hours post fertilization
GABA- Gamma-Aminobutyric acid, or γ -aminobutyric acid
GDE1- Glycerophosphodiester phosphodiesterase 1
GPCR- G-protein-coupled receptor
GPCR55- G-protein-coupled receptor 55
GIRK- G-protein-gated inwardly rectifying potassium channels
GRKs-G-protein-coupled receptor kinases
Hh- Hedgehog
hr- Hours
ICL- Intracellular loop
ICS- Intracellular solution
Ihh- Indian hedgehog
IP3- Inositol trisphosphate
KIF7- Kinesin family member 7
KA- Kainic acid
LPI- L-lysophosphatidylinositol

LL- Lateral line

MS- Multiple sclerosis

M-cell- Mauthner cell

NMJ- Neuromuscular junction

MiP- Middle primary motor neuron

MN- Motor neuron

min- Minutes

NAPE- N-acyl-phosphatidylethanolamine

NAPE-PLD- (NAPE)-specific phospholipase D

mEPC- Miniature endplate current

MAPKs - Mitogen-activated protein kinases

MGL- monoacylglycerol lipase

PKA- Protein kinase A

PKB- Protein kinase B

PI3K- Phosphatidylinositol 3-kinase

PIP2- Phosphatidylinositol bis-phosphate

pLL- Posterior lateral line

PLA2- Phospholipase A2

PLC- Phospholipase C

RT-qPCR- Reverse transcription quantitative real time PCR

Shh- Sonic hedgehoge

s- seconds

SUFU- Suppressor of fused

THC- δ^9 Tetrahydrocannabinol

TRPA1- Transient receptor potential cation channel, subfamily A, member 1

TRPV1- The transient receptor potential cation channel, subfamily V, member 1

TRPV2- The transient receptor potential cation channel, subfamily V, member 2

Wnt- Wingless

2-AG-2-arachidonoylglycerol

(-) THC - (-) trans δ^9 THC

Chapter 1

Introduction and literature review

1.1 Introduction

According to the world drug report 2020, cannabis use has increased worldwide in recent years. For instance, the estimated number of cannabis users was more than 250 million in 2018, which was 20 million more than in 2016 (United Nations Office on Drugs and Crime, 2020). One contributing factor is likely to be the legalization of cannabis use for recreational and medicinal purposes in many regions such as Canada, Europe, Australia and several states in the USA. Legalizing and decriminalizing cannabis might encourage further use and supports the misconception that it has little or no harmful effects (Leyton, 2019; Ramo et al., 2012). Recent reports show that cannabis use has increased from 17% to 20% among people aged 15 or older (Rotermann, 2021), and cannabis use has been predicted to increase significantly in the coming years.

Traditionally, people have used cannabis for medicinal and recreational purposes since 500 BC (Spicer, 2002). However, it has also been proposed as a gateway drug for new users, especially among a younger population (George & Vaccarino, 2015). In addition, cannabis is also one of the most commonly used illicit drugs among a wide range of people, including pregnant women. The ease of availability and its social acceptance could facilitate the increase in

cannabis use during pregnancy. In fact, in the USA, cannabis use increased from 5.7 % to 12.1 % between 2003 and 2017 among pregnant women (ages 12-44) (Roncero et al., 2020; Volkow et al., 2019). In Canada, about 12.6 % of pregnant women (ages between 15-44) reported using cannabis in 2015, which increased to 16.9 % in 2016 (Canadian Tobacco Alcohol and Drugs, 2017). Cannabis is often taken during pregnancy to tame morning sickness (Badowski & Smith, 2020; Koren & Cohen, 2020; Roberson et al., 2014) and more than 21 % of pregnant women in the USA who experienced severe nausea during pregnancy stated they were more likely to use cannabis. The same study indicated that about 6 % of pregnant women reported taking cannabis in the month before pregnancy while 2.6 % of women reported using cannabis during pregnancy. A study in British Columbia reported that 77 % of pregnant women had nausea and vomiting during pregnancy, and 60 % of them used cannabis to treat the condition. Given that cannabinoids can cross the placenta, cannabis exposure can pose a severe risk to the development of the offspring (Fried, 1995; George & Vaccarino, 2015). Since more and more people are using this drug and an increasing number of countries are looking to legalize recreational cannabis use, it is important to understand its effects on embryonic development.

About 554 chemical compounds have been identified in cannabis (*Cannabis sativa*), including 113 different plant-derived cannabinoids (phytocannabinoids). Although cannabis has been used medicinally for thousands of years, the first cannabinoid to be isolated was cannabitol (CBN) (Howlett, 2005), while chemical synthesis of the second cannabinoid to be isolated, cannabidiol (CBD), occurred in 1940. The main psychoactive component tetrahydrocannabinol (THC), was identified and isolated in 1964 (Fig 1.1) (Gaoni & Mechoulam, 1964). Significant progress on cannabis research occurred when Allyn Howlett's group discovered the first cannabinoid receptor, CB₁R, in 1984 (Howlett, 2005; Pertwee, 2006). And shortly thereafter,

Mechoulam's group identified endogenous cannabinoids, anandamide (AEA) and 2-arachidonyl glycerol (2-AG) from porcine brain and canine gut respectively (Devane et al., 1992; Mechoulam et al., 1995). These endogenous cannabinoids were referred to as endocannabinoids (eCBs) and they are natural ligands of CB₁R (Fig 1.1 and 1.2). The discovery of the eCBs coupled with advances in understanding their receptor biology revealed important information on their physiological and developmental functions, and suggested key roles in maintaining homeostasis. Consistent with this, it was found that the dysregulation of eCB signalling is linked to various diseases, such as multiple sclerosis, cardiovascular diseases, schizophrenia, and cancer (Maurya & Velmurugan, 2018).

Smoking cannabis facilitates the interaction of plant-derived cannabinoids (THC, CBD and CBN) with the endocannabinoid system (ECS), leading to a disruption in the balance of the system, and resulting in abnormal chemical and physiological changes in the organism. Several epidemiological and clinical studies have reported a range of adverse effects of cannabis, including depression, anxiety, developmental deformities, impairment in learning and memory, decision-making and attention deficits (Churchwell et al., 2010; Crippa et al., 2009; Degenhardt et al., 2003; Moore et al., 2007; Solowij et al., 2002). In addition, some animal studies provide evidence of neurotoxic effects (Sarne et al., 2011; Sarne & Mechoulam, 2005). However, there is little evidence regarding the mechanism of how cannabinoids such as THC, CBD and CBN, modulate these types of adverse effects.

Another pressing concern is that the cannabinoid content of recreational and medical cannabis has increased dramatically over the past two decades. For instance, ElSohly et al., (2016) reported that the THC content of recreational cannabis in the United States increased from 4% in 1995 to 12% in 2014. Hence, understanding how cannabinoids affect the structures

and functions of the nervous system, impact neurological development, and induce neurobiological changes is important given the increased prevalence of cannabis use and the elevation in the cannabinoid content in cannabis.

1.2 Endocannabinoid system

The ECS is composed of three components: i) receptors for activating downstream signalling, ii) ligands (cannabinoids) that bind to the receptors, and iii) synthesizing & degrading enzymes for cannabinoids. The two primary eCBs produced by an organism (human, rodent and zebrafish) are 2-AG and AEA, and they act as ligands on cannabinoid receptors. There are two main types of cannabinoid receptors: CB₁R and CB₂R that belong to the rhodopsin-like G-protein-coupled receptor (GPCR) family with seven transmembrane-spanning domains (Fig 1.4 and Fig 1.5). CB₁R and CB₂R are coupled to the G_{i/o} family of G-proteins that inhibit adenylate cyclase (AC) activity. They have also been shown to activate inwardly rectifying potassium channels and inhibit voltage-gated Ca²⁺ channels (Fig 1.6) (Turu & Hunyady, 2010).

1.2.1 Cannabinoid receptors activation and signalling

It had long been thought that cannabinoids interact with receptors to produce their wide-ranging effects as psychotropic agents, analgesics or antiemetic compounds, but it was not until 1990 that the first cannabinoid receptor (CB₁R; SKR6) was cloned from a rat cerebral cortex cDNA library (Matsuda et al., 1990). The translated genetic sequence (encoded by the *CNR1* gene) gave rise to a 473 amino acid protein of the G-protein-coupled family of receptors, which

contained seven putative hydrophobic or membrane-spanning domains, and several potential glycosylation sites. When expressed in Chinese hamster ovary (CHO) K1 cells the protein displayed cannabinoid stereo-selectivity and cannabinoid-induced inhibition of AC activity (Matsuda et al., 1990). Consequently, the human homologue (472 amino acid protein) and mouse homologue (473 amino acid protein) were rapidly identified (Gerard et al., 1991; Gérard et al., 1990). Three years after the initial cloning of the rat CB₁R, a second type of G-protein-coupled cannabinoid receptor (CX5) was cloned from a human promyelocytic leukemia cell line (HL60) (Galve-Roperh et al., 2013). This receptor was highly expressed in macrophages obtained from spleen and its amino acid composition exhibited significant divergence from the CB₁R that was cloned from rat brain. Evidence has now accumulated to show that both CB₁R and CB₂R are negatively coupled to AC and are typically expressed in very different regions of the body. CB₁R are mainly limited to the central nervous system (CNS) while CB₂R are largely confined to the peripheral nervous system and the immune system. A detailed tissue distribution of cannabinoid receptors is reviewed elsewhere (Howlett et al., 2002; Jordan & Xi, 2019). Radiolabeling of CB₁R in the brain with the tritiated CB₁R receptor agonist [³H] CP55,940 showed high density expression in regions of the basal ganglia such as the substantia nigra pars reticulata and globus pallidus, as well as in the hippocampus and cerebellum (Herkenham et al., 1990). However, expression was sparse in the thalamus and lower brainstem regions (Herkenham et al., 1990). The subcellular location of receptors provided clues of their functional roles. Because CB₁R are highly localized to presynaptic membranes, they were thought to act as modulators of synaptic release. Indeed, physiological studies confirmed this hypothesis and showed that activation of CB₁R altered synaptic transmission in a homeostatic manner. But how does this occur? What are the mechanisms that underlie these effects? To answer these questions we need to examine the

literature on the pharmacology of CB₁R activation. Both CB₁R and CB₂R are negatively linked to AC activity (Fig 1.6) and protein kinase A (PKA) (Howlett, 2005; Turu & Hunyady, 2010). When the receptors are expressed in cell lines, they initiate a pertussis toxin-mediated event that requires G_{i/o} signalling and that results in a reduction in the production of cyclic AMP (cAMP) (Pertwee, 2008). The downregulation of PKA suppresses PKA-mediated signalling events. In addition, dissociated G-protein βγ subunits stimulate phosphatidylinositide 3-kinase (PI3K) and protein kinase B (PKB), which induce the phosphorylation of mitogen-activated protein kinases (MAPKs). Activated MAPKs can influence a range of downstream activity (Howlett, 2005; Turu & Hunyady, 2010; Zou & Kumar, 2018) (Figure 1.6).

Cannabinoid receptors may also mediate signalling through non-G-protein pathways. Two proteins that are associated with non-G-protein pathways and that have been shown to interact with cannabinoid receptors are i) G-protein-coupled receptor kinases (GRKs), and ii) β-arrestins (Lefkowitz & Shenoy, 2005). The non-G-protein pathway also includes the adaptor protein AP-3, GPCR-associated sorting proteins (GASP) and the cannabinoid-interacting protein 1a (CRIP1a). These partners regulate downstream signalling such as MAPKs, tyrosine kinases, ERK-dependent induction of protein translation (Witherow et al., 2004), and phosphatidylinositol 3-kinase (PI3K)-mediated phospholipase A2 (PLA2) activation (Walters et al., 2009). The non-G-protein pathway can also modulate Kif3A-dependent activation of the protein Smoothed in the cilium (Kovacs et al., 2009; Kovacs et al., 2008) and protein phosphatase 2A (PP2A)-mediated dephosphorylation of Akt (Beaulieu et al., 2005). Upon binding, a ligand can selectively activate either the G-protein or the β-arrestins pathway, which is called “biased signalling” while the ligands are called “biased ligands”.

Ligand binding studies show that the eCB, AEA, is capable of inhibiting AC activity in membranes possessing CB₁R (Childers et al., 1994; Howlett & Mukhopadhyay, 2000), but this same agonist shows markedly less efficacy on CHO cells expressing CB₂R, suggesting that AEA has differential effects on CB₁R vs CB₂R. In contrast, the other main eCB, 2-AG, acts as a full agonist at the cannabinoid receptors when inhibiting forskolin-induced cAMP accumulation (Gonsiorek et al., 2000). A critical determinant of the downstream effects of CBR activation is the isoform of AC that associates with the receptor. For instance, ligand binding to CBR co-expressed with AC isoforms 1, 3, 5, 6 or 8 leads to inhibition of cAMP, whereas co-expression with AC isoforms 2, 4, or 7 leads to stimulation of cAMP production (Rhee et al., 1998; Rhee et al., 1997). Thus, CB₁R/CB₂R are capable of activating G_s in addition to G_{i/o} even though much of the endogenous or physiological activity appears to lead to an inhibition of cAMP.

The search for additional cannabinoid receptors led to the publication of convincing evidence in 2007 that the orphan receptor GPCR55 is a cannabinoid receptor (Ryberg et al., 2007). Cloning, sequencing and expression of GPCR55 showed that the CB₁R/CB₂R ligand [³H] CP55940 exhibited high specificity for GPCR55. Moreover, this receptor can also be activated by THC, AEA, 2-AG and the CB₁R selective agonist noladin ether. Interestingly, 2-AG displays almost 200-fold greater potency as an agonist at GPCR55 compared with the prototypical CB₁R and CB₂R, and THC has a greater efficacy at GPCR55 compared with CB₁R or CB₂R. GPCR55 couples to G α ₁₃ (Ryberg et al., 2007), but has also been linked to increases in intracellular Ca²⁺ via a mechanism that involves G_q, G₁₂, RhoA, actin, phospholipase C (PLC) and Ca²⁺ release from IP₃-gated stores (Lauckner et al., 2008). In other words, cannabinoid receptors are linked to multiple second messenger systems that have the potential to couple enzyme activity to ion channel behavior, as well as, to gene activation. An investigation into the role of GPCR55 at

presynaptic terminals of CA3-CA1 synapses show that activation of GPCR55 by L-lysophosphatidylinositol (LPI) transiently increases the Ca^{2+} release probability by elevating presynaptic Ca^{2+} through activation of local Ca^{2+} stores, implying a possible role in short-term potentiation in the hippocampus (Sylantsev et al., 2013). Based upon these findings there have been suggestions that the GPCR55 receptor could be renamed a type 3 cannabinoid receptor, CB_3R . Nonetheless, GPCR55 shows significant characteristics of a true cannabinoid type receptor and fully determining its distribution within the body, subcellular localization, temporal expression patterns and downstream signalling pathways will lead to a greater understanding of the function of eCBs and effects of phytocannabinoids. Lastly, three other orphan GPCRs, that share about 35% identity with cannabinoid receptors, have been detected in the mammalian CNS: GPCR3 in the mouse brain, GPCR6 in the human brain and GPCR12 in the rat brain (Lee et al., 2001).

There is now significant evidence for a direct interaction between cannabinoids and transient receptor potential (TRP) channels such as the TRP vanilloid type 1 and 2 (TRPV1 and TRPV2) and TRP ankyrin type 1 (TRPA1) (Zygmunt et al., 1999). TRPV1 and TRPV2 channels are cation channels that allow the passage of Na^+ , K^+ and Ca^{2+} across cell membranes and are activated by capsaicin or heat above temperatures of 40 °C and above ~50 °C respectively, whereas TRPA1 are menthol- and cold-activated cation channels (Zheng, 2013). TRPV1 are activated by the eCBs 2-AG and AEA (Akopian et al., 2008), while TRPV2 and TRPA1 are activated by THC and CBD (Akopian et al., 2008; Kim et al., 2008; Qin et al., 2008). TRPV1 are largely found in the cerebellum, basal ganglia, hippocampus, diencephalon and DRG neurons (Ahluwalia et al., 2000; Cristino et al., 2006). TRPV2 tend to be localized to sensory neurons of the DRG, spinal cord, and trigeminal ganglia, but are also found in the cerebellum (Caterina &

Julius, 1999; Kowase et al., 2002). TRPA1 is extensively colocalized with TRPV1 in sensory neurons (Diogenes et al., 2007; Diógenes et al., 2007; Story et al., 2003). Activation of these receptors typically leads to membrane depolarization and activation, but TRPV1 and TRPA1 are known to exhibit functional desensitization. In other words, activation of TRPV1 and TRPA1 by cannabinoids may lead to an immediate depolarization, but this will be followed by sensitization and subsequently inhibition because further activation by ligands, heat or cold will be muted as the channels are in a desensitized state. Some evidence exists for the direct interaction between cannabinoids and ion channels and it has been hypothesized that some of the CB₁R/CB₂R-independent cannabinoid effects occur in this manner.

1.2.1.1 Interaction of cannabinoid receptors with THC, CBD and CBN

Our understanding of the mechanisms that underlie key interactions between the cannabinoid receptors and their agonists and antagonists was further increased with the elucidation of the crystal structure of the human CB₁R in 2016 (Huang et al., 2020). To date, two crystal structures of CB₁R have been generated. Hua et al. (2016) reported a crystal structure of the inactive form of CB₁R bound to the antagonist AM6538, whereas the second was reported with the active form of CB₁R bound to the inverse agonist taranabant (Shao et al., 2016). CB₁R consists of seven transmembrane alpha helices (TMH1-7), three extracellular loops (ECL1-3) and three intracellular loops (ICL1-3). The G_{i/o} family of proteins (G_{i1}, G_{i2} and G_{i3}, and G_{o1} and G_{o2}) interact with cannabinoid receptors via the receptor's intracellular loops (ICL3 or ICL4) (Howlett & Shim, 2011; Hryhorowicz et al., 2019).

The extracellular surface of CB₁R is involved in ligand binding (Hua et al., 2016; Shao et al., 2016) and, in particular, the extracellular loop ECL2 dictates ligand trafficking to the binding pocket of the cannabinoid receptors (Ahn et al., 2009; Shim, 2010; Wheatley et al., 2012). Furthermore, ECL2 maintains the shape of the active site where the ligand binds, thus, plays a crucial step in the functioning of GPCRs (Woolley & Conner, 2017). The ECL2 of CB₁R contains 21 amino acid residues (tryptophan W255 to isoleucine I271) and helps to stabilize TMH4 and THM5. The disulfide bond between Cys257 and Cys264 of ECL2 is essential for CB₁R stability in an inactive state (Fay et al., 2005). Findings also showed that specific residues are necessary for ligand interaction and accommodate the cyclic core of cannabinoids. For instance, six residues (Cys257, Cys264, F268, P269, H270 and I271) are critical for allosteric modulation and four residues (F268, P269, H270 and I271) are critical for accommodating the cyclic core and alkyl side chain of cannabinoids (THC, CBD and CBN) (Ahn et al., 2009).

TMH6 contains a conserved CWxP structural motif and consists of residues C6.47, W6.48 and P6.50 that play a vital role in CB₁R activation. Amino acid residue P6.50 in TMH6 acts as a hinge which likely facilitates the conformational change during CB₁R activation following agonist binding (Marino & Gladyshev, 2010; Zhang et al., 2018). Another highly conserved motif in GPCR named the “DRY motif” consists of aspartic acid, arginine, and tyrosine, and plays an important role in cannabinoid receptor (CB₁R and CB₂R) conformation and activity. A double mutation in the DRY motif (D213 and R214) resulted in a change in CB₁R signalling, i.e. CB₁R showed bias towards β -arrestin signalling rather than G-protein activation (Gyombolai et al., 2014).

Two mechanisms have been proposed to explain how the binding of the CB₁R agonists within the binding pocket might activate G-proteins. One mechanism suggests that cannabinoid

binding might disrupt the hydrogen bond interaction between D163 in TM2 and N394 in TM7. Barnett-Norris et al. (2002) proposed a second mechanism that includes an interaction between TM3 R214 (in the highly conserved sequence of D-R-Y-x-x-ile) and TM6 D338. The formation of a hydrophobic interaction between TM6 and the alkyl side chain of cannabinoid agonists serves as a trigger to move TM6. The motion of TM6 might alter the conformation of ICL3, which in turn activates G-protein (Howlett & Shim, 2011).

1.2.2 Ligands

The ligands for cannabinoid receptors are divided into several families/groups depending on the route of synthesis. For instance, eCBs are synthesized within the organism, phytocannabinoids are synthesized by plants, and synthetic cannabinoids are produced by human-designed chemical reactions. AEA and 2-AG are endocannabinoid ligands, whereas THC, CBD and CBN are three major phytocannabinoids that are represented by C21 terpenophenolic compounds (Fig 1.1 and 1.2; Table 1.1). Thus far, more than one hundred phytocannabinoids have been identified and subdivided into 10 classes of compounds (Turner et al., 2017). The immediate precursor of all phytocannabinoids is the acidic form tetrahydrocannabinolic acid (THCA), representing the first biogenic cannabinoid compound synthesized in the plant.

1.2.2.1 Phytocannabinoids

δ^9 -THC (IUPAC: 6aR, 10aR) (referred to THC afterwards) was first isolated in 1942 (Wollner et al., 1942) and typically constitutes 17-18% of the total phytocannabinoid content of cannabis plants (Turner et al., 2017). The structure was elucidated in 1964 (Gaoni & Mechoulam, 1964) (Fig 1.1). There are two forms of the acidic precursor of THC: THCA-A which is the major precursor and THCA-B which is a minor compound. Nine types of THC cannabinoids have been identified. Amongst those, δ^8 - tetrahydrocannabinol, the second major psychoactive component in cannabis is about 20% less potent than δ^9 THC (Turner et al., 2017). δ^9 -THC has four stereoisomers that vary in their double bond position and cis or trans ring junction: (+) trans δ^9 THC, (-) trans δ^9 THC, (+) cis δ^9 THC and (-) cis δ^9 THC (Pertwee, 2006). The (-) trans δ^9 THC form (referred to as (-) THC from here on) is found in natural cannabis because its production is energetically favored naturally (Khan et al., 2016; Pertwee, 2006) (Fig 1.1). Hence, consumable cannabis products or preparations might have a mixture of stereoisomers. For instance, a trace amount of (-) THC was detected in a commercially available CBD oil preparation (Runco et al., 2016). So, a detailed characterization of the composition and monitoring of the stability of these cannabis products is essential because they could potentially result in a change of potency, pharmacology or even toxicity. (-) THC is commercially available as dronabinol, which is used for medical purposes such as stimulating appetite to prevent anorexia in a patient with AIDS and as an antiemetic for cancer patient after chemotherapy (Khan et al., 2016).

THC is highly lipophilic and accumulates in adipose tissue and the spleen which act as long-term storage sites (Nahas et al., 2002). It is estimated that up to 37% of THC present in cigarettes can be delivered to the body during smoking while up to 30% is destroyed via pyrolysis (Perez-Reyes, 1990). When smoked, THC enters the blood stream extremely rapidly

with rising levels detected in blood plasma within 1–2 min of the first inhalation (Huestis, 2007). In controlled experiments, puffs of a 3.5% THC cigarette result in peak THC blood plasma levels of approximately 270 ng/ml (Huestis, 2007), and in experiments where the THC content of cigarettes was kept at either a “low” dose of 1.75% or a “high” dose of 3.55%, the blood plasma levels obtained from individuals smoking the higher dose cigarettes were variable and ranged from 90 ng/ml to 250 ng/ml (Huestis, 2007). These data indicate that the bioavailability varies substantially with each individual, and factors such as weight, gender, age, health and physiological background will likely impact the extent to which THC and other cannabinoids affect an individual. THC taken orally usually peaks in the circulation within 1–2 h, with blood plasma levels lower than those obtained during smoking (McGilveray, 2005). THC accumulates in fatty tissue and organs such as the heart, liver and spleen (Nahas et al., 2002). It readily crosses the blood-brain barrier and can be found in high quantities in the brain (McGilveray, 2005). THC released from fat has a half-life of several days and in some instances may take up to several weeks to fully clear from adipose tissue (Huestis, 2007; Huestis et al., 1996). Much of the metabolism of THC occurs in the liver where it is converted to 11-hydroxy-THC or 11-nor-9-carboxy-THC (Huestis, 2007). This conversion is rapid and occurs within minutes of THC detection in blood plasma (Huestis et al., 1992; Huestis et al., 1996; Huestis et al., 1992). Whereas 11-hydroxy-THC is psychotropically active, 11-nor-9-carboxy-THC is not (Mario Perez-Reyes et al., 1972) and is the principle component found in urine analyses as a proxy for determining cannabis consumption (Huestis et al., 1996). Numerous additional oxidative metabolites occur, but in lesser quantities.

CBD, the major non-psychoactive cannabinoid, is the third most abundant cannabinoid in the cannabis plant after δ^9 -THC and δ^8 -THC and comprises approximately 8% of the total

phytocannabinoid content. Isolated in 1940, it was another 23 years before the molecular structure was elucidated in 1963 (Mechoulam & Shvo, 1963). Seven CBD-type cannabinoids have been described thus far, and CBD and its precursor cannabidiolic acid (CBDA) are the most abundant cannabinoids in industrial hemp or *Cannabis Sativa*.

CBN is an oxidative product of THC and is non-psychoactive in nature. The amount of CBN in freshly consumed cannabis products is much less than THC and CBD (Zamengo et al., 2019). Interestingly, the acidic form of CBN (cannabinolic acid, CBNA) is present in large amounts in the cannabis plant and is converted to CBN upon heating. It has been shown that the THC content in cannabis decreases over time at a rate of 3-5% per month at room temperature (Lerner & Zeffert, 1968) and converted to CBN that is proportional to THC degradation (Repka et al., 2006; Zamengo et al., 2019). Heat and UV light accelerates the degradation of THC (Ross & Elsohly, 1998). For instances, a significant degradation of THC occurred in a range of 37-100 °C (Coffman & Gentner, 1974; Turner & Elsohly, 1979). A recent study also showed the influence of storage conditions where authors reported that the conversion of THC to CBN was faster in the first years than in subsequent years. The effect seemed more profound when the herbal sample was stored in natural light at 22 °C compared to darkness at 4 °C (Trofin et al., 2011). Thus, several studies described that CBN is predominantly present in significant quantities in stored, dried and aged cannabis products (Harvey, 1990). Hence, it is essential to consider how cannabis products are being processed or stored for medicinal and recreational purposes (Harvey, 1990).

Several studies have examined the effects of THC and CBD on developing organisms (Achenbach et al., 2018; Ahmed et al., 2018; Carty et al., 2019; Carty et al., 2018), but information on the effect of CBN during early development is scarce. This is in part due to the

low concentration of CBN in freshly prepared cannabis; however, as THC oxidizes, the concentration of CBN increases and over time may build up to significantly high concentrations (Ross & Elsohly, 1998). Recent findings have shown that after a year of dark-storage, almost 22 % of the THC content is degraded to CBN with a transformation rate of 4.4 % every three months (Andre et al., 2016; Ross & Elsohly, 1998). Therefore, improper handling and long-term storage of cannabis will result in increased levels of CBN.

1.2.2.2 Endocannabinoids and synthetic cannabinoids

After identifying CB₁R in 1990, the Mechoulam lab discovered the first endogenous cannabinoid neurotransmitter, AEA (N-arachidonylethanolamine) (Devane et al., 1992). A few years later, in 1995, a second endogenous ligand, 2-AG, was identified (Mechoulam et al., 1995; Sugiura et al., 1995). 2-AG is more potent and more broadly expressed throughout the body (Savinainen et al., 2001). It is also found in the human brain at levels that are more than 150 times higher than AEA (Stella et al., 1997). AEA binds preferentially to CB₁R and activates signalling cascades, which regulate appetite, mood swings, glucose metabolism, pain perception and fertility. However, 2-AG binds efficiently to CB₁R and CB₂R and regulates immune function, plays roles in brain injury, stroke and oxidative stress, and modulates a wide range of mental and physiological processes.

2-AG and AEA are structurally similar molecules, and while both contain arachidonic acid (Fig 1.1) (Lu & MacKie, 2016), the routes of synthesis and degradation are distinct and are mediated by multiple pathways (Fig 1.3). The membrane-bound inositol phospholipid is the ultimate precursor for the synthesis of these compounds. More precisely, 2-AG is synthesized

from phosphatidylinositol bis-phosphate (PIP₂) by the phospholipase C beta (PLC β) enzyme, while AEA is produced from N-arachidonyl phosphatidylethanolamine by N-acyltransferase (NAT) and N-acyl-phosphatidylethanolamine (NAPE)-specific phospholipase D (NAPE-PLD) enzymes. Sequential hydrolysis of PIP₂ occurs by the actions of PLC β followed by hydrolysis of diacylglycerol by diacylglycerol lipase (DAGL) (Murataeva et al., 2014). Two isoforms of DAGL have been reported: DAGL α and DAGL β (Bisogno et al., 2003). Knockout studies in mice have shown that DAGL α is responsible for synthesizing the majority of 2-AG (Tanimura et al., 2010). The alternative pathway for synthesizing 2-AG involves cleavage of PIP₂ by phospholipase A, followed by hydrolysis of phosphate ester bond by lysophospholipase C (Lu & MacKie, 2016).

The synthesis of AEA is more complex in comparison to 2-AG and involves four routes of synthesis: i) hydrolysis of NAPE by a NAPE-PLD; ii) cleavage of the NAPE by NAPE- PLC followed by dephosphorylation of the resulting phospho-AEA by phosphatase; iii) dual hydrolysis of NAPE by the phospholipase B and alpha/beta domain hydrolases 4 (ABHD4), followed by hydrolysis by glycerophosphodiester phosphodiesterase 1 (GDE1); and iv) liberation of AEA by the action of a lyso-NAPE-PLD (Lu & MacKie, 2016).

Three hydrolytic enzymes are responsible for the degradation of 2-AG: i) monoacylglycerol lipase (MGL), ABHD6, and ABHD12 (Blankman et al., 2007). Additionally, 2-AG can be hydrolyzed by fatty acid amino hydrolase (FAAH) (Lu & MacKie, 2016) and oxidized by cyclooxygenase-2 (COX-2) (Hermanson et al., 2014). In contrast, AEA is degraded by a single enzyme, FAAH (Cravatt et al., 1996) into arachidonic acid (AA) and ethanolamine

by a process that depends on multiple enzymes such as NAAA (N-acylethanolamine-hydrolyzing acid amide), COX and LOX (lipoxygenase) (Lu & MacKie, 2016).

In addition to phytocannabinoids and eCBs, several hundred synthetic cannabinoids have been synthesized to date (An et al., 2020). These cannabinoids can be categorized into the followings: i) CB₁R-specific agonists such as ACEA, ACPA, methanandamide and O-1812; ii) CB₂R-specific agonists such as JWH-133, JWH-105, PM-226, HU-308, GW-405833 and L-759633; iii) CB₁R-specific antagonists such as AM-251, Otenabant (CP-945,598), AM-281, Rimonabant (SR141716), Taranabant (MK-0364) and Surinabant (SR147778); and iv) CB₂R-specific antagonists such as AM-630, JTE-907 and SR144528 (Table 1.2 and 1.3).

1.2.2.3 Agonist, antagonist and inverse agonist

Three parameters can define the properties of a ligand- i) affinity, ii) efficacy and iii) potency. Affinity describes the tightness of the bond between the receptor and the ligand, whereas the intrinsic efficacy of a ligand is characterized by the ability of the ligand-bound receptor to elicit downstream signalling. Potency is determined by comparing the effects of the ligand with a reference ligand at the same receptor. In other words, potency is a measurement of the concentration of the ligand needed to produce the half-maximum effect. Based on these parameters (affinity, efficacy and potency), the ligand can be further classified into four groups- i) full agonist, ii) partial agonist, iii) neutral antagonist and iv) inverse agonist (Table 1.1).

A ligand that binds to the orthosteric site and activates the downstream signalling pathway is called an agonist and exhibits either full or partial responses. When an agonist shows

maximum receptor activity, it is called a full agonist, whereas if the receptor activity remains below the maximum response, it is categorized as a partial agonist. The binding of an agonist (either full or partial) to a receptor locks the conformation into an active state, whereas an inverse agonist stabilizes it into an inactive state. For example, THC inhibits AC activity; however, the extent of the inhibition is not the same as for several other agonists (Lyons et al., 2018). Thus THC is categorized as a partial agonist at CB₁Rs (Howlett et al., 2002) because the maximum effect it produces is well below that of the agonists CP55940 and WIN55212 (Breivogel & Childers, 1998; Gerard et al., 1991; Griffin et al., 1998). In addition, THC binds to and activates CB₂R; however, the binding affinity is much lower than CB₁R (Table 1.1). Therefore, THC has been shown to act as a partial agonist at CB₂R and inhibits the AC second messenger system in several cell lines including CHO cells (Bayewitch et al., 1996; Bolognini et al., 2012).

In contrast, an antagonist is a ligand that binds to, but does not activate or inactivate the receptor, and therefore results in no physiological response. CBD has a very low affinity for CB₁R and CB₂R and acts as an antagonist at these receptors in the submicromolar concentration range (Table 1.1 and 1.4) (Thomas et al., 2007). While CBD exhibits low affinity for CB₁R and CB₂R, it acts as a potential antagonist of GPCR55 (Sylantsev et al., 2013; Whyte et al., 2009). For example, CBD was shown to inhibit excitatory output from pyramidal cells by preventing the activation of GPCR55 in rat hippocampal slices (Sylantsev et al., 2013), and it has been shown to work as a potent antagonist at GPCR55 through GTPγS-binding assays (Ryberg et al., 2007). Behavioral experiments in mice showed that THC activation of CB₁R leads to inhibition of locomotion (activity) and reduction of body temperature, pain sensitivity and catalepsy. These effects were blocked by the CB₁R antagonist rimonabant at concentrations above 1 μM (Martin

et al., 1991; Varvel et al., 2005), but rimonabant has non-specific actions above 1 μ M, suggesting that additional receptors might be involved in producing the functional antagonism. For instance, a higher concentration of rimonabant can produce the antagonistic effect of GPCR55 (Sharir & Abood, 2010), the antagonistic effect of A1 adenosine receptors (Savinainen et al., 2003) and the antagonistic effect of TRPV1 channels (De Petrocellis et al., 2001). Some biological systems have a basal level of activity of a particular receptor type in the absence of an agonist, which is referred to as constitutive activity. For instance, cannabinoid receptors exhibit a basal level of activation or constitutive activity. When a ligand binds to activated receptors and inactivates them, this signalling is called inverse agonist signalling. An inverse agonist works as an antagonist in a non-constitutively active system.

THC can exert a mixed agonist-antagonist effect, i.e. in some experimental conditions it behaves as an agonist whereas under some experimental condition it acts as an antagonist (Turner et al., 2017). The mixed effect is most likely dependent on i) the proportion of cannabinoid receptors that are in their “active-state” and coupled to their effector molecules/mechanism, and ii) the proportion of cannabinoid receptors that are in their “inactive-state” and uncoupled to their effector molecule/mechanism. The mixed effect can also be modulated by other synthetic or eCBs present in the tissue (Turner et al., 2017). In addition, the mixed effect can be regulated by the orthosteric or allosteric sites. For instance, studies suggest that THC can act as an agonist or an antagonist at GPCR55 in a concentration-dependent manner (McHugh et al., 2012). The orthosteric sites can be defined as the binding sites of the endogenous ligands of GPCRs, while the allosteric binding sites are distinctive but linked to the orthosteric binding sites and are considered to be regulatory. The binding of THC to the orthosteric site of GPCR55 might produce agonistic properties. In contrast, the binding of THC

to the allosteric sites can induce conformational changes in the orthosteric binding site of GPCR555, resulting in antagonistic properties of THC.

Further, the allosteric binding site can modulate the conformation and functionality of the receptor or protein in multiple ways: positively (enhancing the affinity/efficacy), negatively (decreasing the affinity/efficacy), or neutrally (no change in activity). THC has been proposed to act as an allosteric modulator at 5-HT_{3A} and glycine receptors (Hejazi et al., 2006) and can inhibit 5-HT_{3A}-induced currents in HEK293 cells (Barann et al., 2002). Similarly, CBD can act as a negative allosteric modulator at CB₁R, where it may change the potency and the efficacy of the orthosteric ligand at CB₁R (Laprairie et al., 2015). For instance, CBD reduced the efficacy of the orthosteric ligands THC and 2-AG at CB₁R (Price et al., 2005).

CBN is reported to act as an agonist at CB₁R, but it binds to CB₂R with a higher affinity than CB₁R (Table 1.1 and 1.4). However, the binding of CBN to CB₂R and its downstream effects have been controversial. Rhee et al. (1997) reported that CBN acts as an agonist at CB₂R through a cAMP assay, whereas others showed an antagonistic effect of CBN at CB₂R in GTPYS assay (MacLennan et al., 1998). Similarly, a fluorescence-based Ca²⁺ assay showed that CBN works as a potential agonist and desensitizing agent at TRPA1 and TRPV2 receptors, whereas it appears to act as an antagonist on TRPM8 channels (De Petrocellis et al., 2011). These discrepancies could potentially be explained by the following: i) use of different ligand concentrations, ii) active and inactive state of the receptors, iii) different types of assay, iv) collection of tissue samples from different regions (based on that, the proportion of CB₁R and CB₂R would be different), and v) in vivo as opposed to in vitro experiments. In addition, a ligand can have a greater affinity for an individual receptor conformation than other conformation(s). In that case, the amount of ligand present in the system can redistribute the proportion of each

conformational state. Hence, the concentration of ligand might dictate the distribution of the conformational state of the receptor and thus inhibit or induce the physiological response (Kenakin, 1995). It is clear that further research is needed to unfold the pharmacology of CBN at different receptors.

1.3 Exposure to cannabinoids during development

Acute and chronic exposure paradigms are typically used in animals to study the immediate and long-term developmental effects of cannabinoids. This allows researchers the freedom to manipulate all aspects of the exposure paradigm. The impact of the cannabinoids depends on a range of factors, including the age of the organism, the length of the exposure, the concentration of the cannabinoids, the types and purity of the cannabinoids, and if the cannabinoid originated from animals, plants or were synthesized in the laboratory.

1.3.1 Effect of acute cannabinoid exposure in animal studies

The age of the organism when exposed to cannabinoids is a critical factor in determining the effect of cannabinoids on brain development. Evidence suggests that cannabinoids are less toxic or harmful to the adult central nervous system compared with embryonic organisms (Lubman et al., 2015; Mokrysz et al., 2016). Acute or short-term exposure to cannabinoids during prenatal, neonatal and adolescent periods can be harmful (Downer & Campbell, 2010) due to the critical involvement of the endocannabinoid system in brain development (Galve-Roperh et al., 2008). For instance, neonatal rodents exposed to cannabinoids experience cortical

cell death, whereas adults exposed to cannabinoids exhibit no detectable effects on neocortical cells (Downer et al., 2007). Furthermore, prenatal exposure has been shown to alter the development of major neurotransmitter systems in the brain, which might have a long-lasting impact on the organism (Kumar et al., 1990; Molina-Holgado et al., 1996)

It is essential to differentiate between the types of cannabinoids (i.e. THC, CBD and CBN), the source of cannabinoids (i.e. synthetic or natural) and the composition of cannabinoids in cannabis extracts especially because some cannabis species contain a more significant percentage of cannabinoids than others. For example, CBD accounts for up to 40% of the active component in *Cannabis sativa* (Campos et al., 2012), which is the predominant species of cannabis plant. THC has been shown to increase anxiety (Schramm-Sapyta et al., 2007), whereas CBD was found to be anxiolytic in rodent studies (Campos & Guimarães, 2008; Moreira et al., 2006; Resstel et al., 2009). Furthermore, THC has been shown to induce a psychotic-like effect in rodent models (Malone & Taylor, 2006), while CBD acts as an anti-psychotic drug (Moreira & Guimarães, 2005; Zuardi et al., 1991).

Studies have shown that the acute administration of cannabinoids impairs learning, memory, and attention in adult rodents (Egerton et al., 2006; Lichtman et al., 2002; Lichtman et al., 2004; Sullivan, 2000). Acute exposure of cannabinoids in rats led to alterations in neuronal activity in different brain regions, including hippocampus and prefrontal cortex, which indicates potential disruption of cognitive processes (learning, memory) (Campbell & Clark, 1988; Egerton et al., 2006; Lichtman et al., 2002; Sullivan, 2000). Even exposure to very low doses of THC (0.0001-0.0002 mg/kg) has resulted in long-term impairment in spatial learning and memory formation in mice (Amal et al., 2010; Tselnicker et al., 2007).

Administration of a single dose of THC (0.0286 mg/kg) in humans resulted in an increase in brain-derived neurotrophic factor (BDNF) levels in blood serum. However, the authors reported no effect of THC on BDNF levels amongst light cannabis users (D'Souza et al., 2009). BDNF is a crucial factor in synaptic plasticity and is associated with the reduction of anxiety and depression (D'Souza et al., 2009). Furthermore, acute administration of cannabinoids in humans is found to impair cognitive function, such as learning, short-term and working memory, attention, and executive functions (Ranganathan & D'Souza, 2006; Solowij & Pesa, 2011).

1.3.2 Effect of chronic exposure of cannabinoids in animal studies

Chronic cannabinoid exposure is reported to exert immunosuppressive and anti-inflammatory properties (Klein, 2005; Walter & Stella, 2004). Very high dose and long-term cannabinoid exposure in rats and monkey (up to 60 mg/kg for 1-3 months) have resulted in adverse effects on the hippocampus, amygdala and cerebral cortex (Harper et al., 1977; Heath et al., 1980; Landfield et al., 1988; Lawston et al., 2000; Scallet et al., 1987) including changes such as reducing synapse numbers, dendritic length, pyramidal cell density and shrinkage of neural cell bodies. Daily THC exposure (20 mg/kg) in adolescent rats over 3 to 6 months resulted in learning impairment and increased locomotion activity (Stiglick & Kalant, 1985). Chronic cannabinoid exposure during adolescence caused persistent deficits in learning and memory (O'Shea et al., 2004; Quinn et al., 2008; Renard et al., 2014) and led to more severe and persistent abnormal behavior compare to exposure during adulthood (Schneider, 2008).

1.4 Zebrafish as a model organism

Zebrafish is an elegant and popular model to study developmental biology, synaptic plasticity, toxicology, drug efficacy and behavior; this is indicated by the increasing number of publications per year from roughly a hundred publications in 1990 to several thousand in 2020 (Ellis, 2019; Hill et al., 2005). Zebrafish embryos offer certain distinct advantages over mammalian models for toxicity and exposure studies. One feature that makes it valuable for embryological and toxicological studies is that the embryos develop outside the mother in a chorion or egg casing, allowing one to accurately control the concentration and the time course of exposure compared with placental animals. Other benefits of using zebrafish as an experimental organism include their high fecundity and semi-transparent zebrafish embryos, which can be used for whole preparation imaging and identifiable neurons can be studied throughout development. The developmental stages of zebrafish are well characterized, and a complete genome sequence is available (Howe et al., 2013). It is a unique model where in vivo patch-clamp recordings can be obtained from neuromuscular junction (NMJ) and identifiable neurons such as the Mauthner cell (M-cell), while maintaining functional synaptic connections within an intact brain-spinal cord preparation (Roy & Ali, 2013; Saint-Amant & Drapeau, 2003). Last but not the least, zebrafish has a high degree of homology (~ 70%) to the mammalian genome and 84% of human disease-related genes have a zebrafish counterpart (Ellis, 2019). Drawbacks include the absence of a maternal-embryo interaction during gestation. Nonetheless, the advantages offered by a zebrafish model for toxicity and teratogenicity are significant and allow for a wide range of studies that may be difficult to perform in other preparations.

Zebrafish larvae are highly susceptible to various stimuli such as touch, olfaction, chemosensation, audition, vestibular input and vision. They also exhibit a wide range of complex behaviors, making them attractive organisms to study human disorders (Kalueff et al., 2014). In particular, zebrafish exhibit defensive, social, anxiety, and cognitive behaviors making them ideal candidates for studying neurological and psychiatric disorders (Basnet et al., 2019; Friedrich et al., 2012; Levitas-Djerbi & Appelbaum, 2017; Morris, 2009). Recent progress in zebrafish research documented a wide range of behaviors at different developmental stages. For instance, Kalueff et al. (2013) described more than a hundred different zebrafish behaviors, including spontaneous coiling activity, escape response, and free-swimming.

During development, zebrafish exhibit characteristic behaviors at specific time points (Kalueff et al., 2013). For instance, starting around 17 hpf, the embryos exhibit spontaneous coiling movements within the egg casing (chorion). This repetitive side-to-side movement of the tail of an embryo is the earliest type of activity, and is governed by a neuronal circuit (interneuron and primary MNs) located in the spinal cord (Saint-Amant & Drapeau, 2000; Zindler et al., 2019). The lateral line (LL) is a sensory organ in fish that detects water movement and plays an essential role in locomotion; this becomes morphologically visible at 18 hpf (Mizoguchi, Togawa, Kawakami, & Itoh, 2011). The posterior lateral line (pLL) is composed of an array of neuromasts in the trunk and tail that sit on the surface of the skin in embryos. In comparison, the neuromasts on the head form the anterior lateral line (aLL). Each neuromast (10-500 μm in length) is a rosette-like structure and consists of hundreds of mechanosensory cells, called hair cells, surrounded by supportive cells. Sensory hair cells are specialized mechanotransductive receptors required for hearing and vestibular function (Mizoguchi et al., 2011). Each sensory hair cell has a ciliary bundle (extending from the cell surface), composed of

a single long kinocilium and many shorter stereocilia (Webb, 2011). Another critical locomotor behavior exhibited by zebrafish is the escape response or C-start response (Berg et al., 2018; Roberts et al., 2011). The escape behavior develops at 24-27 hpf and occurs in response to visual, tactile and acoustic stimuli. This locomotor response is generated by well-defined neuronal circuits, that includes cells such as the M-cell, its homologues, Mid2 and Mid3 cells (Saint-Amant & Drapeau, 1998), and MNs. The M-cell, the largest interneuron in the CNS first appears around 8 hpf, but functional synapses onto the M-cells are not formed until 17-18 hpf (Ali et al., 2000; Kimmel et al., 1990). Primary MNs first appear between 9 and 16 hpf while axogenesis begins at 17 hpf and muscle innervation occurs shortly afterwards (Fig 1.7). Secondary MNs first appear around 15 hpf and innervate muscle fibers around 26-28 hpf (Myers et al., 1986; Westerfield et al., 1986). Free swimming starts at 48-72 hpf, shortly after hatching; however, more fully developed swimming (beat and glide type) starts at 96 hpf. Embryos exhibit M-cell-mediated fast escape activities in response to auditory/vestibular (AV) stimuli starting around 75 hpf (Kohashi et al., 2012). Zebrafish larva exhibit synaptic plasticity phenomena (habituation) associated with the escape response (both short and long term) to AV stimuli starting from 96 hpf (Roberts et al., 2016, 2011). Adult fish have also been shown to exhibit learning and memory through simple memory tests such as the novel object approach (NOA) test (Hamilton et al., 2017; Krook et al., 2019; May et al., 2016). In these studies, it was found that zebrafish prefer familiar objects over novel ones, contrasting preference shown by rodents.

1.4.1 ECS in Zebrafish

Phylogenetic analyses showed that the eCBs is highly conserved between zebrafish and humans, establishing zebrafish as an effective model for studying cannabinoid signalling in vivo. Zebrafish express all of the ECS genes necessary for cannabinoid signalling, including genes encoding CB₁R and CB₂R, FAAH and MAGL. Furthermore, zebrafish ECS genes have been shown to be linked to development (Akhtar et al., 2013; Carty et al., 2019), locomotion (Sufian et al., 2019), immune system function (Liu et al., 2013), cognitive process (Ruhl et al., 2014), anxiety (Ruhl et al., 2014; Stewart & Kalueff, 2014), energy balancing (Migliarini & Carnevali, 2008; Pai et al., 2013), and addiction (Braidia et al., 2007). In zebrafish CB₁R mRNA expression has been detected as early as the 3 somite stage (10 hpf) through RT-qPCR (Migliarini & Carnevali, 2009) and in situ hybridization experiments have documented the spatial expression of CB₁R as early as 1 dpf in the preoptic area. By 2 dpf, CB₁R expression is detected in the telencephalon, hypothalamus and hindbrain region (Lam et al., 2006; Watson et al., 2008). Additionally, CB₁R expression has been detected outside of the central nervous system in the liver and ovary (Migliarini & Carnevali, 2008, 2009). However, a recent study reported the presence of CB₁R and CB₂R mRNA as early as 1 hpf during development (Oltrabella et al., 2017). In the adult, CB₂R mRNA has been detected in the brain, retina, heart, gill, muscle and spleen of the zebrafish (Rodriguez-Martin et al., 2007).

mRNA molecules for the synthesizing enzyme DAGL, *dagla* is present in the telencephalon, hypothalamus, tegmentum and hindbrain at 2 dpf (Watson et al., 2008). FAAH protein expression has been detected in the adult zebrafish retina through immunocytochemistry (Yazulla & Studholme, 2001). Further, the presence of *gdel*, *mgl*, *abhd4* and *faah2a* transcripts has been reported during early development as early as 1 cell stage through in situ hybridization (Thisse et al., 2001).

1.4.2 Muscle structure of zebrafish

Muscle is composed of bundles of muscle fibers or myocytes. A muscle fiber is an elongated multinucleated cell composed of myofibrils, which consist of repeated units called sarcomeres. Within the sarcomere, one can find an array of proteins, including thick and thin filaments comprised of bundles of myosin and actin, respectively. Each sarcomere can be subdivided into different bands, lines, and zones. The I band is the region that contains only thin filaments, whereas the A band is the central region of the sarcomere and has both thick and thin filaments. The H zone contains only the area of thick filaments. The M line runs down the center of the sarcomere, through the middle of myosin filaments. In contrast, Z lines define the boundary of each sarcomere. More than 20 muscle fibers are arranged in parallel and are encapsulated by a layer of connective tissue called perimysium, forming a muscle fascicle. Several fascicles are grouped together in a muscle structure (Fig 1.8).

Towards the end of the segmentation period (24 hpf), zebrafish skeletal muscle contains four types of fibers: slow muscle, muscle pioneer cells, fast muscle cells and medial fast fibers (Naganawa & Hirata, 2011; Ochi & Westerfield, 2007). However, in adult zebrafish, skeletal muscle contains mainly two types of fibers: slow-twitch and fast-twitch fibers (Waterman, 1969). Each muscle fiber has distinct morphological properties and occupies a specific region of the axial muscle. Slow muscle fibers are located superficially and are composed of mitochondria-rich, red muscle. Slow muscle fibers undergo their first spontaneous contraction as early as 17 hpf, and by 21 hpf they mediate the spontaneous coiling behavior (Saint-Amant & Drapeau,

1998). In comparison, fast muscle fibers are found just underneath the red fibers and are involved in fast darting behaviors that start towards the end of the hatching period.

Muscle fiber development requires the concerted effort of multiple developmental signals, including growth factors and muscle-specific transcription factors. One such factor is sonic hedgehog (Shh) which plays a crucial role in zebrafish muscle development and is necessary to induce the development of slow muscle and pioneering muscle cells (Ochi & Westerfield, 2007). Another factor, fibroblast growth factor (Fgf), has been linked to muscle development, repair, and regeneration, and plays a crucial role in zebrafish morphogenesis and fast cell differentiation (Nguyen-Chi et al., 2012; Saera-Vila et al., 2016).

1.4.3 Zebrafish motor neurons

Most vertebrate muscles are innervated by a single motor axon (forming a single endplate), whereas individual zebrafish skeletal muscles are innervated by multiple neurons (Westerfield et al., 1986). Based on the origin, size, location and innervation pattern of trunk musculature, zebrafish motor neurons can be categorized into two classes: primary and secondary. Primary MNs appear between 9 and 16 hours post-fertilization (hpf), whereas secondary MNs are born at 22 hpf and continue to appear even after 25 hpf (Myers et al., 1986). Primary motor neurons have relatively large cell bodies, averaging $11.3 \pm 1.4 \mu\text{m}$ in diameter, and large axons (Myers et al., 1986). Secondary MNs are smaller in diameter ($6.7 \pm 1.0 \mu\text{m}$) with smaller axon widths. Each hemi-segment within the trunk contains 3- 4 primary motor neurons and about 20-24 secondary motor neurons.

Primary motor neurons can be classified into three types depending on their location in the spinal cord: Caudal (CaP), Middle (MiP) and Rostral (RoP) primary MNs (Eisen et al., 1986) (Fig 1.7). The CaP is born around 17 hpf and has a cell body that is located in the middle of the spinal cord with an axon that projects ventrally along the medial surface of the myotome. The growing axon pauses for about an hour upon reaching the horizontal myoseptum and then extends further ventrally to innervate all white muscle in the ventral region of the trunk (Eisen et al., 1986, Westerfield et al., 1986). The cell bodies of MiP MNs are located in between the RoP and CaP. The axon follows the path of the CaP until it reaches the horizontal myoseptum, where it extends to innervate the dorsal musculature. RoP MNs are located at the rostral end of a segment and follow the path of the MiP extension to reach the horizontal myoseptum. At this point, they grow laterally and innervate muscles at the dorsal segment of the ventral muscles (Eisen et al., 1986). In summary, the CaP, MiP, and RoP specifically innervate the ventral, dorsal, and middle musculature, respectively.

Based on the muscle innervation pattern, Menelaou & Mclean (2012) categorized secondary MNs into three classes: dorsally projecting secondary MNs (dS), ventrally projecting secondary MNs (vS) and dorsoventrally projecting secondary MNs (dvS). The dorsally projecting secondary MNs (dS) innervate muscles on the dorsal side of the body, and ventrally projecting secondary MNs (vS) are located dorsal to the dS and innervate ventral muscles only. Whereas dorsoventrally projecting secondary MNs (dvS), the largest secondary MNs in diameter, innervate muscles both on the dorsal and ventral side of the body. Axons of dS, vS and dvS have more extensive branching at deep musculature than superficial layers, suggesting they preferentially innervate white muscle fibers (Menelaou & McLean, 2012). Axonal growth of secondary MNs is initiated around 26 hpf. Several axon guidance molecules, including

sema3A1, sema3A2, GDNF, neuropilin, chondroitin sulphate, have been identified that play crucial roles in the proper development of primary and secondary axogenesis (Menelaou & McLean, 2012). Shh signal transduction is also essential for the normal development of motor neuron progenitors and somites.

1.4.4 Hair cell development in zebrafish

Primary cilia, also called immotile cilia, are sensory organelles associated with most cell types, that respond to chemical and mechanical stimuli in the environment and communicates those signals to the organism (Bangs et al., 2015). This organelle is essential to process cellular signals, such as sonic hedgehog (Shh), Wingless (Wnt) and Notch by detecting extracellular cues, thus necessary for animal development. The structure and function of the cilia are highly conserved throughout evolution (Pazour et al., 2002, 2000). The backbone of the cilium, the axoneme, is composed of nine microtubule doublets consisting of α - and β -tubulin polymers. The axoneme is anchored to the cell body and transition zone. The transition zone separates cilia from the cell body and regulates protein trafficking into cilia, creating an exclusive ciliary environment. This zone is composed of Y-shaped linker protein and ciliary necklace membrane protein, and distal appendages. Since cilia do not contain the molecular machinery for protein translation and synthesis, proteins must be transported to the ciliary tip and back via anterograde and retrograde intraflagellar transport mechanism, respectively

In vertebrates, Hedgehog (Hh) signalling critically depends on the primary cilium. Therefore, dysregulation of Hh is linked to numerous human diseases collectively called ciliopathies, and which include birth defects and diverse types of cancers. Aberrant activation

can lead to dysregulation of other vital pathways such as Wnt and Notch. Hh is a secreted protein that acts as a ligand that is evolutionarily conserved, and plays a crucial role in embryonic development and adult tissue homeostasis. Thus, Hh is a critical signalling pathway for organogenesis, regeneration and homeostasis. There are three Hh proteins recognized as ligands: Shh, Indian hedgehog (Ihh) and desert hedgehog (Dhh). Shh, plays a role in nervous system cell type specification (Ma et al., 2019; Patten & Placzek, 2000), whereas Ihh involves skeletal development (Iwasaki et al., 1997; Vortkamp et al., 1996), and Dhh is essential for spermatogenesis (Szczepny et al., 2006). In mice, Shh affects the patterning of the neural progenitors (interneurons and motor neurons) during embryogenesis, which depends on the gradient of Shh.

Activation of Shh can occur in two ways: 1) the canonical pathway which consists of the ligand-dependent activation of the pathway, and 2) the non-canonical pathway consists of a Gli-independent mechanism. In canonical signalling, the HH ligand binds to its receptor *ptch1* and releases SMO repression, activating the Shh pathway by activating *Gαi*. As a result, it inhibits AC, limiting the conversion of ATP into cAMP. The inhibition of cAMP ultimately inhibits PKA accumulation, which prevents the post-translational modification of the Gli transcription factor into its repressor form (Gli R). In summary, shh pathway activation facilitates the transcription of genes necessary for an organism's normal development by inhibiting PKA activity. In the absence of the HH ligand, *ptch1* inhibits SMO activity that increases AC and PKA activity and which leads to cleavage of Gli into its Gli R state (Fig 1.9). Gli R inhibits the transcription of target genes, which are necessary for development. The downstream effects of the cascade results in the translocation of Gli protein to the nucleus, which begins the transcription of the essential gene, including *ptch1* and *Gli 1*, in a negative and positive feedback loop, respectively.

Also, Gli protein translocation can induce modulation of Wnt and Noggin (Carballo et al., 2018). Ptch2 is another receptor for Shh, which shares about 54% homology with ptch1, but the expression and signalling are different from ptch1. And ultimately, it has decreased inhibition capacity to Smo (Fig 1.9).

In non-canonical signalling, activation of the pathway occurs through a Gli-independent mechanism, including type 1: downstream of Smo, and type 2: independent of Smo (Brennan et al., 2012). The non-canonical Shh signalling regulates several signalling cascades, including Ca^{2+} , cell proliferation and survival, chemotaxis and cell migration through actin rearrangement, and axonal guidance through ERK and Src kinase pathway activation.

A number of positive and negative regulators has been reported that influence the hedgehog pathway positively and negatively, respectively. For instances, PKA is a negative regulator of the Shh pathway and becomes enriched in the cilium when SMO is active. Other regulators such as GPCR161, Kinesin family member 7 (KIF7), suppressor of fused (SUFU) and TULP3 also become enriched in the cilium shortly after activation of SMO. GPCR161 is a negative regulator of Shh signalling; activation of HH signalling (i.e. HH ligand binding) enriches SMO along the membrane and GPCR161 exits from the cilia. KIF7 is essential for the trafficking of Gli proteins to the tip of the cilia. There are three types of Gli protein: Gli 1, Gli 2 and Gli 3. Gli 1 mainly works as an activator; whereas Gli 2 and Gli 3 are the predominant activator and repressor proteins, respectively. Finally, SUFU forms an inhibitory complex with Gli proteins (in the absence of HH ligand) and inhibits the translocation of Gli into the nucleus to prevent the pathway's activation. TULP3 is also a negative regulator as it is responsible for recruiting GPCR161, anchored to $G\alpha_s$ that activate AC to increase cAMP concentration in the

cilia. In contrast, GSK3 β works as a positive regulator of the Shh pathway by phosphorylating SUFU and promoting the release of SUFU from Gli proteins.

Emerging evidence suggests that the HH pathway can interact with other critical signalling pathways such as PKA, Wnt/ β -catenin and Notch. Particularly, HH and Wnt can interact in two ways: 1) by Gli 1 and Gli 2 activity, which can positively regulate the expression of secreted frizzled-related protein-1 (sFRP) that leads to inhibition of Wnt signalling, and 2) by the downstream activity of GSK3 β that is an essential component of inhibition complexes for HH and Wnt pathway.

Genetically engineered rodents lacking cilia die around E11.5, and mutants lacking Shh signalling die at E9.0 (Casparly et al., 2002; Kasarskis et al., 1998; Zhang et al., 2001). Ventral neural cell fates were not specified in the mutants lacking cilia or Shh signalling, as the relevant target genes were not induced. Also, loss of cilia ablates the formation of Gli activator (Gli A) or Gli repressor (Gli R); hence, the target genes were either not activated or repressed. In contrast, the mutant of SMO only produces the repressor of Gli (Gli R), so the target genes are repressed and had a more severe phenotype as they repress genes in non-neural tissue.

Cannabinoids activate the shh pathway possibly through two mechanisms of action: 1) by directly inhibiting Smo and preventing the signalling of Smo through Gai proteins, 2) by stimulating CB₁R that are present in the primary cilia (Fish et al., 2019). Potentially, CB₁R form heterodimers with Smo, and CB₁R-Smo heterodimers are associated with Gas proteins. Activation of Gas signalling stimulates AC, increasing PKA activity, leading to increases in Gli R activity.

1.4.5 Swimbladder development in zebrafish

The swimbladder is a gas-filled sac that is located dorsal to the gut and is used for buoyancy. It is essential for survival of most teleost species because it minimizes the energy required to maintain a vertical position in the water column (Alexander, 1972). In zebrafish, swimbladder development begins during embryogenesis and it becomes fully functional by 5 dpf (Yue et al., 2015). The development of the swimbladder process takes place in three phases: budding, growth or elongation and inflation (Winata et al., 2009). The budding phase involves the initiation of the swimbladder bud that forms as an evagination of the foregut, which consists of endothelial cells. This budding process starts at 36 hpf and lasts until 65 hpf. The elongation step (65-96 hpf) involves the growth of the swimbladder bud to form the pneumatic ducts. The swimbladder has three distinct tissue layers during this phase: an epithelial layer, surrounded by a mesenchymal layer, followed by a mesothelial layer (Winata et al., 2009). Finally, the inflation phase involves the development of a fully inflated single-chambered (known as a posterior chamber) swimbladder at 4-5 dpf via air gulping (Goolish & Okutake, 1999). The development of the anterior chamber of the swimbladder occurs at 20-21 dpf when a two-chambered swimbladder becomes visible in adult zebrafish (Winata et al., 2009).

Zebrafish swimbladder is thought to be a homolog of the tetrapod lung. Studies have shown that the zebrafish swimbladder fails to inflate following exposure to various drugs (Jönsson et al., 2012; Yue et al., 2015). Defective swimbladder development is commonly reported after exposure to oils or polycyclic aromatic hydrocarbons (PAHs) (Price & Mager, 2020). However, the exact mechanism underlying these effects on swimbladder development is unknown. Failed primary inflation and diminished swimbladder function are two possible

causes, which are likely responsible for the altered development of the swimbladder. Failure in primary inflation could result from a failure to swim-up to the water's surface to gulp air. Swim-up is a laborious movement that requires the integration of multiple physiological functions, including proper muscle and CNS development, and visual coordination. Impairment to any of these physiological systems could lead to failed swim-up behavior such as underdeveloped musculature and impaired vision. Abnormal development of the cardiovascular system is also linked to defective swimbladder function in PAHs exposure (Incardona et al., 2004). In that study, the authors predicted failed inflation of swimbladder as a secondary consequence of cardiovascular impairment (Incardona et al., 2004).

Further, the swimbladder development can be impacted by diminished swimbladder activity because if the swimbladder function is compromised, swimbladder volume cannot be maintained even though primary inflation occurs. Compromised swimbladder function can include reduced gas secretion rate by the gas gland or impairment of cardiac function. In addition, studies also suggest that each layer of the swimbladder has a unique expression of gene markers such as Shh and Wnt signalling, which may play a role in swimbladder development (Winata et al., 2009).

1.5 Research Objectives and hypothesis

Epidemiological and clinical studies in humans indicate that exposure to cannabis during development might have adverse effects. However, there are many inconsistencies and contradictions among these reports due to various confounding factors, including the types of cannabis used in the study: i) high in CBD *Cannabis sativa* (or hemp), ii) high in THC content

Cannabis indica, and iii) synthetic cannabis product. Surprisingly, very little is known about the mechanisms of actions of cannabinoids in light of its widespread use. Therefore, the objective of my study was to determine the effects of different types of cannabinoids on development in zebrafish. Specifically, I have studied the impact of brief exposures of cannabinoids on zebrafish development (i.e., gross development and synaptic development & maturation). My research mainly focuses on exposure during gastrulation, which occurs between 5.25-10.75 hpf in zebrafish (Kimmel et al., 1995) (Fig 1.10). Because gastrulation is a critical stage in embryonic development when the differentiation of cell lines becomes apparent for the first-time during embryogenesis. Three germ layers- ectoderm, mesoderm and endoderm are formed during this stage, and key neurons including M-cells (giant pair of neurons in zebrafish CNS) and primary motor neurons are born. In humans, gastrulation occurs in week 3 of embryogenesis (Nishimura et al., 1974) and is early enough that pregnancy may remain undetected. Hence, I hypothesize that cannabinoid exposure during gastrulation disrupts the proper development of zebrafish.

Further, epidemiological studies indicated that prenatal cannabis smoking promotes impaired cognitive function, abnormal behavior and neuropsychiatric defects among their children. These results suggest that cannabis has a profound and persistent effect on CNS development. However, the transgenerational effect of cannabis smoking is not well documented yet. Also, how cannabis exposure during development can have a persistent impact, i.e. the mechanism of gene regulation, which affects the next-generation offspring, is not known either. Therefore, to address these questions, I propose the following two objectives:

Objective 1: Determine whether cannabinoid exposure during gastrulation alters the development of zebrafish embryos and adults.

Objective 2: Study the multigenerational effect of brief exposure of cannabinoids on zebrafish.

In this thesis, I tried to decipher the effects of prenatal cannabinoid exposure on the development of zebrafish embryos and adults. Subsequently, I tried to determine whether the brief 5.5 hr exposure to cannabinoids altered the development of the next generation of animals. Understanding how cannabis impacts an organism's development, particularly the brain or neuronal development, will enrich our knowledge, which will ultimately help clarify the inconsistency and contradiction presented in a vast literature.

Figure 1. 1 Chemical structure of phytocannabinoids and endocannabinoids

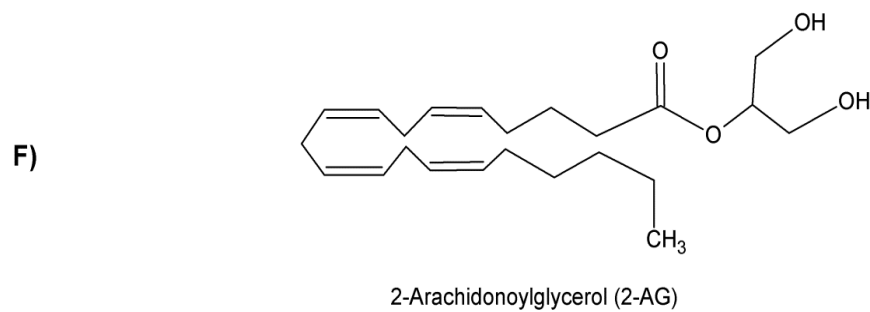
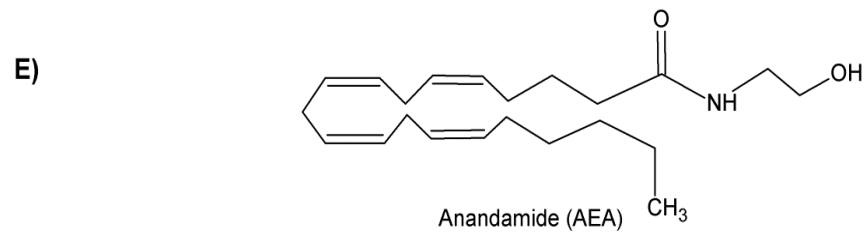
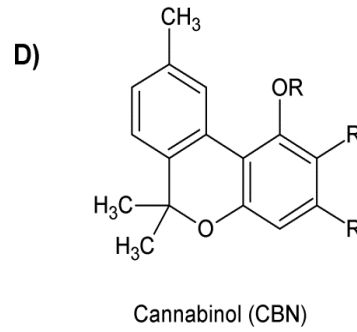
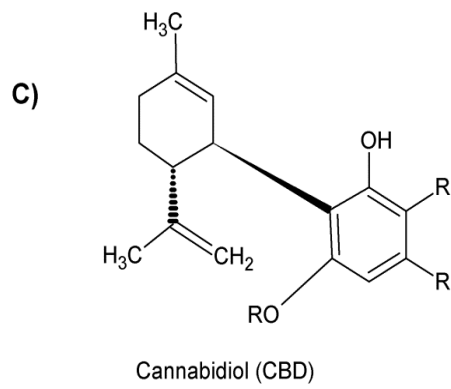
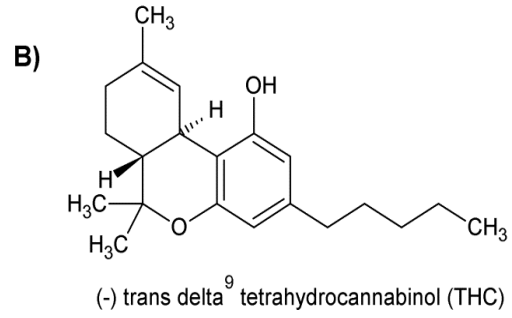
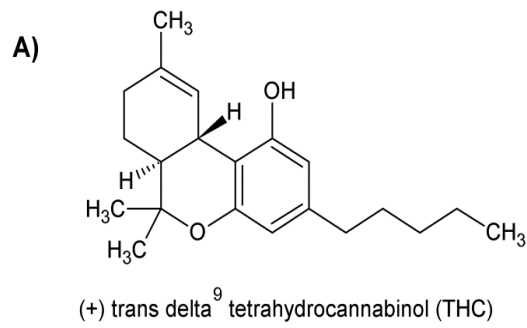


Figure 1.1 Chemical structure of phytocannabinoids and endocannabinoids. Chemical structure of several phytocannabinoids (A-D), (+) trans- Δ^9 -tetrahydrocannabidiol, (-) trans- Δ^9 -tetrahydrocannabidiol, cannabidiol (CBD), cannabinol (CBN), and the endocannabinoids (E-F), anandamide (AEA) and 2-arachidonoylglycerol (2-AG).

Figure 1. 2 Phytocannabinoids and endocannabinoids bind to cannabinoid receptors

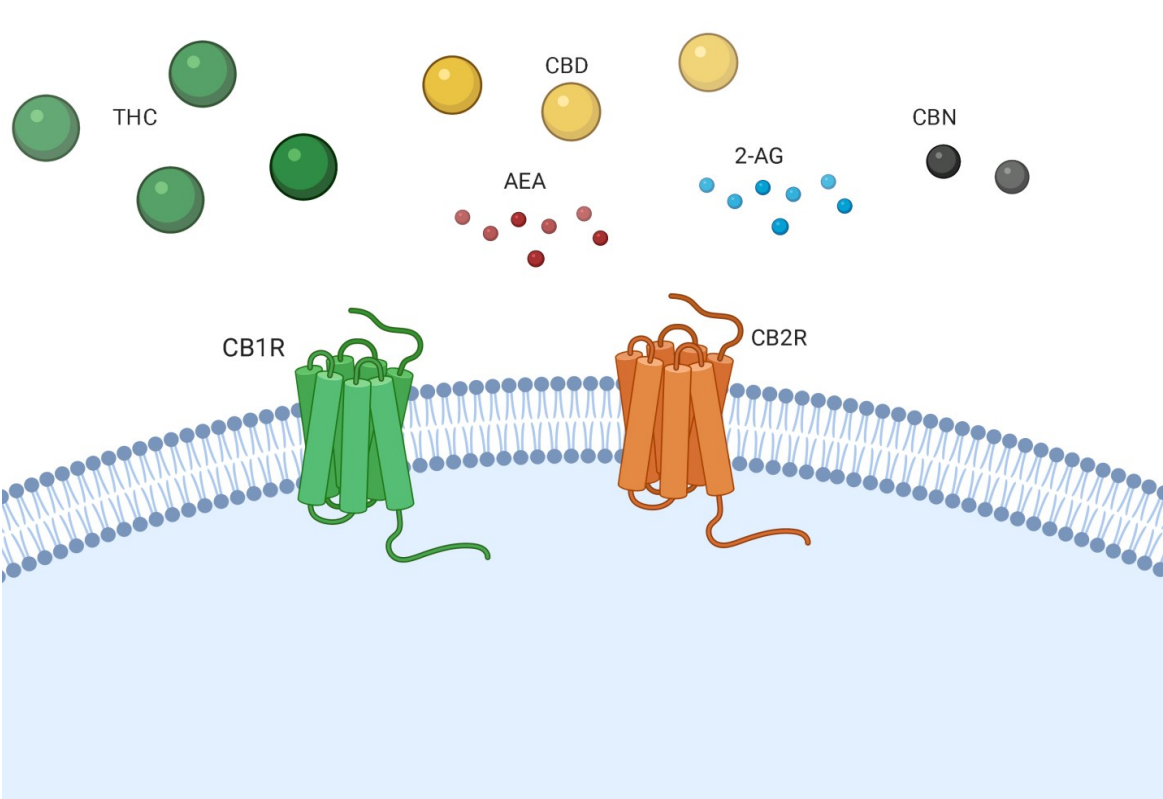


Figure 1.2 Phytocannabinoids and endocannabinoids bind to cannabinoid receptors. Ligand phytocannabinoids and endocannabinoids are depicted in different colors: THC in green circle, CBD in yellow circle, CBN in black circle. Smaller circles represent endocannabinoids: AEA in red circle and 2-AG in blue circle. These cannabinoids work through CB₁R and CB₂R. CB₁R is shown in green color and CB₂R is shown in orange color.

Figure 1. 3 Endocannabinoid system (ECS)

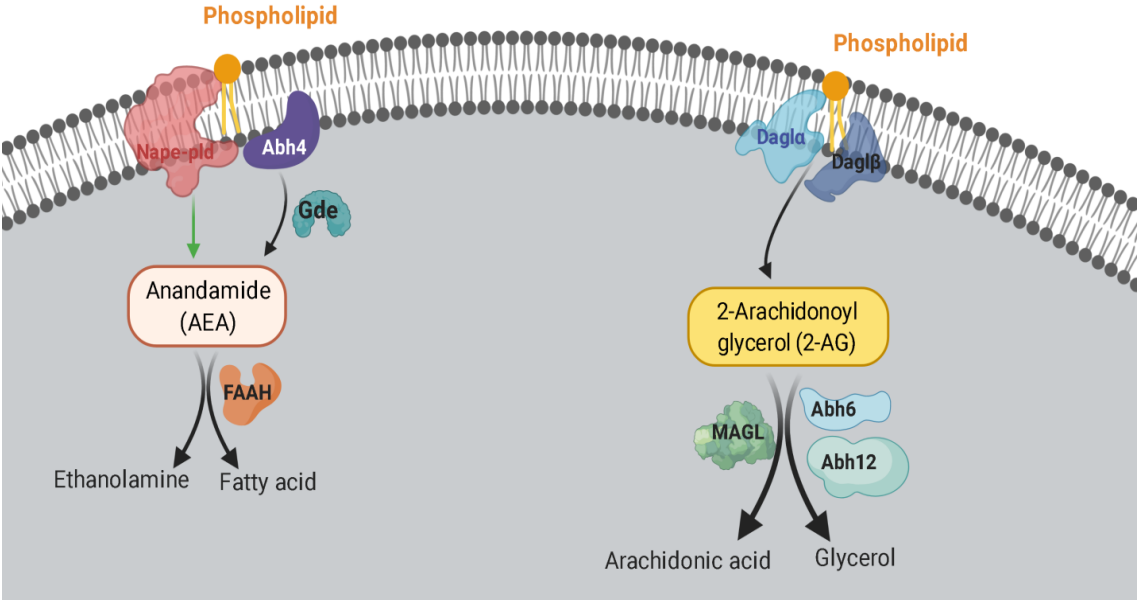
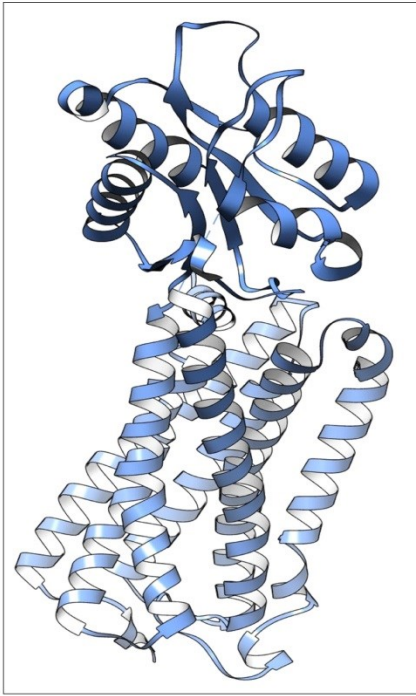


Figure 1.3 Endocannabinoid system (ECS). The routes of synthesis and degradation 2-AG and AEA are distinct and are mediated by multiple pathways. 2-AG is synthesized from phosphatidylinositol bis-phosphate (PIP₂). Sequential hydrolysis of PIP₂ occurs by the actions of phospholipase C beta (PLC β) followed by hydrolysis of diacylglycerol by diacylglycerol lipase (DAGL). Two isoforms of DAGL have been reported: DAGL α and DAGL β . Monoacylglycerol lipase (MGL), ABHD6, and ABHD12 are responsible for the degradation of 2-AG. Additionally, 2-AG can be hydrolyzed by fatty acid amino hydrolase (FAAH) and oxidized by cyclooxygenase-2 (COX-2). AEA is produced from N-arachidonyl phosphatidylethanolamine by N-acyltransferase (NAT) and N-acyl-phosphatidylethanolamine (NAPE)-specific phospholipase D (NAPE-PLD) enzyme. Hydrolysis of NAPE by a NAPE-specific phospholipase D (NAPE-PLD). Dual hydrolysis of NAPE by the phospholipase B and alpha/beta domain hydrolases 4 (ABHD4), followed by hydrolysis by GDE1. AEA is degraded by a single enzyme, FAAH into arachidonic acid (AA) and ethanolamine.

Figure 1. 4 Protein Structure of active form of CB₁R and CB₂R

A)



B)

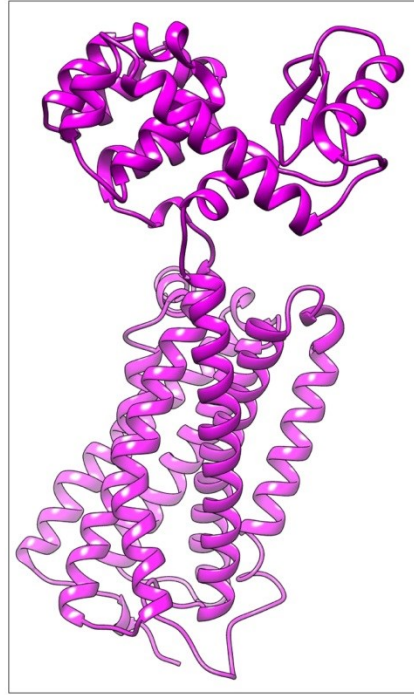
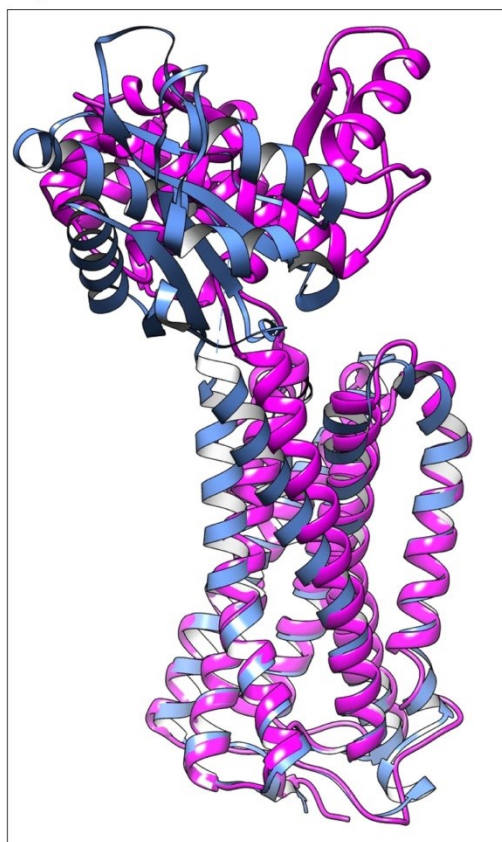


Figure 1.4 Protein Structure of active form of CB₁R and CB₂R. A) Protein structure of active CB₁R (5xra). B) Protein structure of active CB₂R (6kpc).

Figure 1. 5 Superimposition of active and inactive structures of CB₁R (A) and CB₂R (B).

A)



B)

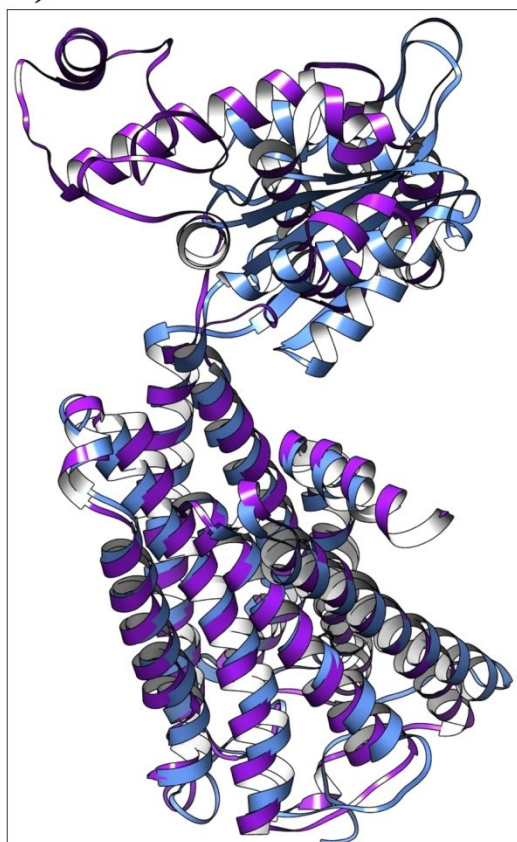


Figure 1.5 Superimposure of active and inactive structures of CB₁R and CB₂R. A) active CB₁R (5xra) in blue and active CB₂R (6kpc) in purple are superimposed. B) A) inactive CB₁R (5tgz) in light blue and inactive CB₂R (5zty) in magenta are superimposed.

Figure 1. 6 Schematic outline of second messenger pathway activation

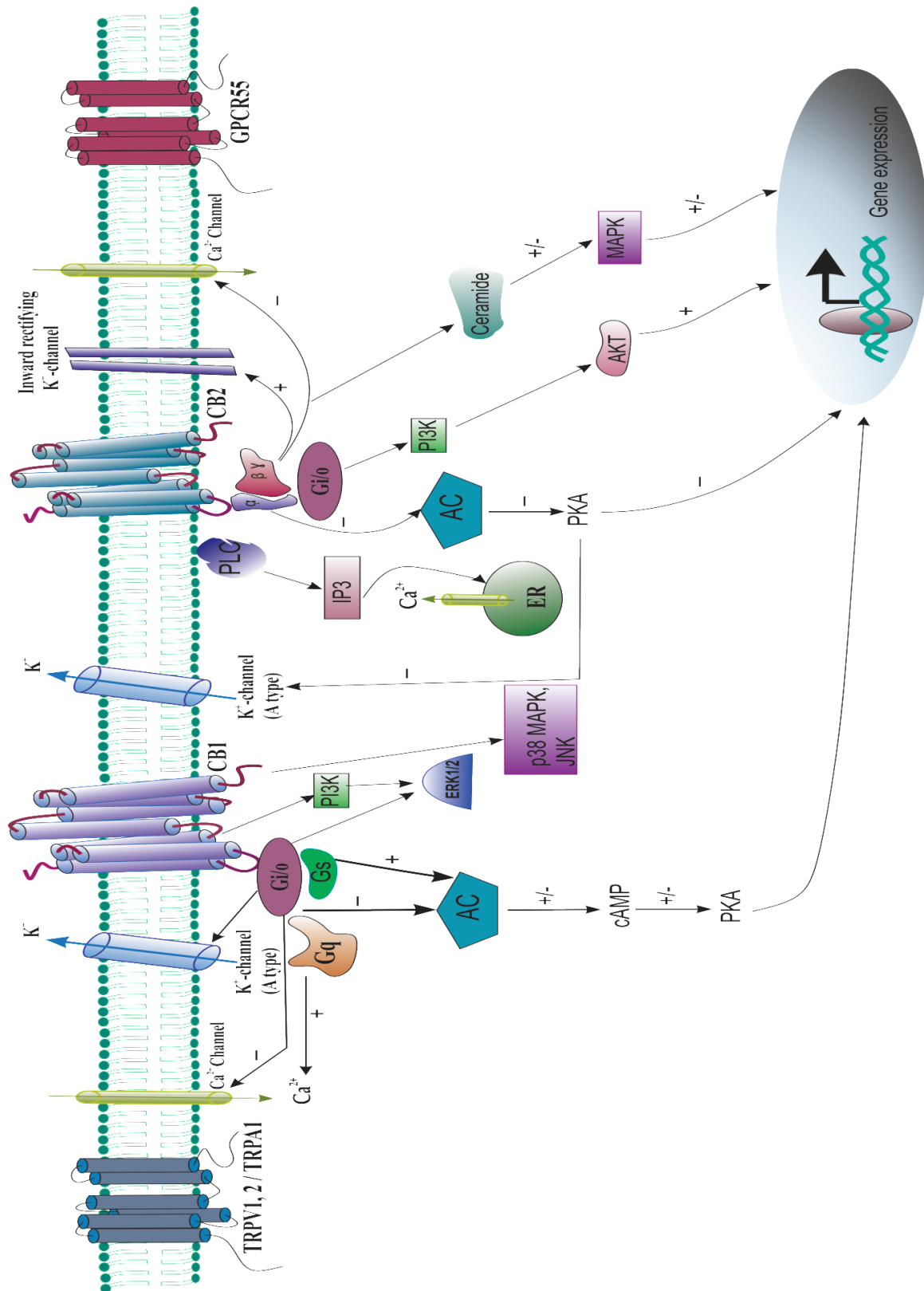
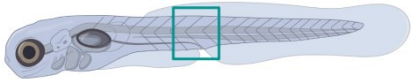


Figure 1.6 Schematic outline of second messenger pathway activation by cannabinoid

receptors. The prototypical G-protein coupled receptors for cannabinoids are CB₁R and CB₂R, but GPCR55 has been suggested to be a possible third cannabinoid receptor. CB₁R and CB₂R are negatively coupled to adenylyl cyclase (AC) via G_{i/o}, while GPCR55 is potentially linked to the G_{q/11}. Cannabinoids are also known to bind to transient receptor potential channels such as TRPV1, TRPV2 and TRPA1. Possible downstream effects include the regulation of genes and ion channel activity (A-type K⁺ channels).

Figure 1. 7 Schematic of primary motor neuron branching in zebrafish.

A)



B)

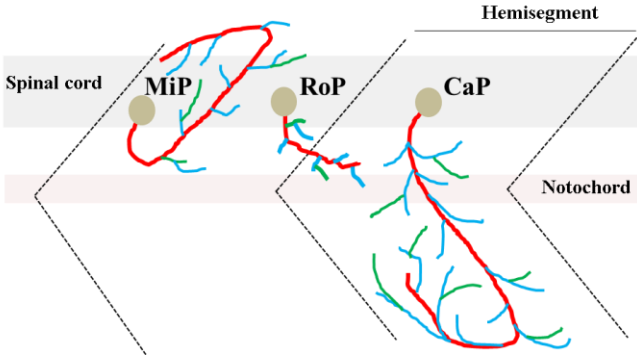


Figure 1.7 Schematic of primary motor neuron branching in zebrafish. A) Schematics of an embryo. B) Each motor neuron has characteristic soma location and axonal branching, based on which they are further divided. Primary MNs are subdivided into Middle Primary MN (MiP), Rostral Primary MN (RoP) and Caudal Primary MN (CaP).

Figure 1. 8 Ultrastructure of muscle organization.

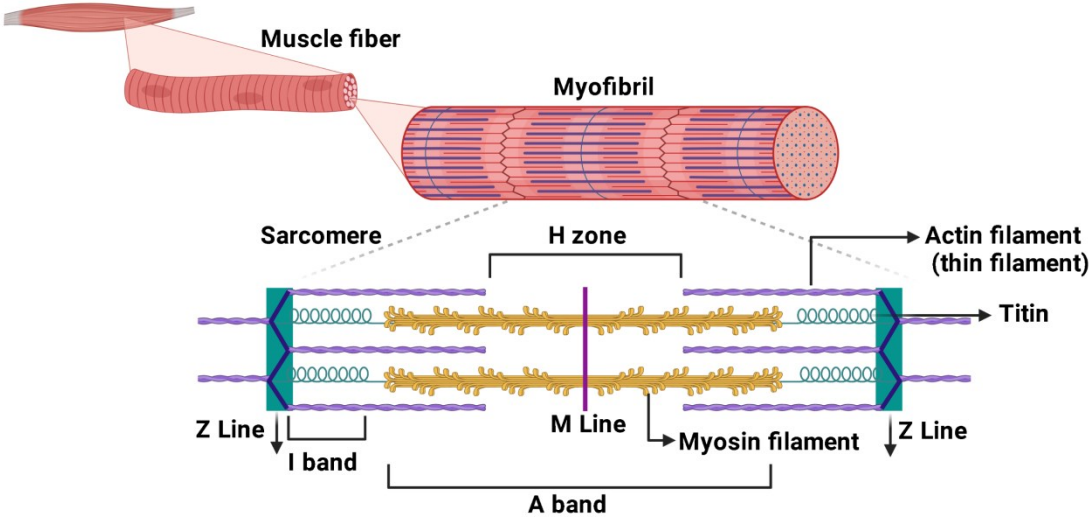


Figure 1.8 Ultrastructure of muscle organization. The schematic outline shows the ultrastructure of sarcomere assembly. Sarcomeres are seen as a series of dark and light bands under microscope, referred as A-band and I-band respectively. They are comprised of thick filaments and thin filaments sequentially organized and bound to Z disk. Principal proteins associated with the myofilament structures are indicated at the bottom. Image created using Biorender.com.

Figure 1. 9 Schematic outline showing activation and inactivation of the Hedgehog pathway.

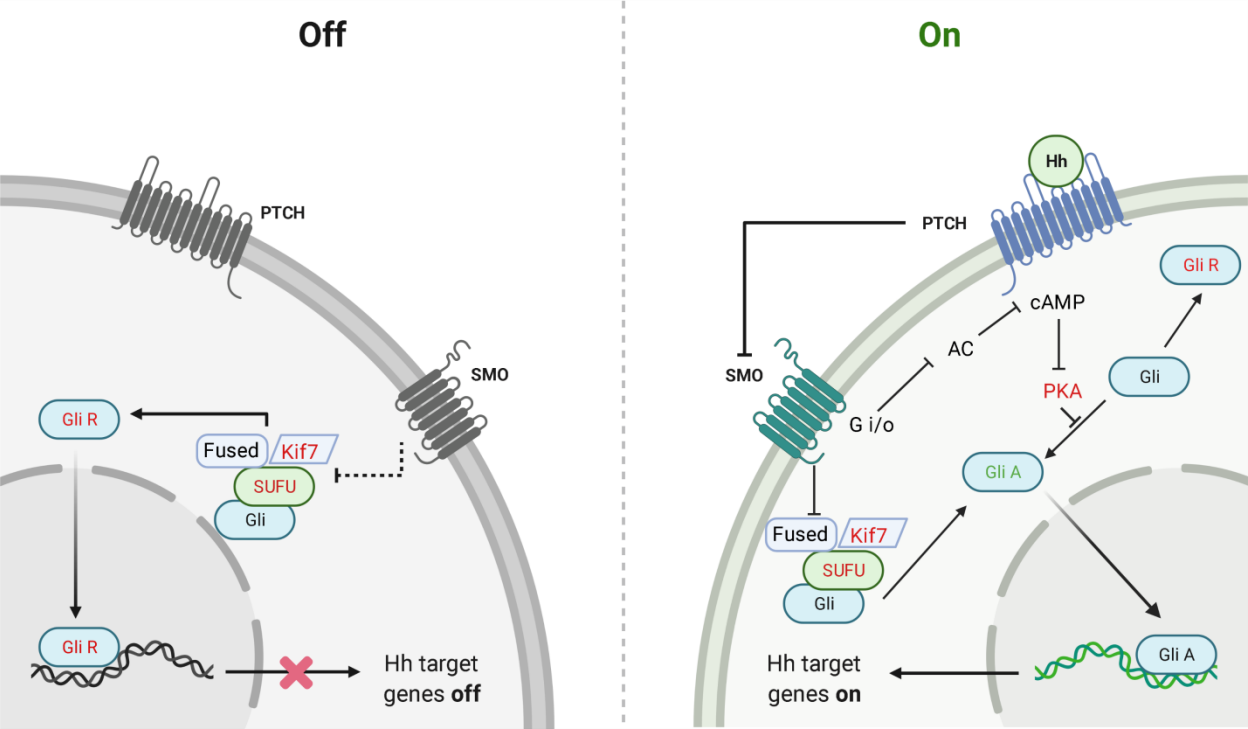


Figure 1.9 Schematic outline showing activation and inactivation of the Hedgehog pathway.

In the absence of the HH ligand, ptch1 inhibits SMO activity that increases AC and PKA activity and which leads to cleavage of Gli into its Gli R state (left). In the presence of HH ligand, HH ligand binds (i.e. cannabinoids) to its receptor ptch1 and releases SMO repression, activating the Shh pathway by activating $G\alpha_i$. As a result, it inhibits adenylate cyclase (AC), limiting the conversion of ATM into cAMP. The inhibition of cAMP ultimately inhibits PKA accumulation, which prevents the post-translational modification of the Gli transcription factor into its repressor form (Gli R). This ultimately facilitates the transcription of genes necessary for an organism's normal development by inhibiting PKA activity. Image created using Biorender.com.

Figure 1. 10 Schematic outline of cannabinoid exposure

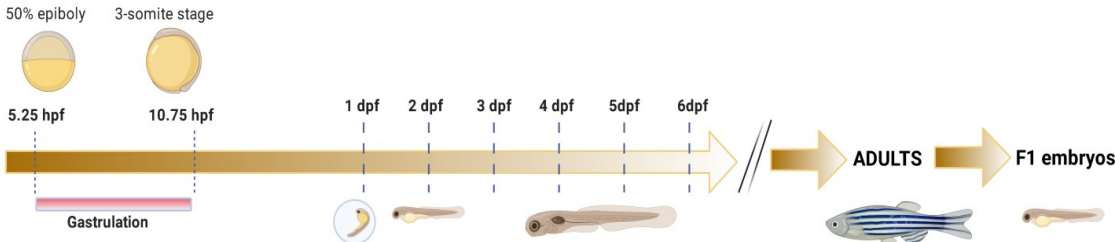


Figure 1.10 Schematic outline of cannabinoid exposure. Cannabinoid exposure was carried out during gastrulation period of zebrafish. Once the gastrulation period is over, at 10.75 hpf, the embryos were washed off with the fresh embryo media and allowed them to grow.

Table 1. 1 Properties of phytocannabinoids and endocannabinoids at CB₁R and CB₂R

Type of ligand	Name	Action
Phytocannabinoids	THC	Partial CB ₁ R and CB ₂ R agonist
	CBD	1. Antagonists of CB ₂ R 2. Negative allosteric modulator of CB ₁ R
	CBN	1. Agonist of CB ₁ R 2. Agonist and antagonist of CB ₂ R
Endocannabinoids	AEA	Partial agonist of CB ₁ R
	2-AG	Agonist of CB ₁ R and CB ₂ R

Table 1. 2 Structure and properties of synthetic agonists at CB₁R and CB₂R

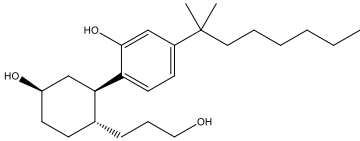
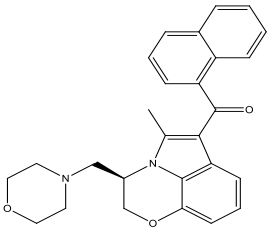
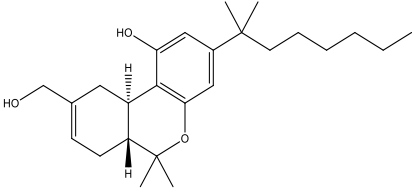
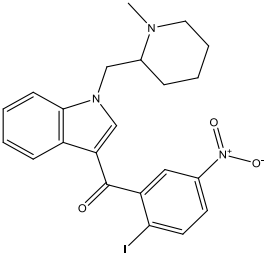
Type of ligand	Name	Action	Structure
Synthetic Agonist	CP55940	Agonist of CB ₁ R and CB ₂ R	
	WIN55212-2	Agonist of CB ₁ R and CB ₂ R	
	HU-210	Agonist of CB ₁ R and CB ₂ R	
	AM-1241	Agonists of CB ₂ R	

Table 1. 3 Structure and properties of synthetic antagonists at CB₁R and CB₂R

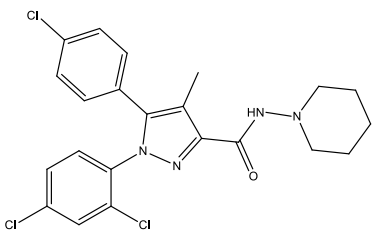
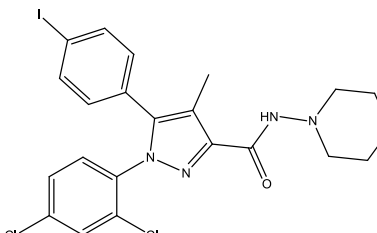
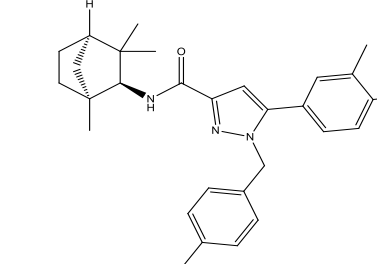
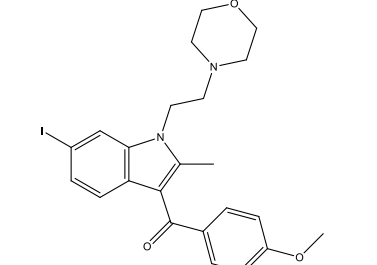
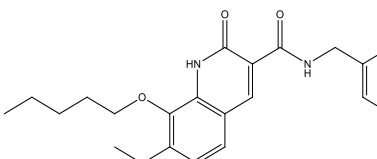
Type of ligand	Name	Action	Structure
Antagonists	SR141716A (Rimonabant)	Inverse agonists of CB ₁ R	
	AM251	Inverse agonists of CB ₁ R	
	SR144528	Inverse agonists of CB ₂ R	
	AM630	Inverse agonists of CB ₂ R	
	JTE907	Inverse agonists of CB ₂ R	

Table 1. 4 *Ki* values for phytocannabinoids and endocannabinoids at CB₁R and CB₂R

Compound name	<i>Ki</i> (at CB₁ receptor)	<i>Ki</i> (at CB₂ receptor)
THC	5-80 nM ^a	3-32 nM ^a
CBD	4350 nM ^a	2860 nM ^a
CBN	120-1130 nM ^a	96-300 nM ^a
AEA	61 nM (mice) ^b	1930 nM ^b
2-AG	472 ± 55 nM ^b	1,400 ± 172 nM ^b

- a. Pertwee RG (2008) The diverse CB₁ and CB₂ receptor pharmacology of three plant cannabinoids: Δ⁹-tetrahydrocannabinol, cannabidiol and Δ⁹-tetrahydrocannabivarin. *British Journal of Pharmacology* 153, 199–215; doi: <https://doi.org/10.1038/sj.bjp.0707442>

- b. Bow EW and Rimoldi JM (2016) The structure–function relationships of classical cannabinoids: CB₁/CB₂ Modulation. *Perspect Medicin Chem.* 2016; 8: 17–39; doi: 10.4137/PMC.S32171

Chapter 2

Materials and methods

2.1 Animal care and exposure to THC, CBD and CBN

The fish used in this study were wild type zebrafish (*Danio rerio*) embryos of the Tubingen Longfin (TL) strain that were maintained at the University of Alberta Aquatic Facility. All animal housing and experimental procedures in this study were approved by the Animal Care and Use Committee at the University of Alberta (AUP #00000816) and adhered to the Canadian Council on Animal Care guidelines for humane animal use. For breeding, 3 to 5 adults, usually consisting of 3 females and 2 males, were placed in breeding tanks the evening before eggs were required. The following morning, fertilized eggs were collected from the breeding tanks, usually within 30 mins of fertilization. Embryos and larvae were housed in incubators on a 12 h light/dark cycle, and set at 28.5 °C. Embryos were exposed to egg water (EW; 60 mg/ml Instant Ocean) containing either THC (2, 4, 6, 8 and 10 mg/L diluted from a stock solution obtained from Sigma; Δ^9 -Tetrahydrocannabinol solution 1.0 mg/ml in methanol) or CBD (1, 2, 3 and 4 mg/L diluted from a stock solution obtained from Sigma; CBD solution 1.0 mg/ml in methanol), or equivalent amounts of methanol during the period of gastrulation, which occurs between 5.25 hpf to 10.75 hpf. The exposure medium was then replaced at 10.75 hpf with 25 mL of fresh EW. Embryos were washed several times in EW and then incubated in fresh EW until further experiments at 48 hpf. For immunohistochemical studies, pigment formation was blocked by adding 0.003% phenylthiourea (PTU) dissolved in egg water at 24 hpf. All protocols were carried out in compliance with guidelines described by the Canadian Council for Animal Care (CCAC) and the University of Alberta.

For Chapter 4, embryos were exposed to egg water (EW; 60 mg/mL Instant Ocean) containing either 6 mg/L THC (diluted from a stock solution obtained from Sigma; Tetrahydrocannabinol solution 1.0 mg/mL in methanol) or equivalent amounts of methanol during the period of gastrulation, which occurs between 5.25 hpf and 10.75 hpf. The exposure medium was then replaced at 10.75 hpf with 25 mL of fresh EW. The dose of THC (6 mg/L) was selected based on my previous work identifying critical concentration that affects survival and embryonic development (Ahmed et al., 2018).

For Chapter 5, embryos were exposed to egg water (EW; 60 mg/ml Instant Ocean) containing CBD (a stock solution obtained from Sigma, CBD solution 1.0 mg/ml in methanol) or equivalent amounts of methanol (vehicle) during the period of gastrulation, which occurs between 5.25 hpf to 10.75 hpf. The exposure medium was then replaced at 10.75 hpf with 25 mL of fresh EW. Embryos were washed several times in EW and then incubated in fresh EW until further experiments at 48, 72, 96 and 120 hpf.

For Chapter 6, embryos were exposed to egg water (EW; 60 mg/ml Instant Ocean) containing CBN (0.01-4 mg/L diluted from a stock solution obtained from Sigma; solution 1.0 mg/ml in methanol) or equivalent amounts of methanol or combination of appropriate drugs during the period of gastrulation, which occurs between 5.25 hpf to 10.75 hpf. The exposure medium was then replaced at 10.75 hpf with 25 mL of fresh EW. Embryos were washed several times in EW and then incubated in fresh EW until further experiments at 48 hpf. Antagonists of CB₁R (AM251 (Seleckchem, cat # S2819), CP945598 (Apexbio, cat #1435; referred as CP94)) and CB₂R (AM630 (Tocris Bioscience, cat #1120), JTE907 (Tocris Bioscience, cat #2479)) were used in some experiments.

For Chapter 7, embryos were exposed to egg water (EW; 60 mg/ml Instant Ocean) containing (-) THC (a stock solution obtained from Sigma, (-) THC solution 1.0 mg/ml in methanol) or equivalent amounts of methanol (vehicle) during the period of gastrulation, which occurs between 5.25 hpf to 10.75 hpf. The exposure medium was then replaced at 10.75 hpf with 25 mL of fresh EW. Embryos were washed several times in EW and then incubated in fresh EW until further experiments at 24, 48 and 120 hpf.

2.2 Embryo imaging and morphological observations

Embryos were imaged at 2 dpf using a Lumenera Infinity2-1R color microscope camera mounted on a Leica stereomicroscope. Embryos were placed in a 16-well plate with one embryo per well and were anesthetized in 0.02% MS222 (Tricaine methanesulfonate, sigma-Aldrich, cat # E10521) Morphological observations were performed using a dissecting microscope; embryos were placed in a 16-well plate with one embryo per well and anesthetized in 0.02% MS222. Measurements of embryo length were done using a microscope eyepiece equipped with a micrometer.

The number of fish still alive and the number of fish that had hatched out of the chorion were recorded on each day until 5 dpf. Gross deformities were observed at 2 dpf where body length of the fish, the number of larvae exhibiting pericardial edema and axial malformations was counted for each treatment.

2.3 Immunohistochemistry

Znp-1 and Zn-8 staining

Embryos (2 dpf) were fixed in 2% paraformaldehyde for 1–2 h and washed with 0.1 M phosphate buffered saline (PBS) every 15 min for 2 h. The preparations were then permeabilized for 30 min in 4% Triton-X 100 containing 2% BSA and 10% goat serum. Tissues were incubated for 48 h at 4 °C in either mouse monoclonal anti-znp-1 (Developmental Studies Hybridoma Bank, DSHB) which targets an isoform of synaptotagmin 2 that is highly localized in zebrafish primary motor axons (Fox & Sanes, 2007; Trevarrow et al., 1990), or mouse monoclonal anti-zn-8 (DSHB) (Trevarrow et al., 1990), which targets the DM-GRASP protein on the surface of secondary motor axons (Fashena & Westerfield, 1999; Sylvain et al., 2010). All primary antibodies were diluted at 1:250 in PBS. Tissues were washed in PBS twice every 15 min for 2–3 h and then incubated for 4 hours at room temperature in the secondary antibody, Alexa Fluor® 488 goat anti-mouse IgG, (Molecular Probes, Life Technologies), at a dilution of 1:1000. The embryos were then washed for 7 h with PBS and mounted in MOWIOL mounting media. All embryos were imaged on a Zeiss LSM confocal microscope and photographed under a 40 × objective. Images were compiled using Zeiss LSM Image Browser software and are shown as maximum intensity z-stack compilations. In Chapter 3, for primary motor axon branches, 9 square boxes (Fig. 3.7 A; each about 1500 μm² area) were evenly placed over the trunk (3 in dorsal, 3 in middle and 3 in lateral regions) and the number of branches per square box were counted and averaged for each fish. In other Chapters (Chapter 5, 6 and 7), image J plugins neurite tracer was used to trace all the branching of primary motor (in one hemi segment) and the number of branches were counted and averaged.

3A10, RMO44, F59 and F310 staining

In Chapter 4, tissues were incubated for 48 h at 4 °C in either mouse monoclonal anti-3A10 (Developmental Studies Hybridoma Bank (DSHB), Iowa City, IA, USA) (1:250) which targets neurofilaments associated with M-cell (Hatta, 1992) or anti-RMO44 (Thermo Fisher Scientific, Waltham, MA, USA) (1:250) which labels several types of reticulospinal neurons. Tissues were also incubated in anti-F59 (DSHB, 1:50) which targets myosin heavy chain isoform of red muscle fibers (Miller et al., 1985) or anti-F310 (DSHB, 1:100) that targets myosin light chain of white muscle fibers (Kok et al., 2007). Tissues were washed in PBS twice every 15 min for 2–3 h and then incubated for 4 h at room temperature in the secondary antibody, Alexa Fluor®488 goat anti-mouse IgG or Alexa Fluor®555 goat anti-mouse IgG, (Molecular Probes, Thermo Fisher Scientific), at a dilution of 1:1000. The embryos were then washed for 7 h with PBS and mounted in MOWIOL mounting media. Images were compiled using Zeiss LSM Image Browser software and are shown as maximum intensity z-stack compilations.

α -bungarotoxin staining

For the labelling of nicotinic acetylcholine receptors (nAChRs), embryos at 2 dpf were permeabilized as previously stated and incubated with 100 nM Alexa-488 conjugated α -bungarotoxin (Molecular Probes, Thermo Fisher Scientific) for 4 h at room temperature. Embryos were then washed for 7 h with PBS and mounted in MOWIOL mounting media. All embryos were imaged on a Zeiss LSM 710 confocal microscope (CA, USA) and photographed

under a 40x objective. Images were compiled using Zeiss LSM Image Browser software and are shown as maximum intensity z-stack compilations. To quantify the number and size of the α -bungarotoxin puncta Image J (ImageJ 1.51r, National Institutes of Health, Bethesda, MD, USA) was used.

2.4 Electrophysiology

Whole-cell patch clamp recordings were taken from muscle cells of embryos at 2 dpf. Patch-clamp electrodes were pulled from borosilicate glass (GC150T; World Precision Instruments, Sarasota, FL, USA) on a P-97 pipette puller (Sutter Instrument Co., Novato, CA, USA) and fire-polished (Micro-Forge MF-830; Narishige, Japan); once filled with intracellular solution (ICS), these tips had series resistances of 2–4 M Ω . ICS consisted of (mM): 130 CsCl, 8 NaCl, 10 Hepes, 10 EGTA, 2 CaCl \cdot 2H $_2$ O, 4Mg-ATP, 0.4 Li-GTP; the pH was adjusted to 7.4 and osmolarity was adjusted to 290 \pm 2 mOsmol L $^{-1}$. An extracellular solution (ECS), which consisted of (mM): 134 NaCl, 2.9 KCl, 1.2 MgCl $_2$, 10 Hepes and 10 glucose, with an osmolarity of 280 \pm 2 mOsmol L $^{-1}$, adjusted to pH 7.8, was bubbled with air and continuously washed over the preparation, starting \geq 5 minutes prior to recording. The ECS contained the voltage-gated Na $^+$ channel blocker tetrodotoxin (TTX; Tocris, UK) at a concentration of 1 μ M in order to block action potentials during mEPC recordings. White muscle fibers were easily and accurately identified based on their orientation within each segment using Nomarski Differential Interference Contrast (DIC) optics, and whole cell voltage-clamp recordings were taken over periods of 1 minute. Whole cell currents were recorded at a holding potential of -60 mV using an Axopatch 200B amplifier (Axon Instruments, Sunnyvale, CA, USA), low-pass filtered at 5 kHz

and digitized at 50 kHz. Once in the whole-cell recording mode, the fibers had series resistances from 3–6 M Ω . Synaptic currents were recorded in 1-minute epochs. After each 1-minute recording the series resistance was checked and if it had changed by more than 20%, the recording was aborted. Recordings were maintained as long as the membrane resistance remained greater than 10 \times the series resistance. Series resistances were compensated by 70% using the amplifier's compensation circuitry.

2.4.1 Analysis of mEPCs

Miniature endplate currents (mEPCs) were monitored using a Macintosh iMac computer running AxoGraph X v1.1.1 software (Axon Instruments). Recordings were examined by the software, and synaptic events were detected using a template function. Overlapping or misshapen events were removed, and the remaining events were averaged and the properties (amplitudes, decay time constants, frequencies) of the averaged trace were recorded. Events with slow rise times and low amplitudes originate from neighbouring, coupled cells and were excluded from the analysis, therefore, only fast rise time events were included in my analysis since these events originated from the cells we were patch clamping rather than from nearby, electrically-coupled muscles (Luna & Brehm, 2006). Single decay time constants were fit over the initial (fast) decay portion and over the distal (slow) portion of the decay. For each n , currents were recorded from a single white muscle fiber from a single embryo.

2.5 Locomotion in embryos and larva

2.5.1 Locomotory response to sound and touch

To image the zebrafish escape response, I used a high speed AOS video camera (AOS S-PRI 1995; 1250 FPS; shutter speed: 800 μ s) mounted on a dissecting microscope (Roy et al., 2015). For the sound stimulus, six larvae, aged 5 dpf, were placed in 35 mm \times 10 mm petri dishes with embryo media and were allowed to acclimate to their environment for 30 minutes prior to sound stimulus application. The sound stimulus was a sawtooth waveform (500 Hz, intensity was 85–95 dB), created using audacity software (version 2.2.1). A computer speaker was positioned next to the petri dishes to deliver auditory/vibrational (AV) stimulation to embryos. Escape responses were recorded immediately prior to delivering the stimulus and then for about 1000 ms following the stimulus. This period of time was long enough to film the escape response and periods of swimming following the C-bend. The locomotion to an auditory pulse was scored as an escape response when the animal began the characteristic C-bend after the stimulus. For the touch response, 10 larvae were placed in a 35 mm \times 10 mm petri dish and were allowed to acclimate to their environment prior to application of the mechanical stimulus. The mechanical stimulus consisted of a light touch to the head with a pair of forceps. C-starts were captured with the AOS high speed video camera.

2.5.2 Spontaneous coiling activity (Locomotion at 1 dpf)

Quantifications of spontaneous coiling activity were performed using DanioScope (Noldus) software to analyze video recordings of 1 dpf embryos that were still encased within their chorion. Video recordings of 1 dpf embryos were taken under a dissecting microscope. The

spontaneous coiling activity (%) of 1 dpf embryos was measured to represent the proportion of time that embryos were actively moving, while the burst count/minute represented the mean number of contractile movements performed by embryos averaged per minute.

2.5.3 Escape Response in 2 dpf Embryos

Escape responses of 2 dpf embryos were tested and recorded as previously described (Shan et al., 2015). Briefly, 2 dpf embryos were immobilized in 2% low-melting point agarose (LMPA; Sigma-Aldrich; St. Louis, MO, USA) dissolved in embryo medium. LMPA was cut away from the embryo's trunk and tails allowing them to move, while the heads remained embedded in the gel. Embryo media was added to the petri dish to ensure that the embryos remained immersed in solution. Borosilicate glass micropipettes were pulled, filled with solution and then positioned close to embryo's otolith without touching the embryo. Embryos were stimulated using a 15 ms pulse of phenol red (Sigma-Aldrich) dissolved in embryo media ejected from a Picospritzer II (General Valve Corporation, Cambridge, MA, USA). Embryonic responses were recorded for about 900 ms following the stimulus using an AOS video camera (AOS S-PRI 1995; 1250 FPS; shutter speed: 800 μ s) mounted on a dissecting microscope. The video-recordings were analyzed using a Motion Analysis Software, ProAnalyst[®] (Xcitex Inc., Cambridge, MA, USA).

2.5.4 Escape response to touch using EthoVision (Locomotion at 2 dpf)

Individual 2 dpf larvae were gently placed into the center of a petri dish (14 cm in diameter) containing 200 mL of egg water, pH 7.0. A fishing line was used to touch the head of the larvae to trigger an escape response. The petri dish was placed on top of an infrared backlight source and a Basler GenlCaM (Basler acA 1300-60) scanning camera with a 75 mm f2.8 C-mount lens, provided by Noldus (Wageningen, Netherlands) was used for individual larval movement tracking. EthoVision® XT-11.5 software (Noldus) was used to quantify the swimming distance (cm) and swimming velocity (cm/s).

2.5.5 Free Swimming (Locomotion at 3-6 dpf)

To track behavioral activities, such as velocity, swim bouts and activity, larvae at 3-6 dpf were placed in a 96-well plate. Larvae were placed gently into the center of wells containing 150 µl egg water, pH 7.0 and 48 wells were used each time from a 96-well plate in my study (Costar #3599). Prior to video recording, larvae were acclimated in the well plate for 60 minutes. Plates were placed on top of an infrared backlight source and a Basler GenlCaM (Basler acA 1300-60) scanning camera with a 75 mm f2.8 C-mount lens, provided by Noldus (Wageningen, Netherlands) was used for individual larval movement tracking.

EthoVision® XT-11.5 software (Noldus) was used to quantify activity (%), velocity (mm/s), swim bouts frequency and cumulative duration of swim bouts for one hour. To exclude background noise, displacement ≥ 0.2 mm was defined as active movement. Activity was defined as % pixel change within a corresponding well between samples (motion was captured by taking 25 samples/frames per second) as reported before (Leighton et al., 2018). The absolute values of mean activity may appear small due to pixel percentage in my region of interest (a well) that are

changing at any time is small and bursts of activity may occur such that total movement is short within any given minute.

2.6 Behavioral experiments in adults

2.6.1 Open field (OF) test

The open field test is a common behavioral test in research to assess anxiety-like behavior and locomotion in zebrafish (Hamilton et al., 2021; A. Stewart et al., 2012). Open field tests took place in a white circular plastic arena with a diameter of 34 cm and a height of 16 cm. For each trial, the arena was filled to a height of 6 cm with fresh habitat water that was changed after every third trial. Behavior of individual fish in the open field test was evaluated for a 10-min trial in the test arena used for shoaling testing. Individual fish were placed in the center of the arena. The distance moved (cm) and time spent in the center zone, the thigmotaxis zone, and the transition zone (between the center and thigmotaxis zone) of the arena were calculated using the EthoVision system. The zones were created within EthoVision XT (v. 11, Noldus, VT, USA) motion tracking software and include a ‘center’ zone that has a diameter of 8.5 cm, a thigmotaxis zone which spanned 8.5 cm from the walls of the arena, and a ‘transition’ zone in between the two zones. A greater amount of time spent in the center zone indicates decreased anxiety-like behavior.

2.6.2 Novel object approach (NOA) test

The novel object approach test is another test to quantify anxiety of the embryo (Dean et al., 2020; Hamilton et al., 2017; A. Stewart et al., 2012). This test involves placing a 4.25 cm tall LEGO® figurine into the center of the open field testing arena and measuring by the tendency of the fish to approach and spend time near the novel object (Hamilton et al., 2017a; Johnson and Hamilton, 2017; Krook et al., 2019). The object was multicolored to avoid any innate color preference of the fish. Each 10-min trial began immediately after the object was placed in the arena. Distance moved (cm) and time spent in the center zone of the arena, the thigmotaxis zone, and the transition zone were calculated using the EthoVision system. Arena water was replaced following every 4th trial.

2.6.3 Shoaling test

For each shoaling test, five fish ($n = 1$ shoal) were netted from the original tank and placed in the center of the behavioral arena. This circular arena was formed from non-toxic plastic and had a diameter of 34 cm and a depth of 15 cm. The arena, which was surrounded by white corrugated plastic to reduce visual stimuli, was filled to a depth of 6 cm with habitat water maintained between 26 and 28 °C. Water in the arena was replaced following every 4th 30-min trial to ensure that the water in the arena was truly fresh and animal is not under stress. Shoaling behavior of 5 fishes in the arena was recorded for 10 min using video camera mounted 1.0 m over the arena. From these videos, EthoVision XT software (v. 10, Noldus, Leesburg, VA, USA) was used to quantify inter-individual distance (IID) and distance moved for each shoal in each

condition. Quantification of time that the fish spend in various zones of the arena can also be used as a proxy for anxiety-like behavior, with increased time near the walls indicative of increased anxiety (Stewart et al., 2012). We quantified the average time each fish in the shoal spent in the center zone of the arena and in the thigmotaxis zone.

2.7 Transmission Electron Microscopy (TEM)

The embryos (5 dpf) were fixed overnight in 2.5% glutaraldehyde, 4% formaldehyde and 5 mM CaCl₂ in 0.1 M cacodylate buffer (pH 7.2). They were then post-fixed for 90 min in 1% OsO₄ in 0.1 M cacodylate buffer containing 5 mM CaCl₂ and 0.8% potassium ferricyanide. Embryos were then dehydrated in acetone and embedded in Epon. Ultra-thin sections were cut and stained with uranyl acetate and lead citrate. Later, samples were analyzed using a JEOL 1210 transmission electron microscope (Jeol; Tokyo, Japan).

2.8 Scanning Electron Microscopy (SEM)

At 5 dpf, embryos were collected into fixative: 2.5% glutaraldehyde, 2% paraformaldehyde in 0.1 M phosphate buffer fixative, pH 7.4. The embryos were then washed in buffer and dehydrated through a graded series of ethanol. After the ethanol series the embryos went through a series of ethanol:Hexamethyldisilazane (HMDS) mixtures, ending with pure HMDS. From HMDS, the embryos were air dried overnight. Embryos were mounted on SEM

stubs and sputter-coated with gold-palladium. The samples were examined in a Zeiss EVO 10 scanning electron microscope using acceleration voltage of 15 kV.

2.9 RT-qPCR

In Chapter 4, to analyze the expression of different nAChR subunits, mRNA was extracted from whole embryos (n = 30–50 embryos, N = 5 batches) using a Trizol reagent according to manufacturer protocol. The concentration and purity of the RNA was determined by NanoDrop spectrophotometry (Thermo Fisher Scientific). A Maxima First Strand cDNA Synthesis kit (Thermo Fisher Scientific) was used to synthesize cDNA from 1 µg of the mRNA stocks according to the manufacturer's protocol. cDNA was diluted to 1:40 in 1x TE buffer for RT-qPCR reaction. TaqMan gene expression assays (Thermo Fisher Scientific) for zebrafish *chrn1*, *chrng* and *chrne* that were previously validated (Ahmed & Ali, 2016) were used for RT-qPCR reaction. RT-qPCR was carried out with the 7500 Fast system (Applied Biosystems). For each reaction (10 µL), 5 µL of 2x TaqMan Gene Expression Master mix, 0.5 µL of 20x TaqMan Gene Expression Assay, and 2.5 µL of Nuclease-free water was added to 2 µL of cDNA diluted to 1:40. The thermal profile included a holding step of 50 °C for 2 min followed by another holding step of 95 °C for 10 min, and 40 cycles including denature at 95 °C for 5 s and anneal/extend at 60 °C for 1 min. All samples were run in triplicate and the threshold cycle (Ct) was determined automatically by SDS software (Applied Biosystems). Outliers possibly originating from inaccurate pipetting were omitted and Ct values were averaged. Housekeeping gene Beta-actin (*actb1*) was used as internal control for my calculation. Comparative Ct Method

(ddCt) was used for data representation using vehicle control as calibrator. No template controls (NTC) were included for each assay in every plate as negative control.

In Chapter 5, RNA was prepared from the vehicle and cannabinoid treated embryos (n = 30–50 embryos, N = 5 batches) using TRIzol reagent (Invitrogen) by homogenization. cDNAs were synthesized from 1 µg of purified RNA using Maxima cDNA kit (Thermo Fisher Scientific) and used as templates. cDNA was diluted to 1:40 in 1x TE buffer for RT-qPCR reaction. qPCR was performed using SYBR Green PCR master mix and the 7500 Fast system (Applied Biosystems). The housekeeping gene Beta-actin (*actb1*) was used as an internal control for my calculation. The Comparative Ct Method (ddCt) was used for data representation using vehicle control as calibrator. A list of Primers (used in the RT-qPCR) is presented in table 5.1.

2.10 RNAseq library preparation and data analysis

RNA was extracted from the vehicle- and THC-treated embryos (5dpf) using TRIzol reagent (Ambion) according to the manufacturer's manual. I checked the concentration (ng/µL) and purity (260/230 ratio) of the extracted RNA using an absorption spectrometer; ensured that the 260/230 value is ~ 2.0 before proceeding with RNASeq. The concentration and RNA Integrity Number (RIN) for RNA samples was confirmed using Bioanalyzer 2100 system (Agilent Technologies). One microgram of total RNA was used for construction of the Illumina libraries (Illumina, San Diego, California). The mRNA was enriched using oligo-dT magnetic beads and fragmented to 100–300 bp. Later, cDNA was synthesized and performed 3' adenylation, multiplex compatible adapter ligation (containing indexes), and RT-qPCR

amplification. RNAseq was run as paired-end at 75 bp read length using Illumina Nextseq platform and biological replicates were used. Data obtained by Illumina sequencing was further analyzed using Illumina basespace. A reference genome file is prepared using Dragen reference builder application for my analysis where I provided the latest reference zebrafish genome obtained from Ensemble database (Ensemble, GCRz11). Later, RNA sequencing file was aligned with the reference genome to get annotation-assisted alignment for each sample. Finally, I performed quantification of differential expression of RNA transcripts (between two samples) using Dragen RNA differential expression application (v3.6.3). To visualize the data R software package (R4.1.0) was used.

2.11 Statistics

In this thesis, all values are reported as means \pm SEM (standard error of the mean). In all instances, tests for normality/homoscedasticity were first done using the D'Agostino-Pearson normality test; appropriate parametric or non-parametric tests were performed accordingly. Comparisons between two samples were achieved by t-tests or Mann-Whitney U tests. Multiple sample comparisons were achieved using ANOVA followed by either Dunnett (comparisons between treatment with controls only) or Turkey (multiple pair-wise comparisons between all groups), or with Kriskle-Wallis multiple comparison (using the statistical software built in to GraphPad prism) ($p < 0.05$).

Chapter 3

Motor neuron development in zebrafish is altered by brief (5.5-h) exposure to THC (tetrahydrocannabinol) or CBD (cannabidiol) during gastrulation

In this study, I set out to determine if exposure to THC and CBD during zebrafish development has an effect on cells involved in locomotion. Importantly, I focused my exposure parameters during a period of development known as gastrulation. Here, I specifically wanted to determine if a brief pulse of cannabinoids during a key developmental period would alter embryonic development. My results indicate that heart rate, gross morphology, neuronal branching, synaptic activity and locomotor responses such as the C-start escape response are adversely affected by exposure to THC or CBD.

3.1 Results

3.1.1 Gross Morphology

My goal in this study was to determine if brief exposure to the primary psychoactive and non-psychoactive ingredients in marijuana (THC and CBD, respectively) during gastrulation, had adverse effects on embryonic development, specifically focusing on aspects of locomotion. I exposed zebrafish embryos to various concentrations of THC (2, 4, 6, 8 and 10 mg/L), CBD (1, 2, 3 and 4 mg/L) and their vehicle controls (0.1–1% methanol) (Fig. 3.1 A), and examined a range of anatomical features as well as hatching, survival and heart rate. I also examined untreated embryos as additional controls for all treatments (THC, CBD and methanol). The dose-dependent effects on morphology and body length are shown in Fig. 3.1 B, C. Consistent with a

previous study, I found that vehicle controls (0.1–1% methanol) had no adverse morphological effects (Maes et al., 2012) (Figs 3.2 A and 3.3 A). Embryos exposed to increasing concentrations of THC and CBD developed with curved tails, cardiac edema and deformities such as blebbing at the tip of the tail. Additionally, there was a dose-dependent reduction in body length of 2 dpf embryos (Fig. 3.1 D, E). For instance, the mean body length of embryos exposed to 6 mg/L THC was 2.88 ± 0.04 mm ($n = 61$) compared with vehicle controls of 3.27 ± 0.03 mm ($n = 22$; $p < 0.001$). (Fig. 3.1 D). Similarly, the mean body length of embryos exposed to 3 mg/L CBD was 2.14 ± 0.07 mm ($n = 25$) compared with 3.19 ± 0.02 mm in vehicle controls ($n = 32$; $p < 0.001$) (Fig. 3.1 E).

To assess survival, I documented mortality rates in the first 5 days of development. Vehicle controls showed no difference in survival from untreated animals (Figs 3.2 B and 3.3 B). Embryos exposed to 2–8 mg/L THC experienced similar survival rates for the first 3 days of development (Fig. 3.4 A). By day 5, embryos treated with 8 mg/L THC had a survival rate of only 31 ± 10 % ($p < 0.05$; $n = 4$ experiments), while embryos treated with 10 mg/L THC only had a 5 ± 5 % survival rate (Fig. 3.4 A; $p < 0.05$; $n = 4$ experiments). The effects of CBD on survival were more severe. For instance, by day 1 there was only about 47 ± 8 % survival in the 4 mg/L-treated group ($p < 0.01$; $n = 5$ experiments) and 54 ± 3 % survival in the 3 mg/L-treated group (Fig. 3.4 C; $p < 0.01$; $n = 5$ experiments). By 5 days post fertilization, survival rates were 65 ± 11 %, 56 ± 14 %, 20 ± 6 % and 5 ± 2 % in the 1–4 mg/L CBD-treated groups respectively (Fig. 3.4 C; $p < 0.01$; $n = 5$ experiments), compared with ~ 80 % survival in untreated and vehicle controls (Fig. 3.4 C).

Rates of hatching were also negatively impacted by exposure to THC and CBD. In most cases, 100 % of untreated animals and vehicle controls hatched by 3 dpf (Fig. 3.4 B, D, and

Figs 3.2 C and 3.3 C), whereas only about 75 % of THC-treated animals (regardless of THC concentration) (Fig. 3.4 B) and 50–90 % of CBD-treated animals (87 ± 1 % for 1 mg/L, 58 ± 3 % for 2 mg/L and 63 ± 11 % for 3 mg/L) (Fig. 3.4 D) had hatched. Embryos treated with 4 mg/L CBD did not hatch at any age and died by 5 dpf (Fig. 3.4 C and D).

Exposure to THC during gastrulation altered the basal heart rate of 2 dpf embryos compared with vehicle controls (Fig. 3.5 A). Exposure to 2 mg/L THC had no significant effect on heart rate, but embryos treated with 4 mg/L THC exhibited heart rates that were lower than controls (Fig. 3.5 A), while exposure to 6, 8 and 10 mg/L THC significantly reduced heart rates by up to 50 % (Fig. 3.5 A; $p < 0.001$; $n = 21$ – 22). The heart rate of untreated embryos was 99 ± 1 ($n = 26$) beats per minute. Embryos treated with 2 mg/L THC exhibited a heart rate of 93 ± 2 ($n = 26$) beats per minute, while embryos treated with 4, 6, 8 and 10 mg/L THC had heart rates of 83 ± 1 ($n = 22$), 61 ± 4 ($n = 22$), 72 ± 1 ($n = 21$) and 59 ± 4 ($n = 21$), respectively (Fig. 3.5 A). Embryos treated with CBD also exhibited a dose-dependent decrease in heart rate. For instance, embryos treated with 1, 2, 3 and 4 mg/L CBD had heart rates of 61 ± 3 ($n = 42$), 36 ± 2 ($n = 40$), 29 ± 2 ($n = 25$) and 25 ± 2 ($n = 20$) beats per minute, respectively, compared with controls that ranged from 97 ± 11 to 103 ± 12 beats per minute (Fig. 3.5 B; $p < 0.001$). These data indicate that a 5-h exposure to THC and CBD during gastrulation significantly lowers the heart rate of newly hatched zebrafish embryos. For the remainder of the study I treated embryos with single concentrations of THC and CBD (6 mg/L THC and 3 mg/L CBD) because these concentrations were in the 30–80% range for hatching and survival of 2 dpf embryos.

3.1.2 Electrophysiology

One of my goals was to determine if exposure to THC and CBD during gastrulation altered the activity of locomotor systems, specifically focusing on the NMJ. Therefore, I asked whether synaptic activity at the NMJ was affected by exposure to cannabinoids. To investigate this, I recorded miniature endplate currents (mEPCs) from the white fibers associated with trunk musculature. Embryonic zebrafish have two types of muscle fibers, tonic red fibers and twitch white fibers that are easily identifiable under the microscope. I particularly focused on white fibers as mammalian skeletal musculature is mostly comprised of twitch fiber types. In zebrafish, white fibers make up the bulk of the trunk musculature and are innervated by both primary and secondary motor neurons (Westerfield et al., 1986). I only analyzed the fast rise time mEPCs in my recordings since these events occurred on the cells I was recording from rather than from neighboring, electrically-coupled cells. The frequency of the fast rise time mEPCs recorded from vehicle controls was 0.1 ± 0.01 Hz ($n = 9$), whereas in the THC (6 mg/L)-treated embryos the mEPC frequency was reduced by almost 50% to a value of 0.04 ± 0.006 Hz ($n = 8$) ($p < 0.01$; Fig. 3.6 A,C), and in the CBD-treated animals, it was 0.02 ± 0.01 Hz ($n = 9$) compared with vehicle controls (0.13 ± 0.02 , $n = 10$) ($p < 0.001$). In fact, in some preparations I recorded only 2–4 mEPCs over a 4-min time period. There was no change in mEPC amplitude compared with vehicle controls ($p > 0.05$; data not shown).

I had previously found that the decay time course of mEPCs recorded from white fibers of 2 dpf embryos was bi-exponential in nature due to the presence of multiple classes of nAChRs (Ahmed & Ali, 2016; Mongeon et al., 2011). Because changes in the kinetics often signify a change in the subunit composition of synaptic receptors, I examined the exponential decay of mEPCs but found that there was no significant difference amongst any of the treatments (Fig. 3.6

B). These data imply that the nAChR subtypes that are normally expressed at zebrafish NMJs are not altered by exposure to THC or CBD.

3.1.3 Motor neuron immunolabelling

My electrophysiological data suggested that activity at zebrafish NMJs was affected by exposure to THC and CBD. A reduction in mEPC frequency usually indicates a change in presynaptic properties, therefore I asked whether the morphology of primary and secondary motor neurons was altered by THC or CBD treatment. To determine motor neuron innervation patterns, I immunolabelled primary and secondary motor neurons with anti-znp1 and anti-zn8 respectively. The anti-znp1 antibody recognizes a form of synaptotagmin 2 that is present in zebrafish primary motor neurons (Fox & Sanes, 2007; Trevarrow et al., 1990), while the anti-zn8 antibody recognizes DM-GRASP protein that is highly localized to the cell membranes of secondary motor neurons (Fashena & Westerfield, 1999; Trevarrow et al., 1990). First, I examined the axons of primary motor neurons labelled with anti-znp1 and found that exposure to 6 mg/L THC had no quantifiable effect on the number of branches emanating from the main, primary axon (Fig. 3.7 A, B), whereas exposure to 3 mg/L CBD resulted in a significant reduction in the number of axonal branches (Fig. 3.7 C, D). Specifically, I found that the number of branches (per 1500 μm^2 area; Fig. 3.7A) was reduced from a mean value of 11 ± 1 ($n = 6$ embryos) in vehicle controls to 8 ± 1 ($n = 8$ embryos) in CBD-treated animals (Fig. 3.7 F, $p < 0.01$).

Immunolabelling of secondary motor neurons with anti-zn8 showed a more severe effect of THC and CBD exposure, compared with primary motor neurons. The nature of the fluorescent

labelling allowed us to specifically quantify dorsal, ventral and lateral branching patterns, as shown in Fig. 3.8 (labelled D, V and L). I was unable to see dorsal branches of secondary motor neurons in embryos treated with either 6 mg/L THC or 3 mg/L CBD (Fig. 3.8 B, D, E, H; $p < 0.01$), whereas ventral branches were always present but often looked thinner than controls (Fig. 3.8 B, D, F and I). Lateral branches were usually present in THC-treated animals but were largely absent following CBD treatment (Fig. 3.8 B, D, G and J; $p < 0.01$). Taken together, these data suggest that the normal development and innervation patterns of primary and secondary motor neurons were affected by exposure to THC and CBD during gastrulation.

3.1.4 nAChR labeling

To determine if the expression of nicotinic acetylcholine receptors (nAChRs) at NMJs was altered by THC and CBD exposure, I used fluorescently tagged α -bungarotoxin to label postsynaptic membranes of neuromuscular junction NMJs (Fig. 3.9). The fluorescent labelling of NMJs consistently appeared brighter in the THC-treated embryos compared with controls. The total number of (nAChR) puncta was greater in THC-treated embryos compared with vehicles by approximately 22% ($p < 0.05$; Fig. 3.9 A, B and E). In contrast, there was a 13 % reduction in the total number of nAChR puncta in CBD-treated embryos (Fig. 3.9 C, D and G). The size of the puncta ranged from a minimum of less than $1 \mu\text{m}^2$ to a maximum of $300 \mu\text{m}^2$. The smallest puncta appeared to be discrete entities and may represent extrasynaptic nAChRs or developing endplates, whereas large puncta ($>10 \mu\text{m}^2$) likely represent mature NMJ clusters. Further analysis revealed that there were fewer puncta with a minimum size of $\sim 5 \mu\text{m}^2$ in CBD-treated

animals compared with controls (Fig.3. 9 D, H). These findings suggest that synaptic development at the NMJ was altered following cannabinoid treatment during gastrulation.

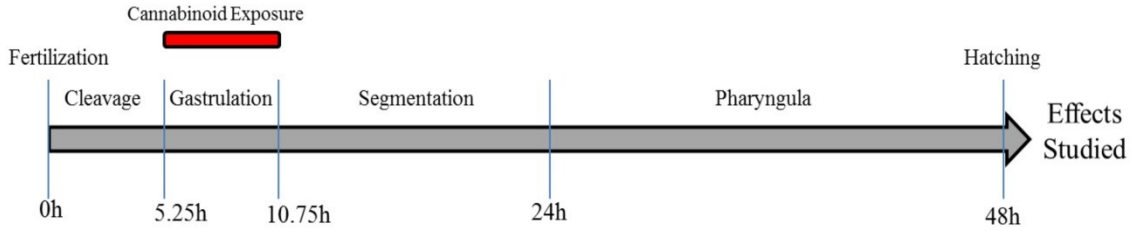
3.1.5 Locomotion

Cannabinoid-exposed embryos were able to swim (data not shown). To determine if exposure to cannabinoids altered their ability to respond to stimuli such as touch or an AV input, I stimulated free-swimming 5 dpf larvae with a mechanical or sound stimulus since the AV input onto Mauthner cells develops at 4 dpf. Vehicle control larvae responded to touch about 100% of the time (Fig. 3.10 A, B). Embryos treated with THC or CBD also showed strong touch response rates of 100% (n = 51 fish in 4 experiments) and 88% respectively (Fig. 3.10 A, B) (n = 25 fish in 3 experiments). However, the response to sound was very different. Vehicle control larvae responded approximately 68% of the time and following THC treatment exhibited a drastic reduction in response where only 6% responded to the sound pulse (n = 30 fish in 5 experiments) (Fig. 3.10 C). CBD-treated embryos only responded at a rate of 40% (n = 30 fish in 5 experiments) when given a sound stimulus. These findings show that motor systems are still functional following cannabinoid treatment, but there appears to be a selective effect on different sensory modalities.

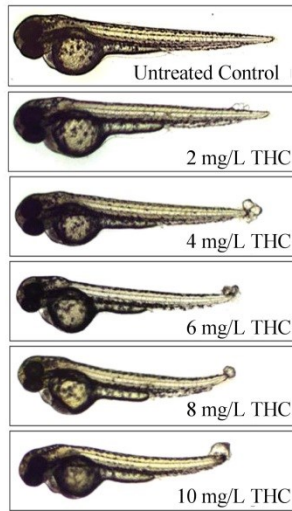
Taken together these results suggest that cannabinoid treatment during the 5-hour time period of gastrulation altered a number of characteristics in developing zebrafish embryos including morphology, heart rate, activity at the neuromuscular junctions, MN branching and ability to respond to sound stimuli.

Figure 3. 1 Effect of THC and CBD exposure on zebrafish embryos

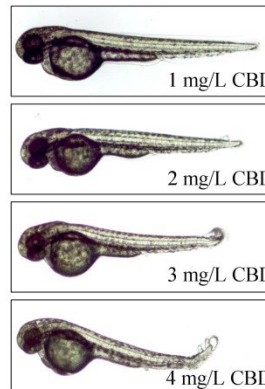
A)



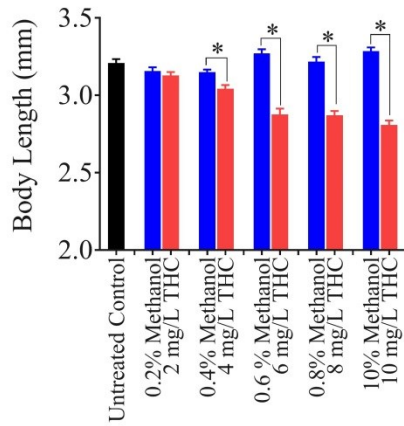
B)



C)



D)



E)

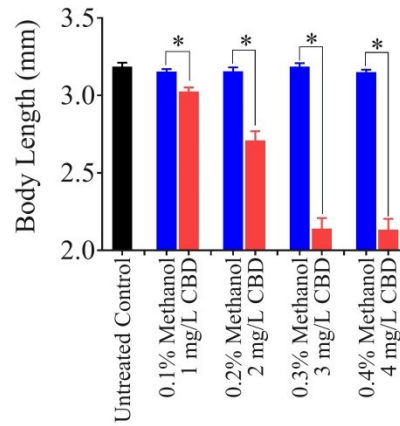


Figure 3.1 Effect of THC and CBD exposure on zebrafish embryos. (A) A schematic of the exposure paradigm of cannabinoids in this study. Red bar shows the duration of the cannabinoid exposure which occurred for 5 h during gastrulation. (B, C) Embryos were untreated (control), or exposed to 2 mg/L, 4 mg/L, 6 mg/L, 8 mg/L or 10 mg/L THC or 1 mg/L, 2 mg/L, 3mg/L or 4mg/L CBD (from 5.25 hpf to 10.75 hpf and then allowed to develop in normal embryo media. Representative images were taken at 48–52 hpf; representative images are presented. (D) Bar graph showing the body lengths of fish in untreated control (black, n = 59), different concentrations of THC (pink, n = 54, 48, 61, 57 and 55 for 2, 4, 6, 8 and 10 mg/L THC-treated fish, respectively) or corresponding vehicle control (blue, n = 39, 37, 22, 25 and 20 for 0.2, 0.4, 0.6, 0.8 and 1 percent methanol-treated fish, respectively). (E) Bar graph showing the body lengths of fish in untreated control (black, n=51), different concentrations of CBD (pink, n = 52, 52, 25 and 19 for 1, 2, 3 and 4 mg/L CBD-treated fish, respectively) or corresponding vehicle control (blue, n = 36, 39, 32 and 37 for 0.1, 0.2, 0.3, and 0.4 percent methanol-treated fish respectively). ***Significantly different from vehicle control, $p < 0.001$. Comparisons between multiple groups were done by one-way ANOVA followed by a Tukey post-hoc multiple comparisons test ($p < 0.05$).

Figure 3. 2 Effect of vehicle control of THC (methanol) on morphology, survival and hatching of zebrafish embryos.

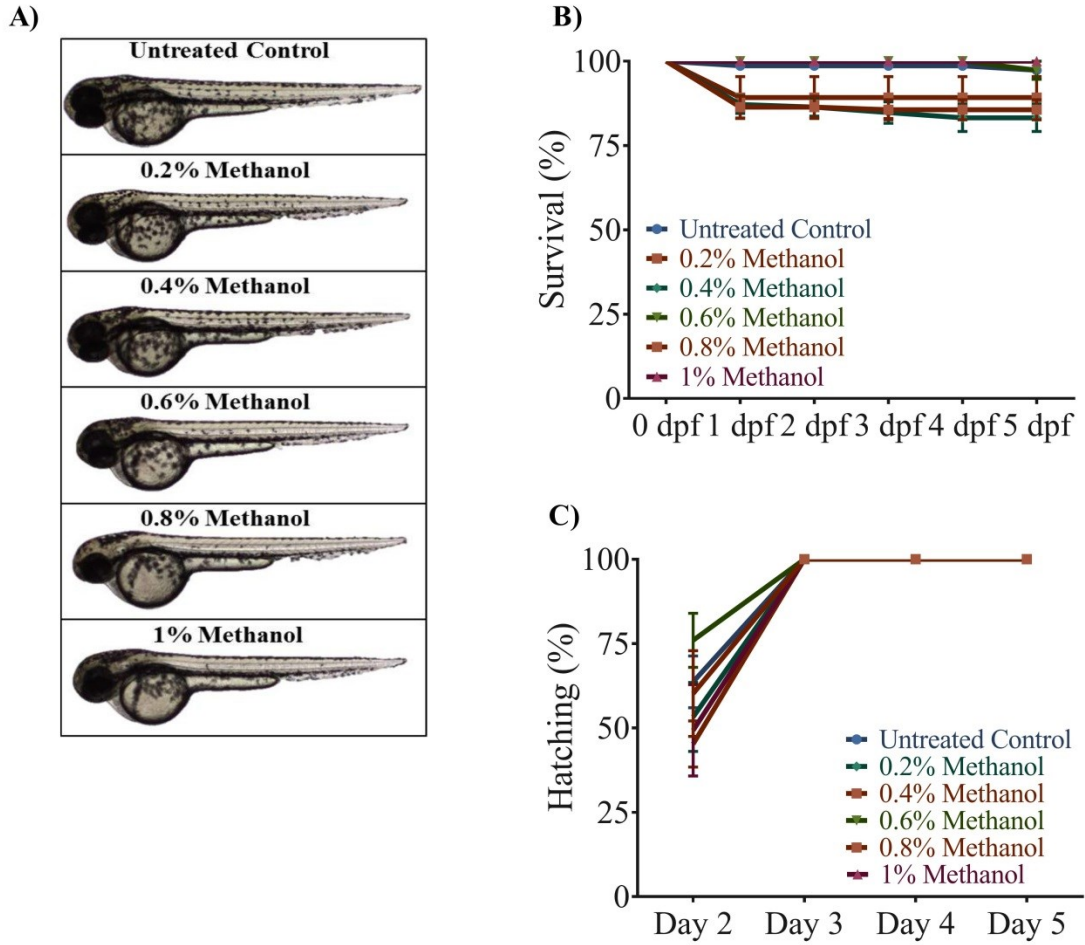


Figure 3.2 Effect of vehicle control of THC (methanol) on morphology, survival and hatching of zebrafish embryos. (A) Embryos were untreated (control), or exposed to 0.2%, 0.4%, 0.6%, 0.8% or 1% methanol (from 5.25 hpf to 10.75 hpf) and then allowed to develop in normal embryo media. Images were taken at 48-52 hpf; representative images are presented. (B) Line graph showing the percentage of embryos that survived within the first 5 days of development following methanol exposure during gastrulation (N=5 experiments and n=125 embryos for each treatment). (C) Line graph showing the percentage of embryos that hatched within the first 5 days after egg fertilization following methanol exposure (N = 5 experiment and n = 125 embryos for each treatment). Comparisons between multiple groups were done by two-way ANOVA followed by a Tukey post-hoc multiple comparisons test ($p < 0.05$).

Figure 3. 3 Effect of vehicle control of CBD (methanol) on morphology, survival and hatching of zebrafish embryos.

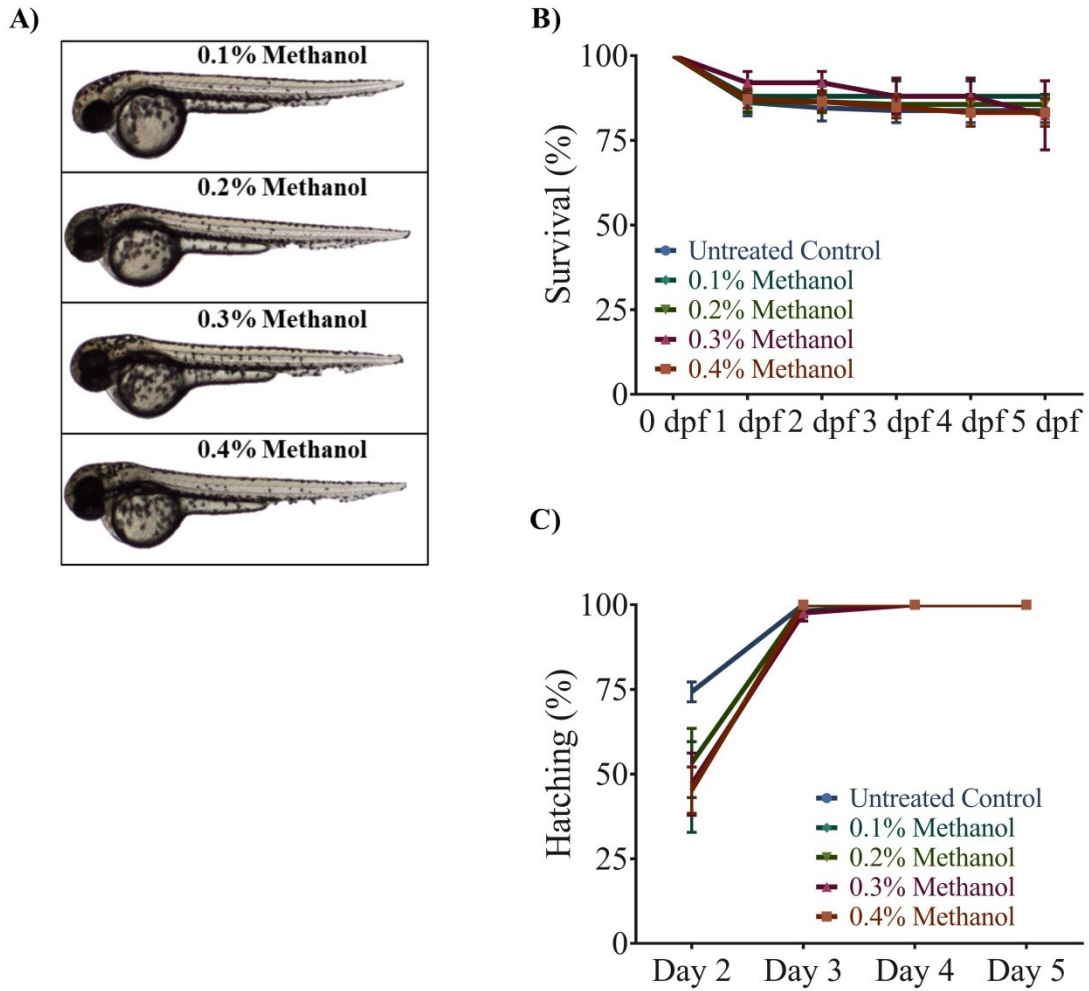


Figure 3.3 Effect of vehicle control of CBD (methanol) on morphology, survival and hatching of zebrafish embryos. (A) Embryos were exposed to 0.1%, 0.2%, 0.3% or 0.4% methanol (from 5.25 hpf to 10.75 hpf) and then allowed to develop in normal embryo media. Images were taken at 48-52 hpf. (B) Line graph showing the percentage of embryos that survived within the first 5 days of development following methanol exposure during gastrulation (N = 5 experiments and n = 125 for each treatment). (C) Line graph showing the percentage of embryos that hatched within the first 5 days after egg fertilization following methanol exposure (N = 5 experiments and n = 125 embryos for each treatment). Comparisons between multiple groups were done by two-way ANOVA followed by a Tukey post-hoc multiple comparisons test ($p < 0.05$).

Figure 3. 4 Effect of THC and CBD exposure on survival and hatching.

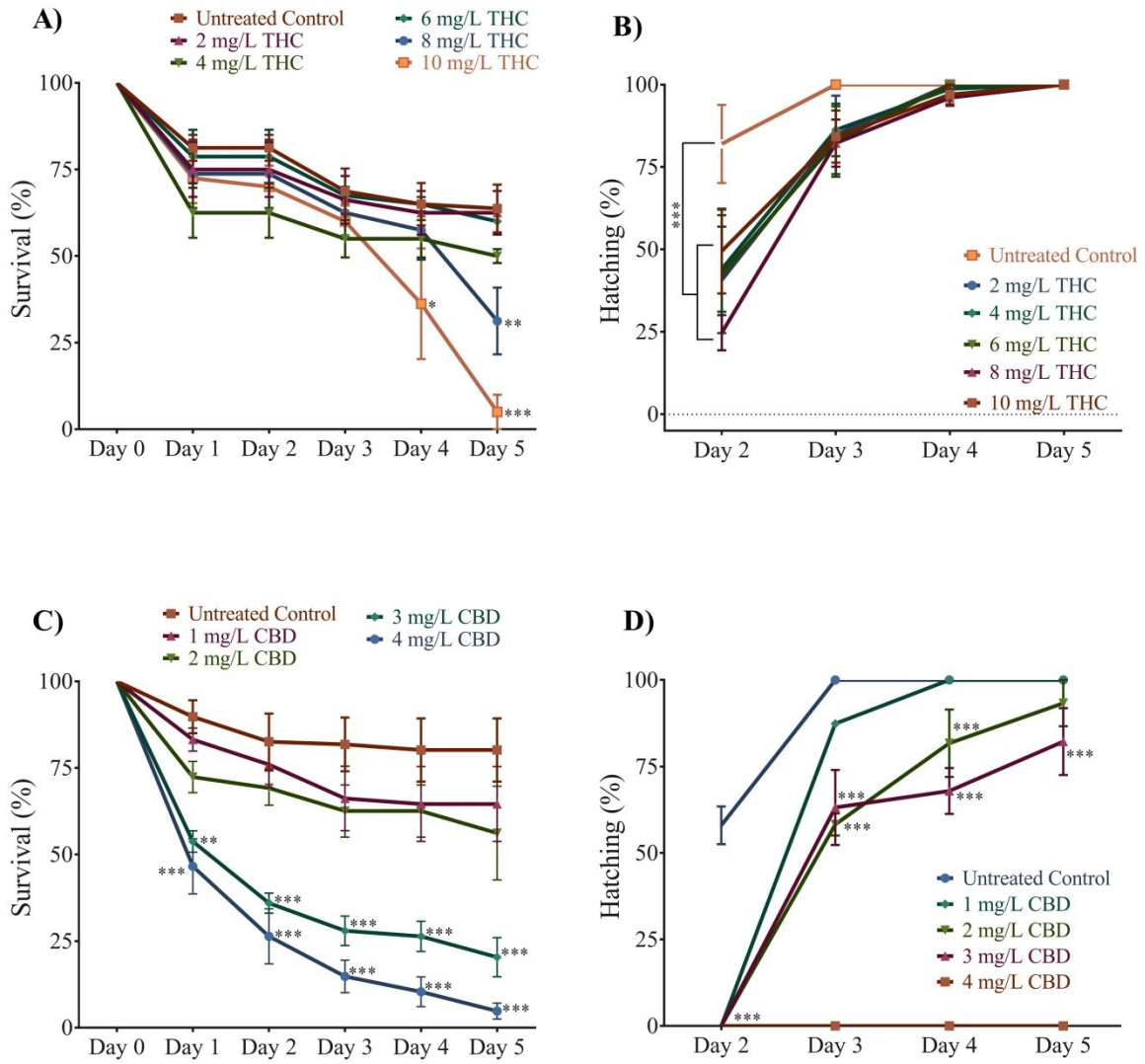


Figure 3.4 Effect of THC and CBD exposure on survival and hatching. (A, B) Line graph showing the percentage of embryos that survived and hatched within the first 5 days of development following THC exposure during gastrulation (N = 4 experiments and n = 20 embryos for each treatment). (C, D) Line graph showing the percentage of embryos that survived (N = 5 experiment and n = 25 embryos for each treatment) and hatched within the first 5 days after egg fertilization following CBD exposure (N = 3 experiment and n = 25 embryos for each treatment). ***Significantly different from vehicle control, $p < 0.001$, **Significantly different from vehicle control $p < 0.01$, *Significantly different from vehicle control $p < 0.05$. Comparisons between multiple groups were done by two-way ANOVA followed by a Tukey post-hoc multiple comparisons test ($p < 0.05$).

Figure 3. 5 Effect of THC exposures on heart rate.

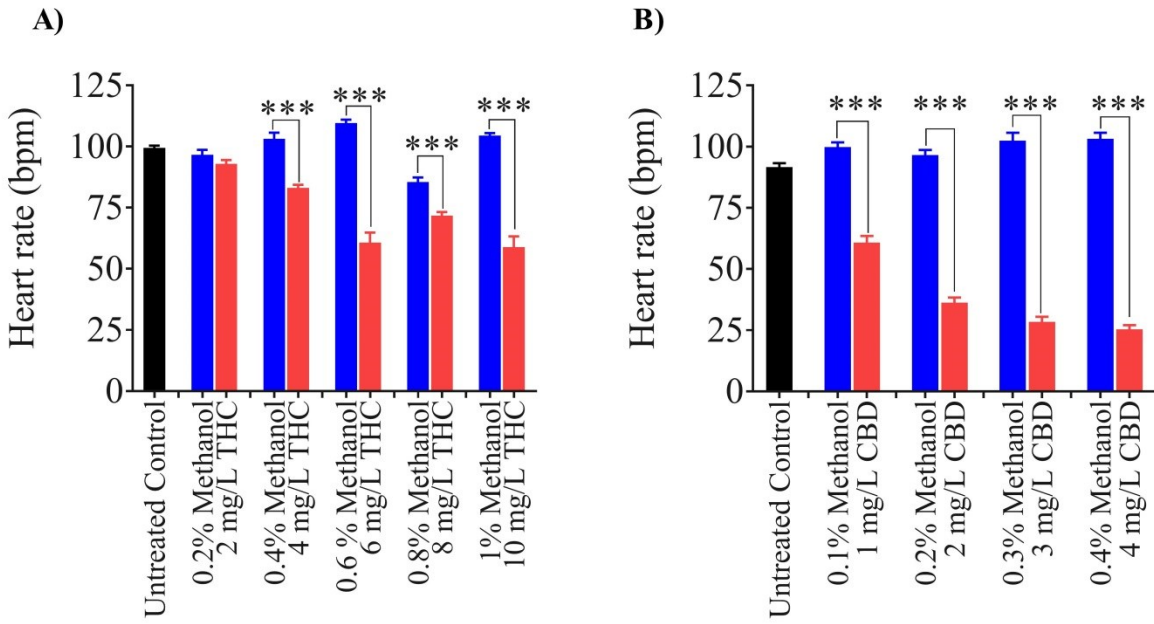


Figure 3.5 Effect of THC exposures on heart rate. (A) Bar graph showing the heart rate of untreated control embryos (n = 29), 2–10 mg/L THC-exposed embryos (n = 26, 22, 22, 21 and 21 for 2, 4, 6, 8, and 10 mg/L THC, respectively) and corresponding vehicle controls (methanol-treated embryos; n = 31, 25, 35, 26 and 28 for 0.2, 0.4, 0.6, 0.8, and 1 percent methanol, respectively). (B) Bar graph showing the heart rate of untreated control embryos (n=22), 1–4 mg/L CBD-exposed embryos (n = 42, 40, 25 and 20 for 1, 2, 3 and 4mg/L CBD respectively) and corresponding vehicle treated embryos (n = 25, 31, 24 and 25 for 0.1, 0.2, 0.3 and 0.4 percent methanol, respectively). ***Significantly different from vehicle control, $p < 0.001$. Comparisons between multiple groups were done by one-way ANOVA followed by a Tukey post-hoc multiple comparisons test ($p < 0.05$).

Figure 3. 6 Miniature endplate currents (mEPCs) recorded from zebrafish white muscle

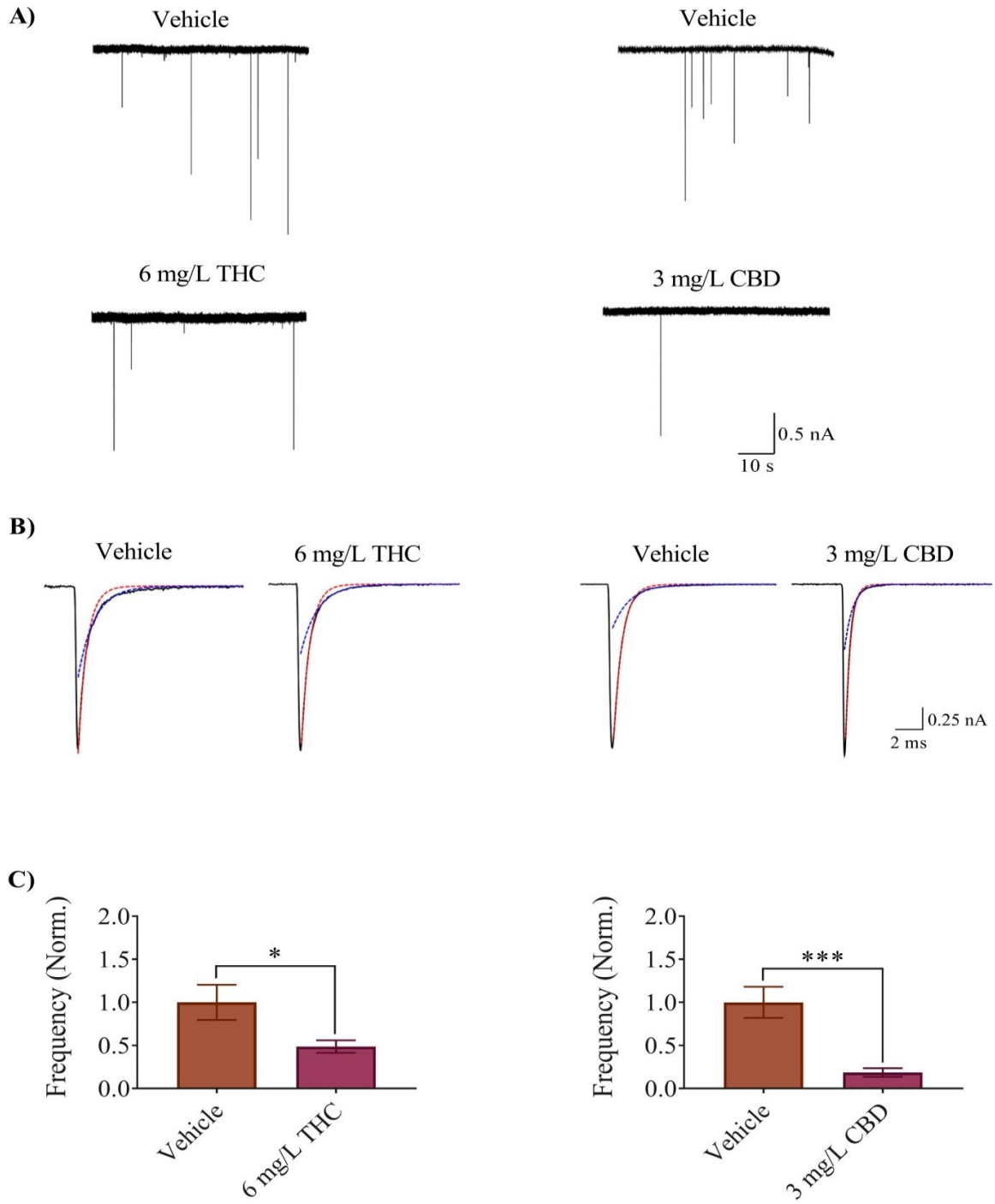


Figure 3.6 Miniature endplate currents (mEPCs) recorded from zebrafish white muscle fibers of vehicle control and 6 mg/L THC-treated embryos (left column), and vehicle control and 3 mg/L CBD-treated embryos (right column). (A) Representative raw traces obtained from 2 dpf vehicle control (0.6% Methanol, 0.3% Methanol), 6 mg/L THC-treated embryos and 3 mg/L CBD-treated embryos. (B) Averaged mEPCs obtained from white muscle (black line) fit with a single exponential decay over the fast component (τ fast, red dashed line) or slow component (τ slow, blue dashed line). Averaged mEPCs acquired from vehicle control (0.6% Methanol 6 events; 0.3% Methanol 36 events in total from 6 fish), 6 mg/L THC-treated embryos (11 events in total from 7 fish) and 3 mg/L CBD (6 events from 5 fish) (C) Bar graph of the mean mEPC frequency of vehicle and THC-treated embryos (left), and vehicle and CBD-treated embryos (right). *** Significantly different from vehicle control, $p < 0.001$ and *Significantly different from vehicle control $p < 0.05$. Significance was determined using a non-parametric Mann-Whitney analysis.

Figure 3. 7 Antibody labelling (anti-znp1) of axonal branches of primary motor neurons at 2 dpf

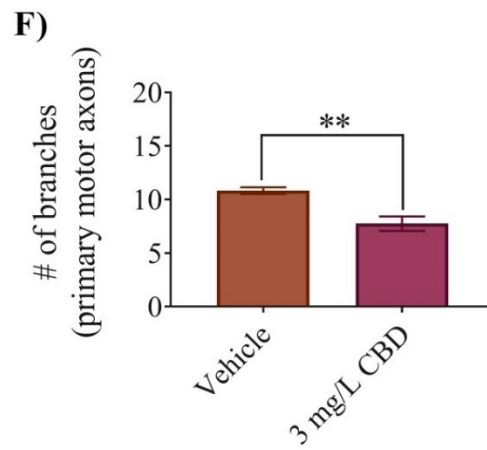
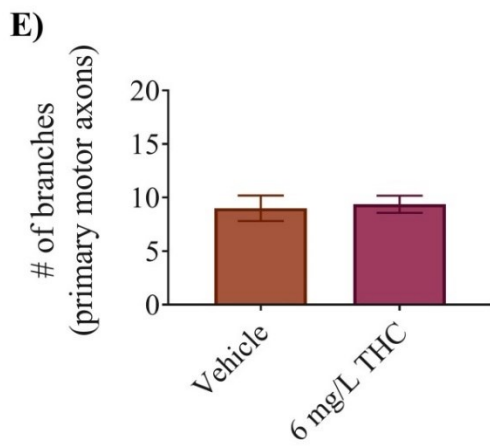
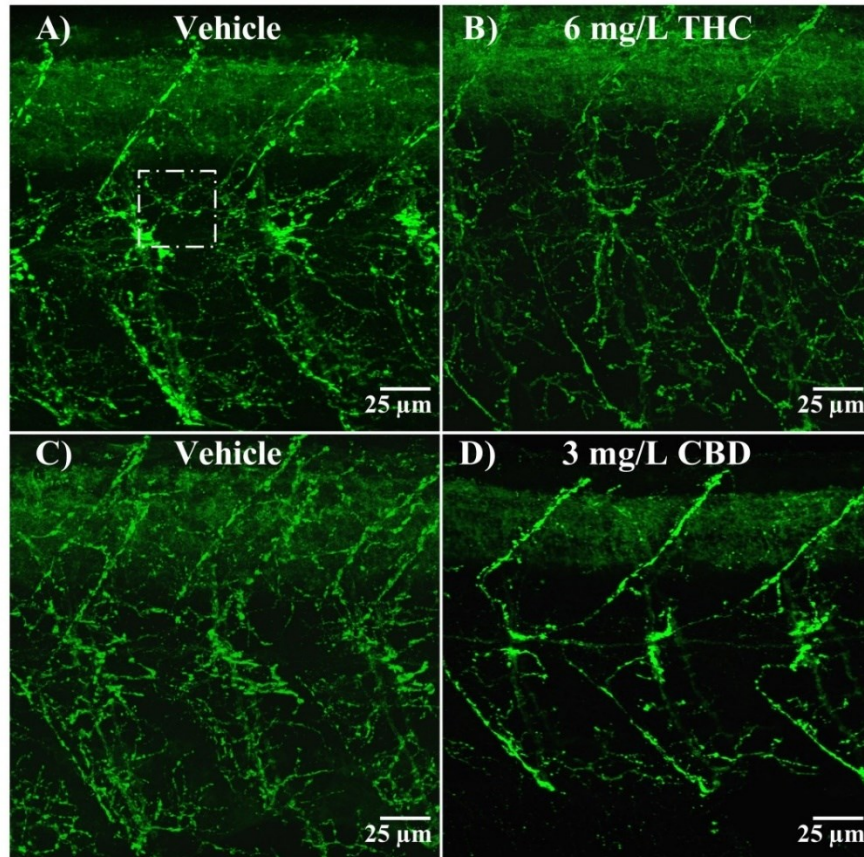


Figure 3.7 Antibody labelling (anti-znp1) of axonal branches of primary motor neurons in 2 dpf embryos in vehicle controls, 6 mg/L THC-treated embryos and 3 mg/L CBD-treated embryos. (A–D) Branching patterns and labelling of axons appear to be similar between controls and THC-treated embryos but reduced in CBD-treated embryos. (E) Bar graph showing the number of branches emanating from primary motor axons in vehicle control (n=7) and 6 mg/L THC-treated embryos (n=8), counted from 9 different square areas (each 1500 μm^2 area). (F) Bar graph showing the number of branches emanating from primary motor axons in vehicle control (n=6) and 3mg/L CBD-treated embryos (n=8), counted from 9 different square areas (each about 1500 μm^2 area). **Significantly different from vehicle control $p<0.01$, * Significantly different from vehicle control, $p<0.05$. Significance was determined using a non-parametric Mann-Whitney analysis.

Figure 3. 8 Antibody labelling (anti-zn8) of axonal branches of secondary motor neurons at 2 dpf

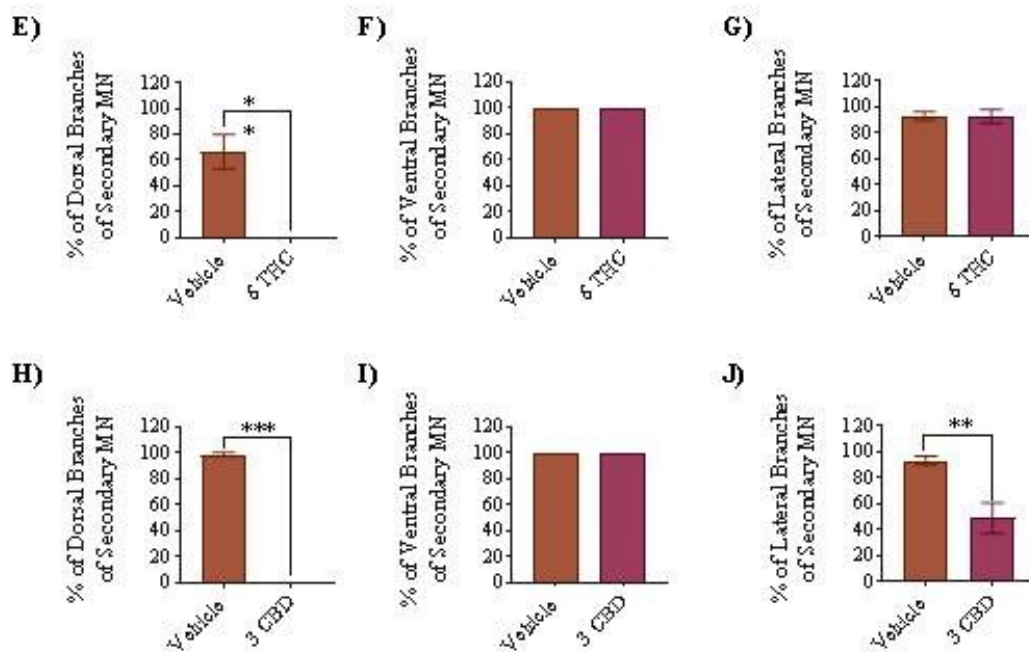
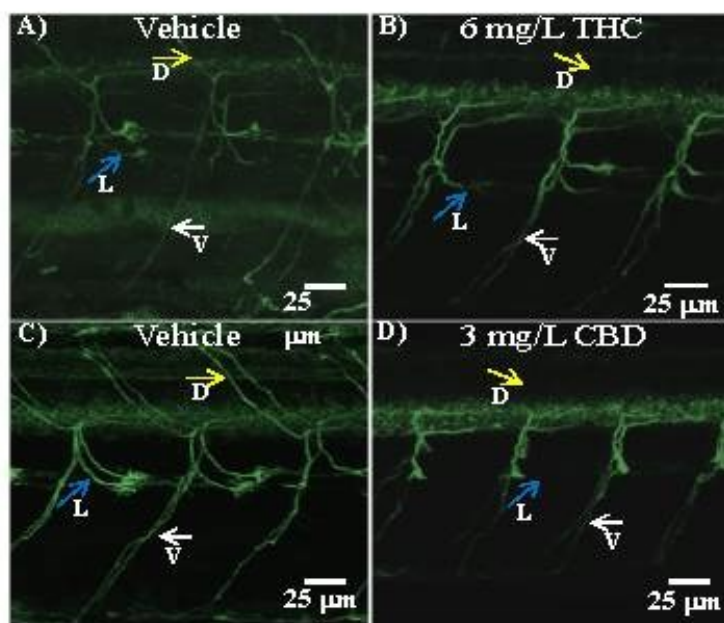


Figure 3.8 Antibody labelling (anti-zn8) of axonal branches of secondary motor neurons in 2 dpf embryos in vehicle control, 6 mg/L THC-treated embryos and 3mg/L CBD-treated embryos. (A–D) Dorsal, ventral and lateral branches emanating from secondary motor neurons are indicated by yellow, white and blue arrows. Dorsal branches were absent in THC- and CBD-treated embryos (B, D). Fewer lateral branches are visible in CBD-treated embryos. (E–G) Bar graph comparing percentage of dorsal branches (E), ventral branches (F) and lateral branches (G) emanating from secondary motor neurons in vehicle control (n=11) and 6 mg/L THC-treated embryos (n=11). (H–J) Bar graph comparing percentage of dorsal branches (H), ventral branches (I) and lateral branches (J) emanating from secondary motor neurons in vehicle control (n=11) and 3 mg/L CBD treated embryos (n=9). ***Significantly different from vehicle control $p < 0.001$, **Significantly different from vehicle control $p < 0.01$, *Significantly different from vehicle control $p < 0.05$. Significance was determined using a non-parametric Mann-Whitney analysis.

Figure 3. 9 Expression of nicotinic acetylcholine receptors (nAChRs) at 2 dpf

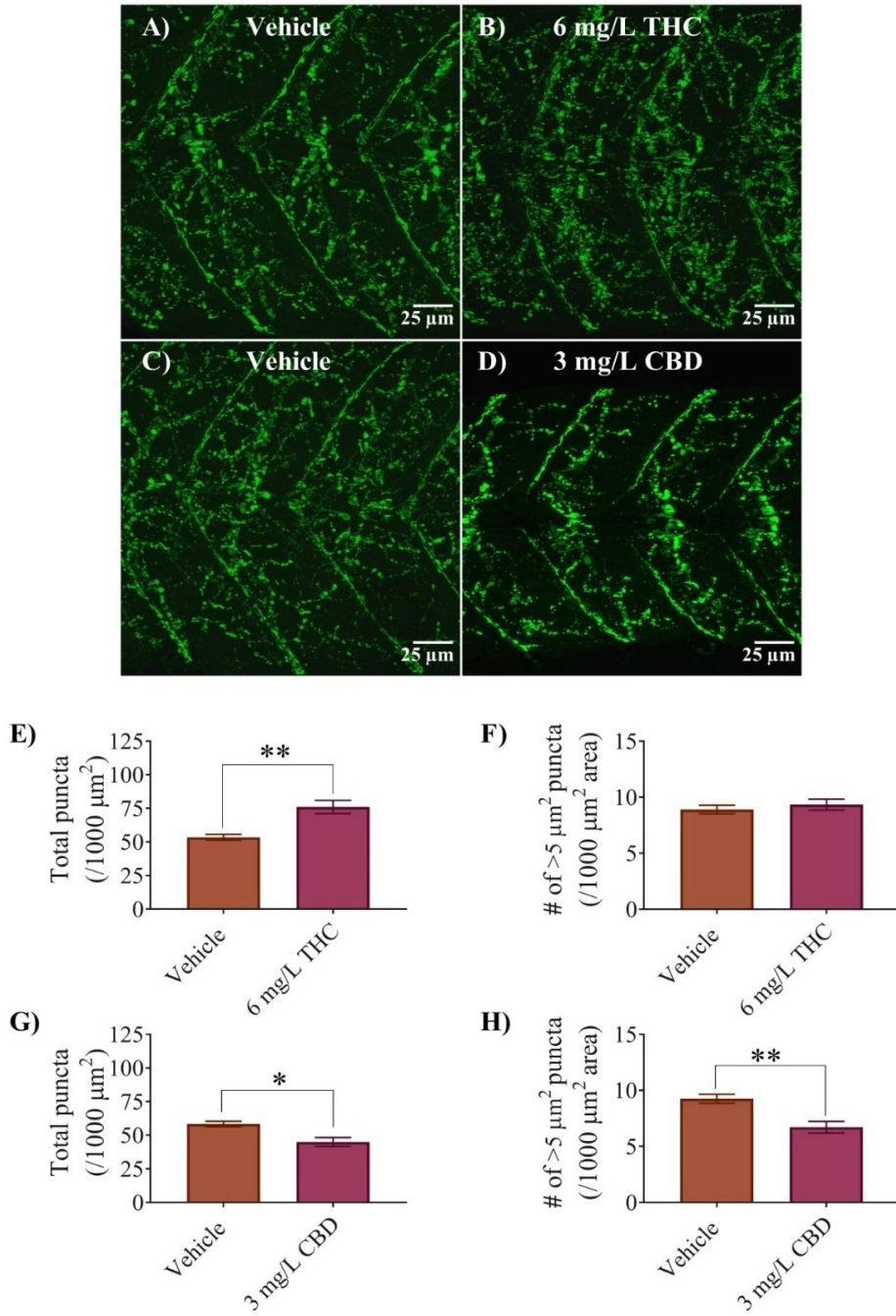


Figure 3.9 Expression of nicotinic acetylcholine receptors (nAChRs) in 2 dpf embryos of controls, 6 mg/L THC- and 3mg/L CBD-treated fish. (A–D) α -bungarotoxin labelling of postsynaptic membranes at the NMJ in zebrafish trunk musculature. (E) Bar graph representing the total number of α -bungarotoxin puncta counted over per 1000 μm^2 area and compared between vehicle control (n=10) and 6 mg/L THC-treated embryos (n=6). (F) Bar graph representing the number of α -bungarotoxin puncta with a minimum area of $\sim 5 \mu\text{m}^2$, compared between vehicle control (n=10) and 6 mg/L THC-treated embryos (n=6). (G) Bar graph representing the total number of α -bungarotoxin puncta counted over a 1000 μm^2 area and compared between vehicle control (n=8) and 3 mg/L CBD-treated embryos (n=7). (H) Bar graph representing the number of α -bungarotoxin puncta with a minimum area of $\sim 5 \mu\text{m}^2$, compared between vehicle control (n=8) and 3 mg/L CBD-treated embryos (n=7). ** Significantly different from vehicle controls $p < 0.01$, *Significantly different from vehicle control $p < 0.05$. Significance was determined using a non-parametric Mann-Whitney analysis.

Figure 3. 10 Quantification of the response rate of 5-dpf zebrafish larvae to touch and sound stimuli

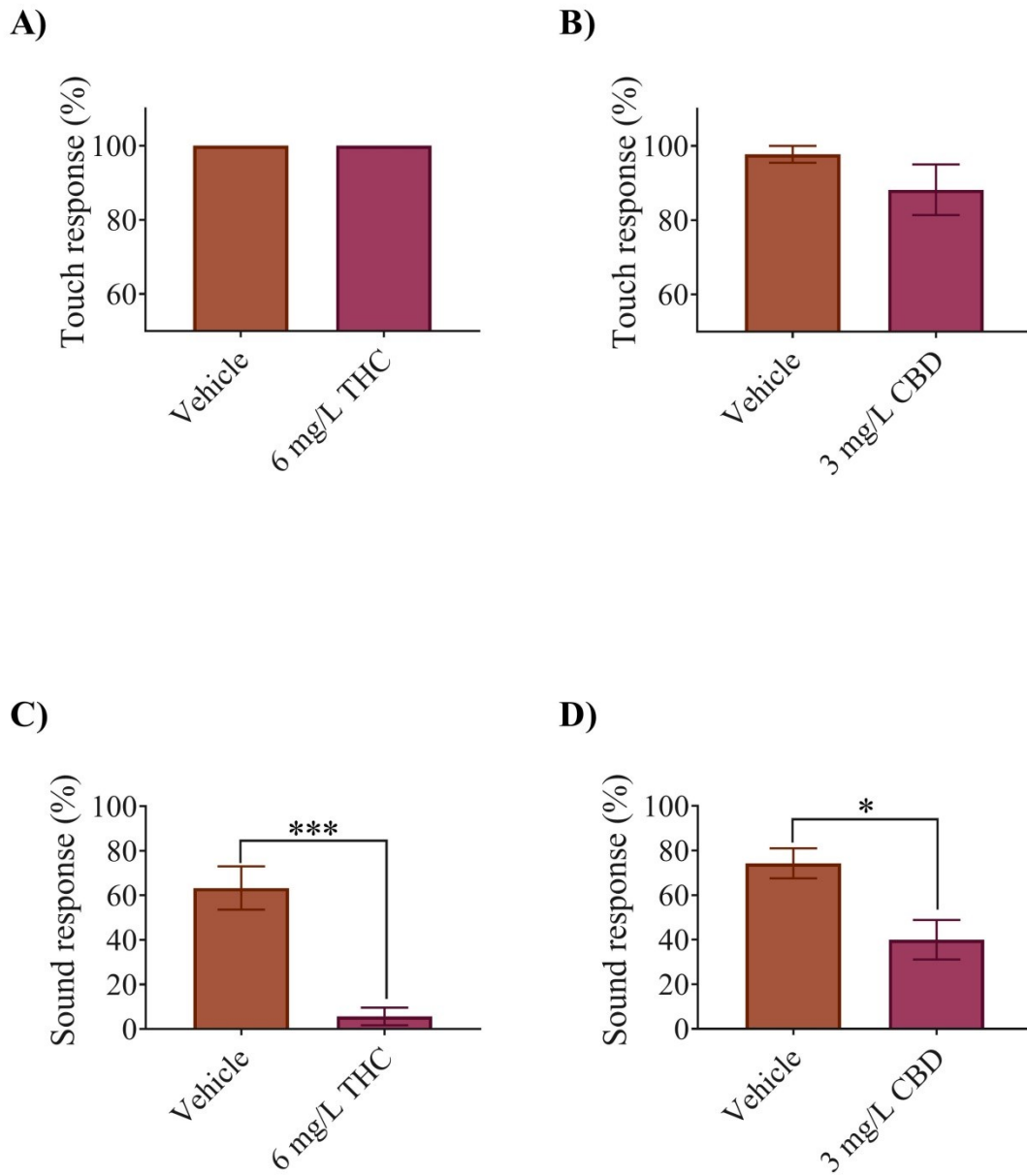


Figure 3.10 Quantification of the response rate of 5-dpf zebrafish larvae to touch and sound stimuli. (A) Bar graph comparing the ratio of larvae responding to a touch stimulus in vehicle control (n=39 embryos in 4 experiments) and 6 mg/L THC groups (n=51 embryos in 4 experiments). (B) Bar graph comparing the ratio of larvae responding to a touch stimulus in vehicle control (n=42 embryos in 4 experiments) and 3 mg/L CBD groups (n=25 embryos in 3 experiments) (C) Bar graph comparing the ratio of larvae responding to a sound stimulus in vehicle control (n=30 embryos in 5 experiments) and 6 mg/L THC groups (n=30 embryos in 5 experiments). (D) Bar graph comparing the ratio of larvae responding to a sound stimulus in vehicle control (n=24 embryos in 4 experiments) and 3 mg/L CBD groups (n = 30 embryos in 5 experiments). *** Significantly different from controls $p < 0.001$, *Significantly different from vehicle control $p < 0.05$. Significance was determined using a non-parametric Mann-Whitney analysis

Chapter 4

Early Exposure to THC Alters M-Cell Development in Zebrafish Embryos

I had previously found that zebrafish embryos exposed to THC during gastrulation exhibited altered fast escapes in response to acoustic but not mechanosensitive stimuli (Chapter 3), indicating a possible deficit with M-cell form or function. My results from the present study indicate that M-cells are largely intact following exposure to THC during gastrulation and that there appears to be minor but significant changes to neuronal morphology. Moreover, muscle morphology and locomotor responses are also impacted by exposure to THC.

4.1 Results

4.1.1 THC exposure reduces axonal diameter of M-cell

In chapter 3, I found that zebrafish embryos exposed to THC from 1–10 mg/L exhibited morphological and neuronal changes that ranged from no effect at the lower concentrations, to disorganized neuronal morphology and alterations in responses to sound at the higher concentrations. In the present study I continue my work by examining the morphology of M-cells following exposure to the primary psychoactive ingredient in cannabis, THC. I exposed zebrafish embryos to 6 mg/L THC as I had done previously and compared these embryos with vehicle controls (0.6% methanol). An immunohistochemical analysis of M-cell morphology was performed at 2 dpf with anti-3A10. Embryos exposed to THC exhibited M-cells that were largely similar to controls but appeared disheveled and possessed slightly thinner and wisper looking axons (Fig 4.1 A–E). The diameter of the M-cell body was unchanged ($p > 0.05$; $n = 8–10$) (Fig

4.1 C), whereas the M-cell axon diameter was significantly smaller in the treated group compared with controls ($p < 0.05$). Specifically, the M-cell diameter in the control group was $2.0 \pm 0.1 \mu\text{m}$ ($n = 8$) while it was $1.5 \pm 0.1 \mu\text{m}$ ($n = 11$) in the THC-treated group (Fig 4.1 F). To confirm these findings, I performed an additional immunohistochemical analysis of the M-cells by labelling reticulospinal neurons using the anti-RMO44 antibody. I found that there was an overall reduction in the intensity of the fluorescent labelling of many neurons in the THC-treated animals compared with controls (Fig 4.1 G, J). The diameter of the M-cell body remained unchanged (Fig 4.1 I); however, the diameter of the M-cell axon was significantly smaller ($1.2 \pm 0.06 \mu\text{m}$, $n = 9$) in the treated group compared with vehicle controls ($1.8 \pm 0.1 \mu\text{m}$, $n = 7$) ($p < 0.05$) (Fig 4.1 L). These results, obtained using two distinct and independent antibodies, strongly suggest that the M-cells exhibit small but significant changes following exposure to 6 mg/L THC in the gastrulation stage.

4.1.2 Escape response properties were altered due to THC exposure

To determine if the properties of the escape response had been altered by exposure to THC, I recorded the C-bend following a mechanosensitive stimulus to the head of 2 dpf embryos. The C-bend response rate between the two groups was similar and there were no overt differences between the treatments. However, the angle of the C-bend was significantly greater in the THC-treated animals compared with vehicle controls (Fig 4.2 A; $p < 0.05$; $n = 7-13$). Analysis of the maximum speed and acceleration showed no significant differences in these parameters (Fig 4.2 B, C; $p > 0.05$; $n = 7-13$). On the other hand, the time to maximum bend of

the trunk was greater in the THC-treated animals (Fig 4.2 D, $p < 0.05$; $n = 7-13$), likely because the bend angle was greater.

4.1.3 White and red muscle fibers appear thinner and slightly disorganized in THC treated embryos

Since a deficit in muscle development may contribute to the characteristics in the C-bend response, I decided to examine muscle morphology. I performed an immunohistochemical analysis of the trunk muscles in conjunction with labelling of the nicotinic receptors using fluorescently tagged α -bungarotoxin. The trunk muscles of embryonic and larval zebrafish embryos are composed of a single layer of outer red muscles and several layers of inner white muscles (Waterman, 1969). The outer red muscle of vehicle control animals developed in an orderly fashion with clear and precise boundaries between the trunk segments (Fig 4.3). The α -bungarotoxin labelling of nAChRs in untreated animals was neatly aligned at the segmental boundaries (Fig 4.3 A–C) as described in previous studies (Lefebvre et al., 2007; Park et al., 2014). However, embryos treated with THC exhibited thinner individual muscle fibers (Fig 4.3 E) that appeared less tightly packed, with larger spaces in between the fibers and unclear segmental boundaries. The diameter of THC-treated red muscle fiber was reduced to 5.1 ± 0.2 μm from control values of 6.3 ± 0.3 μm in vehicle exposed fibers (Fig 4.3 G, $p < 0.05$; $n = 24-34$). However, the lengths of the fibers remained unchanged (Fig 4.3 H). Moreover, the nAChR expression, that was largely confined to the segmental boundaries, was somewhat disorganized (Fig 4.3 D-F).

A corresponding analysis of the white fibers using the F310 antibody combined with α -bungarotoxin labelling of nAChRs provided a similar result (Fig 4.4). The white fiber diameter for control embryos was $7.8 \pm 0.3 \mu\text{m}$ (Fig 4.4 G), whereas it decreased to $4.6 \pm 0.3 \mu\text{m}$ for THC-treated embryo muscle fibers (Fig 4.4 G, $p < 0.05$; $n = 18\text{--}22$). I did not observe any significant changes in the length of individual fibers (Fig 4.4 H). The white fibers exhibited periodic regions of disorganization with intermittent nAChR expression (Fig 4.4 D–F). Further, the labelling of α -bungarotoxin showed more condensed nAChR that was also disorganized (Fig 4.4 D).

4.1.4 THC does not alter nAChR subunit expression

To determine if the expression of the nAChR subunits was altered following THC exposure, I performed a semi quantitative analysis of the mRNA for the $\alpha 1$, γ and ϵ subunits in relation to the β subunit. However, I found no significant differences in the relative expression of the nAChR subunits (Fig 4.5 A–C), suggesting that differences in nAChR subunits expression do not occur as a result of early THC exposure in my experimental paradigm.

4.1.5 THC exposure alters the locomotion at 5 dpf

Lastly, I allowed the animals to develop until they were 5 dpf, at which age they actively swim to feed. This allowed us to determine if exposure to THC affected their basal level of activity. I found that all aspects of their movement were altered by THC treatment during gastrulation (Fig 4.6 A–D). For instance, the mean distance swam changed from 3200 ± 620

mm/hr in the controls ($n = 77$) to 960 ± 170 mm/h in the THC-treated animals (Fig 4.6 A, $n = 77$; $p < 0.001$). The mean velocity fell from 0.70 ± 0.08 mm/s ($n = 77$) to 0.22 ± 0.03 mm/s ($n = 79$) (Fig 4.6 B, $p < 0.001$), the mean activity fell from 0.073% ($n = 84$) to 0.015% ($n = 84$) (Fig 4.6 C, $p < 0.001$) and the movement frequency fell from 635 ± 72 ($n = 74$) to 247 ± 44 ($n = 74$) (Fig 4.6 D, $p < 0.001$) in 5dpf fish previously exposed to THC. Taken together, these findings suggest that cannabinoid treatment during gastrulation affected neuronal morphology to a small degree, as well as the development of muscle fibers and various aspects of locomotion. These results are consistent with my previous study and suggest that developing organisms exposed to THC may experience subtle alterations in development.

Figure 4. 1 THC exposure reduces M-cell axonal diameter

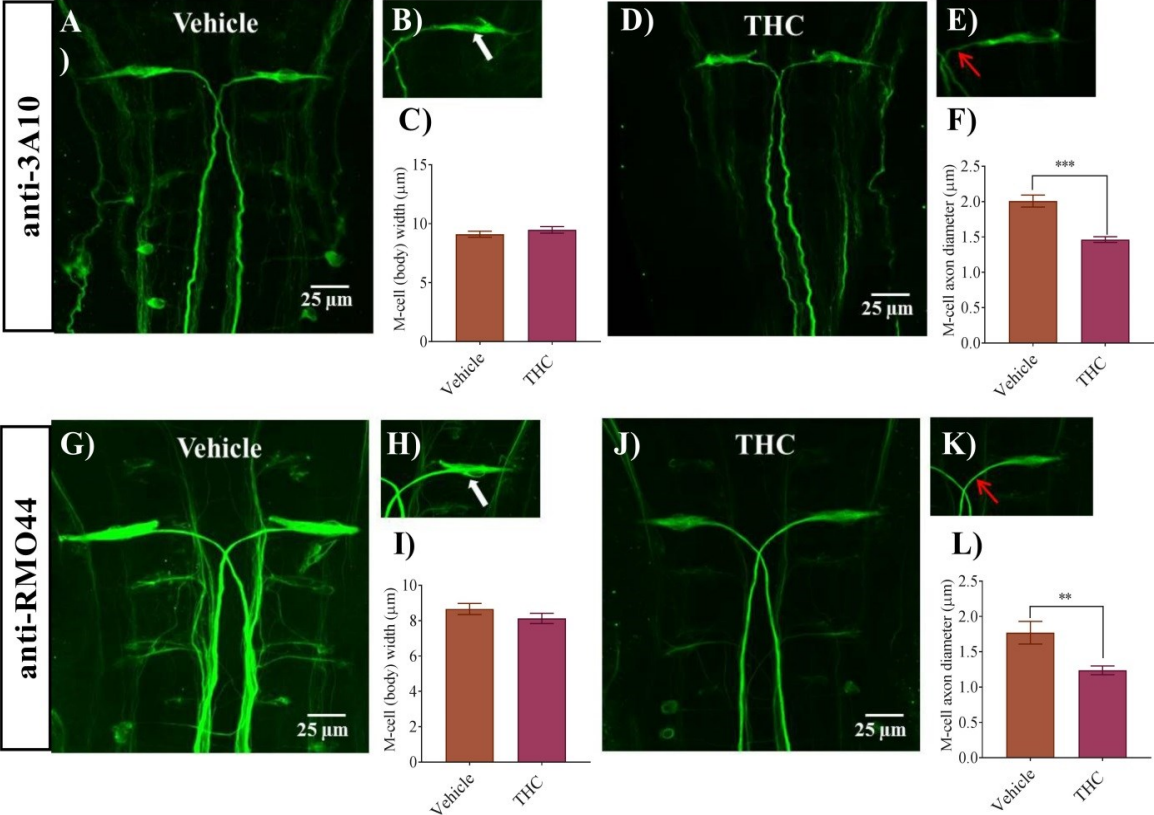


Figure 4.1 THC exposure reduces M-cell axonal diameter. (A, G) Immunolabeling of M-cells with anti-3A10 and anti-RMO44 in a vehicle-treated embryo; (B, H) higher magnification of M-cell body and axon of vehicle-treated embryos. White arrow shows the cell body of the M-cell. (C, I) Bar graph of the width of an M-cell body in vehicle and THC-treated embryos. (D, J) Immunolabeling of M-cells with anti-3A10 and anti-RMO44 in a THC-treated (6 mg/L) embryo; (E, K) higher magnification of M-cell body and axon of a THC-treated embryo. Red arrow points to the proximal axon immediately anterior to the decussation point. (F, L) Bar graph of the diameter of M-cell axons slightly anterior to the decussation point in vehicle and THC-treated embryos. Significance was determined using non-parametric Mann-Whitney analysis. ** Significantly different from vehicle control, $p < 0.01$. *** Significantly different from vehicle control, $p < 0.001$.

Figure 4. 2 Exposure to THC during gastrulation alters escape response parameters

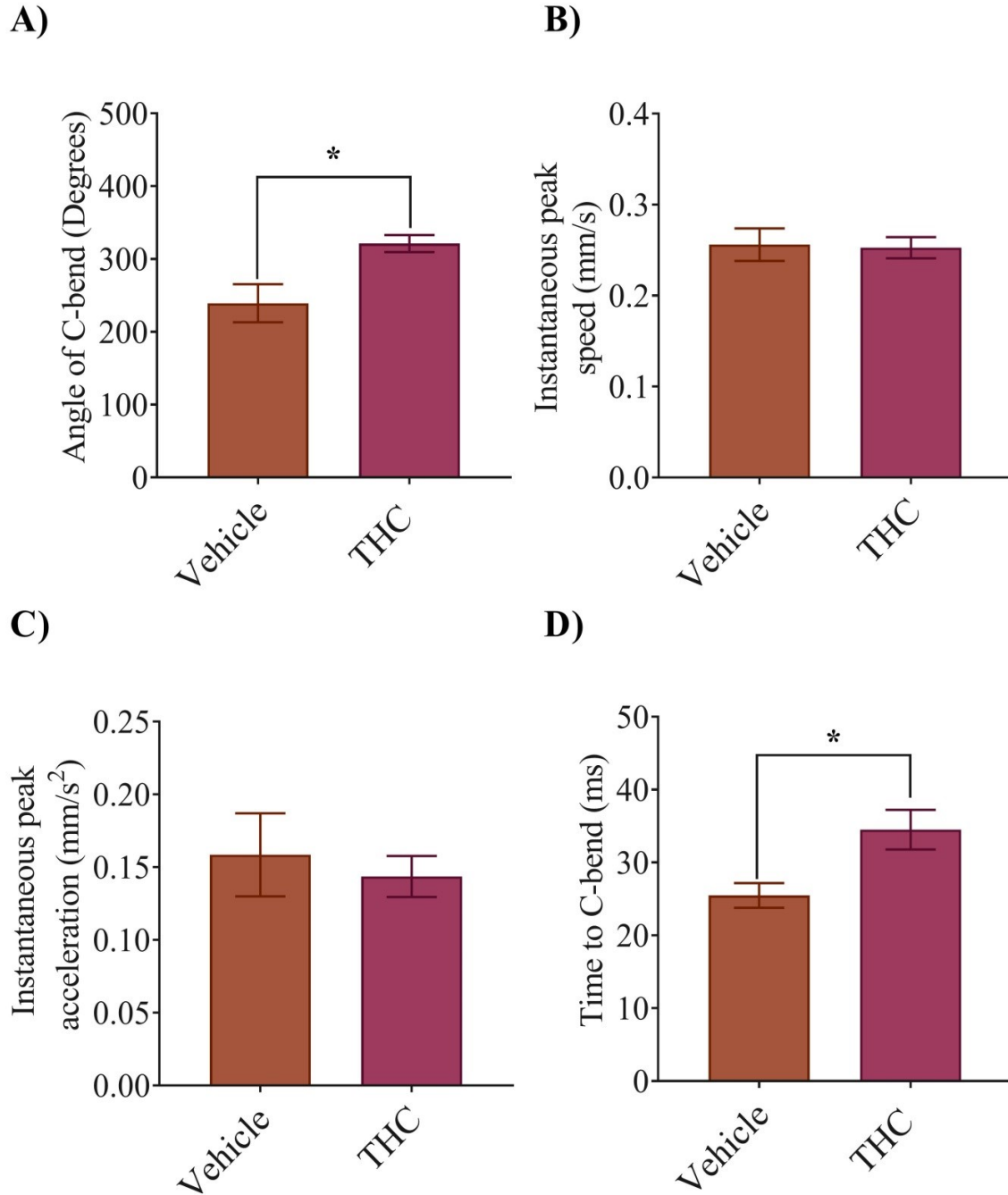


Figure 4.2 Exposure to THC during gastrulation alters escape response parameters.

Analysis and quantification of C-bend parameters was carried out at 2 dpf. Zebrafish embryos exhibit a C-bend in response to a jet of water directed at the head just behind the eyes. (A) Bar graph showing the maximum angle of bend for vehicle and THC-treated (6 mg/L) embryos. (B) Bar graph showing the instantaneous peak speed (mm/s) during C-bend. (C) Bar graph showing the instantaneous peak acceleration during C-bend. (D) Bar graph showing the time for the tail to bend to the maximum angle. Significance was determined using non-parametric Mann-Whitney analysis. * Significantly different from vehicle control, $p < 0.05$.

Figure 4. 3 Co-labeling of red muscle fibers and nAChRs using anti-F59 and Alexa 488 conjugated α -bungarotoxin, respectively

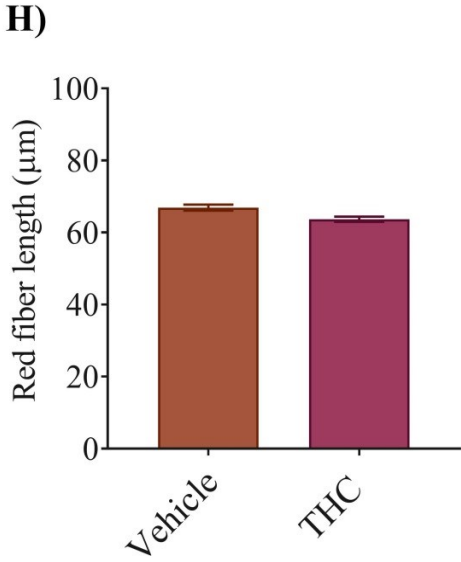
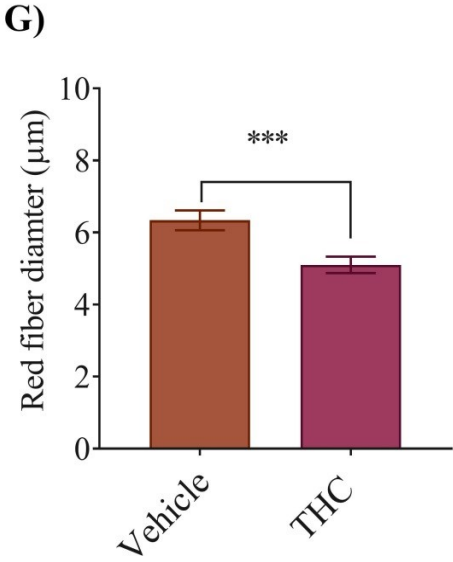
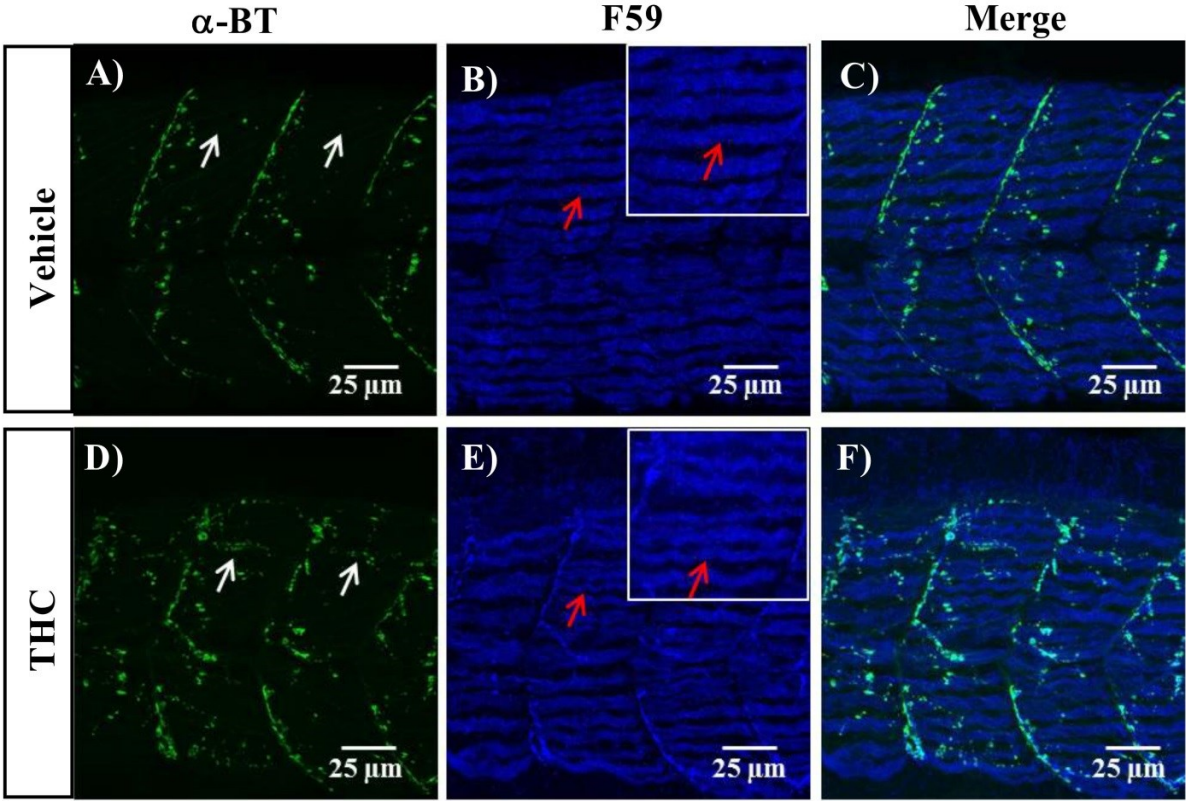


Figure 4.3 Co-labelling of red muscle fibers and nAChRs using anti-F59 and Alexa 488 conjugated α -bungarotoxin respectively. (A) α -Bungarotoxin-labelled nAChRs associated with red muscle fibers in vehicle-treated embryos. (B) Anti-F-59-labelled muscle fibers in vehicle-treated animals. Red arrows point to the edge of a muscle fiber. Inset shows muscle fibers at higher magnification to better determine the size of the fiber. (C) Merged image showing the co-labelled red muscle fiber and nAChR in vehicle-treated animals. (D) α -bungarotoxin-labelled nAChRs associated with red muscle fibers in THC-treated (6 mg/L) embryos. White arrow shows the cluster of nAChRs. (E) Anti-F59 labelled muscle fibers in THC-treated animals. Red arrows point to the edge of a muscle fiber. Inset shows muscle fibers at higher magnification to better determine the size of the fiber. (F) Merged image showing the co-labelled red muscle fiber and nAChR in THC-treated animals. (G) Bar graph showing the diameter of red fibers for vehicle- and THC-treated embryos and (H) measurement of red fiber length. Significance was determined using non-parametric Mann-Whitney analysis. *** Significantly different from vehicle control, $p < 0.001$.

Figure 4. 4 Co-labeling of white muscle fibers and nAChRs using anti-F310 and Alexa 488 conjugated α -bungarotoxin, respectively

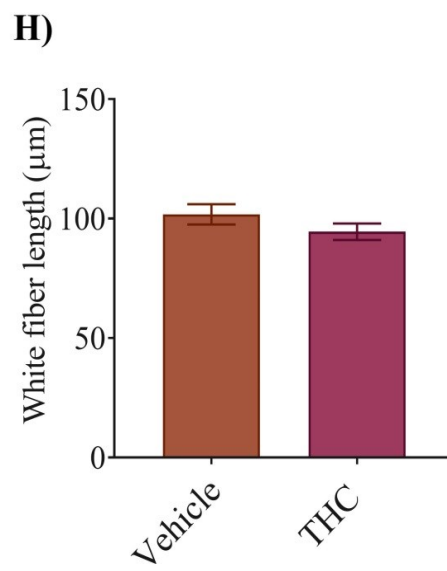
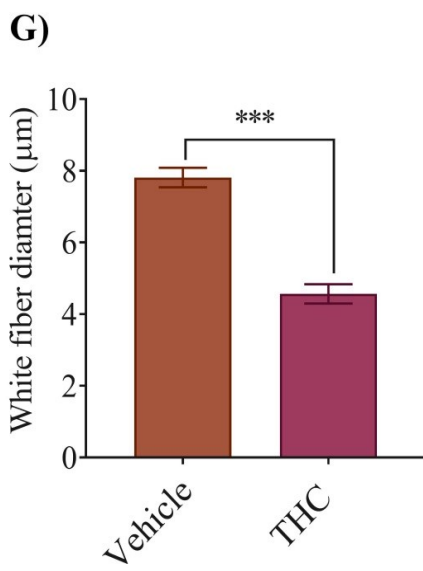
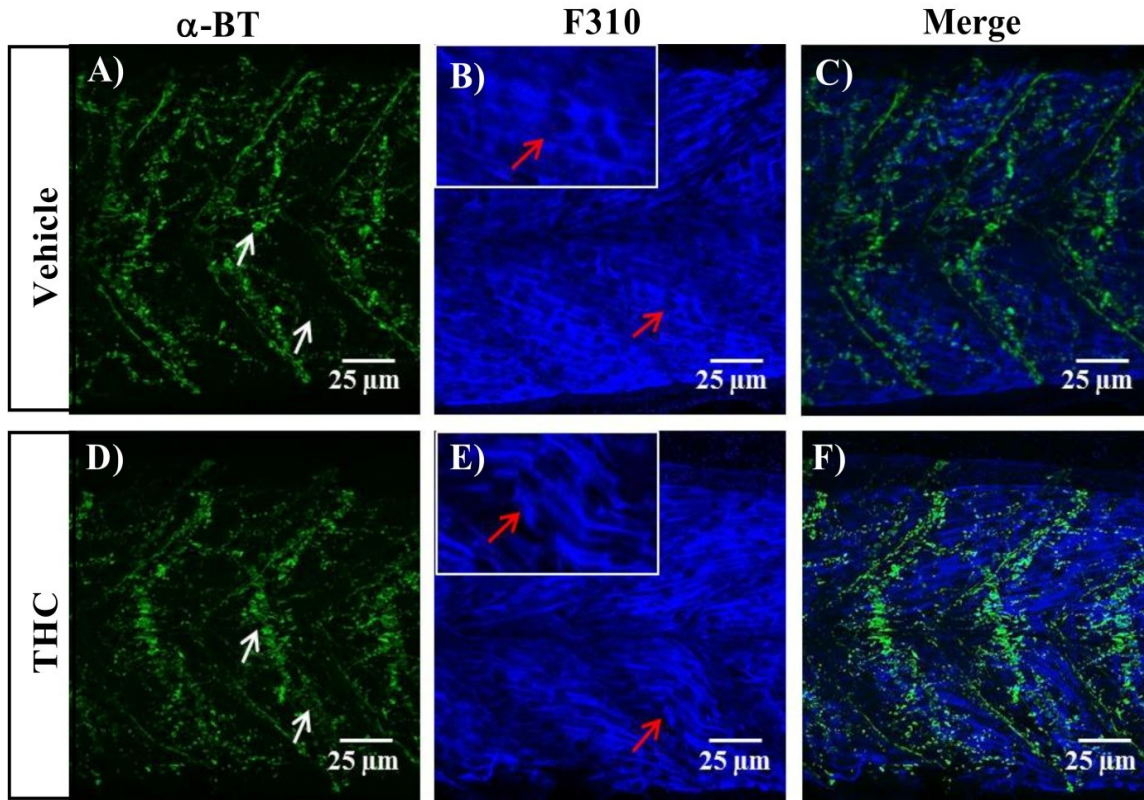


Figure 4.4 Co-labelling of white muscle fibers and nAChRs using anti-F310 and Alexa 488-conjugated α -bungarotoxin, respectively. (A) α -Bungarotoxin-labelled nAChRs associated with white muscle fibers in vehicle-treated embryos. White arrow shows clusters of nAChRs. (B) Anti-F-310-labelled muscle fibers in vehicle-treated animals. Red arrows point to the edge of a muscle fiber. Inset shows muscle fibers at higher magnification to better determine the size of the fiber. (C) Merged image showing the co-labeled white muscle fiber and nAChR in vehicle-treated animals. (D) α -bungarotoxin-labelled nAChRs associated with white muscle fibers in THC-treated (6 mg/L) embryos. White arrow shows clusters of nAChRs. (E) Anti-F310-labelled muscle fibers in THC-treated animals. Red arrows point to the edge of a muscle fiber. Inset shows muscle fibers at higher magnification to better determine the size of the fiber. (F) Merged image showing the co-labeled white muscle fiber and nAChR in THC-treated animals. (G) Bar graph showing the diameter of white fibers for vehicle- and THC-treated embryos and (H) measurement of white fiber length. Significance was determined using non-parametric Mann-Whitney analysis. *** Significantly different from vehicle control, $p < 0.001$.

Figure 4. 5 The relative levels of nAChR subunits (α 1, γ and ϵ) mRNAs were analyzed by RT-qPCR

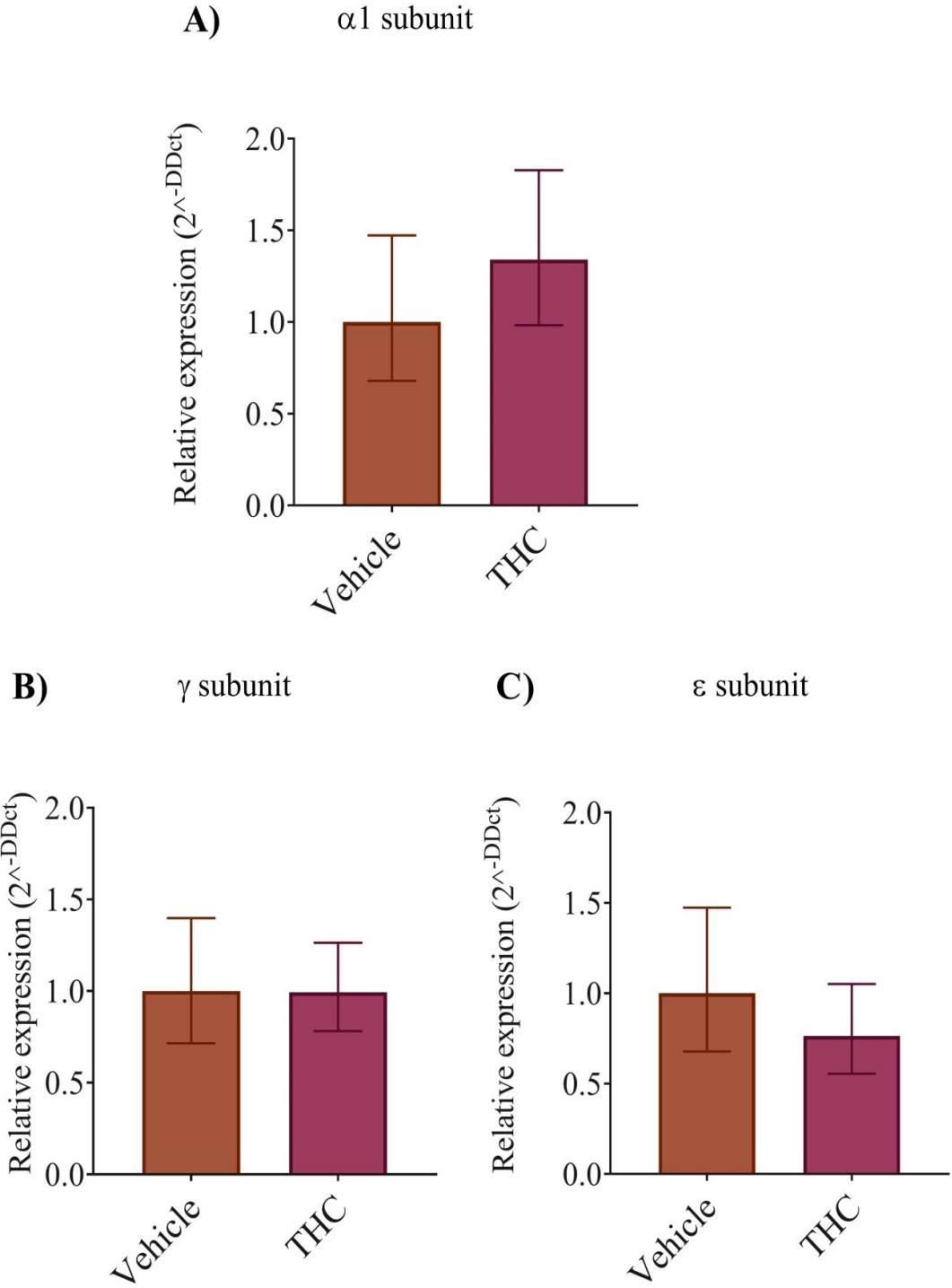


Figure 4.5 The relative levels of nAChR subunits ($\alpha 1$, γ and ϵ) mRNAs were analyzed by real-time RT-qPCR. The relative expression (expressed in relationship to the nAChR β subunit) was measured from vehicle controls and THC-treated embryos using the relative expression in vehicle control as calibrator. (A) The relative level of $\alpha 1$ nAChR expression from vehicle- and THC-treated embryos. (B, C) The relative expression of γ and ϵ , respectively. Data are presented as the mean \pm SE for individual groups (n = 5). Significance was determined using non-parametric Mann-Whitney analysis (p <0.05).

Figure 4. 6 THC exposure affects free swimming activity (locomotion) of zebrafish embryos at 5 dpf

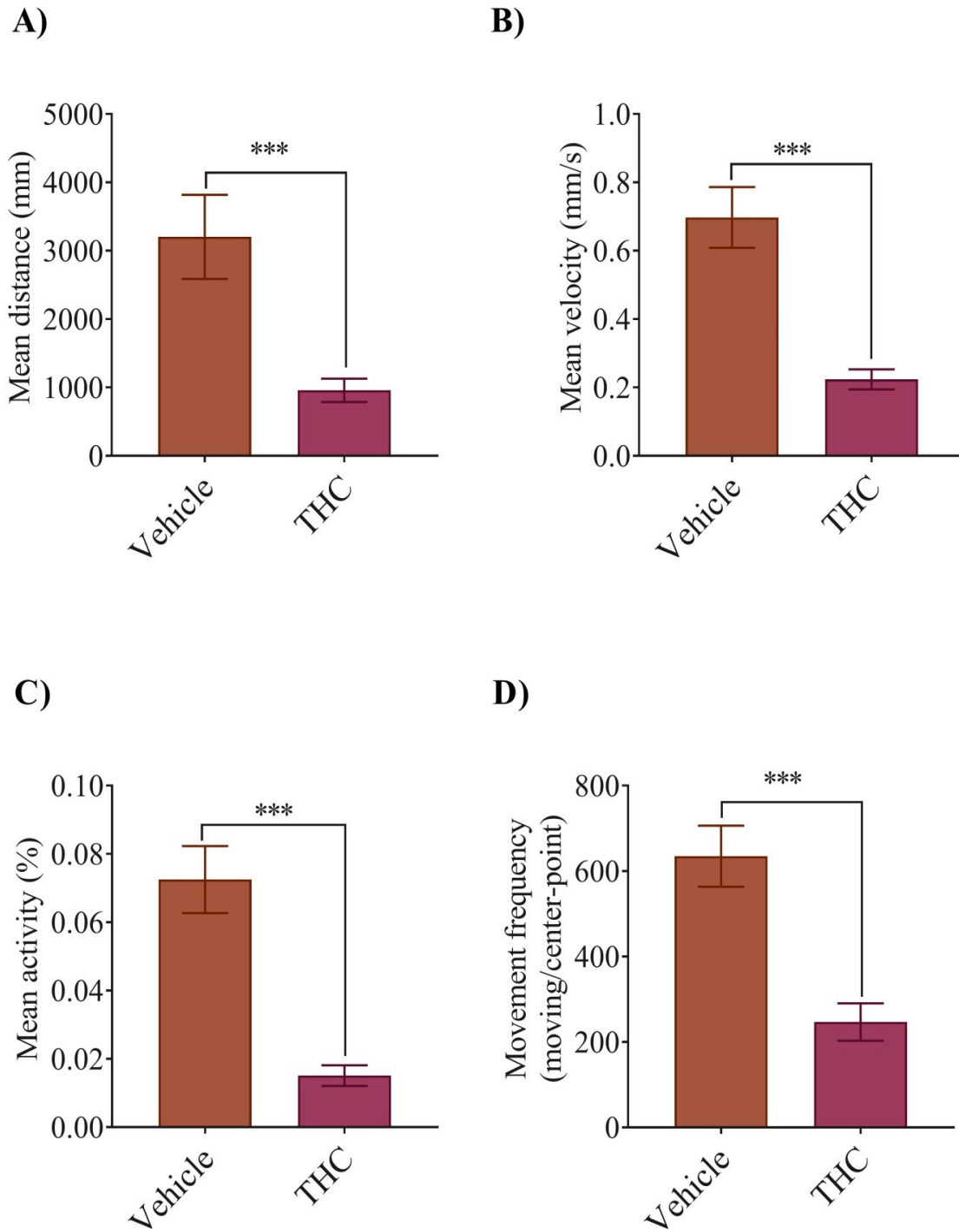


Figure 4.6 THC exposure affects free-swimming activity (locomotion) of zebrafish embryos at 5 dpf. Bar graphs display changes in larval mean distance moved (A), mean velocity (in mm/s for one hour) (B), mean activity (% rate for one hour) (C), and frequency of swim bouts within one hour (D). Significance was determined using non-parametric Mann-Whitney analysis. *** Significantly different from vehicle control, $p < 0.001$.

Chapter 5

Transgenerational effect of CBD on locomotion, motor neuron development and gene expression in zebrafish

In this study, I sought to determine if a brief exposure of CBD during early development (i.e. gastrulation) has a persistent effect on the development of zebrafish offspring. In zebrafish, gastrulation occurs between 5.25 hours post fertilization (hpf) and 10.75 hpf. In humans, gastrulation occurs in the third week of embryogenesis and is early enough that pregnancy may remain undetected. I found that the brief CBD exposure negatively affected the locomotion in the F0 generation, adults and in their offspring (F1). Also, the neuronal branching and the gene expression were significantly altered both in the F0 generation and in their offspring (F1).

5.1 Results

5.1.1 CBD during gastrulation affects the locomotion during development (burst activity, escape response and free swimming)

Spontaneous coiling activity at 1 dpf

In this study, I sought to characterize the adverse effects of a brief exposure of zebrafish embryos to CBD. I was especially interested in determining if brief exposure to CBD during gastrulation has long lasting effects. I treated zebrafish embryos with varying concentrations of CBD (0.01, 0.5, 1, 2, 3 and 4 mg/L) from 5.25 hpf to 10.75 hpf. Embryos were allowed to develop and were examined for locomotor activities in the first week of development. Zebrafish

embryos exhibit the first MN activity around 17-19 hpf and develop the escape response as early as 27 hpf when embryos start to hatch (Saint-Amant & Drapeau, 2000). Embryos start free swimming at 48-72 hpf following hatching. The newly hatched embryos exhibit burst swimming followed by beat and glide swimming by 4 dpf. I first examined burst activity over 1 min time periods in 1dpf embryos. My analysis showed a significant alteration of burst activity (Fig 5.1 A, n=25-44, p<0.05). Among the lower doses (0.001-1 mg/L), 0.1 mg/L CBD treatment resulted in a significant increase in spontaneous coiling activity compare to vehicle control (Fig 5.1 B, n=25-44, p<0.05). However, 0.1 mg/L CBD treatment did not result in a significant increase of spontaneous coiling count per minute (Fig 5.1 C, n=25-44, p>0.05). When the CBD treatment concentration is above 1 mg/L, I observed severely reduced spontaneous coiling activity (Fig 5.1 B, C, n=25-44, p<0.05).

Escape response to touch at 2 dpf

Next, I examined whether the escape behavior was altered in CBD-treated animals. To elicit an escape response, the head of the fish was gently touched with a thin piece of fishing line. Animals treated with CBD concentrations greater than 0.5 mg/L exhibited significantly reduced swimming distances immediately following the C-bend escape (Fig 5.2 B, n = 25-44, p<0.05). Specifically, the mean distance travelled was 1.96 ± 0.30 (n=47), 0.90 ± 0.14 (n=42), 0.29 ± 0.04 (n=49), 0.13 ± 0.01 (n=38) and 0.12 ± 0.01 cm (n=18) for 0.5, 1, 2, 3 and 4 mg/L CBD treatments respectively, which was significantly smaller than control animals that swam 6.51 ± 0.82 cm (n=30; p<0.001). Similarly, animals treated with CBD concentrations greater than 0.5

mg/L exhibited a significant decrease in their swimming velocity immediately following the C-bend, compared with control animals (Fig 5.2 C, n = 25-44, p<0.05).

Swimming behavior at 3, 4, 5 and 6 dpf

Since CBD treatment altered the burst activity and escape responses to touch, I asked whether larval free swimming was also affected by CBD. I didn't find a significant effect of CBD treatment on the swimming distance and activity in 3 dpf and 4 dpf animals (Fig 5.3 A - D, n=20-50, p>0.05). However, CBD exposure produced a bi-phasic effect on the swimming activity at 5 dpf and 6 dpf. At 5 dpf, the larval swimming distance was significantly reduced to 677 ± 125 mm by the lowest concentration of CBD treatment of 0.01 mg/L compared to vehicle control that swam a mean distance of 3218 ± 814 mm (Fig 5.3 E, n = 20-55, p<0.05). Animals treated with 2-4 mg/L CBD showed a significant reduction in swimming distance to 936 ± 190 , 444 ± 79 and 305 ± 115 mm respectively compare with vehicle controls (Fig 5.3 E, n = 20-55, p<0.05). Interestingly, animals treated with 1 mg/L CBD swam a mean distance of 2567 ± 526 mm, which was not significantly different compared with vehicle controls (Fig 5.3 E, n = 20-55, p>0.05). The CBD treated larvae exhibited similar biphasic effect on the swimming activity at 5dpf as well (Fig 5.3 F, n = 20-55, p<0.05).

At 6 dpf, the mean swimming distance of 1 mg/L CBD treatment was not significantly different compare with control animal (Fig 5.3 G, n = 20-50, p>0.05). The mean swimming distance was significantly decreased in animals treated with every concentration of CBD except 1 mg/L (Fig 5.3 G, n = 20-50, p<0.05). Similarly, the activity was also significantly reduced if the CBD concentration is either below or higher than 1 mg/L (Fig 5.3 H, n = 20-50, p<0.05).

5.1.2 Brief exposure to CBD during gastrulation affects the locomotion in adult zebrafish.

Individual behavior - open field test

To determine if brief exposure to CBD during gastrulation has effects that persist into adulthood, I reared animals to adults and examined a number of behaviors. I chose to rear animals treated with 3 mg/L CBD because this concentration significantly affected survival and hatching rates, which was reported in my previous study (Chapter 3). First, I wanted to observe whether CBD-treated zebrafish had locomotor deficits in open field test. To achieve this objective, I recorded the swimming activity of adult zebrafish for 10 minutes in an open arena. I found that the CBD-treated adult zebrafish traveled a significantly shorter distance, averaging 1834 ± 106 cm compared to 4511 ± 197 cm of the controls (Fig 5.4 A, n=20-50, $p < 0.05$). I also observed that the CBD-treated animals spent significantly less time in the center zone (Fig 5.4 B, n=20-50, $p < 0.05$) suggesting a greater level of anxiety than the controls. However, the time spent in the transition and thigmotaxis zone were not significantly different compared to control animals (Fig 5.4 C, D: n=20-50, $p > 0.05$).

Individual behavior - novel object approach test

To test the anxiety-like behavior on individual fish I performed a novel object approach (NOA) test where fish explore a novel object (LEGO[®] figurine) and I measured the amount of time they spent exploring the object. CBD-treated individual fish spent significantly less time in

the center and transition zone (Fig 5.4 F, G; $n=272$, $p<0.05$), and significantly more time in the thigmotaxis area compared to control animals (Fig 5.4 H; $n=272$, $p<0.05$). The decreased times spent in the center zone and increased time spent in the thigmotaxis zone are indicative of anxiety-like behavior in CBD-treated fish.

Shoaling behavior

Next, I performed a shoaling test to determine anxiety-like behavior. Control fish exhibited a mean inter-individual distance (IID) of 7.3 ± 0.35 cm ($n = 10$ shoals) while time spent in the thigmotaxis and center zones was 244 ± 16 s and 60 ± 9 s, respectively. The total distance travelled by control fish shoals was 4265 ± 232 cm ($n = 10$ shoals). In contrast, CBD-treated fish exhibited a significantly greater mean IID of 9.7 ± 0.22 cm (Fig 5.5 A, $n = 24$, $p<0.05$) and time spent in the thigmotaxis zone was significantly increased to 385 ± 12 s (Fig 5.5 B, $n = 24$, $p<0.05$). Time spent in the center zone significantly decreased to 36 ± 3 s in CBD-treated fish compared with control animals (Fig 5.5 C, $n = 24$, $p<0.05$). However, the total distance moved by CBD-treated fish during shoaling experiments was not significantly different compared with control fish.

5.1.3 The exposure of CBD during gastrulation in F0 generation has a persistent effect on the locomotion of F1 embryos.

Burst activity of F1 embryos at 1 dpf

At 1 dpf, zebrafish embryos normally exhibit contractile coiling movements within their chorion. These burst behaviors were assessed in the embryos of adult fish that were treated with CBD while in the gastrula stage. In other words, I now tested the next generation of animals to determine if CBD-treated fish had offsprings that exhibited altered activity patterns (Fig 5.6 A, B). Embryos from CBD-treated parents exhibited significantly reduced levels of burst activity of 1.74 ± 0.15 % compare to control embryos of 2.62 ± 0.22 %, whose parents were untreated fish that were from the same batch of animals as the CBD-treated fish (Fig 5.6 C, n = 20-50, p<0.05). Similarly, the burst count per minute was significantly decreased for the embryos of CBD-treated parents (Fig 5.6 D, n = 20-50, p<0.05).

Escape response of F1 fish to touch at 2 dpf

Next, I tested whether escape responses were different in the offspring of F1 generation (5.7 A, B). I found that that the CBD-treated offspring swam a significantly shorter distance of 6.37 ± 0.7 cm compare to that of controls of 9.60 ± 1.0 cm, immediately following the C-bend (Fig 5.7 C, n = 35-39, p<0.05). Also, the escape response swim velocity of CBD-treated offspring was significantly decreased to 0.31 ± 0.03 cm/s compared with that of control animals of 0.48 ± 0.06 cm/s (Fig 5.7 D, n = 35-39, p<0.05).

Free-swimming behavior of F1 fish at 3, 4, 5 and 6 dpf

I assessed free-swimming behavior and found that the swimming distance and the activity of F1 offspring at 3 dpf and 4 dpf were not significantly different from controls (Fig 5.8 A-D, n = 77-102, $p > 0.05$). However, 5 and 6 days old offsprings of CBD-treated parents exhibited a significant reduction in the swimming distance and the activity compared with control offsprings (Fig 5.8 E-H, n = 77-94, $p < 0.05$). For instance, offsprings from CBD-treated fish had a mean swimming distance of 1243 ± 391 mm and 1125 ± 209 mm at 5 dpf and 6 dpf respectively, which were significantly shorter than the corresponding distances of 4666 ± 2240 mm and 5335 ± 1361 mm respectively covered by control animals (Fig 5.8 E and G, n = 77-94, $p < 0.05$). Similarly, the swimming activity of 5 dpf and 6 dpf offsprings of CBD-treated animals was reduced by 50% compared with control offsprings (Fig 5.8 F and H, n = 84-102, $p < 0.05$).

5.1.4 F1 embryos produced from CBD-treated parents (F0 generation) exhibited altered MN branching.

Since the F1 embryos generated from F0, CBD-exposed parents exhibited significant changes in locomotor activity I asked whether the development of the motor neurons was altered. To determine this, I immuno-labelled embryos with anti-ZnP1 to investigate the morphology of primary MNs (schematic is presented in 5.9 A, B). I found that the labeling of primary MN was significantly altered from control animals (Fig 5.9 C). Quantification of the number of ventral secondary and tertiary axonal branches emanating from the MN axon indicated a significant reduction in the number of branches in CBD-treated F0 embryos compared with controls (Fig 5.9 D and F, left pairs, n=6, $p < 0.05$). Similarly, a significant reduction of the secondary and tertiary ventral branching was observed in F1 embryos from CBD-treated parents compared with vehicle

treated F1 embryos from vehicle-treated parents (Fig 5.9 D and F, right pairs, n=6, p<0.05). In contrast to the ventral branch patterns, I observed an interesting trend in the number of secondary and tertiary dorsal branches. In the case of F0 embryos, only the number of tertiary dorsal branches was significantly reduced by CBD exposure compared with vehicle controls (Fig 5.9 G, left pairs, n = 6, p<0.05). Interestingly, the number of secondary and tertiary dorsal branches of F1 embryos from CBD-treated parents was significantly increased compared with F1 embryos from vehicle treated parents (Fig 5.9 E and G, right pairs, n = 6, p<0.05).

5.1.5 Brief embryonic exposure of CBD altered the gene expression in F0 and F1 generations

Because there were significant changes in the locomotor activity and developmental morphology of MNs in F1 embryos from CBD-exposed parents, I asked whether there were any changes in gene expression in these animals. Therefore, I examined the gene expression of developmental biomarkers such as *c-fos*, *bdnf*, *sox-2* and *nrf2*. CBD exposure during gastrulation in the F0 generation caused a significant reduction in the expression of *bdnf* and *sox-2* in F0 animals, whereas *c-fos* and *nrf2* expression was unchanged (Fig 5.10 A, n=6, p<0.05). In contrast, there were fewer changes in the gene expression in F1 generation. Specifically, only the expression of *c-fos* and *bdnf* were significantly reduced whereas the expression of *sox2* and *nrf2* remained unchanged (Fig 5.10 B, n=6, p<0.05).

5.1.6 Embryonic exposure of CBD affected the expression of ECS genes in F0 and F1 generations

Next, I asked if CBD exposure during gastrulation in F0 generation altered the expression of ECS genes in the F0 and F1 generations. Since the ECS consists of several types of receptors, and endocannabinoid synthesizing and degrading enzymes, I tested the expression of genes encoding receptors: CB₁R, CB₂R, TRPV₁, GPCR55 and *Cnrip1a*; eCB synthesizing enzymes: *Nape-pld*, *abhd4*, *gde*, *dagla* and *daglb*; and eCB degrading enzymes: *faah*, *mgll*, *abhd6a*, *abhd6b* and *abhd12*. I found that CBD treatment led to a reduction in the expression of genes encoding for GPCR55 and *cnrip1a* in the CBD-exposed F0 generation (Fig 5.11 A, n=6-8, p<0.05). Among the AEA synthesizing enzymes (*Nape-pld*, *abhd4* and *gde*) in the F0 generation, only *Nape-pld* expression was significantly reduced by CBD treatment (Fig 5.11 B, n=6, p<0.05). However, the gene expression of both 2-AG synthesizing enzymes, *dagla* and *daglb*, were significantly reduced in F0 generation fish exposed to CBD (Fig 5.11 D, n=6-8, p<0.05). The gene expression of the AEA degrading enzyme (*faah*) F0 animals was not affected by embryonic CBD exposure whereas the gene expression of the 2-AG degrading enzymes, *abhd6a* and *abhd6b*, were significantly decreased in CBD-treated F0 generation animals (Fig 5.11 E, n=6-8, p<0.05).

When examining the F1 generation, I found that CBD exposure at gastrulation of F0 embryos had also prominent effect on eCB synthesizing and degrading enzymes in F1 generation fish relative to F0 animals. For instance, CBD exposure only significantly reduced the gene expression of *abhd6a* (2-AG degrading enzyme) in F1 generation (Fig 5.12 E, n=6-8, p<0.05) while the expression of other eCB synthesizing and degrading enzyme genes remained

unchanged. Unlike the situation with F0 animals, F1 animals from CBD-treated parents had significantly elevated expression levels of *cbr2* and *gpr55* receptor genes relative to progenies of vehicle-treated parents; in contrast, *cnrip1a* expression was depressed as in the F0 animals exposed to CBD (Fig 5.11 A, n=6-8, p<0.05).

Together these results indicate that CBD treatment of zebrafish embryos led to locomotor, motor neuron and genetic changes that persisted into adulthood and even into the next generation of animals.

Figure 5. 1 Effect of CBD exposure on spontaneous coiling activity in F0 embryos at 1 dpf

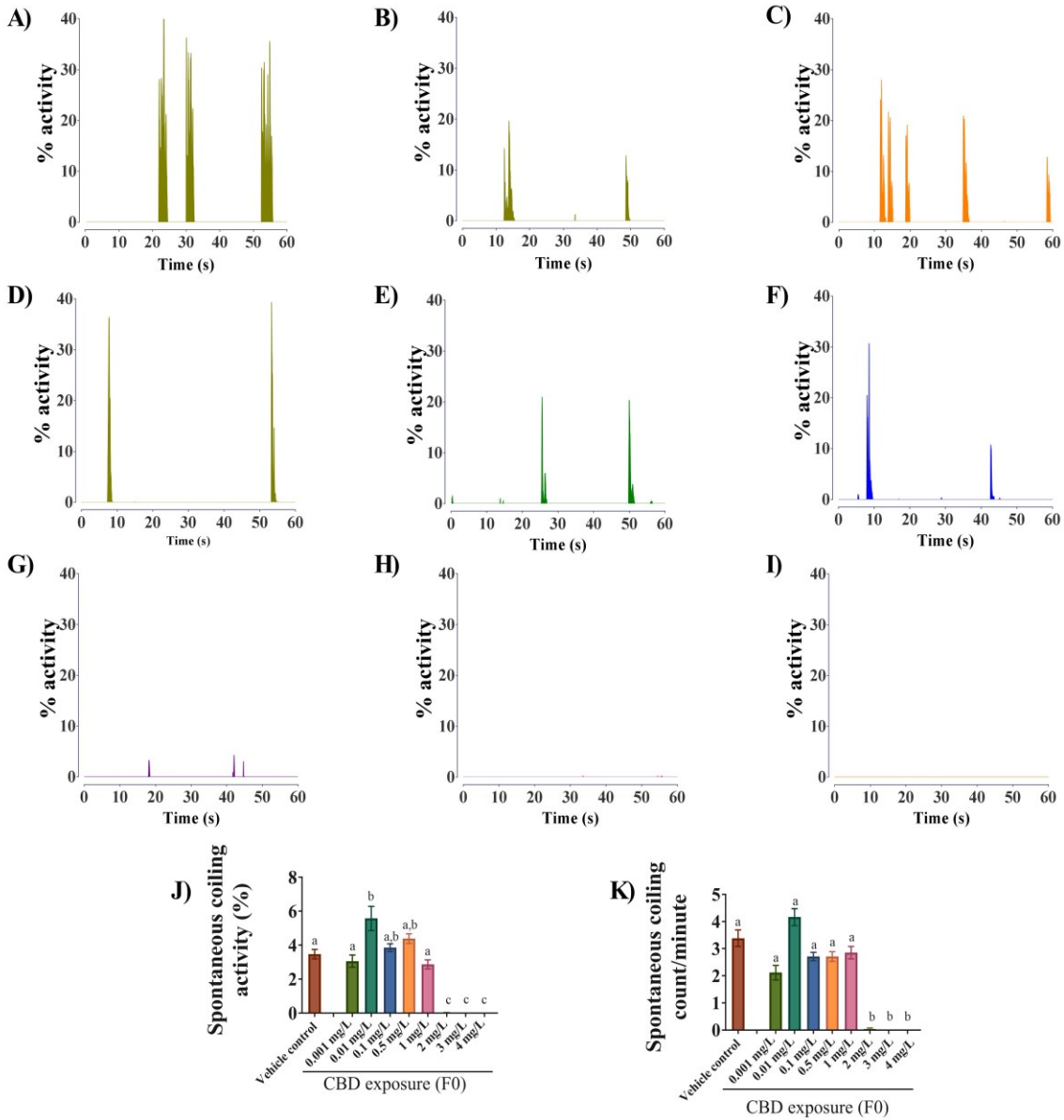
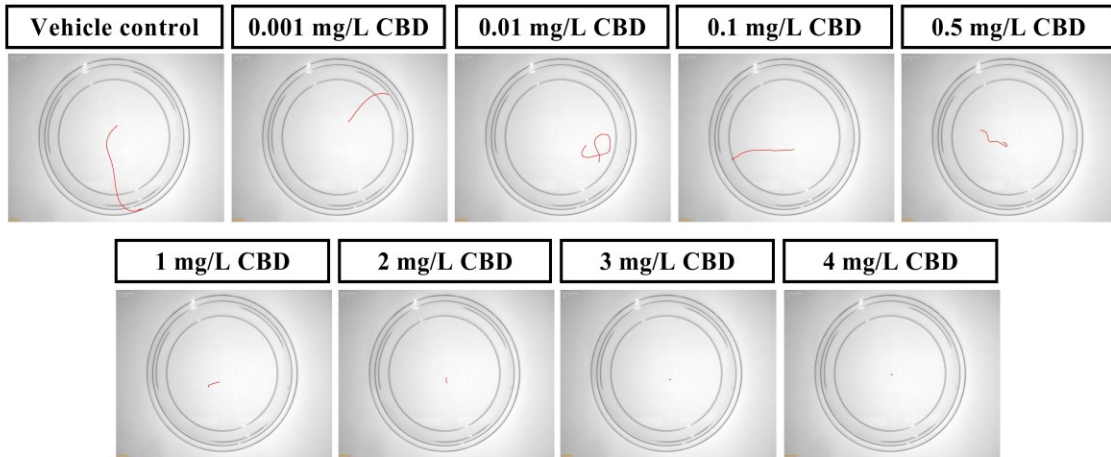


Figure 5.1 Effect of CBD exposure on spontaneous coiling activity in F0 embryos at 1 dpf.

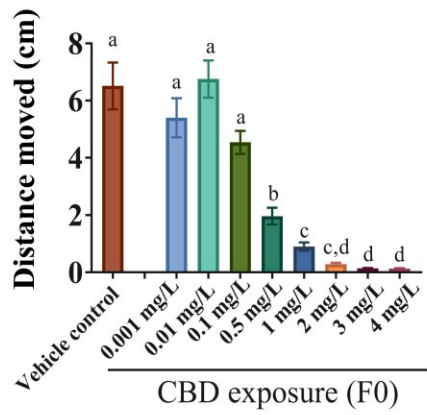
Spontaneous coiling was recorded from F0 embryos at 1 dpf; treated with vehicle, 0.001, 0.01, 0.1, 0.5, 1, 2, 3 and 4 mg/L CBD, respectively. (A-I) Representative traces of spontaneous coiling activity over a minute period is shown for vehicle, 0.001, 0.01, 0.1, 0.5, 1, 2, 3 and 4 mg/L CBD treatment, respectively. (J) Bar graph represents mean spontaneous coiling activity. (K) Bar graph represents mean spontaneous coiling count/minute. N = 3 experiments and n = 20 embryos for each treatment. Significance was determined using Kruskal-Wallis tests followed by Dunn's multiple comparison test. Groups which share the same letter(s) of the alphabet are not statistically different from one another.

Figure 5. 2 Brief exposure of CBD affect the escape behavior at 2 dpf

A)



B)



C)

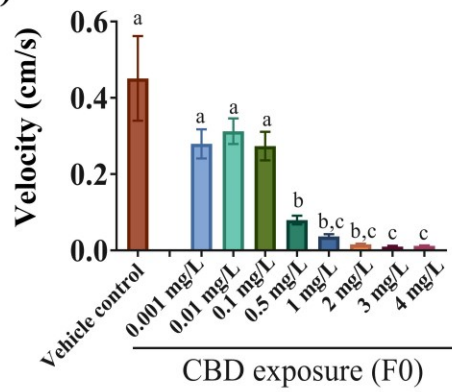


Figure 5.2 Brief exposure of CBD affect the escape behavior at 2 dpf. Escape locomotion was recorded from F0 embryos in response to touch at 2 dpf. (A) Traces of escape behavior in response to touch near head region is shown for vehicle, 0.001, 0.01, 0.1, 0.5, 1, 2, 3 and 4 mg/L CBD treatments. (B) Bar graph represents mean distance travelled by embryos in response to touch. (C) Bar graph represents mean velocity exhibited by embryos during escape responses. N=5 experiments and n = 20 embryos for each treatment. Significance was determined using Kruskal-Wallis tests followed by Dunn's multiple comparison test. Groups which share the same letter(s) of the alphabet are not statistically different from one another.

Figure 5. 3 Effect of CBD exposure on free swimming at 3-6 dpf

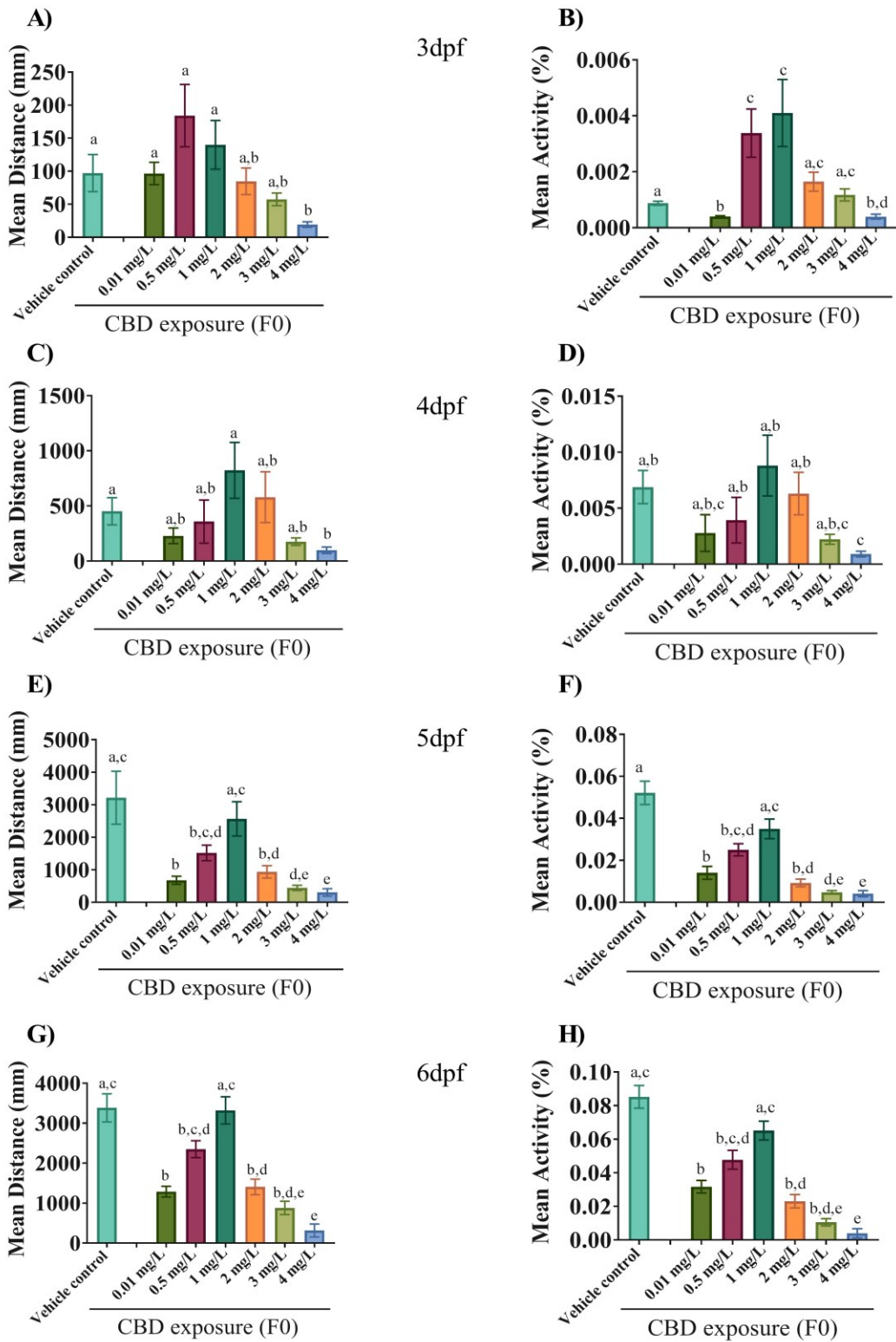
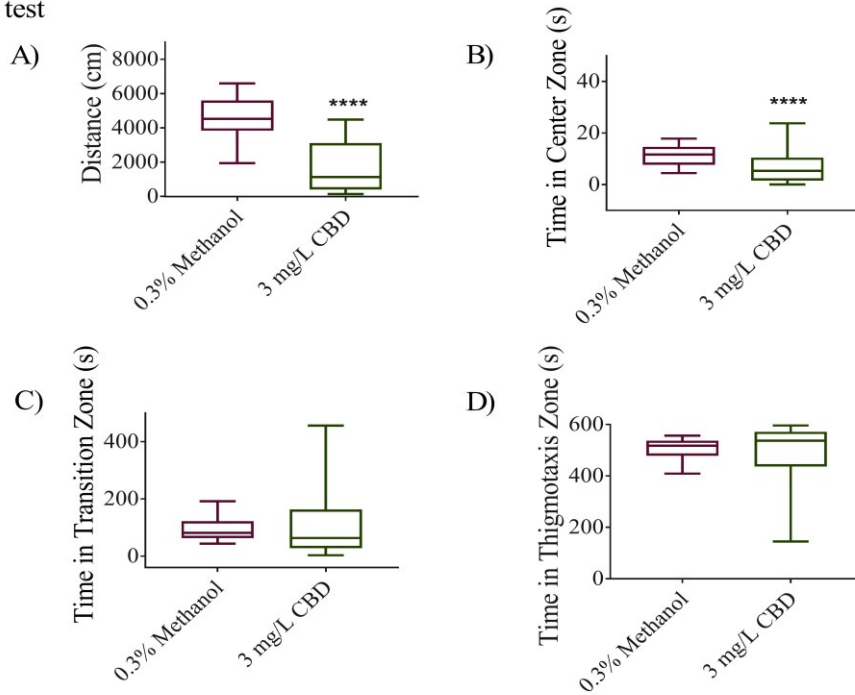


Figure 5.3 Effect of CBD exposure on free swimming at 3-6 dpf. Free-swimming behavior in 3-6 dpf larvae was determined through recording 1 hr of the free-swimming activity of individual larvae; F0 embryos were treated with vehicle, 0.01, 0.5, 1, 2, 3 and 4 mg/L CBD, respectively. (A, B) Free-swimming behavior output from 3 dpf larvae. (A) Bar graph shows mean distance travelled by embryos. (B) Bar graph shows mean activity (%). (C, D) Free-swimming behavior output from 4 dpf larvae. (C) Bar graph shows mean distance travelled by embryos. (D) Bar graph shows mean activity (%). (E, F) Free-swimming behavior output from 5 dpf larvae. (E) Bar graph shows mean distance travelled by embryos. (F) Bar graph shows mean activity (%). (G, H) Free swimming behavior output from 6 dpf larvae. (G) Bar graph shows mean distance travelled by embryos. (H) Bar graph shows mean activity (%). N=5 experiments and n = 20 embryos for each treatment. Significance was determined using Kruskal-Wallis tests followed by Dunn's multiple comparison test. Groups which share the same letter(s) of the alphabet are not statistically different from one another.

Figure 5. 4 Brief exposure of CBD during gastrulation alters the locomotion in adults

Open Field test



Novel Object Approach test

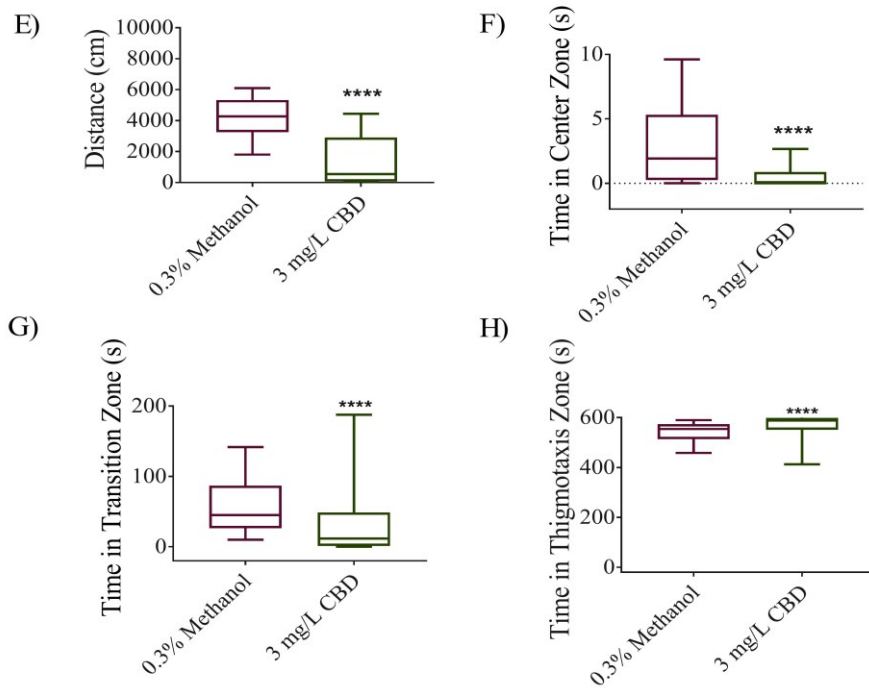


Figure 5.4 Brief exposure of CBD during gastrulation alters the locomotion in adults. Adult zebrafish exhibited alteration in their behavior following a brief exposure of CBD (3mg/L) in F0 embryos. Open field tests in individual adults (panels A – D). Open field test was carried out on adult fish following an exposure to vehicle (n = 25) or 3 mg/L of CBD (n = 20) during gastrulation in F0 embryos. Here, the data is presented in box whisker plots (A-H); lines show the median, the box extends from the 25th to the 75th percentile, and range indicate minimum to maximum. (A) Box plot shows mean distance travelled. (B) Box plot shows time spent in center zone. (C) Box plot shows time spent in the transition zone. (D) Box plot shows time spent in the thigmotaxis zone. (E-H) Novel object approach tests in individual adults. Panels E-H show key novel object approach test outcomes from adult fish following exposure to vehicle (n = 25) or 3 mg/L of CBD (n = 20) during gastrulation in F0 embryos. (E) Box plot shows time spent in center zone. (F) Box plot shows time spent in the transition zone. (G) Box plot shows time spent in the thigmotaxis zone. (H) Box plot shows mean distance travelled. Significance was determined using a non-parametric Mann-Whitney test. **** Significantly different from vehicle control, p <0.0001.

Figure 5. 5 Treatment of CBD in F0 embryos caused an anxiety-like behavior in adult zebrafish

Shoaling test

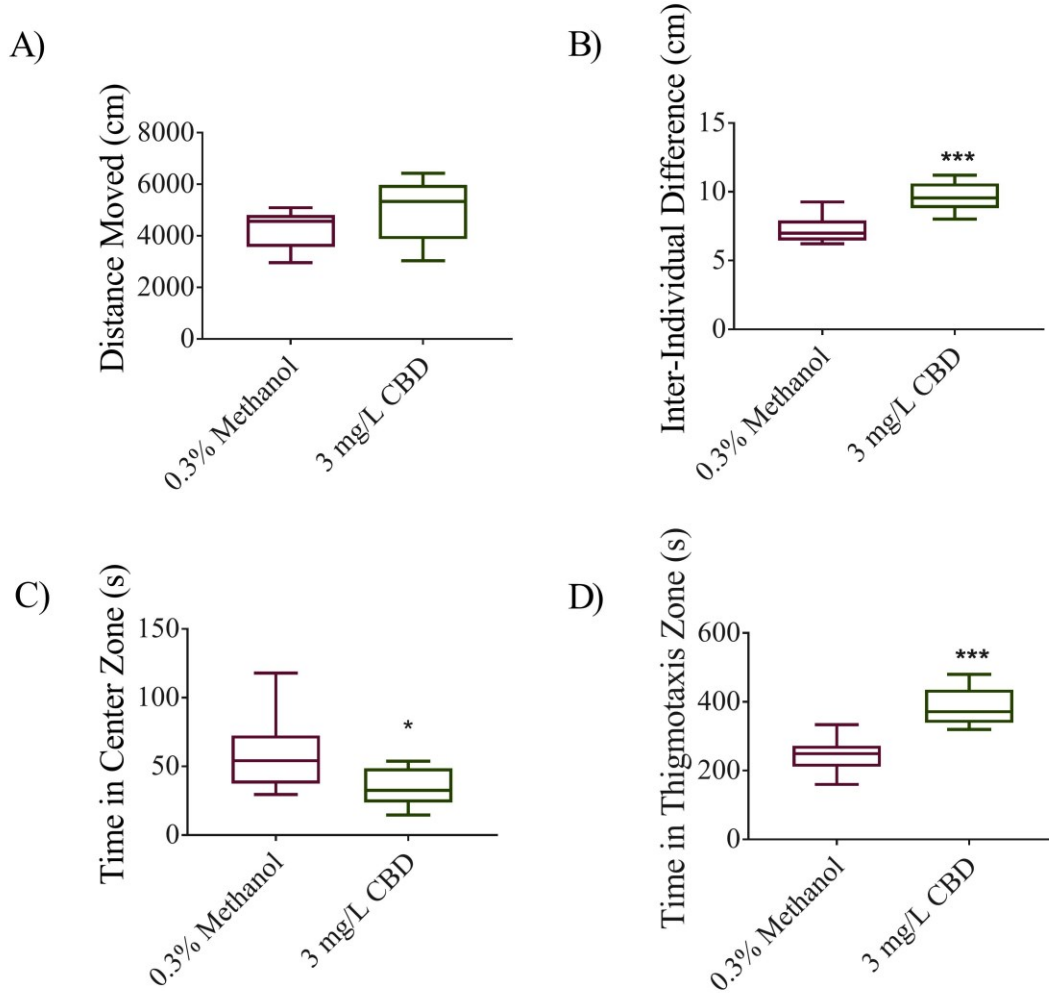


Figure 5.5 Treatment of CBD in F0 embryos caused an anxiety-like behavior in adult zebrafish. Shoaling tests were performed with groups of 5 adults previously exposed to either vehicle (n = 25) or 3 mg/L of CBD (n = 20) during gastrulation as F0 embryos. Here, the data is presented in box whiskers plots (A-D); the line shows the median, the box extends from the 25th to the 75th percentile, and the range indicates the minimum to maximum values. (A) Box-whiskers plot shows the inter individual distance (cm). (B) Box-whiskers plot shows the time spent (s) in the thigmotaxis zone. (C) Box-whiskers plot shows the time spent (s) in the center zone. (D) Box-whiskers plot shows the distance moved. Significance was determined using a non-parametric Mann-Whitney test. *** Significantly different from vehicle control, $p < 0.001$, * $p < 0.05$.

Figure 5. 6 Unexposed F1 embryos showed altered spontaneous coiling activity following CBD exposure in F0 embryos

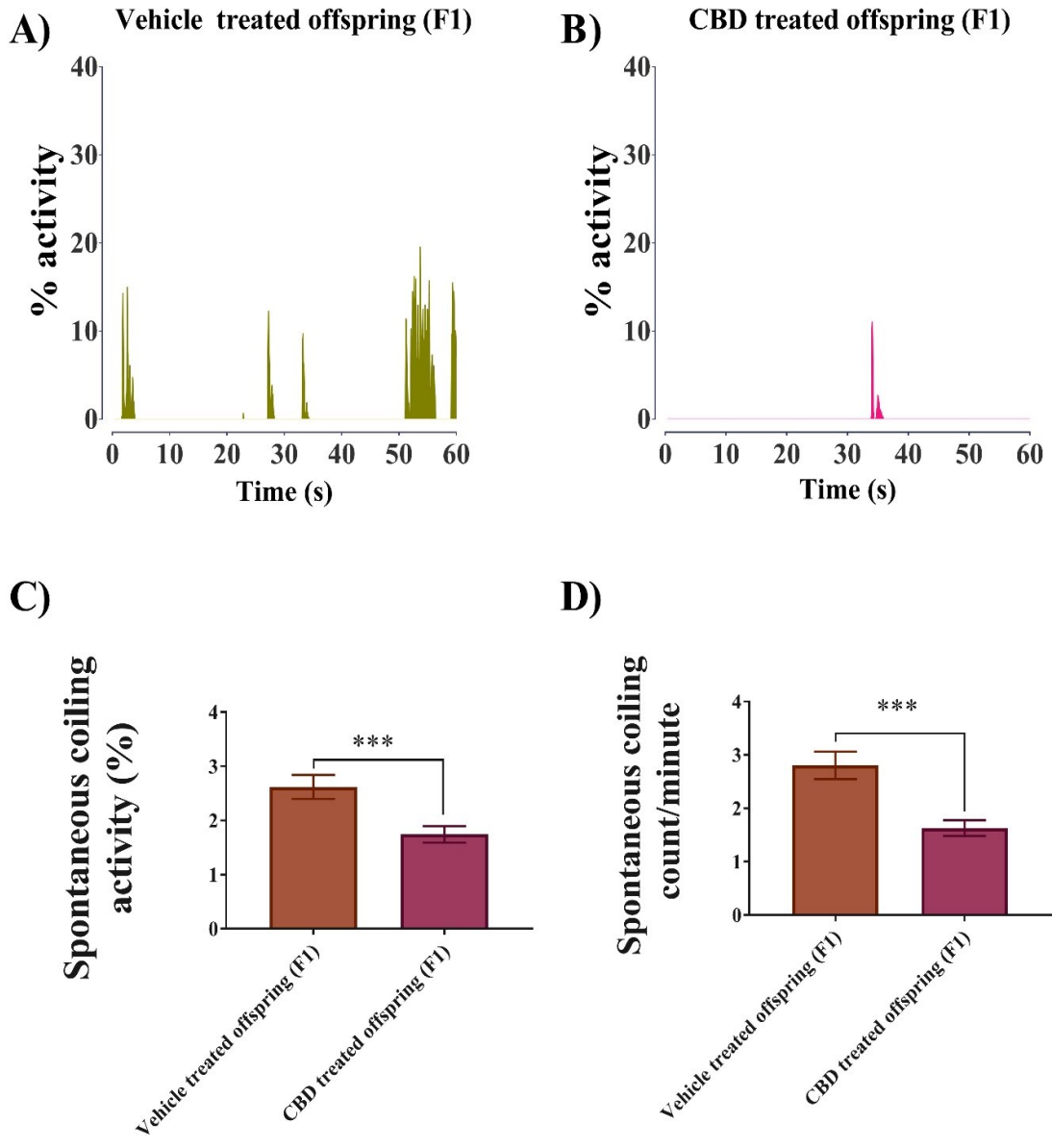
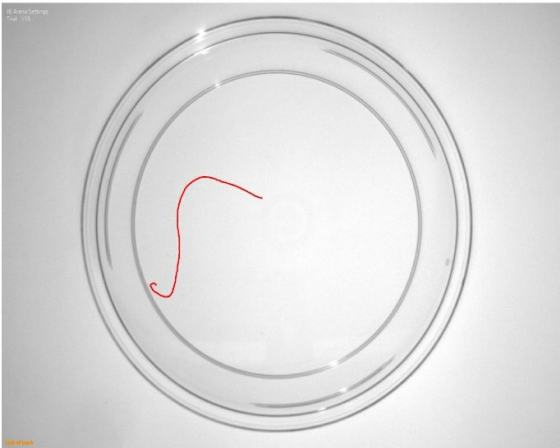


Figure 5.6 Unexposed F1 embryos from parents treated with CBD as F0 embryos during gastrulation showed altered spontaneous coiling activity at 1 dpf. Spontaneous coiling was recorded from unexposed F1 embryos at 1 dpf; F1 embryos were collected from either vehicle or 3 mg/L CBD-treated parents. (A) Representative traces of spontaneous coiling activity over a minute period is shown for unexposed F1 embryos from vehicle-treated parents. (B) Traces of spontaneous coiling activity over a minute period are shown for unexposed F1 embryos from CBD-treated parents. (C) Bar graph represents mean spontaneous coiling activity (D) Bar graph represents mean spontaneous coiling count/minute. N=5 experiments. Significance was determined using a non-parametric Mann-Whitney test. *** Significantly different from vehicle control, $p < 0.001$.

Figure 5. 7 Untreated F1 embryos exhibited decreased escape behavior following brief exposure in F0 generation

A) Vehicle treated offspring (F1)



B) CBD treated offspring (F1)

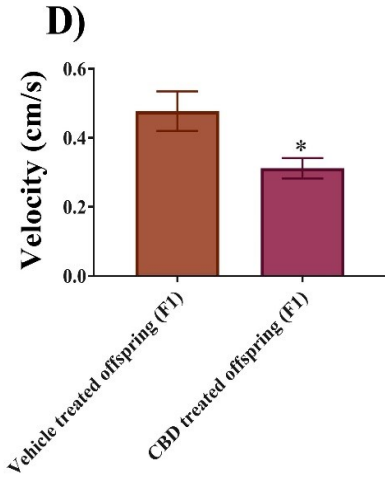
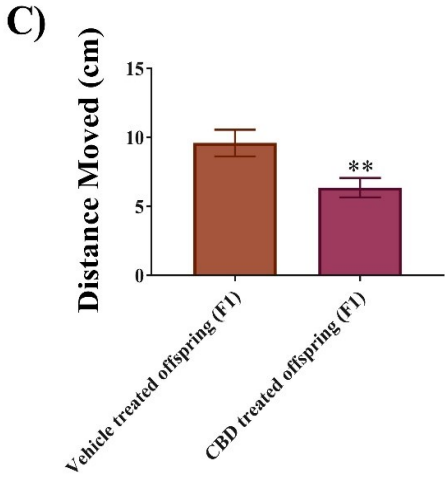
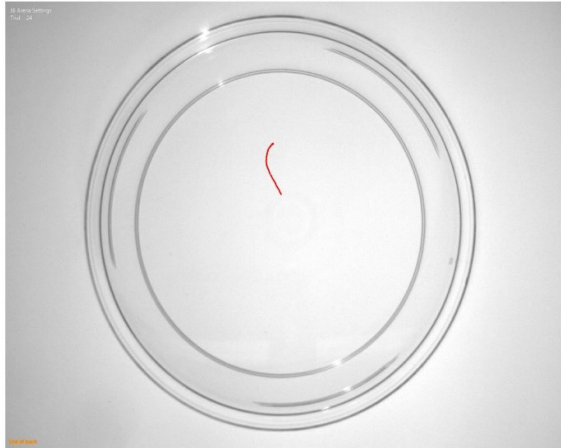


Figure 5.7 Untreated F1 embryos from parents that had been briefly exposed to CBD during gastrulation as F0 embryos exhibited decreased escape behaviour. Escape locomotion was recorded from in response to touch at 2 dpf; F1 embryos were collected from either vehicle- or 3 mg/L CBD-treated parents. (A) Representative traces of escape behavior in response to touch is shown for unexposed F1 embryos from vehicle treated parents. (B) Traces of escape behavior in response to touch is shown for unexposed F1 embryos from 3 mg/L CBD treated-parents. (C) Bar graph represents mean distance travelled by embryos in response to touch. (D) Bar graph represents mean velocity exhibited by embryos during escape response. N=5 experiments. Significance was determined using a non-parametric Mann-Whitney test. ** Significantly different from vehicle control, $p < 0.01$, * $p < 0.05$.

Figure 5. 8 Untreated F1 embryos showed altered free swimming following an exposure of CBD in F0 embryos

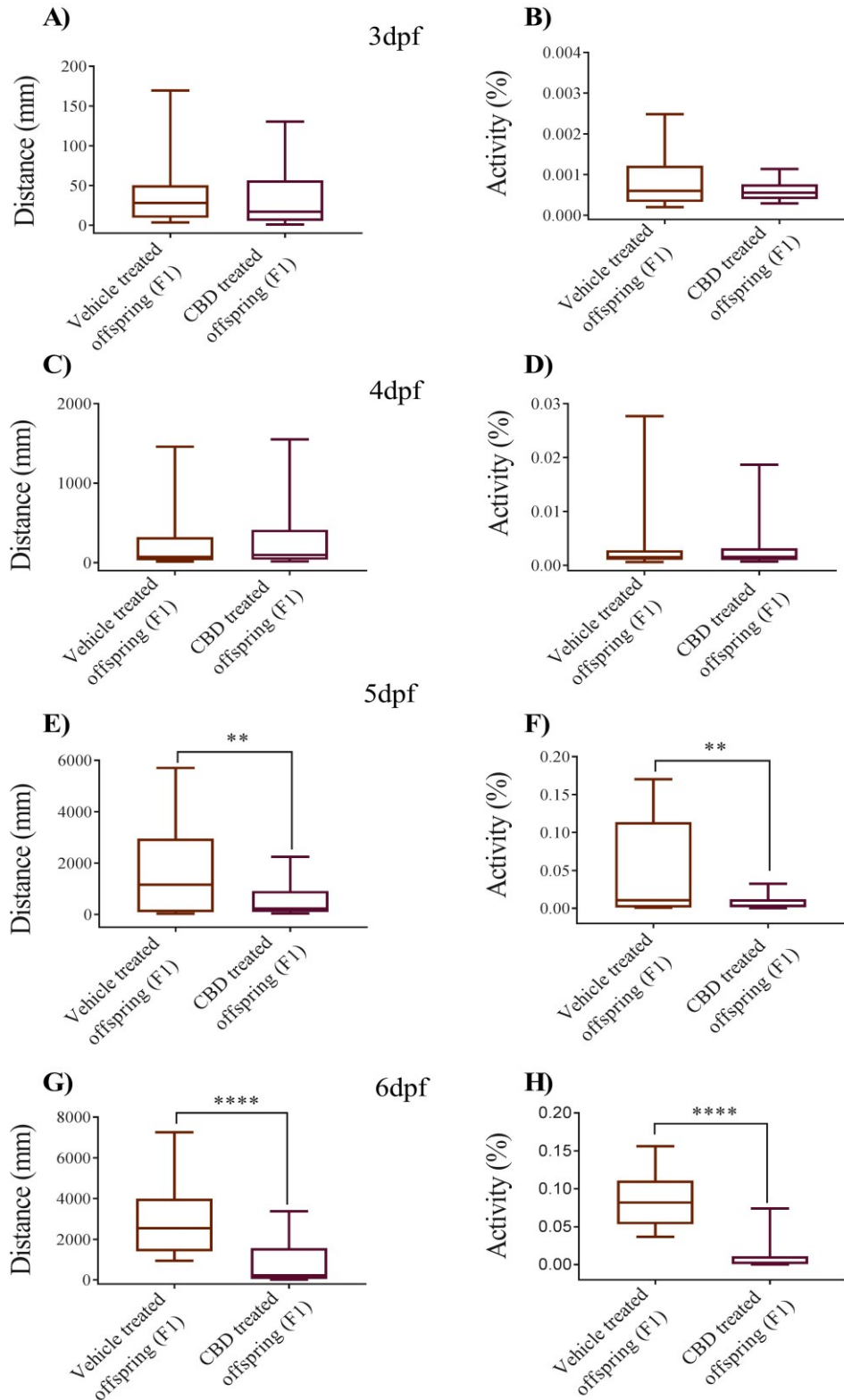


Figure 5.8 Untreated F1 embryos from parents exposed to CBD during gastrulation as F0 embryos showed altered free-swimming behavior. Free swimming behavior of unexposed F1 larvae was determined through recording 1 hr of the free-swimming activity of individual larvae; F1 embryos were collected from either vehicle or 3 mg/L CBD-treated parents. (A-H) Free swimming behavior output for 3-6 dpf larvae. Here, the data is presented in box whiskers plots (A-D); the line shows the median, the box extends from the 25th to the 75th percentile, and the range indicates the minimum to maximum values. (A and B) box plot shows the distance (mm) and activity (%) exhibited, respectively, by embryos at 3 dpf. (C and D) box plot shows the distance (mm) and activity (%) exhibited, respectively, by embryos at 4 dpf. (E and F) box plot shows the distance (mm) and activity (%) exhibited, respectively, by embryos at 5 dpf. (G and H) box plot shows the distance (mm) and activity (%) exhibited, respectively, by embryos at 6 dpf. N=5 experiments. Significance was determined using a non-parametric Mann-Whitney test. **** Significantly different from vehicle control, $p < 0.0001$, ** $p < 0.01$.

Figure 5. 9 Primary MN staining of F1 embryos showed an altered branching pattern

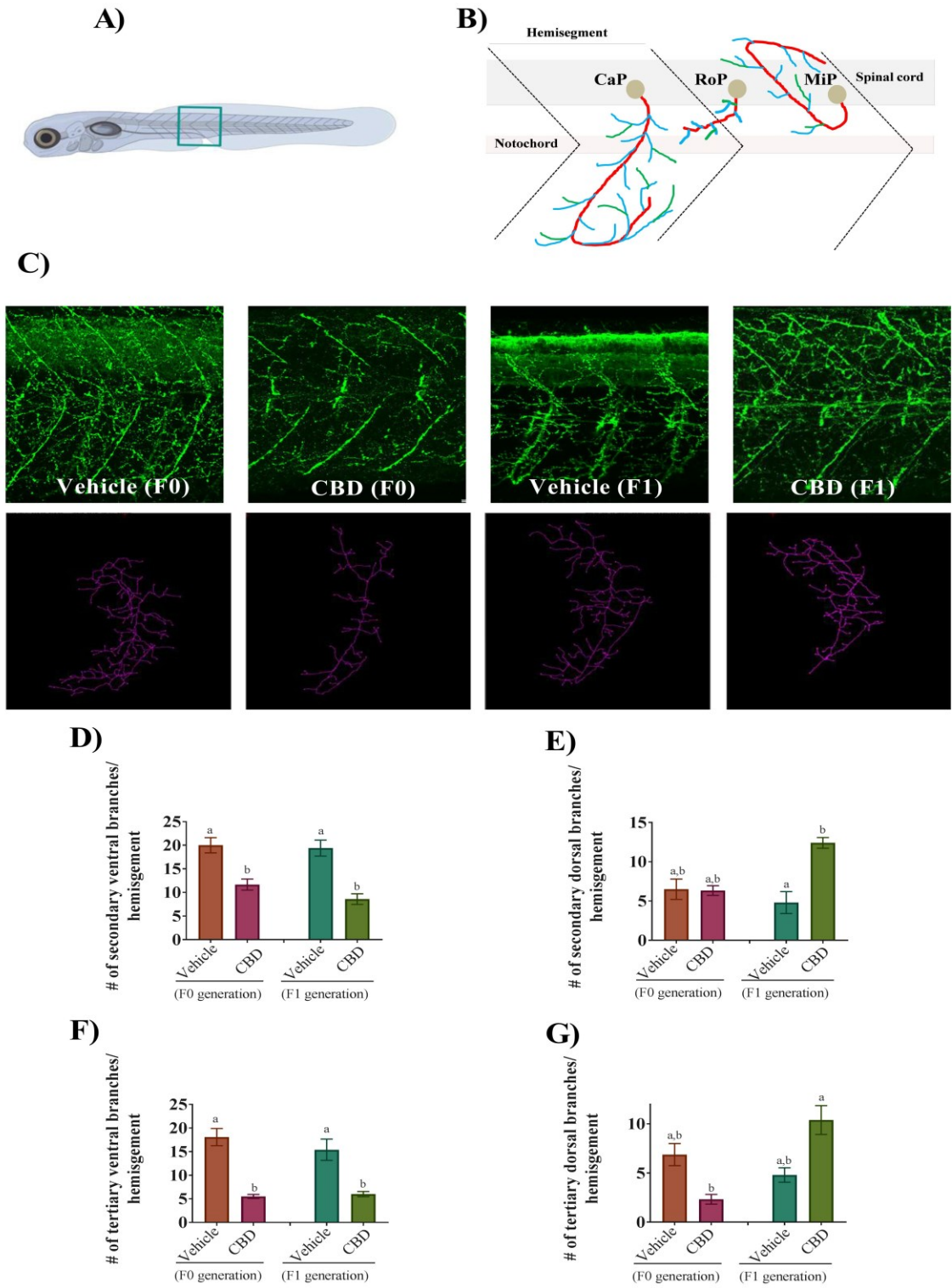
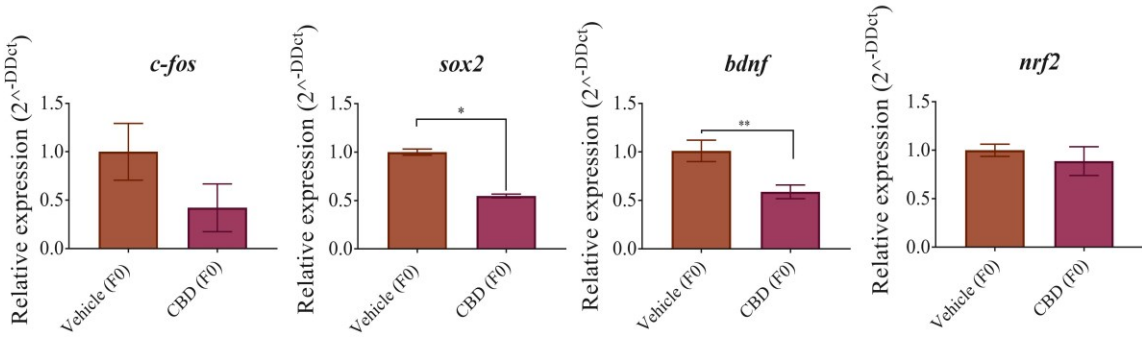


Figure 5.9 Primary MN staining of F1 embryos from parents that had been briefly exposed to 3 mg/L CBD as F0 embryos during gastrulation showed an altered neuronal branching pattern. (A) Schematic of an embryo showing the area where I focused for performing immunostaining. (B) Schematic shows three types of primary MN: CaP (caudal), RoP (rostral) and MiP (middle). (C) Anti- Znp1 staining was used to immunelabel axonal branching of MN in vehicle-treated F0 embryos (n = 6), CBD-treated F0 embryos (n = 6), unexposed F1 embryos from vehicle-treated parents (n = 6) and unexposed F1 embryos from CBD-treated parent (n = 6), respectively (top panel). Representative tracing of MN branching (using image J) in a hemi segment of an embryo (bottom panel). (D, E) Bar graph shows the number of secondary ventral and dorsal branches emanating from the main axon. (F, G) Bar graph shows the number of tertiary ventral and dorsal branches emanating from the main axon. Significance was determined using Kruskal-Wallis tests followed by Dunn's multiple comparison test. Groups which share the same letter(s) of the alphabet are not statistically different from one another.

Figure 5. 10 RT-qPCR of neuronal marker genes

A)



B)

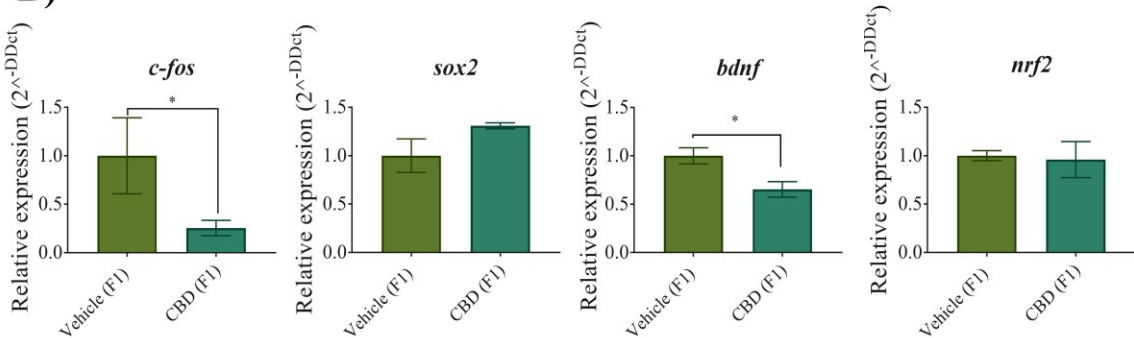


Figure 5.10 RT-qPCR of neuronal marker genes. Expression of neuronal marker genes such as *c-fos*, *sox2*, *bdnf*, *nrf2* as compared with reference gene *actb1*. (A) Bar graph shows the relative expression of neuronal marker genes of vehicle-treated or 3 mg/L CBD-treated embryos (F0 generation). (B) Bar graph shows the relative expression of neuronal marker genes of unexposed embryos (F1 generation) from parent fish that were either exposed to vehicle or CBD as F0 embryos. Significance was determined using a non-parametric Mann-Whitney test. ** Significantly different from vehicle control, $p < 0.01$, * $p < 0.05$.

Figure 5. 11Gene expression of endocannabinoid system related genes (F0 embryos)

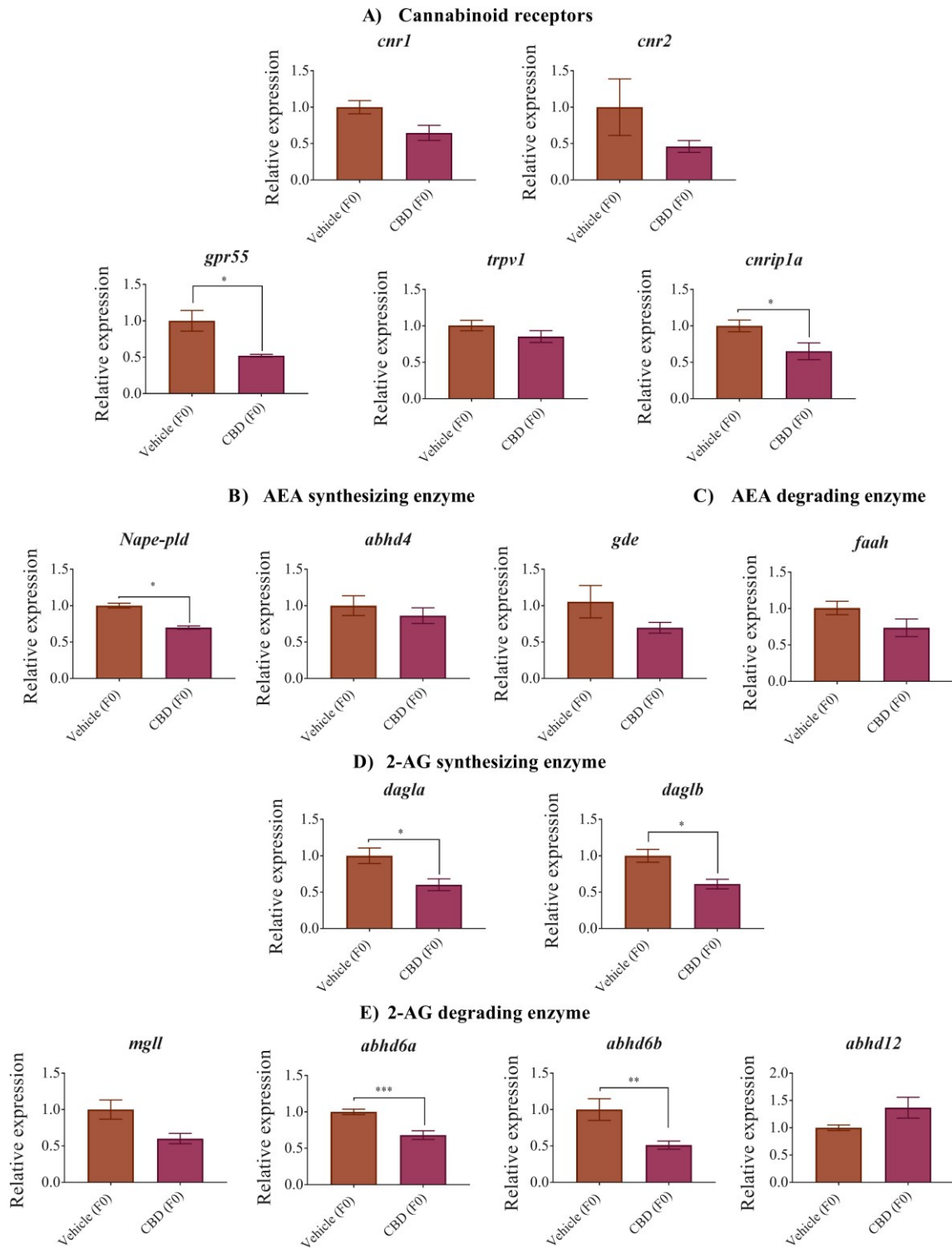


Figure 5.11 RT-qPCR of ECS-related genes in F0 embryos exposed briefly to 3 mg/L CBD.

Bar graphs show differential expression of genes encoding. (A) cannabinoid receptors (*cb1r*, *cb2r*, *gpcr55*, *trpv1*, *cnip1a*), (B) AEA synthesizing enzymes (*nape-pld*, *abhd4*, *gde*), (C) AEA degrading enzyme (*faah*), (D) 2-AG synthesizing enzymes (*dagla*, *daglb*), and (E) 2-AG degrading enzymes (*mgll*, *abhd6a*, *abhd6b* and *abhd12*) as compared with reference gene *actb1*. Significance was determined using a non-parametric Mann-Whitney test. *** Significantly different from vehicle control, $p < 0.001$, ** $p < 0.01$, * $p < 0.05$.

Figure 5. 12 Gene expression of endocannabinoid system related genes (of F1 embryos)

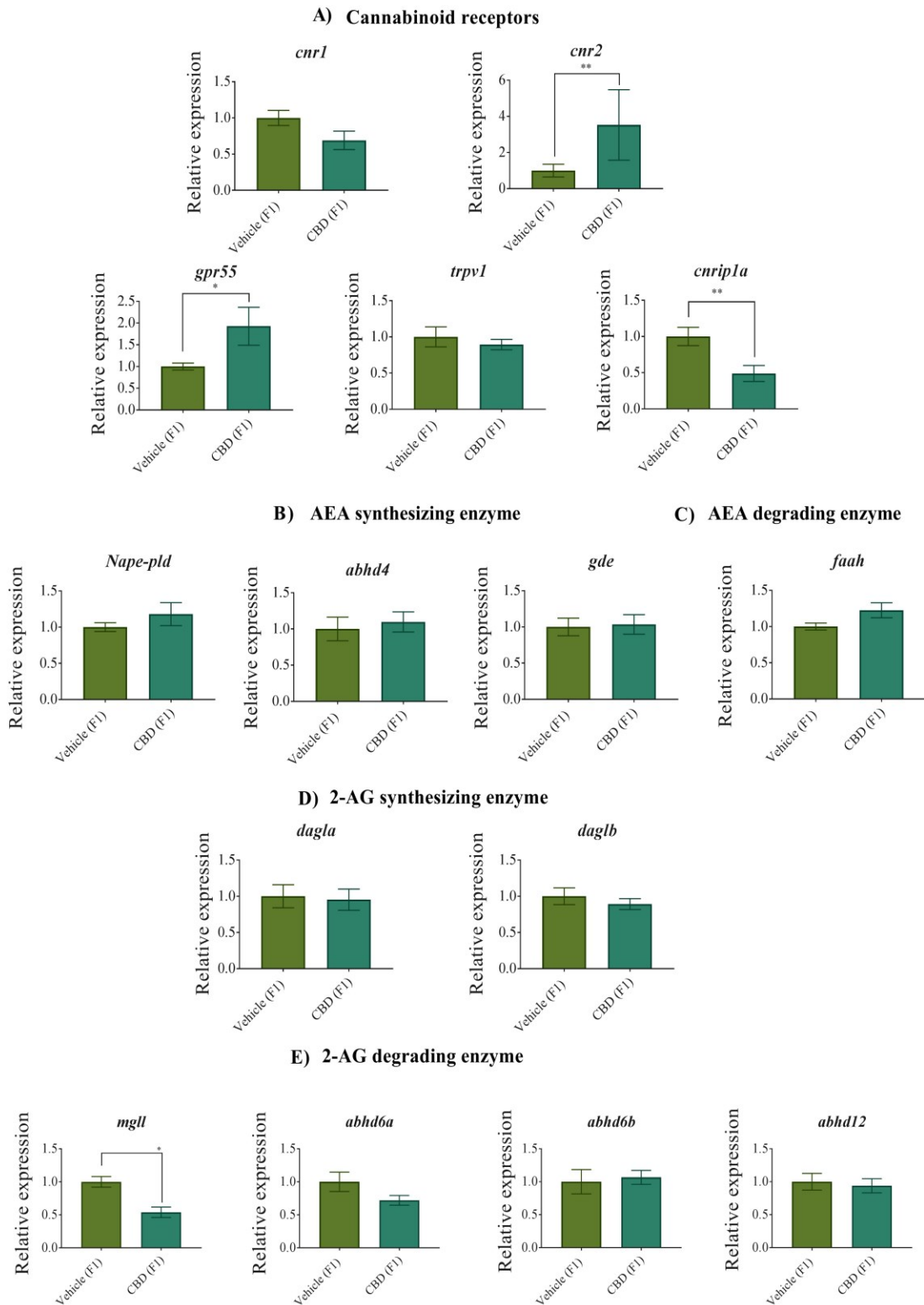


Figure 5.12 Relative gene expression of ECS-related genes of untreated F1 embryos from parents exposed briefly to either vehicle or 3 mg/L CBD as F0 embryos during gastrulation. Bar graphs show relative expression of (A) cannabinoid receptor genes (*cnr1*, *cnr2*, *gpr55*, *trpv1*, *cnip1a*), (B) AEA synthesizing enzyme genes (*nape-pld*, *abhd4*, *gde*), (C) AEA degrading enzyme gene (*faah*), (D) 2-AG synthesizing enzyme genes (*dagla*, *daglb*), and (E) 2-AG degrading enzyme genes (*mgl1*, *abhd6a*, *abhd6b* and *abhd12*) as compared with reference gene *actb1*. Significance was determined using a non-parametric Mann-Whitney test. *** Significantly different from vehicle control, $p < 0.001$, ** $p < 0.01$, * $p < 0.05$.

Table 5. 1 List of primers used for RT-qPCR

Gene name	Forward	Reverse
<i>cnr1</i>	CCCCTGCAGCTGGATAACAG	GCGATTTTCACAGTGGTCTTGA
<i>cnr2</i>	CACACTTTTAGTTTGATCCTTCTAAT CC	GTGAACTCTTGTGTAAACCCTC TTCTCTAT
<i>c-fos</i>	TGTTACCTACCCAGAAAACGA	GTCGGACGACTGATCATTGCT
<i>gpr55</i>	TCTGGCATGCTTCATTCCTTATC	TGTCTTCGTTCCAGTTGTTCGT
<i>mgl1</i>	GTTCTAAACCGCTTGGCTCCTA	CTGTTTGGGATCCCGTGAGA
<i>naple-pld</i>	CGTTTCCTTTATCCTATGAGCATTAT C	GATTAAGTCCAAGATTACCAT TGC
<i>nrf2</i>	AGGCTTTCTCGCCTAACGAAT	AGAGTCTTTTTAAGGCGAGGAA CTAG
<i>sox2</i>	AACGGCTCGCCACCTA	CCACCGAGCCCATGGA
<i>abhd4</i>	AACACCGTCGCCCAGATC	GTAGACGTGATGGGAAGCATCT T
<i>abhd6a</i>	TTGGAGCGGCCTAGAAAATCT	GAGTTTCTTGTTGCTGTTGATTCT CT
<i>abhd6b</i>	GCAAGTTTGACAGTCAGATGCAT	GGAGTGGAGGGAATAAGTGGA A
<i>aAbhd12</i>	CTCCTCATCCCCACGGTTAG	AGAGCCGGAGTGTCTTGAGTTC
<i>cnrip1a</i>	CCAAGAGTGGAGACAGACAACCT	GCCAGACGGTTTCGAACATC
<i>dagla</i>	TCTCCCGCTGATGGAGTGTT	CATAGACGACAATGCAGTTTCC TT
<i>daglb</i>	TTCTCGCAGGTCAGGTATCGA	GTCCGGCATGTGGTCTTTG
<i>faah</i>	TGGATATTTTGTTGTGTCCCATTC	GGTTGTAGAGGGTGGTGTAACT GA
<i>gdel</i>	CCTCTGAACAAGCTGCTCTTCTC	GGAAACGGTCGCTGAATCTG
<i>trpv1</i>	GTGGAACAGGAACATGGGTATAATA A	CACGACTGGGCTCTCTCTGAA
<i>actb1</i>	CGAGCAGGAGATGGGAACC	CAACGGAAACGCTCATTGC

Chapter 6

Cannabinoid receptor 2 (CB₂R) mediates cannabinol (CBN)-induced developmental defects in zebrafish

In the present study, I examined the effects of a range of CBN concentrations (0.01-4 mg/L) on zebrafish development. To my knowledge, this is the first study to report the effect of CBN on neuronal development in embryos.

In this study, I sought to determine if exposure to CBN during gastrulation, altered zebrafish embryonic development via acting through the endocannabinoid receptors CB₁R and CB₂R. I specifically focused the exposure paradigm on a critical stage of early embryonic development known as gastrulation, which occurs 5 hours after egg fertilization in zebrafish. During gastrulation the differentiation of cell lines occurs and embryogenesis starts. In zebrafish, gastrulation occurs between 5.25 hours post fertilization (hpf) and 10.75 hpf (Kimmel et al., 1995). My results indicate that embryonic morphology, heart rate, neuronal branching, locomotor responses and hair cell development are adversely affected by exposure to CBN, and that these effects are mediated through the CB₂Rs.

6.1 Results

6.1.1 CBN affects gross morphology, heart rate, MN development, locomotion and hair cell development

In this study I set out to determine the effect of early cannabinol exposure on zebrafish development. To do this I exposed embryos during the gastrulation stage (from 5 hpf to 10.75 hpf) to concentrations of CBN ranging from 0.01 mg/L to 4 mg/L. I observed significant morphological defects in embryos exposed to CBN at concentrations above 1 mg/L (Fig 6.1 A; n=42, P<0.001), but there were no obvious effects at concentrations of 0.5 mg/L and below. Animals treated with 2, 3 and 4 mg/L CBN exhibited pericardial edema at rates of 26 ± 13 , 36 ± 9 and $56 \pm 14\%$, respectively, compared with vehicle controls of $4 \pm 2\%$ (Fig. 6.2 B). Similarly, there was a significantly higher incidence of axial malformations ranging from mean values of 12% to 82% in animals treated with 1 to 4 mg/L CBN, compared with vehicle mean values of 3% (Fig 6.2 C). Embryos exposed to vehicle controls exhibited a body length of 3.15 ± 0.01 mm while embryos exposed to 0.01-0.5 mg/L had body lengths ranging from 3.08 ± 0.01 to 3.06 ± 0.02 mm. However, embryos exposed to 3 and 4 mg/L CBN had shorter body lengths of 2.48 ± 0.1 mm and 2.45 ± 0.12 mm, respectively (Fig 6.1 B; n=20-30; p<0.001).

There was a dose-dependent effect of CBN on survival, where animals treated with 0.01 mg/L had a survival rate of $83.8 \pm 3.8\%$, which was similar to controls. The rate of survival decreased to $9.6 \pm 4.6\%$ for animals treated with 4 mg/L CBN (Fig 6.1 C; n=100-120; P<0.001). Similarly, the hatching rate was significantly reduced with exposure to increasing concentrations of CBN (Fig 6.2 A). Taken together, these data show that when the exposure concentration was above 0.5 mg/L, CBN has an obvious impact on embryonic development.

In a previous study, I found that exposure to THC and CBD during gastrulation severely affected heart rate in zebrafish embryos (Ahmed et al., 2018). In the present study, I obtained similar results for exposure to CBN, such that quantification of cardiac activity at 2 dpf showed a significant reduction in heart rate for animals treated with CBN at 2 mg/L or higher (Fig 6.1 D; $n=20-50$; $p < 0.01$). Specifically, animals treated with 2 mg/L CBN exhibited a heart rate of 81 ± 3 beats per minute (bpm), which is significantly less than control heart rates of 102 ± 3 bpm. Embryos treated with 4 mg/L CBN had a lower mean heart rate of 59 ± 4 bpm (Fig 6.1 D, $p < 0.01$).

Next, I asked whether CBN exposure during gastrulation altered motor neuron growth and morphology because zebrafish primary motor neurons first appear between 9 and 11 hpf, during gastrulation, while secondary motor neurons start to appear 5 hours later. To determine this, I performed immunohistochemistry using antibodies that target primary (anti-ZnP1) and secondary (anti-Zn8) motor neurons. Immunostaining using the anti-Znp1 antibody showed that exposure to CBN altered the branching pattern of primary motor neurons with the greatest level of severity in animals treated with the highest concentrations of CBN (Fig 6.1 E; $n=5-7$). Exposure to the lowest concentration of CBN (0.01 mg/L) had no visible effects on primary MN branching (Fig 6.1 E; $n=10$). Additionally, immunostaining secondary motor neurons with anti-Zn8 showed that the lateral branching of secondary motor neurons is reduced for CBN treatment (4 mg/L) (Fig 6.1 E; $n=8$).

Because exposure to CBN altered the development of primary and secondary motor neurons, I asked whether locomotion was impacted. I recorded the swimming activity of 5 dpf larva for 60 minutes and measured the swimming activity. Analysis of locomotor activity showed that exposure to CBN in the range of 2 to 4 mg/L significantly reduced the mean

swimming activity of 5 dpf larvae. Specifically, the swimming activity was reduced 10-fold from a control level of $0.1 \pm 0.01\%$ to a value of $0.01 \pm 0.003\%$ in animals exposed to 2-4 mg/L CBN (Fig 6.1 F; n=40-60, $p < 0.05$).

Taken together, these data show that exposure to CBN alters morphological, behavioral and physiological factors in developing zebrafish, but only at high exposure concentrations above 0.5 mg/L CBN.

6.1.2 CBN exposure affects kinocilia development

Hair cells are crucial for the function of a multitude of tissue and organs (Anvarian et al., 2019). Additionally, cilia play important roles during CNS development including neurogenesis, neuronal maturation and cell survival (Youn & Han, 2018). Cilia also play an important role in otolith formation and positioning. The otolith is a biomineralized structure inside the inner ear that lies over patches of sensory hair cells, and which is used for hearing and balance in zebrafish. Structural or functional defect in cilia causes developmental or degenerative diseases which results in ciliopathies. Ciliopathies include polycystic kidney disease (PKD), acrocallosal syndrome, Bardet-Biedl syndrome, Meckel-Gruber syndrome, Joubert syndrome (JBTS), mental retardation and retinal dystrophy etc. (Anvarian et al., 2019; Stooke-Vaughan et al., 2012; Youn & Han, 2018).

Here, I sought to determine whether CBN treatment altered the ability of larvae to respond to an acousto-vestibular (AV) stimulus. To do this, I provided an auditory stimulus to 5 dpf larvae and recorded the ensuing escape response. Quantification of the response rate showed

that embryos exposed to the lowest concentration of CBN (0.01 mg/L) showed no significant change in the response rate (Fig 6.3 A; n=36; p<0.05), whereas embryos treated with higher doses of CBN (e.g. 1 and 4 mg/L) exhibited a major reduction in the response rate of C-bend where only $39 \pm 10\%$ and $14 \pm 10\%$ of animals responded to the sound pulse compared to vehicle controls that responded at a rate of $70 \pm 9\%$ (Fig 6.3 A; n=20-30; p<0.05).

Because CBN-treated embryos exhibited reduced responses to sound, I asked whether this altered response might be due to improper development of cilia associated with the otoliths. For this purpose, I imaged the otoliths at the time of hatching. Embryos treated with lowest concentration of 0.01 mg/L CBN did not exhibit changes in the structure of the otolith. In contrast, animals exposed to the higher concentrations of CBN exhibited severely altered otic vesicles such as completely absent semicircular canals (Fig 6.3 B). Furthermore, the utricular otoliths (UO) and sacular otoliths (SO) were often fused in animals exposed to 4 mg/L CBN (Fig 6.3 B). Next, I sought to determine whether CBN exposure affected the development of kinocilia associated with the otoliths. Since hair cells of the otolith share morphological and functional similarities with hair cells of the posterior lateral line (pLL), I also asked whether CBN treatment altered the development of kinocilia associated with the pLL. To do this, I used SEM to image the neuromasts of zebrafish larvae. Importantly, animals treated with the lowest concentration of CBN (0.01 mg/L) exhibited defects associated with hair cells such as disorganization of the kinocilia (Fig 6.3 C, D) and reduced numbers of neuromasts along the posterior lateral line (Fig 6.3 E, F; p<0.01; n=6). Furthermore, about $53 \pm 8\%$ of the embryos had altered kinocilia in their otoliths compared to controls in which only $7 \pm 2\%$ of the animals had altered kinocilia (Fig 6.3 D; p<0.01; n=6-8). For clarity I characterized hair cells as “altered” when the morphology of their kinocilia appeared unbundled and disorganized as opposed to tight bundles of kinocilia that

were present in control animals. Animals treated with the highest doses of CBN (4 mg/L) exhibited severe changes to cilia development in the otoliths and neuromasts of the pLL (Fig 6.3 C, E). In addition, stereocilia were completely absent inside the otolith as shown in Fig 6.3 C. Almost every embryo examined ($92 \pm 8\%$) showed defective features of their hair cells compared with controls in which only $7 \pm 2\%$ of the animals exhibited altered hair cell features. (Fig 6.3 D, $p < 0.01$; $n = 6-8$). Furthermore, there were significantly high numbers of absent neuromasts along the pLL in animals treated with 4 mg/L CBN as shown in Fig 6.3 E, F ($p < 0.05$; $n = 5$).

6.1.3 Blocking CB₂R activity rescue morphology

Next, I set out to determine if the cannabinoid receptors, CB₁R and CB₂R were involved in mediating the CBN-induced developmental defects. To do this, I used pharmacological blockers of CB₁R (AM251 and CP94) and CB₂R (AM630 and JTE907) to block the activity of these receptors in the presence of CBN. The concentration of CB₁R and CB₂R antagonists were chosen as 10 nM and 10 μ M, respectively, based on dose response studies (Fig 6.4 - 6.7). High concentrations of CB₁R and CB₂R antagonists alone had adverse effects on morphometric, cardiac properties, larval survival, hatching success and locomotion. These concentrations of receptor antagonists chosen had either insignificant or much reduced adverse effects relative to the higher concentrations and yet are still within the effective range (related to IC₅₀) for receptor antagonism. For these experiments, I used a concentration of CBN that had an obvious effect on the embryos, such as 3 mg/L CBN, so that any inhibition of the effects of CBN could be clearly

determined. Moreover, I specifically used two different antagonists for each receptor type to confirm the results in case receptor specificity was an issue in zebrafish.

CBN-treated animals experienced a significant reduction in body length of 2.69 ± 0.06 mm compared to controls of 3.78 ± 0.01 mm (Fig 6.8 A-C; $n=25-80$; $p<0.01$). Co-treatment of CBN with either AM251 or CP94 partially prevented the reduction of body length induced by CBN exposure. Blocking CB₁R activity with AM251 and CP94 resulted in animals which exhibited mean body lengths of 2.84 ± 0.02 and 2.91 ± 0.06 mm, respectively, compared to that in CBN-treated animals of 2.69 ± 0.06 mm (Fig 6.8 A-C; $n=25-80$; $p<0.01$). In contrast, co-treatment of the CB₂R antagonist (JTE907) with CBN resulted in embryos that were normal in appearance and that had body lengths that were similar to vehicle controls (Fig 6.8 A-C; $p<0.01$; $n=25-75$).

With respect to survival, blocking of CB₁R activity with either AM251 or CP94 did not reduce CBN-induced mortality by 5 dpf (Fig 6.8 D, E), indicating the effects of CBN were not due to activation of CB₁R. In contrast, inhibition of CB₂R activity with either AM630 or JTE907 resulted in a significant reduction in mortality with survival rates of 60-70% by 5 dpf in comparison to a survival rate of only 45% in animals treated with 3mg/L CBN alone (Fig 6.8 G; $p<0.01$; $n=100-125$). I then blocked both CB₁R and CB₂R activity together to determine if this resulted in improved morphology, body lengths or survival. However, CBN-exposed animals co-treated with both antagonists showed no significant differences from animals treated with CB₂R antagonists + CBN alone (Fig 6.8 A-E). Taken together, these results suggest that CBN alters aspects of morphological development and survival through activation of CB₂Rs but not CB₁Rs.

Importantly, the effect of CBN on heart rate was largely unaffected by blocking either CB₁R or CB₂R (Fig 6.8 F, G; $p < 0.05$; $n = 30-50$). Co-treatment of CBN with either CP94 prevented the reduction of heart rate induced by CBN exposure (Fig 6.8 G; $p > 0.05$). Interestingly, heart morphology appears largely normal in the presence of CB₂R (data not shown), but the mean heart rate remains slower than controls. Taken together, these findings suggest that CBN works through either CB₁R or CB₂R to alter some aspects of heart development, but that overall, the effects on cardiac activity occur via receptors and intracellular systems that are distinct from the canonical cannabinoid receptor pathways.

6.1.4 CBN induces alterations in MN branching via CB₂R

Next, I wanted to determine if blocking either of the CB₁R or CB₂R prevented the CBN-induced alterations in motor neuron (MN) morphology. Four types of primary MNs have been identified in each hemi segment: the middle primary MN (MiP) project to the dorsal region, the rostral primary MN (RoP) project to the ventral region, the caudal primary MN (CaP) project to the mid region of the trunk and the variable primary MNs (VaP) innervate a region in between rostral and middle MN areas (typically undergoes apoptosis by 36 phf) (Babin et al., 2014; Eisen et al., 1990; Myers et al., 1986). Blocking CB₁R with either AM251 or CP94, did not significantly prevent the CBN-induced deficits in primary motor neuron branching (Fig 6.9 C, D; $p > 0.05$). In contrast, block of CB₂R activity with either AM630 or JTE907 resulted in primary MN branching patterns that were indistinguishable from vehicle controls (Fig 6.9 E, F). Further quantification of the number of secondary and tertiary branches emanating from the main motor

neuron axon was performed for one set of antagonists: CB₁R (AM251) and CB₂R (AM630) (Figure 6.9). Representative traces of such quantifications are shown in Fig 6.10. I analyzed the ventral and dorsal branching separately because this could be done with confidence. Examination of secondary branching in the ventral regions showed that there were no differences between treatment groups (Fig 6.9 I, M). However, CBN treatment caused a significant reduction in the number of secondary branches in the dorsal trunk from 8 ± 1 in the control animals to 2 ± 1 branches after CBN treatment (Fig 6.9 C; $p < 0.05$; $n = 5-6$). Co-exposure of AM251 with CBN, had no significant effect on the number of branches (Fig 6.9 C), whereas animals co-treated with the CB₂R blocker, AM630 and CBN had secondary dorsal branch numbers (7 ± 1) that were similar to controls 8 ± 1 (Fig 6.9 C; $p > 0.05$; $n = 5-6$). Similarly, quantification of tertiary ventral branches showed that the co-treatment of the CB₂R blockers with CBN prevented the effects of CBN treatment alone (Fig 6.9 D; $p > 0.05$; $n = 5-7$). Embryos co-treated with CB₁R antagonists resulted no significant differences in the number of tertiary branches when compared with embryos treated with CBN alone (Fig 6.9 D, E). Next, I tested the ability of a combined treatment of AM251+AM630 to block the effects of CBN. My findings indicate that blocking both receptors simultaneously produced similar results to those elicited by blocking CB₂R alone (Fig 6.9 B-E), where the number of secondary branches in dorsal regions and the number of tertiary branches in ventral regions was comparable to control/vehicle treated animals (Fig 6.9 C, D; $p > 0.05$). Taken together these results suggest that moderately high doses of CBN alter neuronal development via activation of CB₂Rs.

6.1.5 Co-exposure of CBN and CB₂R antagonists prevents locomotor deficits

5 dpf larva exposed to CBN (3 mg/L) during gastrulation exhibited greatly reduced levels of movement compared with vehicle-treated animals. Co-exposure of either of the CB₁R antagonists (AM251 and CP94) with CBN did not prevent the effects of CBN treatment alone (Fig 6.11 A-D). However, co-exposure of either of the CB₂R antagonists (AM630 or JTE907) with CBN significantly reduced the effects of CBN treatment on swimming distance, frequency, activity and velocity (Fig 6.11 A-D; $p < 0.05$; $n = 40-60$). For instance, 3 mg/L CBN-treated animals exhibited significantly reduced mean swimming distances of 474 ± 74 mm compare to values observed in vehicle-treated animals of 4600 ± 945 mm. Whereas, AM630 + CBN and JTE907 + CBN treatment resulted in mean swimming distances of 2046 ± 333 and 2266 ± 296 mm, respectively, indicating that blocking CB₂R activity partially prevented the effect of CBN (Fig 6.11 A; $p < 0.05$; $n = 30-50$). Similarly, the swimming frequency was significantly reduced from 989 ± 178 swim bouts/h in control animals to 267 ± 65 swim bouts/h in 3 mg/L CBN-treated fish. Co-treatment of CB₂R blockers with CBN reduced the CBN-mediated suppression in swimming frequency by ~two-third (723 ± 128 and 786 ± 111 swim bouts/h for AM630 and JTE907, respectively) (Fig 6.11 B; $p < 0.05$; $n = 30-50$). Animals treated with CBN swam less than vehicle controls (Fig 6.11 C; $p < 0.05$) but the effect of CBN on swimming activity was significantly prevented by co-treatment with the CB₂R antagonists (AM630 and JTE907), which resulted in activity levels of $0.06 \pm 0.02\%$ and $0.05 \pm 0.01\%$, respectively; these values were significantly higher than those observed with CBN treatment alone (Fig 6.11 C; $p < 0.05$; $n = 30-50$). With respect to the speed of swimming, I found that animals treated with 3 mg/L CBN exhibited a significant reduction in swimming velocity of 0.31 ± 0.06 mm/s compared to values of 0.93 ± 0.21 mm/s from control fish (Fig 6.11 D; $p < 0.05$). Co-treatment with the CB₂R blocker JTE907 significantly prevented the reduction in swimming velocity (Fig 6.11 D; $p < 0.05$ $n = 30-$

50) while the presence of AM630 resulted in swimming velocities not significantly different from vehicle-treated controls. Finally, animals treated with combinations of CB₁R and CB₂R blockers exhibited mean swimming distances, swimming frequencies and swimming activity that were comparable to those obtained when blocking CB₂R alone (Fig 6.11 A-D; p<0.05 n = 30-50). Taken together my findings show that the effect of CBN treatment on locomotor activity is mediated via actions on CB₂Rs and not CB₁Rs.

6.1.6 Pharmacological blocking of CB₂R inhibits CBN-induced alteration of hair cell development

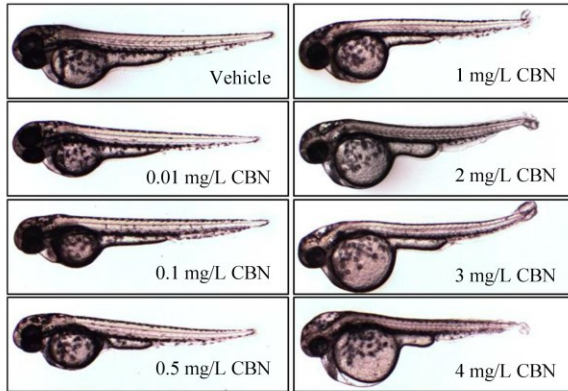
Next, I asked whether blocking CB₁R or CB₂R prevented the CBN-induced deficits in the AV escape response. Analysis of escape responses showed that CBN exposure (3 mg/L) significantly reduced the response rate from a mean value of $68 \pm 11\%$ in vehicle control animals to $17 \pm 5\%$ in the CBN-treated group (Fig 6.12 A; p<0.05; n=24-30). Either AM630 (CB₂R antagonist) or AM251+AM630 co-exposure with CBN resulted in a significant improvement in their escape response rate to $58 \pm 11\%$ and $67 \pm 9\%$, respectively (Fig 6.12 A; p<0.05; n=24-30); whereas application of the CB₁R antagonist, AM251 did not prevent the CBN-induced deficits in escape responses (Fig 6.12 A; p>0.05; n=24-30).

I then asked if co-exposure of either the CB₁R antagonist (AM251) or the CB₂R antagonist (AM630) with CBN prevented the CBN-induced defects in neuromast and cilia development. I found that blocking the activity of either CB₁R or CB₂R partially prevented the CBN-induced alterations of hair cell development associated with the otoliths and the pLL (Fig

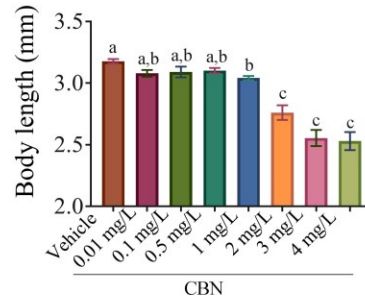
6.12 B-Q and Fig 6.13). For instance, 75 ± 9 % of animals exposed to 3 mg/L CBN experienced neuromast or cilia alterations whereas only 21 ± 1 % and 20 ± 2 % animals co-treated with AM630 or AM251+AM630, respectively, had hair cell deficits (Fig 6.12 R; $p < 0.05$; $n = 8-10$). Co-application of AM630 or combined application of AM251+AM630 with CBN partially prevented the loss of neuromasts along the pLL observed following treatment with CBN. Neuromast quantification showed that treatment of either AM630 or AM251+AM630 with CBN resulted in a neuromast count of 7 ± 1 compared to counts of 2 ± 1 and 11 ± 1 in animals following CBN and vehicle treatments, respectively (Fig 6.12 S; $p < 0.05$; $n = 8-10$). In contrast, co-treatment of AM251 + CBN did not result in a significant reduction of CBN-induced neuromast loss (Fig 6.12 S). Taken together, these findings indicate that the CBN-induced alterations in hair cell morphology along the lateral line are primarily due to activation of CB₂Rs.

Figure 6. 1 Effect of CBN exposure during gastrulation on zebrafish embryos

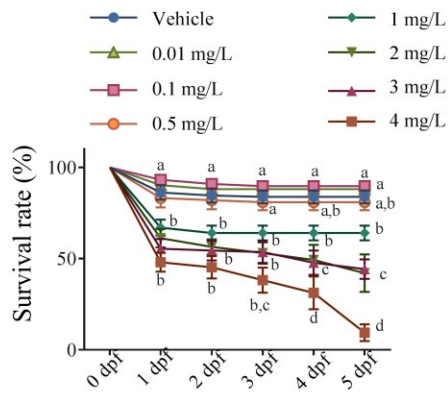
A)



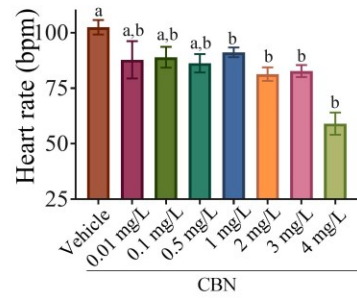
B)



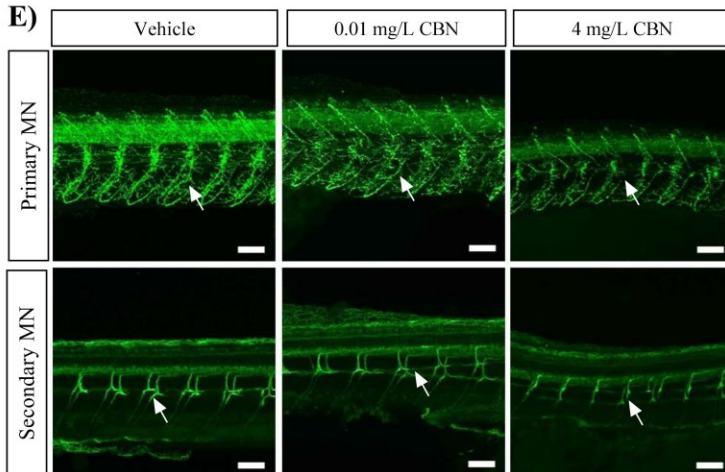
C)



D)



E)



F)

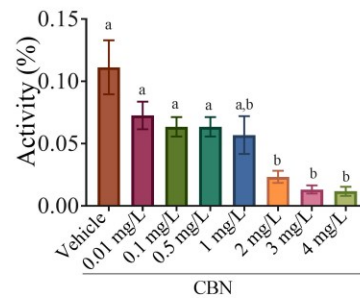


Figure 6.1 Effect of CBN exposure during gastrulation on zebrafish embryos. (A)

Representative images of embryos exposed to 0.4% methanol (vehicle) and 0.01 to 4 mg/L CBN (from 5.25 hpf to 10.75 hpf), and then allowed to develop in normal embryo media. Images were taken at 48–52 hpf. (B) Bar graph showing the body lengths (in mm) of embryos exposed to different media: vehicle control (n = 57), 0.01 mg/L CBN (n = 61), 0.1 mg/L CBN (n = 61), 0.5 mg/L CBN (n = 61), 1 mg/L CBN (n = 42), 2 mg/L CBN (n = 30), 3 mg/L CBN (n = 29), and 4 mg/L CBN (n = 21) at 2 dpf. (C) Line graphs showing the percentage of embryos that survived within the first 5 days of development following exposure to different media: vehicle, 0.01 mg/L CBN, 0.1 mg/L CBN, 0.5 mg/L CBN, 1 mg/L CBN, 2 mg/L CBN, 3 mg/L CBN and 4 mg/L CBN during gastrulation (N = 4 experiments and n = 20 embryos for each treatment). (D) Bar graphs of heart rate of embryos exposed to different media: vehicle control (n = 82), 0.01 mg/L CBN (n = 61), 0.1 mg/L CBN (n = 23), 0.5 mg/L CBN (n = 29), 1 mg/L CBN (n = 25), 2 mg/L CBN (n = 29), 3 mg/L CBN (n = 32), and 4 mg/L CBN (n = 24). (E) Representative images are showing the labelling of primary MN by anti-Znp-1 (upper panel) and secondary MN by anti-Zn8 antibody (lower panel) in fish treated with vehicle (n=5), 0.01 mg/L CBN (n=7), and 4 mg/L CBN (n=7). Branches in a motor axon are indicated with white arrow. Scale bar represents 50 μ m. (F) CBN exposure decreased locomotor activity in larvae at 5 dpf. A 96-well plate was used to record larval swimming activity at 5 dpf. Bar graph shows mean activity (%) for embryos exposed to different media: vehicle control (n = 82), 0.01 mg/L CBN (n = 61), 0.1 mg/L CBN (n = 23), 0.5 mg/L CBN (n = 29), 1 mg/L CBN (n = 35), 2 mg/L CBN (n = 30), 3 mg/L CBN (n = 35), and 4 mg/L CBN (n = 45). For survival, significance was determined using two-way ANOVA followed by tukey's multiple comparison tests. For body length, heart rates and

activity, significance was determined using Kruskal-Wallis tests followed by Dunn's multiple comparison test. Groups which share the same letter(s) of the alphabet are not statistically different from one another.

Figure 6. 2 Effect of CBN exposure on zebrafish hatching and malformation.

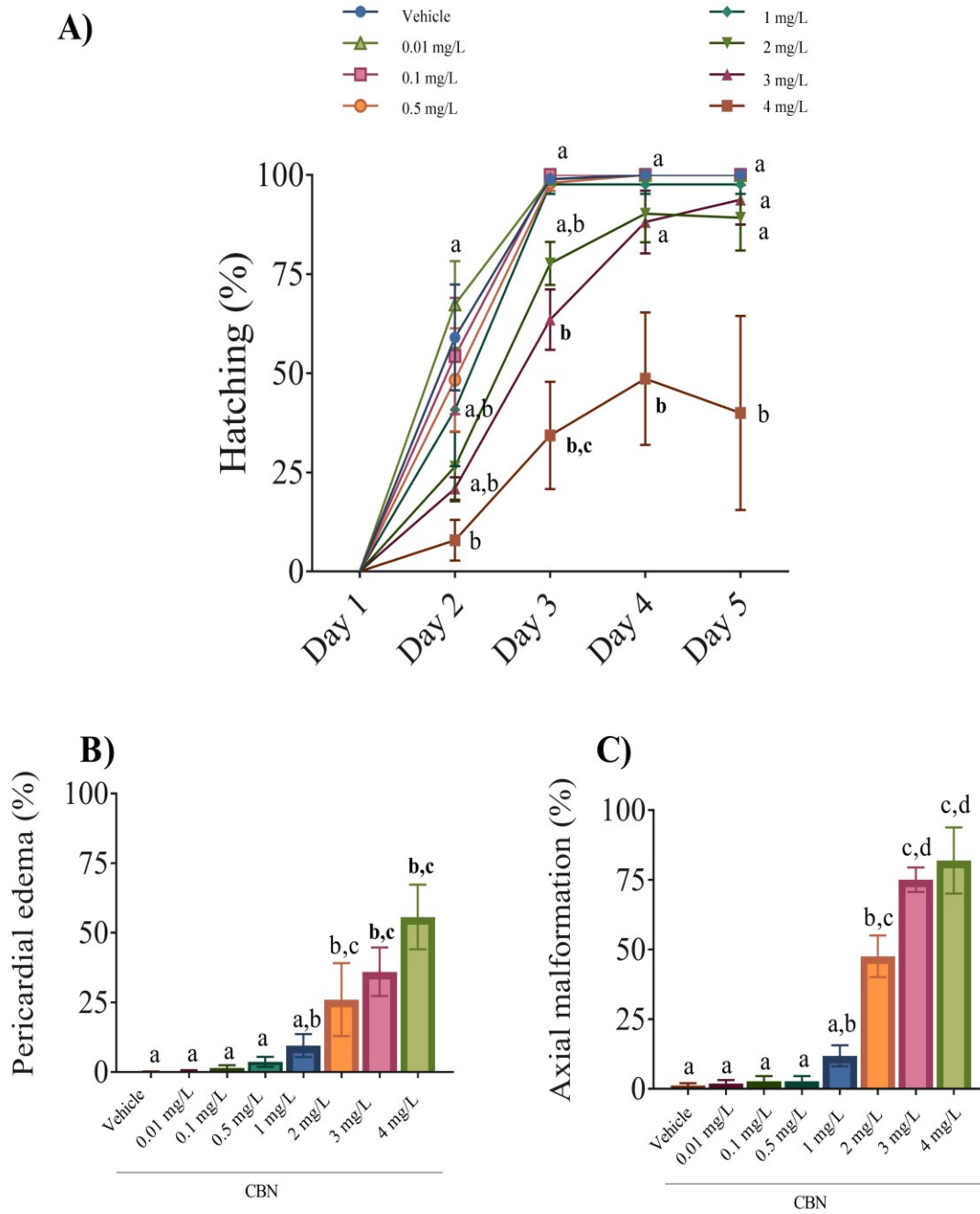


Figure 6.2 Effect of CBN exposure on zebrafish hatching and malformations. (A) Line graphs showing the percentage of embryos that hatched within the first 5 days of development following exposure to different media: vehicle, 0.01 mg/L CBN, 0.1 mg/L CBN, 0.5 mg/L CBN, 1 mg/L CBN, 2 mg/L CBN, 3 mg/L CBN, and 4 mg/L CBN during gastrulation (N = 4 experiments and n = 20 embryos for each treatment). (B) Bar graph showing the pericardial edema (%) at 2 dpf of embryos previously exposed to different media: vehicle control (n = 57), 0.01 mg/L CBN (n = 61), 0.1 mg/L CBN (n = 61), 0.5 mg/L CBN (n = 61), 1 mg/L CBN (n = 42), 2 mg/L CBN (n = 30), 3 mg/L CBN (n = 29) and 4 mg/L CBN (n = 21) . (D) Bar graph showing the axial malformation (%) at 2 dpf of embryos previously exposed to different media: vehicle control (n = 57), 0.01 mg/L CBN (n = 61), 0.1 mg/L CBN (n = 61), 0.5 mg/L CBN (n = 61), 1 mg/L CBN (n = 42), 2 mg/L CBN (n = 30), 3 mg/L CBN (n = 29) and 4 mg/L CBN (n = 21). For hatching, significance was determined using two-way ANOVA followed by tukey's multiple comparison tests. For pericardial edema and axial malformations, significance was determined using Kruskal-Wallis tests followed by Dunn's multiple comparison test. Groups which share the same letter(s) of the alphabet are not statistically different from one another.

Figure 6. 3 CBN exposure affects the development of kinocilia in the otolith and along posterior lateral line (pLL)

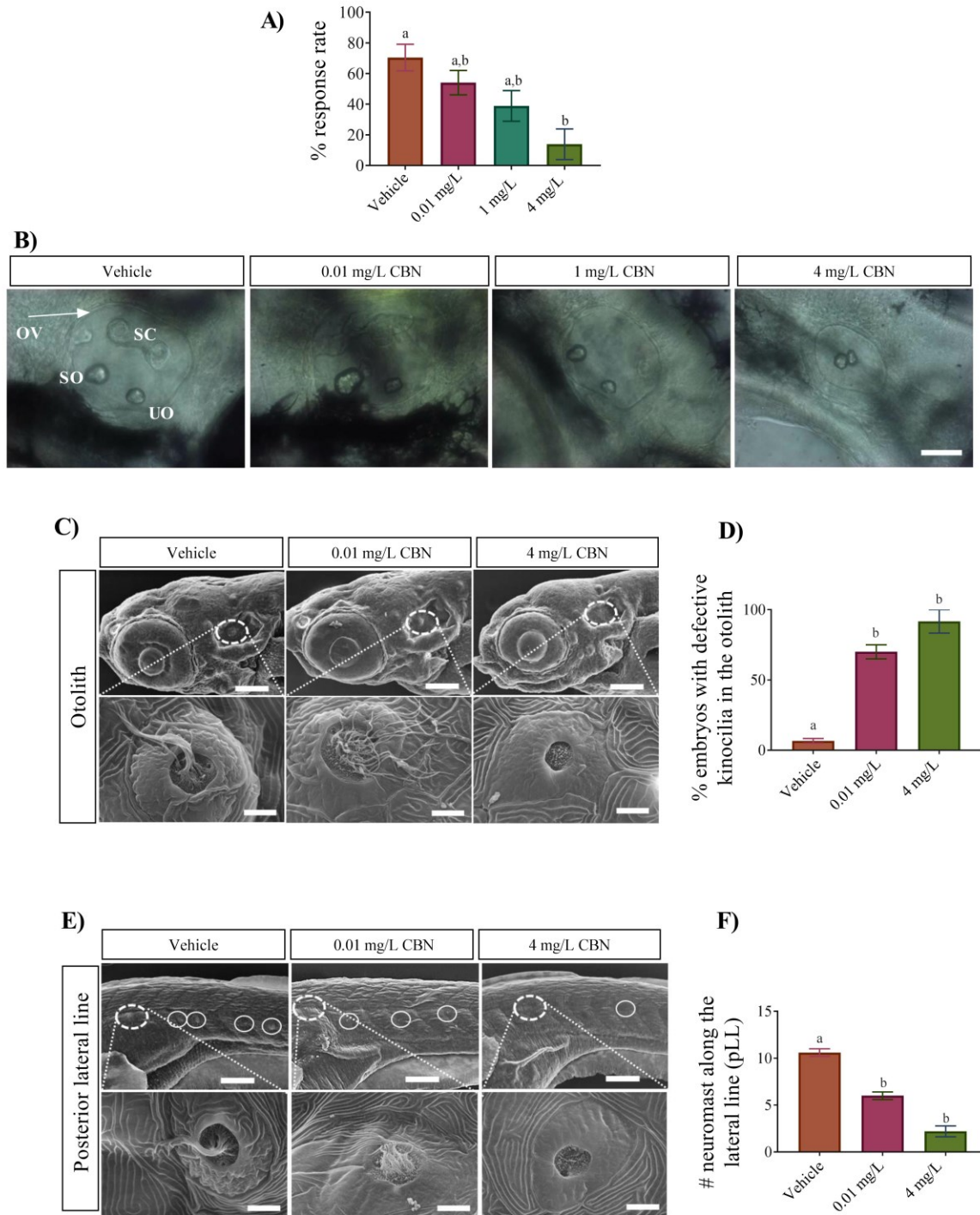


Figure 6.3 CBN exposure at gastrulation affects the development of kinocilia in the otolith and posterior lateral line (pLL). (A) Bar graph represents the (%) of embryos responded to sound stimuli at 5 dpf. Sound pulse was applied to the free-swimming embryos from a speaker and their escape responses were recorded for analysis. (B) Otolith (representative) images were taken from 52 hpf embryos, positioning anterior (head) on right and posterior (tail) on left. The development of otic vesicles (OV), utricular otolith (UO), saccular otolith (SO), and semicircular canal (SC) are visible here. Scale bar represents 50 μm . (C) Scanning electron microscopy (SEM) images of embryos at 5 dpf. Top rows, images were taken from head portion at 500 x magnification. Bottom rows, images were taken from inside the otolith at 1000 x magnification, which is showing the hair cell. Scale bar represents 100 μm (top panel) and 5 μm (bottom panel). (D) Bar graph showing the quantification (%) of embryos that exhibited deformities in hair cell inside the otolith structure. (E) SEM images of embryos along posterior lateral line (pLL) at 5 dpf. Top row is showing images for vehicle control, lowest dose of 0.01 mg/L CBN, and highest dose of 4 mg/L CBN were taken along the portion of lateral line at 500 x magnifications. Bottom row is showing the first neuromast image along the posterior lateral line, which was taken at 10000 x magnification. Scale bar represents 100 μm (top panel) and 5 μm (bottom panel). (F) Bar graph showing the number of neuromasts presents along the posterior lateral line. Significance was determined using Kruskal-Wallis tests followed by Dunn's multiple comparison test. Groups which share the same letter(s) of the alphabet are not statistically different from one another.

Figure 6. 4 Dose response of CB₁R and CB₂R antagonists during gastrulation.

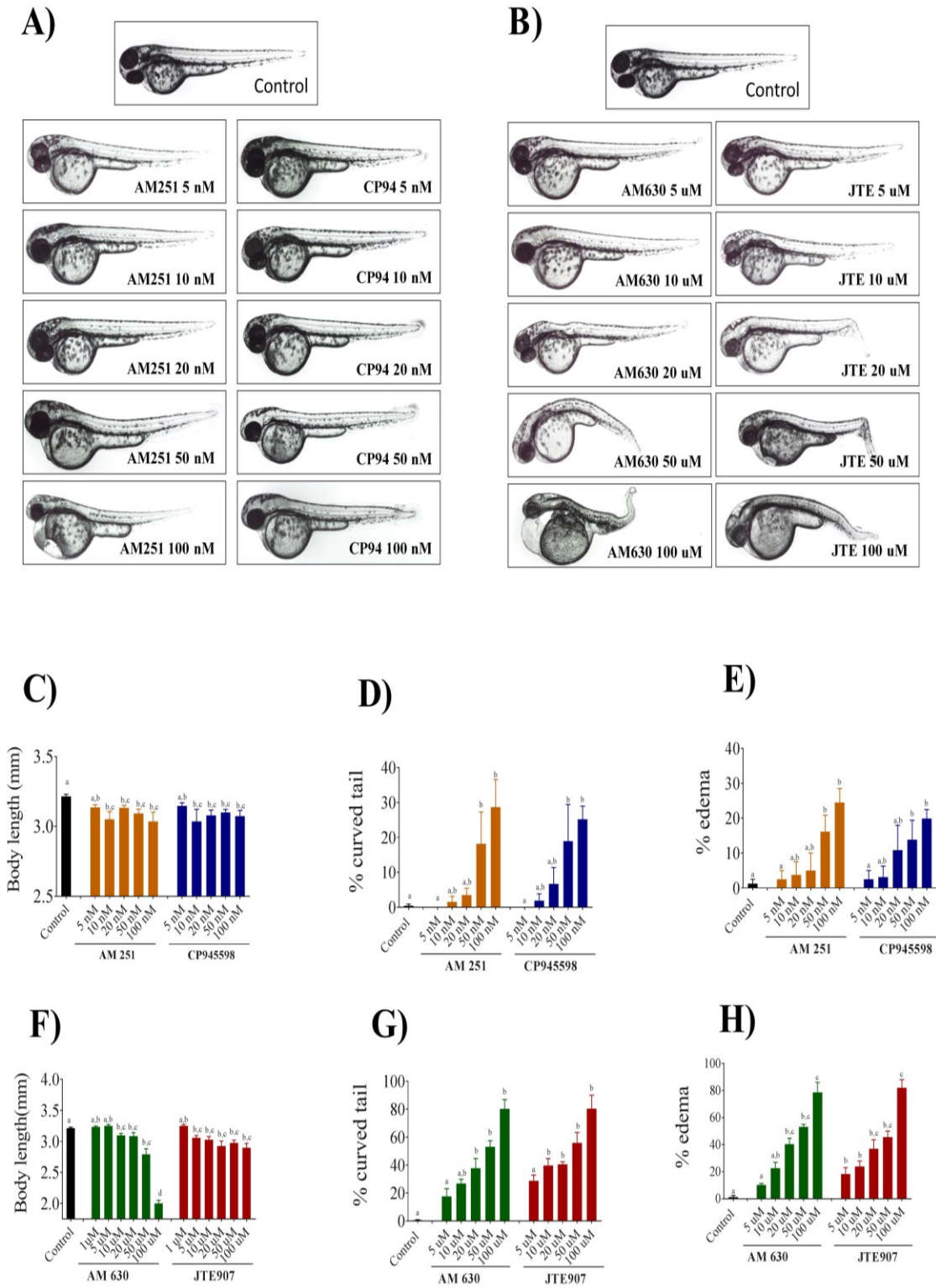
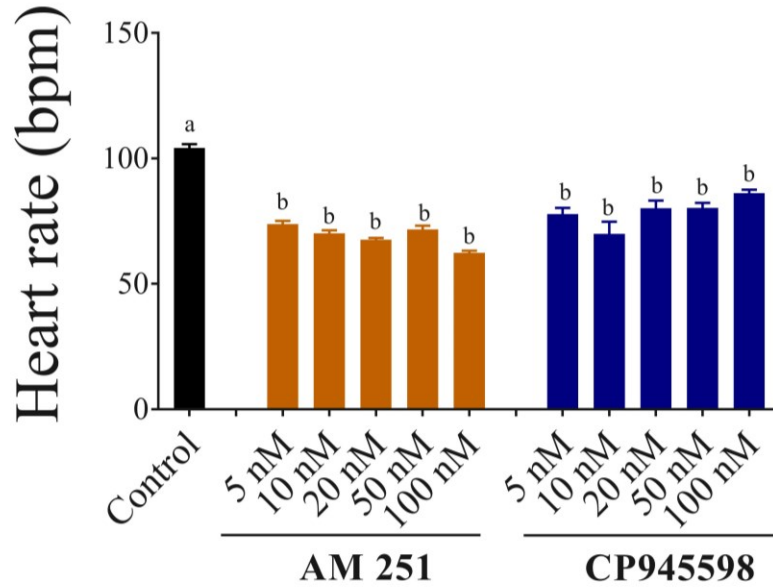


Figure 6.4 Dose response of CB₁R and CB₂R antagonists on morphological features during gastrulation. (A) Representative images of 48-52 hpf embryos previously exposed to DMSO (vehicle control) and 5-100 nM AM251 and CP94 (from 5.25 hpf to 10.75 hpf) and then allowed to develop in normal embryo media. (B) Representative images of 48-52 hpf embryos previously exposed to either DMSO (vehicle control), and 5-100 μM AM630 and JTE907 (from 5.25 hpf to 10.75 hpf) and then allowed to develop in normal embryo media. (C) Bar graph showing the body lengths (in mm) of embryos exposed to different media: DMSO (vehicle control) (n = 60), 5 nM AM251 (n = 60), 10 nM AM251 (n = 60), 20 nM AM251 (n = 55), 50 nM AM251 (n = 40), 100 nM AM251 (n = 30), 5 nM CP945598 (n = 60), 10 nM CP945598 (n = 68), 20 nM CP945598 (n = 66), 50 nM CP945598 (n = 42), and 100 nM CP945598 (n = 40) at 2 dpf. (D) Bar graph showing the curved tail (%) of embryos exposed to different media: DMSO (vehicle control), 5 nM AM251, 10 nM AM251, 20 nM AM251, 50 nM AM251, 100 nM AM251, 5 nM CP945598, 10 nM CP945598, 20 nM CP945598, 50 nM CP945598, and 100 nM CP945598. (E) Bar graph showing the pericardial edema (%) of embryos exposed to different media: DMSO (vehicle control), 5 nM AM251, 10 nM AM251, 20 nM AM251, 50 nM AM251, 100 nM AM251, 5 nM CP945598, 10 nM CP945598, 20 nM CP945598, 50 nM CP945598, and 100 nM CP945598. (F) Bar graph showing the body lengths (in mm) of embryos exposed to different media: DMSO (vehicle control) (n = 50), 5 μM AM630 (n = 50), 10 μM AM630 (n = 40), 20 μM AM630 (n = 50), 50 μM AM630 (n = 40), 100 μM AM630 (n = 40) and 5 μM JTE907 (n = 70), 10 μM JTE907 (n = 68), 20 μM JTE907 (n = 60), 50 μM JTE907 (n = 52), and 100 μM JTE907 (n = 30) at 2 dpf. (G) Bar graph showing the curved tail (%) of embryos exposed to different media: DMSO (vehicle control), 5 μM AM630, 10 μM AM630, 20 μM AM630, 50 μM AM630, 100

μM AM630, 5 μM JTE907, 10 μM JTE907, 20 μM JTE907, 50 μM JTE907, and 100 μM JTE907. (H) Bar graph showing the pericardial edema (%) of embryos exposed to different media: DMSO (vehicle control), 5 μM AM630, 10 μM AM630, 20 μM AM630, 50 μM AM630, 100 μM AM630, 5 μM JTE907, 10 μM JTE907, 20 μM JTE907, 50 μM JTE907, and 100 μM JTE907. Significance was determined using Kruskal-Wallis tests followed by Dunn's multiple comparison test. Groups which share the same letter(s) of the alphabet are not statistically different from one another.

Figure 6. 5 Effect of CB₁R and CB₂R antagonists on heart rate.

A)



B)

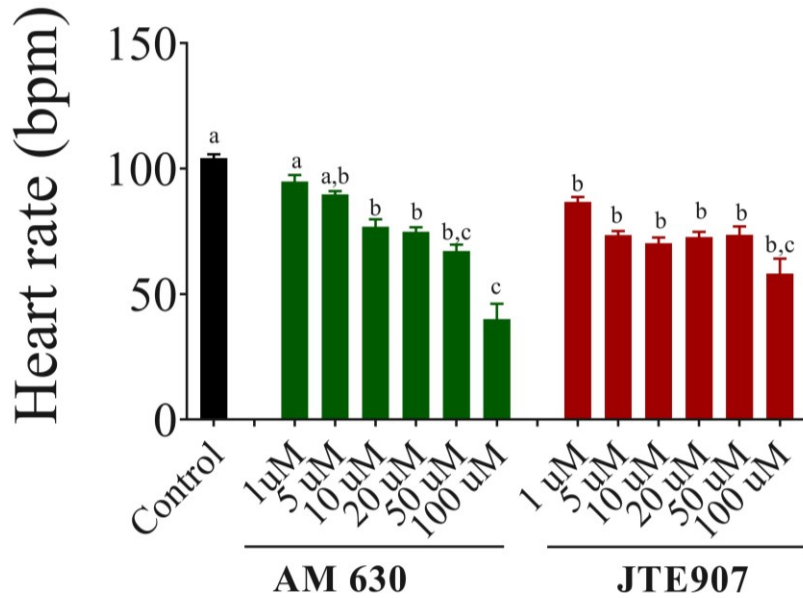


Figure 6.5 Effect of CB₁R and CB₂R antagonists on heart rate. (A) Bar graph showing the heart rate (bpm) of embryos exposed to different media: DMSO (vehicle control), 5 nM AM251, 10 nM AM251, 20 nM AM251, 50 nM AM251, 100 nM AM251, 5 nM CP945598, 10 nM CP945598, 20 nM CP945598, 50 nM CP945598, and 100 nM CP945598. (B) Bar graph showing the heart rate (bpm) of embryos exposed to different media: DMSO (vehicle control), 5 μM AM630, 10 μM AM630, 20 μM AM630, 50 μM AM630, 100 μM AM630, 5 μM JTE907, 10 μM JTE907, 20 μM JTE907, 50 μM JTE907, and 100 μM JTE907. Significance was determined using Kruskal-Wallis tests followed by Dunn's multiple comparison test. Groups which share the same letter(s) of the alphabet are not statistically different from one another.

Figure 6. 6 Effect of CB₁R and CB₂R antagonists on survival and hatching of zebrafish embryos

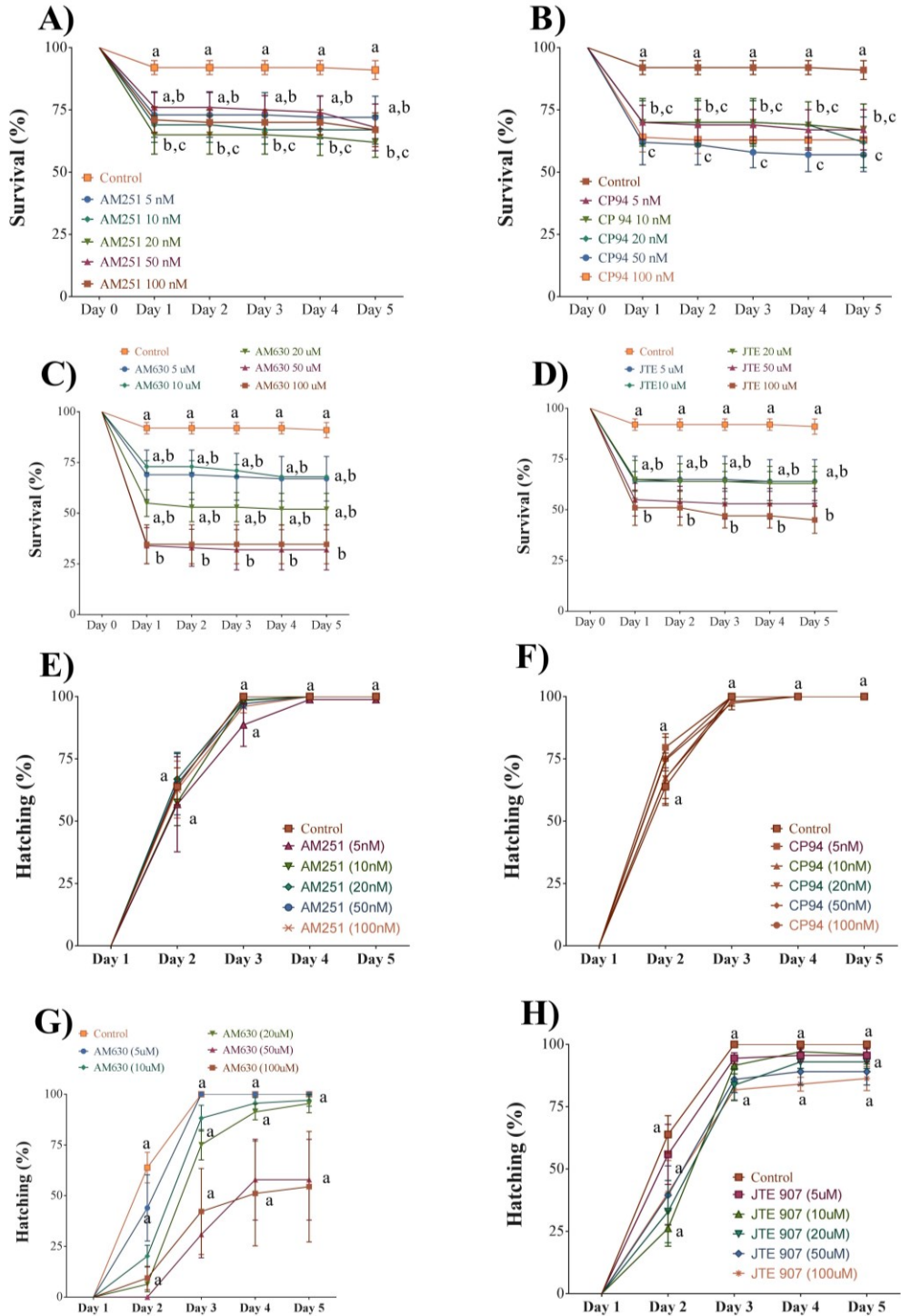


Figure 6.6 Effect of transient exposure to CB₁R and CB₂R antagonists at gastrulation on survival (A-D) and hatching (E-H) by day 5. Line graphs showing the percentage of embryos that survived (A) and hatched (H) within the first 5 days of development following exposure to different media: DMSO (vehicle control), 5 nM AM251, 10 nM AM251, 20 nM AM251, 50 nM AM251, and 100 nM AM251. Line graphs showing the percentage of embryos that survived (B) and hatched (F) within the first 5 days of development following exposure to different media: DMSO (vehicle control), 5 nM CP945598, 10 nM CP945598, 20 nM CP945598, 50 nM CP945598, and 100 nM CP945598. Line graphs showing the percentage of embryos that survived (C) and hatched (G) within the first 5 days of development following exposure to different media: DMSO (vehicle control), 5 μM AM630, 10 μM AM630, 20 μM AM630, 50 μM AM630, and 100 μM AM630. Line graphs showing the percentage of embryos that survived (D) and hatched (H) within the first 5 days of development following exposure to different media: 5 μM JTE907, 10 μM JTE907, 20 μM JTE907, 50 μM JTE907, and 100 μM JTE907. For survival and hatching, significance was determined using two-way ANOVA followed by tukey's multiple comparison tests.

Figure 6. 7 Effect of CB₁R and CB₂R antagonist on locomotion

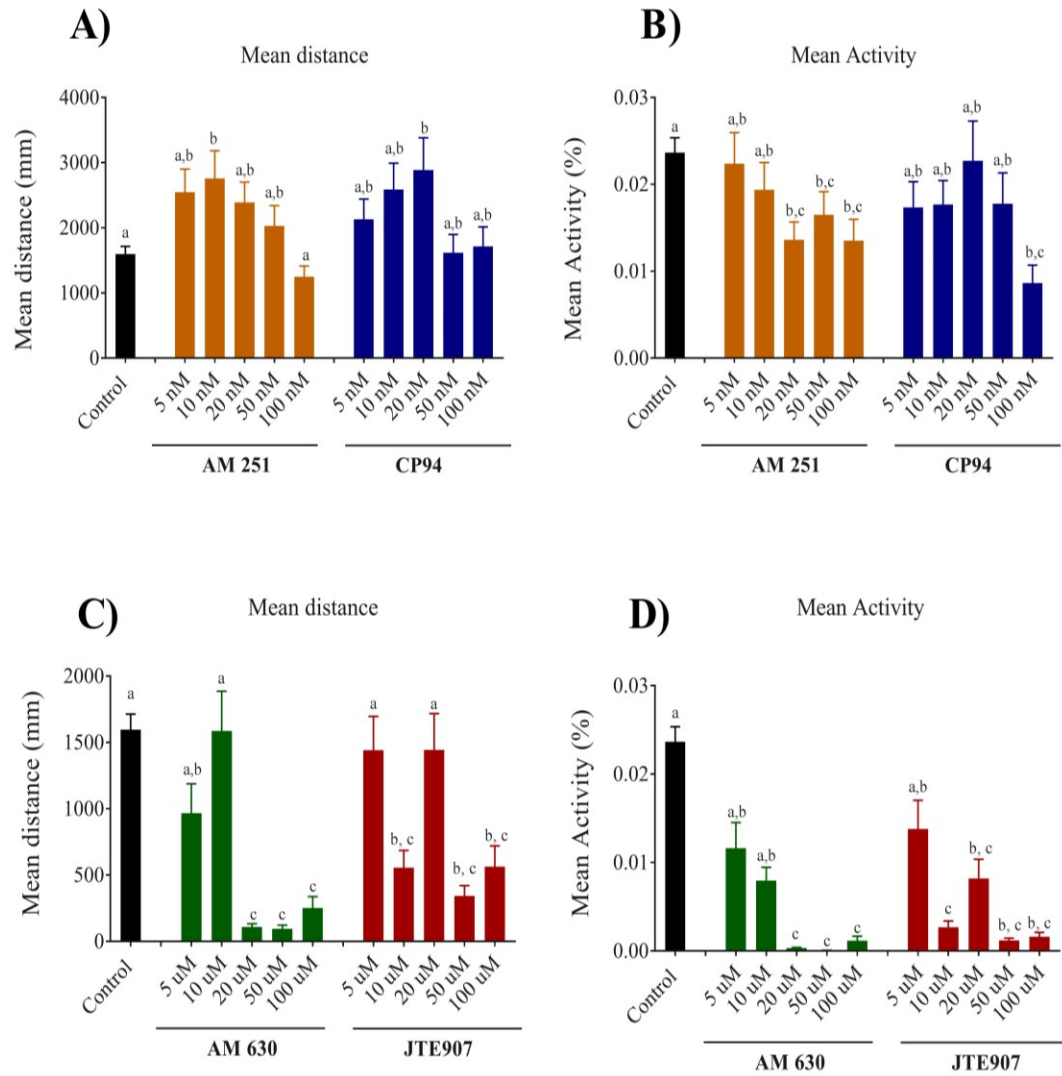


Figure 6.7 Effect of CB₁R and CB₂R antagonist on locomotion. A 96-well plate was used in this experiment where each well contains an individual larva. The free-swimming movement of the fish was recorded for 60 min and the recorded video was analyzed later. (A-B) Tracings were recorded from 5 dpf animals that had been transiently exposed during gastrulation to either DMSO (vehicle control), 5 nM AM251, 10 nM AM251, 20 nM AM251, 50 nM AM251, 100 nM AM251, 5 nM CP945598, 10 nM CP945598, 20 nM CP945598, 50 nM CP945598, or 100 nM CP945598. (A) Bar graph shows total distance (mm) for 1 h. (B) Bar graph shows changes in embryo mean activity (% rate for 1 h). (C-D) Tracings were recorded from 5 dpf animals that had been transiently exposed during gastrulation to either DMSO (vehicle control), 5 μM AM630, 10 μM AM630, 20 μM AM630, 50 μM AM630, 100 μM AM630, 5 μM JTE907, 10 μM JTE907, 20 μM JTE907, 50 μM JTE907, or 100 μM JTE907. (C) Bar graph shows total distance (mm) for 1 h. (D) Bar graph shows changes in embryo mean activity (% rate for 1 h). Significance was determined using Kruskal-Wallis tests followed by Dunn's multiple comparison test. Groups which share the same letter(s) of the alphabet are not statistically different from one another.

Figure 6. 8 Effects of co-exposure of CBN with CB₁R and/or CB₂R antagonists at gastrulation on morphological characteristics, survival, and heart rate

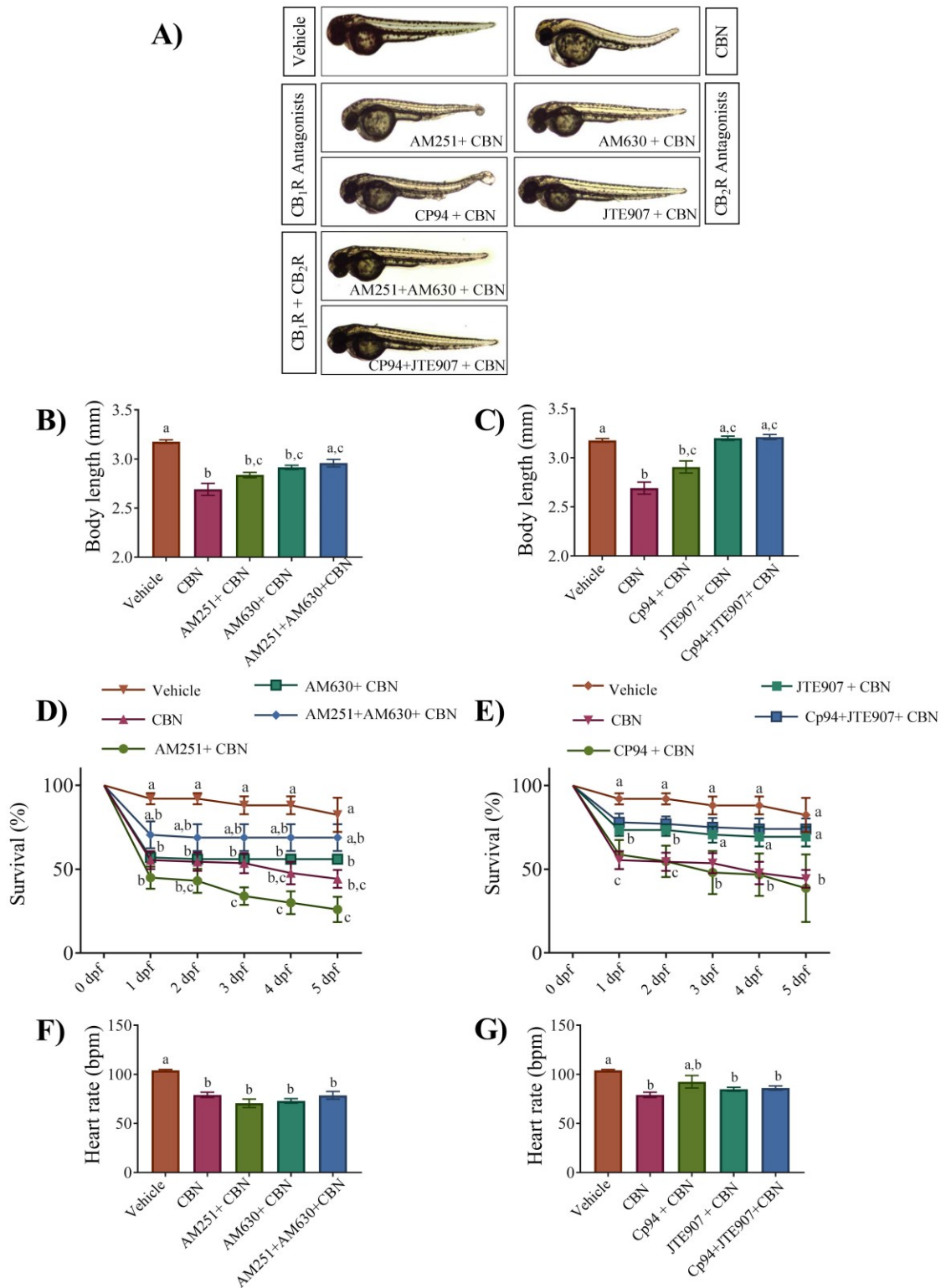


Figure 6.8 Effects of co-exposure of CBN with CB₁R and/or CB₂R antagonists at gastrulation on morphological characteristics, survival, and heart rate. Blocking CB₁R activity does not inhibit CBN-induced anatomical and physiological alteration. However, blocking of CB₂R or CB₁R+CB₂R attenuated CBN-induced alteration (A-E). (A) Representative morphological images of embryos at 2 dpf with co-application of CBN with CB₁R and/or CB₂R antagonists. (B) Bar graphs showing the body length (mm) of the embryos for the set one antagonists (AM251 and AM630 for CB₁R and CB₂R, respectively) in vehicle control (n = 57), 3 mg/L CBN (n = 29), AM251 10 nM + 3 mg/L CBN (n = 21), AM630 10 μM + 3 mg/L CBN (n = 21), and AM251 10 nM + AM630 10 μM + 3 mg/L CBN (n = 36), respectively, at 2 dpf. (C) Bar graphs showing the body length (mm) of the embryos for the set two antagonists (CP94 and JTE907 for CB₁R and CB₂R, respectively) in vehicle control (n = 57), 3 mg/L CBN (n = 29), CP94 10 nM + 3 mg/L CBN (n = 31), JTE907 10 μM + 3 mg/L CBN (n = 234) and CP94 10 nM + JTE907 10 μM + 3 mg/L CBN (n = 31), respectively, at 2 dpf. (D) Line graphs showing the percentage of embryos that survived within the first 5 days of development following co-exposure of the set one antagonist and CBN. Treatments are as vehicle control, 3 mg/L CBN, AM251 10 nM + 3 mg/L CBN, AM630 10 μM + 3 mg/L CBN, and AM251 10 nM + AM630 10 μM + 3 mg/L CBN (N = 4 experiments and n = 25 embryos for each treatment). (E) Line graphs showing the percentage of embryos that survived within the first 5 days of development following co-exposure of the set two antagonists and CBN. Treatments are as vehicle control, 3 mg/L CBN, CP94 10 nM + 3 mg/L CBN, JTE907 10 μM + 3 mg/L CBN, and CP94 10 nM + JTE907 10 μM + 3 mg/L CBN (N = 4 experiments and n = 25 embryos for each treatment). (F) Bar graphs showing heart rate as beats per minute (bpm) at 2 dpf for vehicle control (n = 35), 3 mg/L CBN (n = 59), AM251 10 nM + 3 mg/L CBN (n = 32), AM630 10 μM + 3 mg/L CBN

(n = 33), and AM251 10 nM + AM630 10 μ M + 3 mg/L CBN (n = 20), respectively. (G) Bar graphs showing heart rate as beats per minute (bpm) at 2 dpf for vehicle control (n = 35), 3 mg/L CBN (n = 59), CP94 10 nM + 3 mg/L CBN (n = 21), JTE907 10 μ M + 3 mg/L CBN (n = 25), and CP94 10 nM + JTE907 10 μ M + 3 mg/L CBN (n = 20), respectively. For survival, significance was determined using two-way ANOVA followed by tukey's multiple comparison tests. For body length and heart rates, significance was determined using Kruskal-Wallis tests followed by Dunn's multiple comparison test. Groups which share the same letter(s) of the alphabet are not statistically different from one another.

Figure 6. 9 Combined exposure of CB₂R and CBN inhibits CBN-induced alteration of primary MN branching

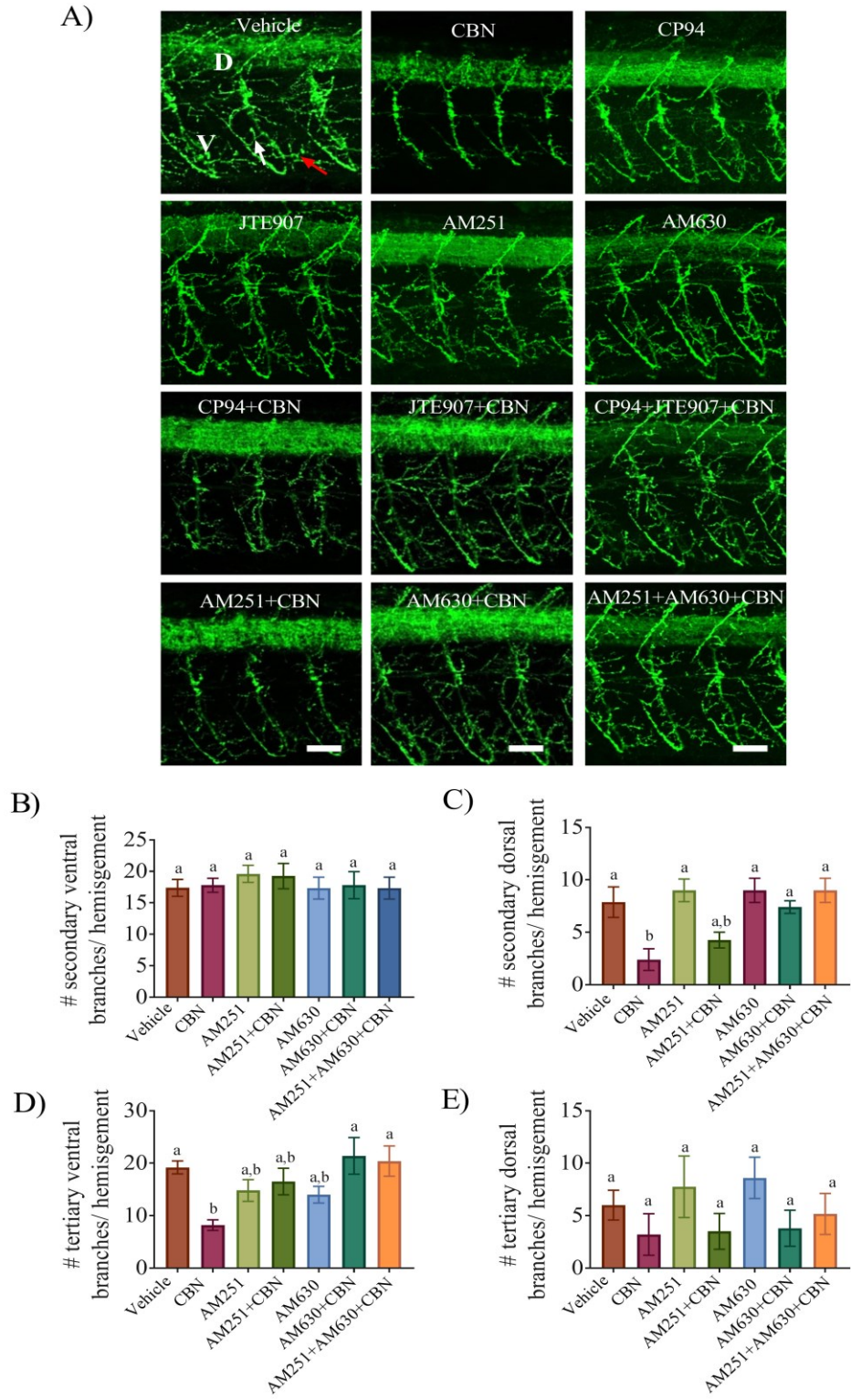


Figure 6.9 Presence of CB₂R antagonists inhibits CBN-induced alteration of primary MN branching. (A) Znp-1 (green) antibody was used to label primary motor neuronal axons and their branches in embryos exposed to either vehicle control (n = 7), 3 mg/L CBN (n = 9), CP50 50 nM (n = 5), JTE907 10 μ M (n = 5), AM251 10 nM (n = 5), AM630 10 μ M (n = 5), AM251 10 nM + 3 mg/L CBN (n = 8), CP94 50 nM + 3 mg/L CBN (n = 9), AM630 10 μ M + 3 mg/L CBN (n = 9), JTE907 10 μ M + 3 mg/L CBN (n = 8), AM251 10 nM + AM630 10 μ M + 3 mg/L CBN (n = 5), or CP94 50 nM + JTE907 10 μ M + 3 mg/L CBN (n = 6) at gastrulation. Dorsal and ventral branches in a motor axon are indicated with the white letters D and V, respectively, whereas secondary and tertiary branches are identified with white and red color arrowhead, respectively, in the vehicle image. Scale bar represents 25 μ m. Bar graphs showing quantification of the secondary and tertiary branches emanating ventrally (B, D) and dorsally (C-E). Significance was determined using Kruskal-Wallis tests followed by Dunn's multiple comparison test. Groups which share the same letter(s) of the alphabet are not statistically different from one another.

Figure 6. 10 Representative tracing of primary MN.

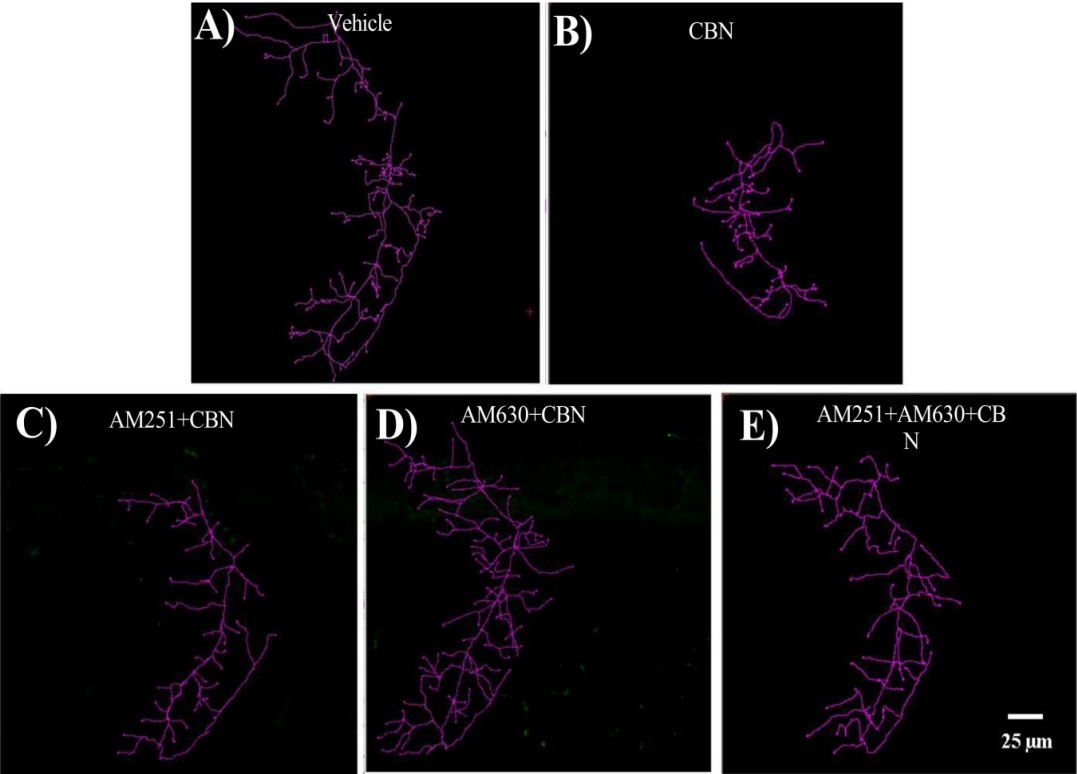


Figure 6.10 Representative traces of primary MN. Neurite image tracing (Image J) was used to trace the MN branching of confocal images. Example tracing shown for (A) vehicle control (n = 7), (B) 3 mg/L CBN (n = 9), (C) 3 mg/L CBN + 10nM AM251 (n = 8), (D) 3 mg/L CBN + 10 μ M AM630 (n = 9), and (E) 3 mg/L CBN + 10 nM AM251 + 10 μ M AM630 (n = 5).

Figure 6. 11 Combined exposure of CBN with CB₂R antagonists exhibited significantly improved locomotion

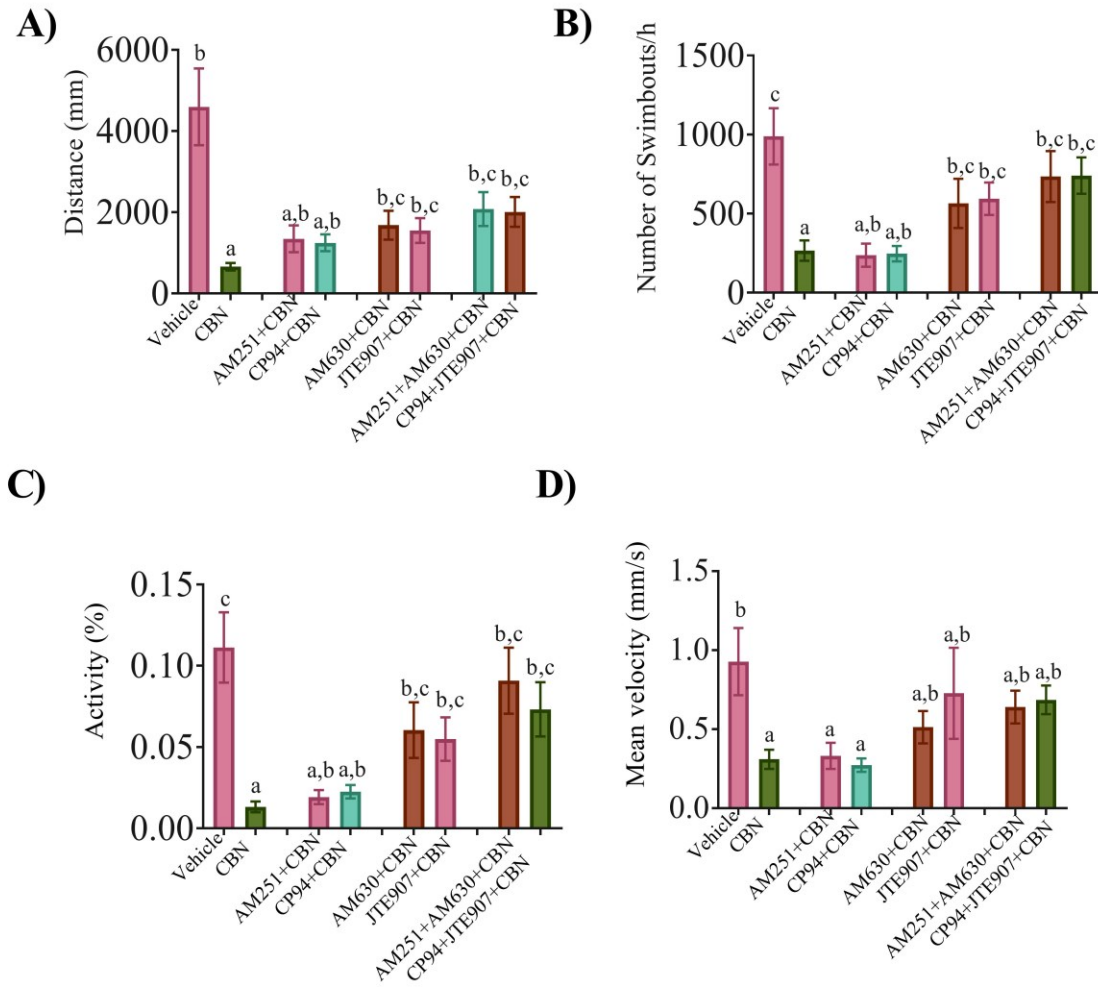


Figure 6.11 Co-treatment with CB₂R antagonists reversed CBN-induced impairment in locomotion. A 96-well plate was used in this experiment where each well contains an individual larva. The free-swimming movement of the fish was recorded for 60 min and the recorded video was analyzed later. Tracings were recorded at 5 dpf for fish exposed transiently at gastrulation to either vehicle control (n = 52), 3 mg/L CBN (n = 40), AM251 10 nM + 3 mg/L CBN (n = 65), CP94 10 nM + 3 mg/L CBN (n = 60), AM630 10 μ M + 3 mg/L CBN (n = 45), JTE907 10 μ M + 3 mg/L CBN (n = 30), AM251 10 nM + AM630 10 μ M + 3 mg/L CBN (n = 40), or CP94 10 nM + JTE907 10 μ M + 3 mg/L CBN (n = 60). (A) Bar graph shows total distance (mm) for 1 h. (B) Bar graph shows frequency of swim bouts within 1 h. (C) Bar graph shows changes in embryo mean activity (% rate for 1 h). (D) Bar graph shows mean velocity (mm s⁻¹ for 1 h). Significance was determined using Kruskal-Wallis tests followed by Dunn's multiple comparison test. Groups which share the same letter(s) of the alphabet are not statistically different from one another.

Figure 6. 12 Blocking CB₁R and CB₂R activity inhibits CBN-induced alteration of kinocilia development partially and fully, respectively.

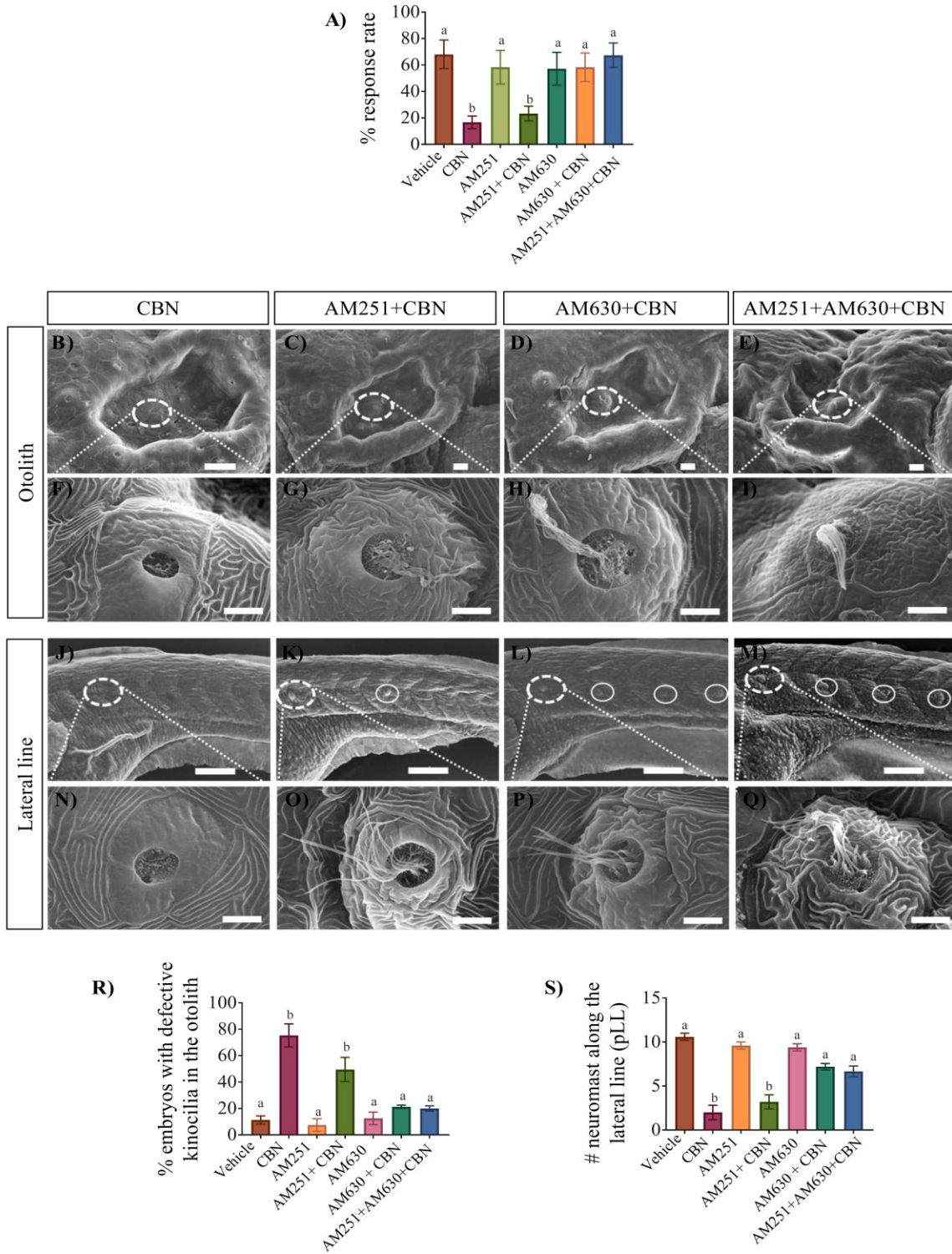


Figure 6.12 Blocking CB₁R and CB₂R activity during CBN treatment at gastrulation inhibits CBN-induced alteration of hair cell development partially and fully, respectively.

(A) Bar graph shows the quantification of response rate (%) to AV stimuli of 5 dpf larvae. (B-I) Representative SEM images from the anterior lateral line (aLL), i.e. otolith and trunk region, i.e., posterior lateral line (pLL) (J-Q), of animals treated with either 3 mg/L CBN (n = 5), AM251 10 nM + 3 mg/L CBN (n = 5), AM630 10 μM + 3 mg/L CBN (n = 5), or AM251 10 nM + AM630 10 μM + 3 mg/L CBN (n = 5). (B-E) and (J–M) Images were taken at 500 x magnification; scale bar represents 20 μm. To show details of the kinocilia inside otoliths (F-I), and neuromasts along pLL (O-Q) images were taken at 10000 x magnification; scale bar represents 5 μm. (R) Bar graph showing the quantification of the percentage of the embryos that exhibited deformities in their hair cell inside the otolith structure. (S) Bar graph showing the number of the neuromasts present along the posterior lateral line. Significance was determined using Kruskal-Wallis tests followed by Dunn's multiple comparison test. Groups which share the same letter(s) of the alphabet are not statistically different from one another.

Figure 6. 13 Blocking CB₂R activity prevented CBN mediated alteration of otolith structure.

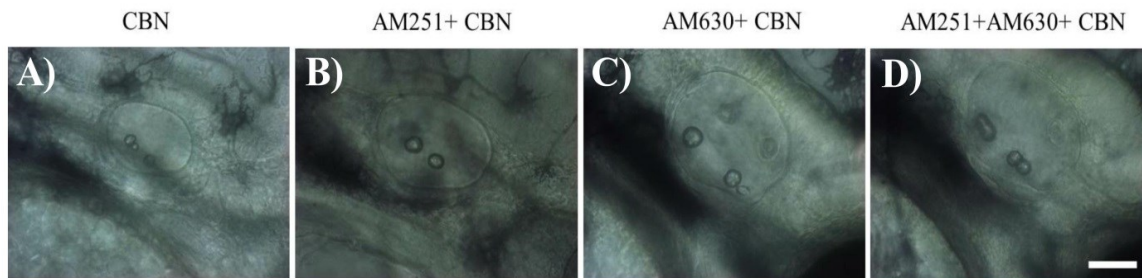


Figure 6.13 Blocking CB₂R activity during CBM exposure at gastrulation prevented CBN-induced alteration of otolith structure. Otolith images were taken from 52 hpf old embryos, positioning anterior (head) on right and posterior (tail) on left; representative images are presented. (A) 3 mg/L CBN (n = 20), (B) 3 mg/L CBN + 10 nM AM251 (n = 20), (C) 3 mg/L CBN + 10 μM AM630 (n = 20), and (D) 3 mg/L CBN + 10 nM AM251 + 10 μM AM630 (n = 20). Scale bar represents 50 μm.

Chapter 7

Brief exposure to (-) THC affects embryonic and adult locomotion; the effect persisted in the offsprings

In this study, I set out to determine if a brief exposure of (-) THC during gastrulation has a persistent effect on zebrafish development (F0 generation) and their offspring (F1 generation). I found that the short (-) THC exposure negatively affected the morphology, locomotion, synaptic activity and MN branching in the F0 generation. Importantly, I found that the concentration of (-) THC was lethal at very low concentrations (0.5 mg/L). In addition, I also observed a persistent effect on locomotion in the adults and their offspring (F1).

7.1 Results

7.1.1 Brief exposure to (-) THC during gastrulation is detrimental to the development of zebrafish embryos

Here, I set out to determine whether exposure to the negative isoform of THC, (-) THC, alters the development of zebrafish embryos. To do this, I exposed zebrafish embryos during gastrulation (5.25-10.75 hpf) to a range of (-) THC concentrations from 0.001 mg/L to 20 mg/L and examined a variety of characteristics including survival, hatching, body length and heart rate. At the end of the exposure period (10.75 hpf), I washed the embryos several times in embryo media and let them grow until they were 5 dpf. Exposure to (-) THC altered morphology and

body length in a dose-dependent manner (Fig 7.1 A and B) such that embryos exposed to higher concentrations of (-) THC exhibited blebbing in the tail region (Fig 7.1 A) and shorter body lengths. Quantification of body length showed that animals treated with 10 and 20 mg/L of (-) THC exhibited a significantly shorter body length of 2.6 ± 0.06 mm (n = 35) and 2.3 ± 0.05 mm (n = 40), respectively, compared to control of 3.2 ± 0.02 mm (Fig 7.1 B, n = 30, $p < 0.05$). Lower doses of (-) THC (0.001 - 1 mg/L) did not significantly alter body length.

Quantification of survival rates showed that only higher concentrations of (-) THC significantly affected survival. At 5 dpf, animals treated with 10 mg/L of (-) THC had a survival rate of 46 ± 6 %, which is significantly reduced compared to control values of 95 ± 3 % (Fig 7.1 C, n = 100, $p < 0.05$). In contrast, a 100 % mortality was observed by 5 dpf in animals treated with the highest concentration of (-) THC 20 mg/L (Fig 7.1 C). Hatching rates were also significantly reduced by exposure to (-) THC, but only in the case of higher concentrations (10 mg/L and 20 mg/L) (Fig 7.1 D, n = 100, $p < 0.05$). Finally, an examination of cardiac activity showed a reduction in heart rate only at higher concentrations of 10 mg/L and 20 mg/L (-) THC where heart rates were 64 ± 5 (n = 56) and 40 ± 3 bpm (n = 70), respectively, compared with control values of 100 ± 2 bpm (Fig 7.1 E, $p < 0.05$).

7.1.2 (-) THC exposure (during gastrulation) affects the locomotion of zebrafish embryos

Next, I asked whether brief exposure to (-) THC during gastrulation altered zebrafish locomotion. I was particularly interested in determining if exposure to (-) THC alters the different types of locomotion that occurs at specific developmental periods in the first week of

development. For example, zebrafish embryos develop spontaneous coiling activity (i.e. burst activity) within the chorion around 17-19 hpf. Later, the embryos develop the escape response around 27 hpf (Saint-Amant & Drapeau, 2000). Finally, embryos develop free-swimming locomotor activities at 72 hpf shortly after hatching, and exhibit beat and glide type swimming by 4-5 dpf. Hence, I wanted to examine whether (-) THC exposure affects spontaneous activity at 1 dpf, touch (escape) responses at 2 dpf and free swimming at 5 dpf, which are characteristic behavior or locomotive response of these developmental ages.

Analysis of spontaneous coiling activity at 1 dpf showed that exposure to (-) THC (0.001-10 mg/L) significantly reduced the coiling activity compared to control embryos (Fig 7.2 A, n = 50-75, $p < 0.05$). Similarly, the spontaneous coiling count per minute was significantly decreased compared to control embryos for all (-) THC treatments (Fig 7.2 B, n=50-75, $p < 0.05$) except 0.1 mg/L.

Zebrafish embryos exhibit a robust characteristic escape activity in response to a touch stimulus to the head. I recorded not only the escape response, but also the swimming activity immediately following the escape because these two locomotor activities are different and are driven by different locomotor circuits. My analysis showed that exposure to the lower concentrations of 0.001- 0.1 mg/L (-) THC did not affect swimming distance. However, the higher concentrations of 1 mg/L and 10 mg/L (-) THC resulted in significant reductions in swimming distances to values of 3.4 ± 0.48 cm (n = 55) and 0.44 ± 0.05 cm (n = 35), respectively, compared with controls of 6.2 ± 1.1 cm (Fig 7.2 C, n = 40, $p < 0.05$). Similarly, swimming velocity was significantly decreased to 0.1 ± 0.02 cm/s (n = 55) and 0.01 ± 0.002 cm/s (n = 35) respectively for 1 mg/L and 10 mg/L (-) THC-treated animals compared with controls values of 0.23 ± 0.03 cm/s (Fig 7.2 D, n = 35-55, $p < 0.05$).

Finally, I recorded the free-swimming activity of 5 dpf larva for one hour. I found that exposure to (-) THC resulted in bi-phasic changes in swimming activity where animals treated with 1 mg/L (-) THC exhibited significantly increased swimming activity compared with control (Fig 7.2 E, n = 30, p<0.05). Exposure of embryos to higher concentrations (10 mg/L; n = 30) or lower concentrations (0.01 and 0.1 mg/L; n = 45 and n = 40 respectively) resulted in a significant reduction of swimming activity (Fig 7.2 E, p<0.05). Analysis of swimming distance showed a similar trend for the (-) THC treatment (Fig 7.2 F).

7.1.3 (-) THC exposure significantly reduced the frequency of mEPCs

The exposure of (-) THC affected the locomotion of the embryos. Therefore, I wanted to examine if the exposure also affected the synaptic activities at NMJs. I recorded miniature endplate currents (mEPCS) from the white fibers of 2 dpf embryos since mammalian skeletal muscle mostly consists of twitch fiber type. I used a single concentration of 10 mg/L (-) THC to treat embryos for the remainder experiment unless mentioned otherwise because this concentration resulted in about 50 % survival and hatching of zebrafish embryos following the exposure. My analysis showed that the (-) THC treatment significantly reduced the mEPCS frequency to 0.03 ± 0.01 Hz compared to control values of 0.08 ± 0.02 Hz (Fig 7.3 A and C, n = 8, p<0.05). However, the average amplitude and the decay kinetics of mEPCS were not significantly different compare to control (Fig 7.3 B, D and E, p> 0.05).

7.1.4 The exposure to (-) THC significantly altered the MN branching

Next, I sought to determine whether (-) THC exposure during gastrulation affected the development of motor neurons. To do this I first used antibodies to immunolabel the primary motor neurons. Immunolabelling of primary MNs (PMNs) with anti-znp1 showed that the (-) THC (10 mg/L) treatment severely impacted the PMNs branching pattern (Fig 7.4 A). To evaluate the effect of (-) THC treatment, I counted the number of primary, secondary and tertiary branches emanating from the motor neuron axon and compared these with corresponding values from controls. Quantification of primary branches of PMN showed no significant difference between (-) THC and vehicle treatment (data not shown). In contrast, (-) THC treatment caused a significant reduction in the number of secondary and tertiary ventral branches of PMN to 12 ± 2 and 6 ± 2 compared to control values of 20 ± 1 and 18 ± 2 , respectively (Fig 7.4 B and C, $n = 6$, $p < 0.05$). Dorsal branches also seem affected by the (-) THC treatment (Fig 7.4 A); however, the quantification did not result in a significant reduction of secondary and tertiary dorsal branches (data not shown).

Next, I wanted to determine if the (-) THC (10 mg/L) treatment affected the branching pattern of secondary MNs. Immunolabelling of the embryos with anti-zn8 showed that the exposure of (-) THC negatively affected the growth of secondary MN at 2dpf (Fig 7.4 D). Only 17 ± 7 % of secondary MNs have ventral branches for the (-) THC treated group compared to values in controls of 100 %, which is a significant alteration of secondary MN branching (Fig 7.4 E, $n = 5$, $p < 0.05$). Similarly, significantly less number of secondary MNs (17 ± 9 %) has lateral branching compared to control of 87 ± 8 % (Fig 7.4 F, $n = 5$, $p < 0.05$).

7.1.5 Brief exposure to (-) THC during gastrulation altered muscle fiber morphology

To complement my studies on motor neural development and to more thoroughly investigate the effect of THC on cells involved in locomotion, I examined if skeletal muscle fibers in zebrafish were altered following exposure to (-) THC. To do this, I used transmission electron microscopy (TEM) to investigate the ultrastructure of muscle fibers. I found that (-) THC treatment severely impacted the morphology of red muscle fibers (including myofibrils and myofilaments) (Fig 7.5 A) and altered the structure of sarcoplasmic reticulum (SR) in white fibers (Fig 7.5 B). Myofibrils (MF) boundary, surrounded by SR, was either absent or disorganized in red fiber of (-) THC treated embryo compared to their vehicle treated animal. Also, myofilaments of the red and white fiber in the (-) THC-treated group did not look sharp and distinct, as observed in the control group (Fig 7.5 B). In addition, SR structure looks altered or swollen in the white fiber of (-) THC treated animal compared to their counterpart (Fig 7.5 B). I also observed the presence of damaged mitochondria or mitochondrial membranes that were visible in the (-) THC treated embryos (white arrow in Fig 7.5 C). The fusion of mitochondria also appeared to occur in animals treated with (-) THC (green arrow in Fig 7.5 C).

7.1.6 Blocking CB₁R activity inhibited (-) THC-induced mortality and morphological alteration

Thus far my findings indicate that high concentrations of (-) THC induce severe alterations in locomotor activity, synaptic activity, MN and muscle development and gross animal morphology. To determine if the cannabinoid receptors CB₁R and CB₂R were involved in

mediating these effects, I asked if blocking either of these receptors would prevent the effects of (-) THC. I used two sets of antagonists for each of CB₁R (AM251 and CP9455) and CB₂R (AM630 and JTE907) and at a range of concentrations (10, 50 and 100 nM for CB₁R and 5, 10 and 50 μM for CB₂R) to confirm my findings. I found that blocking CB₁R with either 10 nM AM251 or 50 nM CP9455 significantly reduced the mortality induced by (-) THC treatment. Combined treatment of (-) THC with 10 nM AM251 or 50 nM CP9455 showed a survival percentage of $72 \pm 5\%$ and $71 \pm 2\%$, respectively, compared with (-) THC-treated embryos of $34 \pm 2\%$ (Fig 7.6 A, n = 125 for each treatment, $p < 0.05$). The CB₂R antagonists (AM630 or JTE907) were not capable of preventing the (-) THC-induced mortality (Fig 7.6 B, n = 125 for each treatment, $p > 0.05$).

Two CB₁R antagonist treatments, 10 nM AM251 or 50 nM CP9455, prevented the (-) THC-induced reduction in body length (Fig 7.6 C, n = 125, $p < 0.05$). In comparison, cotreatment of (-) THC with CB₂R antagonists did not alter (-) THC-induced reduction in body length. Next, I determined if blocking CB₁R or CB₂R inhibited (-) THC-induced reduction of heart rate. I found that the co-treatment of (-) THC with 50 nM CP9455 significantly attenuated (-) THC-elicited alteration of heart rate (Fig 7.6 E, n = 125, $p < 0.05$), whereas neither the CB₁R antagonist AM251 nor the two, CB₂R antagonists tested altered THC-induced reduction of the heart (Fig 7.6 E, F, n = 125, $p > 0.05$). Together, these results suggest that (-) THC acts via CB₁R to alter several aspects of development and is partly responsible for effects on heart rate.

7.1.7 Brief exposure to (-) THC is lethal to zebrafish embryos, disrupts swimbladder development

Next, I asked whether the developmental changes induced by brief exposure to (-) THC during gastrulation persist until adulthood. However, I observed that embryos treated with 10 mg/L (-) THC did not survive past 10 dpf in the nursery. I systematically tested long-term survival following exposure to a range of (-) THC concentrations, from 0.001 to 0.5 mg/L. I found that exposure to 0.5 mg/L (-) THC resulted in a survival rate of $8 \pm 3 \%$ ($n = 125$) compared with control rates of $74 \pm 3.6 \%$ at 15 dpf (Fig 7.7 A, $n = 125$, $p < 0.05$). Even the lowest concentration of 0.001 mg/L (-) THC significantly reduced the survival rate to $41 \pm 5.2 \%$ ($n = 125$) by 15 dpf compare to controls (Fig 7.7 A, $n = 125$, $p < 0.05$). Therefore, I wanted to investigate whether (-) THC treatment caused morphological defects in animals older than 1 week post-fertilization that could contribute to the mortality. Goolish & Okutake (1999) reported that improper swimbladder development is linked to decreased survival of zebrafish by 10 dpf. Therefore, I examined swim bladder development by microscopy and found that the swimbladder was not fully inflated or developed by 5 dpf in animals treated with (-) THC at concentrations higher than 0.5 mg/L (Fig 7.7 B). Under the microscope, it was challenging to identify the area of the swimbladder of some embryos. To avoid ambiguity, I performed H & E staining to examine the swimbladder development. H & E staining showed that the swimbladders of animals treated with 0.5-10 mg/L (-) THC were uninflated (Fig 7.7 C).

7.1.8 Blocking cannabinoid receptor activity did not rescue normal development of swimbladder; however, activation of Shh prevented (-) THC-induced swimbladder defects

I had previously found that blocking CB₁R activity inhibited (-) THC-induced morphological abnormalities, and thus asked whether blocking cannabinoid receptors would prevent (-) THC-elicited swimbladder defects. I found that blocking CB₁R activity with AM251 or CP94 did not inhibit 10 mg/L (-) THC-induced defects of the swimbladder (Fig 7.8 B). Similarly, blocking CB₂R action with AM630 or JTE907 did not prevent the effects of (-) THC. In addition to cannabinoid receptors, (-) THC activity can be mediated through TRP channels such as TRPV1, TRPA1 and TRPM8. Therefore, I tested whether blocking TRP channel activity could prevent the (-) THC-induced defects in the swimbladder. However, I found the application of TRPV1 and TRPM8 channel antagonist (AM9090) did not alter the detrimental effects of (-) THC on the swimbladder (Fig 7.8 B).

The Shh and Wnt signalling pathway has been linked to swimbladder development (Winata et al., 2009). Therefore, I asked whether the activation of these pathways could prevent the (-) THC-induced defects in the swimbladder. Overactivation of Shh pathway with SMO agonist purmorphamine (Pur) (20 µM) resulted a significant defect in the swimbladder development. Whereas, stimulation of Wnt signalling with Bio (0.01 and 0.001 µM) did not resulted an alteration in the swimbladder development. Co-application of the Shh activator Pur (5, 10 and 20 µM) with (-) THC significantly reduced the ability of (-) THC to cause defects in the swimbladder. Exposure to Pur (10 µM) + (-) THC and Pur (20 µM) + (-) THC resulted in increased percentage of embryos with inflated or developed swimbladder of $51 \pm 7\%$ (n = 50) and $54 \pm 15\%$ (n = 60) compared to (-) THC treatment (Fig 7.8 C, n = 50 - 60, p < 0.05). However, co-treatment with the Wnt signalling activator BIO did not prevent (-) THC-induced defects of the swimbladder. Further, combined application of Shh and Wnt signalling activator (Pur and BIO) with (-) THC did not result in an additive effect in reversing the ability of (-) THC

treatment to elicited defects of the swimbladder (Fig 7.8 C). These results indicate that (-) THC-induced defects in the swimbladder is mediated by Shh signalling.

7.1.9 Transcriptomic changes in zebrafish embryos (F0) following brief exposure of (-) THC during gastrulation

Further, I used RNA sequencing technology (RNA-seq) to detect genome-wide transcriptional changes (i.e. differential gene expression) of (-) THC-treated embryos. For doing this, I collected RNA from (-) THC (0.5 mg/L and 3 mg/L) and vehicle control treated embryos at 5 dpf. 3 mg/L and 0.5 mg/L of (-) THC treatments were chosen because they caused 100% and 90% lethality, respectively. Also, I performed RNA-seq at 5 dpf rather than at later times of development because the embryos appear normal till 5 or 6 dpf, and then their survival rates start declining fast. I wanted to avoid additional stress factors or pathway activation, which might trigger in the later developmental stage because the larva started dying at later days of development. Therefore, I focused on 5dpf, and wanted to discover the global differential gene expression that was affected by the (-) THC treatment to understand the mechanism of (-) THC-induced lethality better.

The gene expression of different samples (three samples for each treatment of 3 mg/L and 0.5 mg/L (-) THC) are shown in the heatmap (Fig 7.9 A, B). The clustering of genes showed that the relative expression of genes varies among different samples, which is not surprising. Importantly, findings (tree-structured graph) from the hierarcial clustering showed that samples coming from the vehicle and (-) THC treatment were grouped together. The volcano plot showed a pattern of upregulated and downregulated genes of these treatments (Fig 7.9 C, D). In

total, more than 2750 genes were differentially expressed both in 3 mg/L and 0.5 mg/L of (-) THC-treated embryos. An analysis of differentially expressed genes showed that about 1347 genes were downregulated, whereas 1483 genes were upregulated in 0.5 mg/L (-) THC-treated embryos. In comparison, approximately 1088 genes were downregulated, and 1684 genes were upregulated in 3 mg/L (-) THC-treated embryos (Fig 7.9 B, C). Among upregulated genes, about 812 and 666 genes were unique for 3 mg/L and 0.5 mg/L treatment, respectively; whereas 1072 upregulated genes were common in between these two treatments (7.10 A). In contrast, among downregulated genes, about 727 and 1015 genes were unique for 3 mg/L and 0.5 mg/L treatment, respectively; whereas 699 downregulated genes were common in between these two treatments (7.10 B). Both (-) THC treatments caused significant downregulation of the sonic hedgehog genes such as *ptch2*, *smo*, *gli1*, and *gli2b*. However, regarding the sonic hedgehog ligand gene, 3mg/ L (-) THC treatment caused upregulation of *ihha*, whereas 0.5 mg/L treatment led to downregulation of *shhb*. In addition, both concentrations of THC treatment downregulated Wnt signalling genes such as *wnt4a*, and *wnt9b*, as well as the noggins signalling genes *nog1*, *nog2* and *nog3*.

Screening of ECS-related genes showed that the expression of a number of these genes were altered. Among GPCRs, some of the genes were upregulated, such as *gprc5c*, *gpr146*, *gpr160*, and *gpr186*; whereas *gprc5ba* was downregulated. Also, the expression of TRP channel genes was altered, whereas *trpm1b*, *trpm2*, *trpm6* and *trpm7* were downregulated, *trpm4* (*trpm4a* and *trpm4b.2*) was upregulated. AEA synthesizing genes such as *abhd4*, *abhd14b* were upregulated. In addition, the AEA degrading gene *faah2a* was upregulated while *faah2b* was downregulated. Regarding lipid metabolism, both (-) THC treatments significantly downregulated approximately 20 CYP genes. A number of genes involved in cholesterol

synthesis, such as *hmgcra*, *sqle*, *lss*, *cyp51*, *nsdhl*, *hsd17b7*, *hsd17b12a*, *hsd17b12b*, *ebp*, *sc5d*, were downregulated following (-) THC treatment. Additional analysis (using go profiler) revealed that a number of biological processes were affected as predicted by the observed (-) THC-induced alterations in gene expression (Fig 7.11). Various biological processes related to upregulated genes were significantly altered such as proteolysis, peptidase activity, lipid metabolism and glycosylation (Fig 7.11 A). Similarly, a number of developmental processes were significantly affected, which were linked to downregulated genes. For example, biological process related to nervous system development, neurogenesis, neuron differentiation and development, axon development, axonogenesis, brain development, cellular developmental processes were altered (Fig 7.11 B). Together, these findings suggest that the cannabinoid-induced developmental defects could be due to the downregulation of a number of genes that play important role in the nervous system and cellular development.

7.1.10 Brief exposure to (-) THC during gastrulation has a persistent effect on the locomotion of adult zebrafish

Individual behavior-open field test

I reared the exposed animal to adulthood to examine whether the 5.5 hr exposure to (-) THC had any persistent effects. First, I asked if (-) THC-treated zebrafish exhibited locomotor defects or behavioral changes in an open field. For the open field test, I recorded the swimming activity of adult zebrafish for 10 minutes in an open arena. I found that the distance travelled by (-) THC-treated adult zebrafish was not significantly different compared with control, vehicle-treated zebrafish (Fig 7.12 A, n = 20-50, p>0.05). However, animals treated with 0.5 mg/L (-)

THC spent significantly less time in the center zone of the tank compared with controls. For instance, (-) THC-treated animals spent 5 ± 1 s ($n = 10$) in the center zone while vehicle controls spent 18 ± 3 s ($n = 30$) in the center zone (Fig 7.12 B, $p < 0.05$). Furthermore, ANOVA statistical analysis showed that the time spent in the transition zone by the various group of (-) THC-treated adults was significantly different (Fig 7.12 C, $p < 0.05$). The 0.5 mg/L (-) THC-treated adults spent more time (565 ± 6 s) in the thigmotaxis zone compared with controls (480 ± 29 s) (Fig 7.12 D, $p < 0.05$), which is an indication of shyness of their character.

To test anxiety-like behavior in individual fish, I used a novel object approach (NOA) test where fish explore a novel object (the LEGO[®] figurine) placed into the middle of the tank. I did not find significant differences in the distance travelled by various (-) THC treatment groups (Fig 7.12 E; $p > 0.05$). However, the analysis of time spent showed that the 0.5 mg/L (-) THC-treated adult zebrafish exhibit a trend of spending more time in the thigmotaxis zone and less time in the center zone and transition zone. Although the data is not statistically significant, this is an indication of their character's anxiety or shyness (Fig 7.12 F-H).

7.1.11 The exposure of (-) THC during gastrulation in F0 generation has a transgenerational effect on the locomotion of F1 embryos.

Because (-) THC exposure during gastrulation had a persistent effect into adulthood, I wanted to determine whether a brief exposure of 5.5 hr had transgenerational effects. To do this, I examined different types of locomotion in the embryos (F1 generation) of adult fish that were either treated with (-) THC or with vehicle during the gastrula stage in the F0 generation of embryos. F1 embryos from 0.1 and 0.5 mg/L (-) THC treated parents exhibited significantly

reduced spontaneous activity rate of $2.2 \pm 0.3 \%$ ($n = 40$) and $2.7 \pm 0.3 \%$ ($n = 30$) compared with rates of $4.4 \pm 0.42 \%$ in controls consisting of animals from the same batch of parents that were vehicle-treated as F0 embryos (Fig 7.13 A, $n = 50$, $p < 0.05$). The number of spontaneous coils per minute in 24 hpf animals was significantly decreased for F1 embryos from 0.1 and 0.5 mg/L (-) THC-treated parents relative to controls (Fig 7.13 B, $p < 0.05$). However, the mean duration of spontaneous coiling was significantly increased to 1.1 ± 0.1 s ($n = 30$) for the F1 embryos of 0.5 mg/L (-) THC-treated parents compared to values of 0.6 ± 0.04 s in control F1 embryos (Fig 7.13 C, $n = 50$, $p < 0.05$). Together, this suggests that the F1 offsprings from 0.1 and 0.5 mg/L (-) THC-treated parent exhibit decreased coiling activity.

Next, I wanted to determine if brief exposure to (-) THC during gastrulation in F0 generation affects the escape response in the F1 generation. I found that F1 offsprings from the 0.1 and 0.5 mg/L (-) THC-treated parents traveled a significantly shorter distance of 5.0 ± 0.7 cm ($n = 40$) and 3.9 ± 0.5 cm ($n = 30$), respectively, following the escape response, compared with distance travelled by control fish of 8.7 ± 1.0 cm (Fig 7.13 D, $n = 40$, $p < 0.05$). However, the escape response velocity of F1 offsprings from (-) THC-treated parents was not significantly different compared to controls (Fig 7.13 E, $p > 0.05$).

Figure 7. 1 Effect of (-) THC on the development of zebrafish embryos

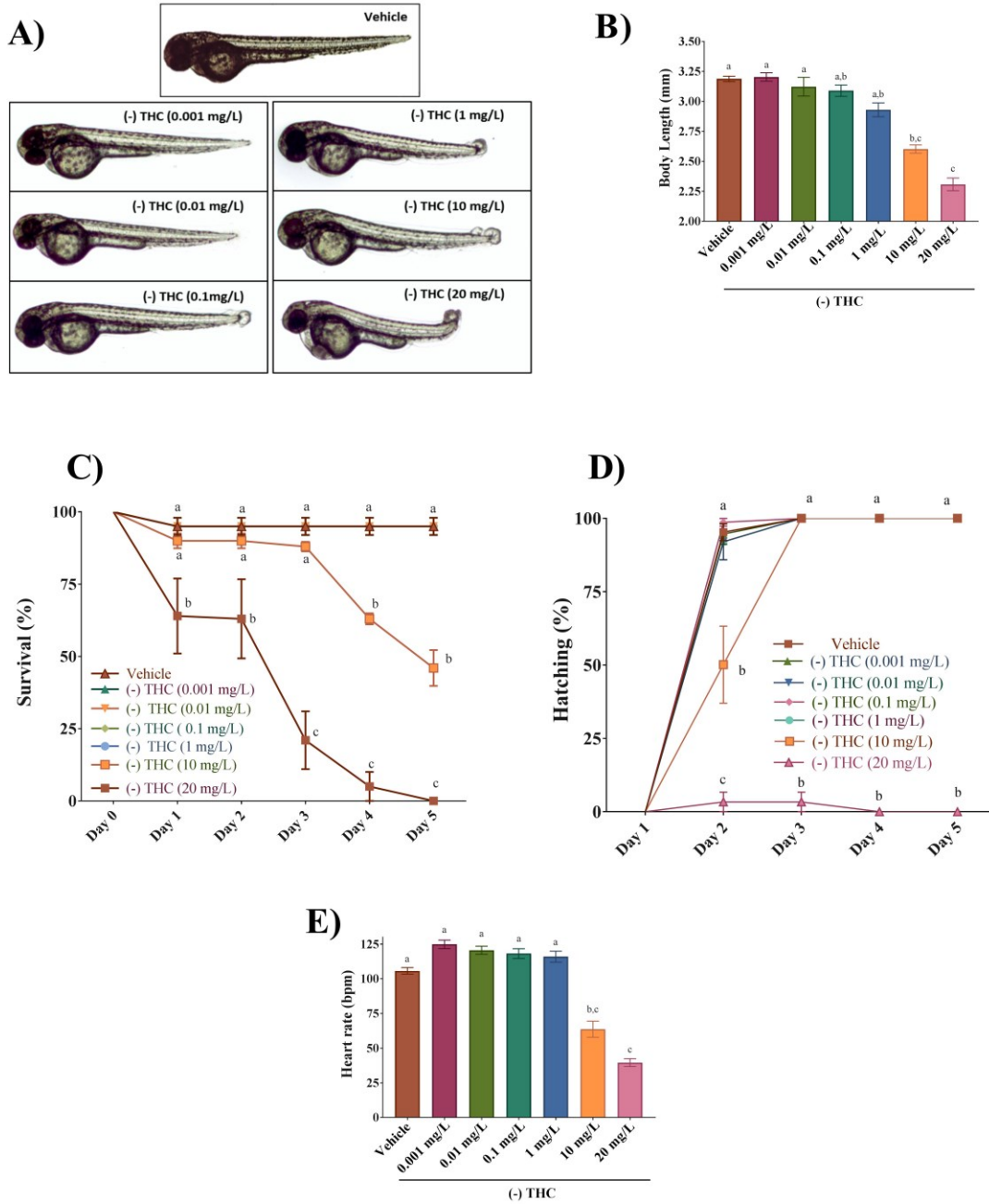
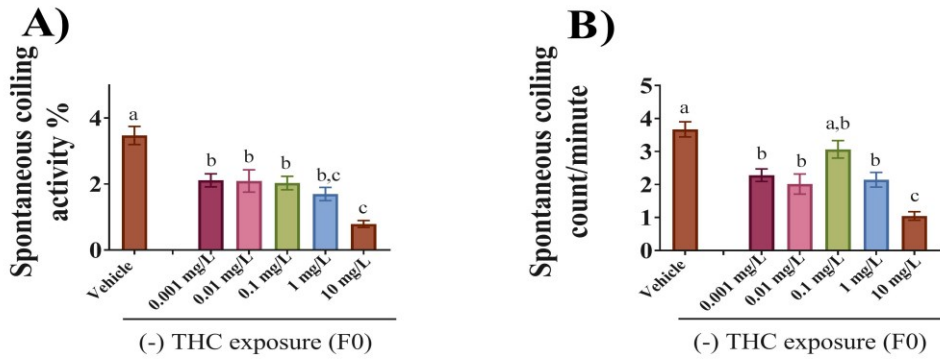


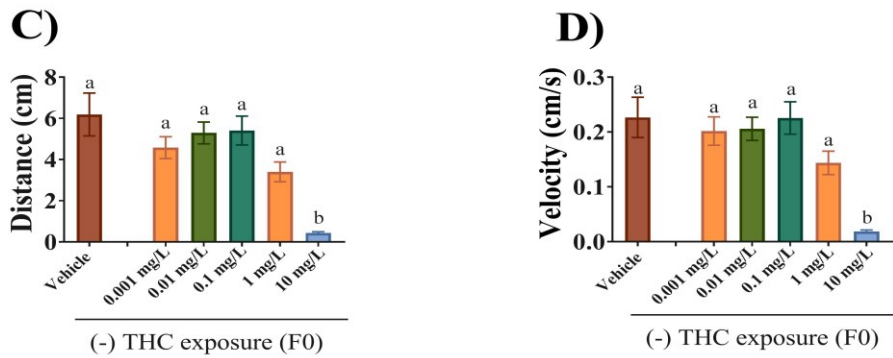
Figure 7.1 Effect of (-) THC on the development of zebrafish embryos. (A) Embryos were treated with vehicle, or exposed to 0.001 mg/L, 0.01 mg/L, 0.1 mg/L, 1 mg/L, 10mg/L, or 20 mg/L (-) THC (from 5.25 hpf to 10.75 hpf) and then allowed to develop in normal embryo media. Images were taken at 48–52 hpf. Representative images are shown. (B) Bar graph showing the body lengths of fish in vehicle control (N=3 experiments and n = 20 embryos for each treatment), and different concentrations of (-) THC (n = 54, 48, 61, 57, 55, and 45 for 0.001, 0.01, 0.1, 1, 10, and 20 mg/L (-) THC-treated fish, respectively). (C) Line graph showing the percentage of embryos that survived within the first 5 days of development following (-) THC exposure during gastrulation (N=3 experiments and n = 20 embryos for each treatment). (D) Line graph showing the percentage of embryos that hatched within the first 5 days of development following (-) THC exposure during gastrulation (N = 3 experiments and n = 20 embryos for each treatment). (E) Bar graph showing the heart rate of vehicle control embryos (n = 30) and 0.001–20 mg/L (-) THC-exposed embryos (n = 26, 22, 22, 21, and 21 for 0.001, 0.1, 0.1, 1, 10, and 20 mg/L (-) THC, respectively). For survival and hatching, significance was determined using two-way ANOVA followed by tukey’s multiple comparison tests. For body length and heart rates, significance was determined using Kruskal-Wallis tests followed by Dunn’s multiple comparison test. Groups which share the same letter(s) of the alphabet are not statistically different from one another.

Figure 7.2 Effect of (-) THC on locomotion during development of F0 embryos

Spontaneous coiling at 1 dpf



Touch response at 2 dpf



Free swimming at 5 dpf

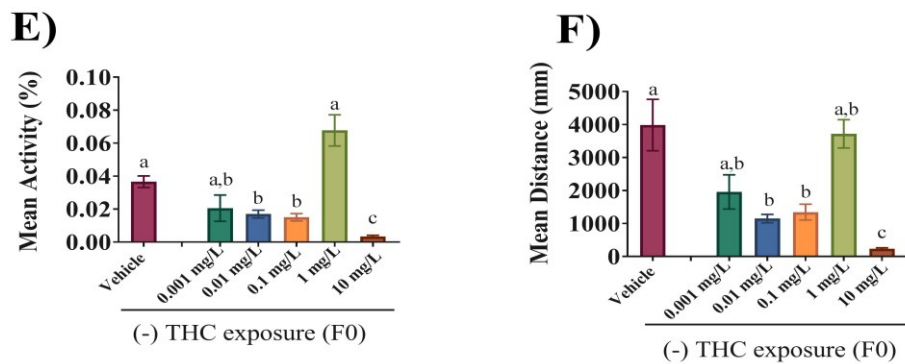


Figure 7.2 Effect of transient exposure to (-) THC on locomotion during development of F0 embryos. (A, B) Spontaneous coiling was recorded from F0 embryos at 1 dpf. Fish were treated during gastrulation with vehicle, 0.001, 0.01, 0.1, 1, or 10 mg/L (-) THC (n = 61, 68, 55, 69, 58, and 49 respectively; N = 5 experiments). (A) Bar graphs represent mean percentage of time showing spontaneous coiling activity. (B) Bar graphs represent mean spontaneous coiling events (count/minute). (D, E) Escape locomotion was recorded from F0 embryos in response to touch at 2 dpf. Fish were treated during gastrulation with vehicle, 0.001, 0.01, 0.1, 1, or 10 mg/L (-) THC (n = 32, 36, 30, 30, 28, and 35, respectively; N= 3 experiments). (C) Bar graphs represent mean distance travelled by embryos in response to touch. (D) Bar graphs represent mean velocity exhibited by embryos during escape response. (E, F) Locomotor behavior in 5 dpf larvae was determined through 1-hr recordings of the free-swimming activity of individual larvae. F0 embryos were treated during gastrulation with vehicle, 0.001, 0.01, 0.1, 1, or 10 mg/L (-) THC (n = 59, 37, 52, 67, 95, and 71, respectively; N= 4 experiments). (E) Bar graphs shows mean activity (%). (F) Bar graphs shows mean distance travelled by embryos. Significance was determined using Kruskal-Wallis tests followed by Dunn's multiple comparison test. Groups which share the same letter(s) of the alphabet are not statistically different from one another.

Figure 7. 3 Effect of (-) THC on synaptic activity at NMJ

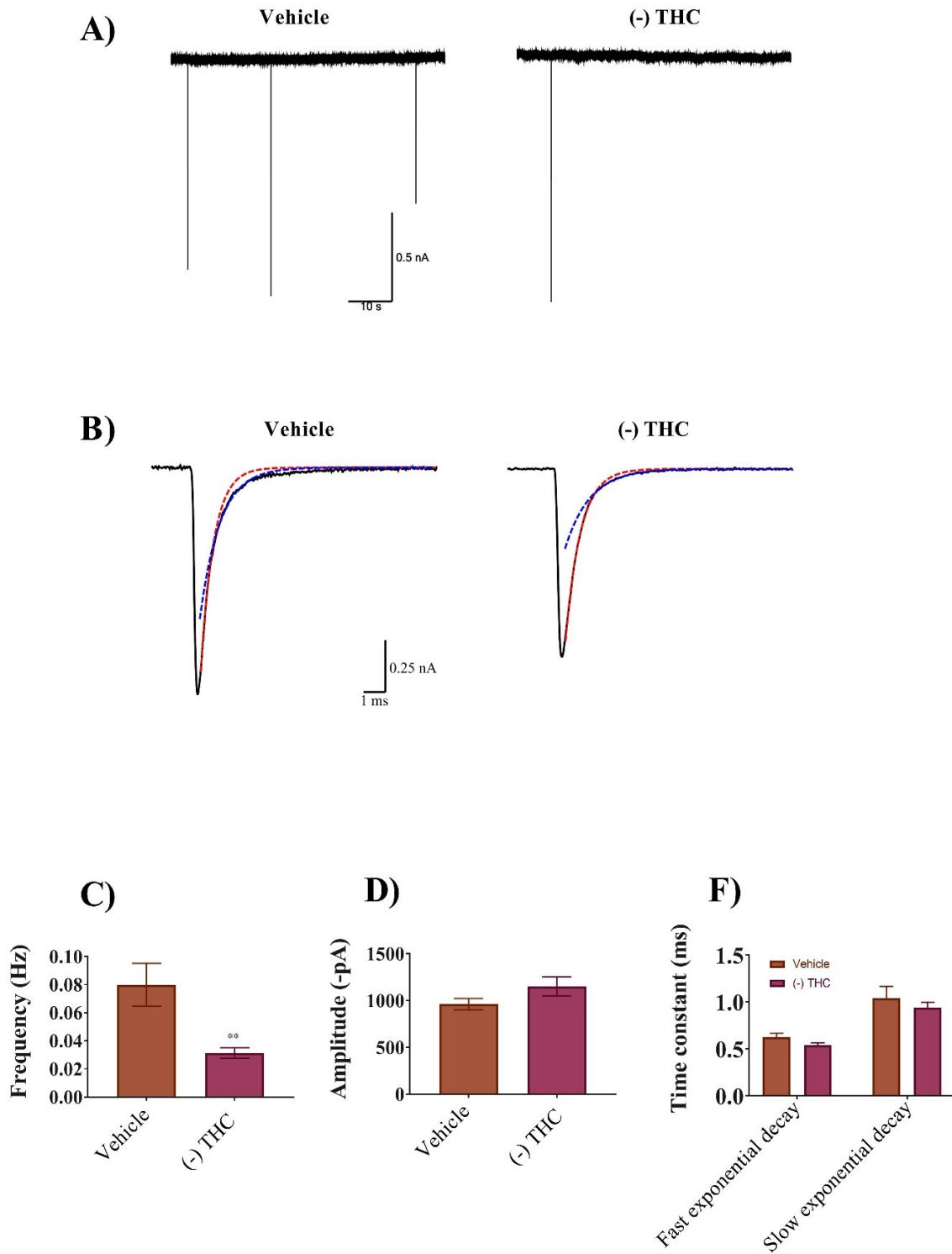


Figure 7.3 Effect of (-) THC on synaptic activity at NMJ. Embryos were exposed to either vehicle or 10 mg/L (-) THC at gastrulation and miniature endplate currents (mEPCs) were recorded from white muscle fibers of 2dpf fish. (A) Example raw traces obtained from 2 dpf vehicle control (n = 7) and (-) THC-treated embryos (n = 9). (B) Averaged mEPCs obtained from white muscle (black line) fitted with a single exponential decay over the fast component (τ_{fast} , red dashed line) or slow component (τ_{slow} , blue dashed line). (C) Bar graph of the mean mEPC frequency of vehicle and (-) THC-treated embryos. (D) Bar graph of the mean amplitude of mEPC of vehicle and (-) THC-treated embryos. (E) Bar graph shows the time constant for mEPC of vehicle and (-) THC-treated embryos. ** Significantly different from vehicle, where $p < 0.01$.

Figure 7. 4 Exposure of (-) THC severely impacted the primary and secondary MN development in F0 embryos

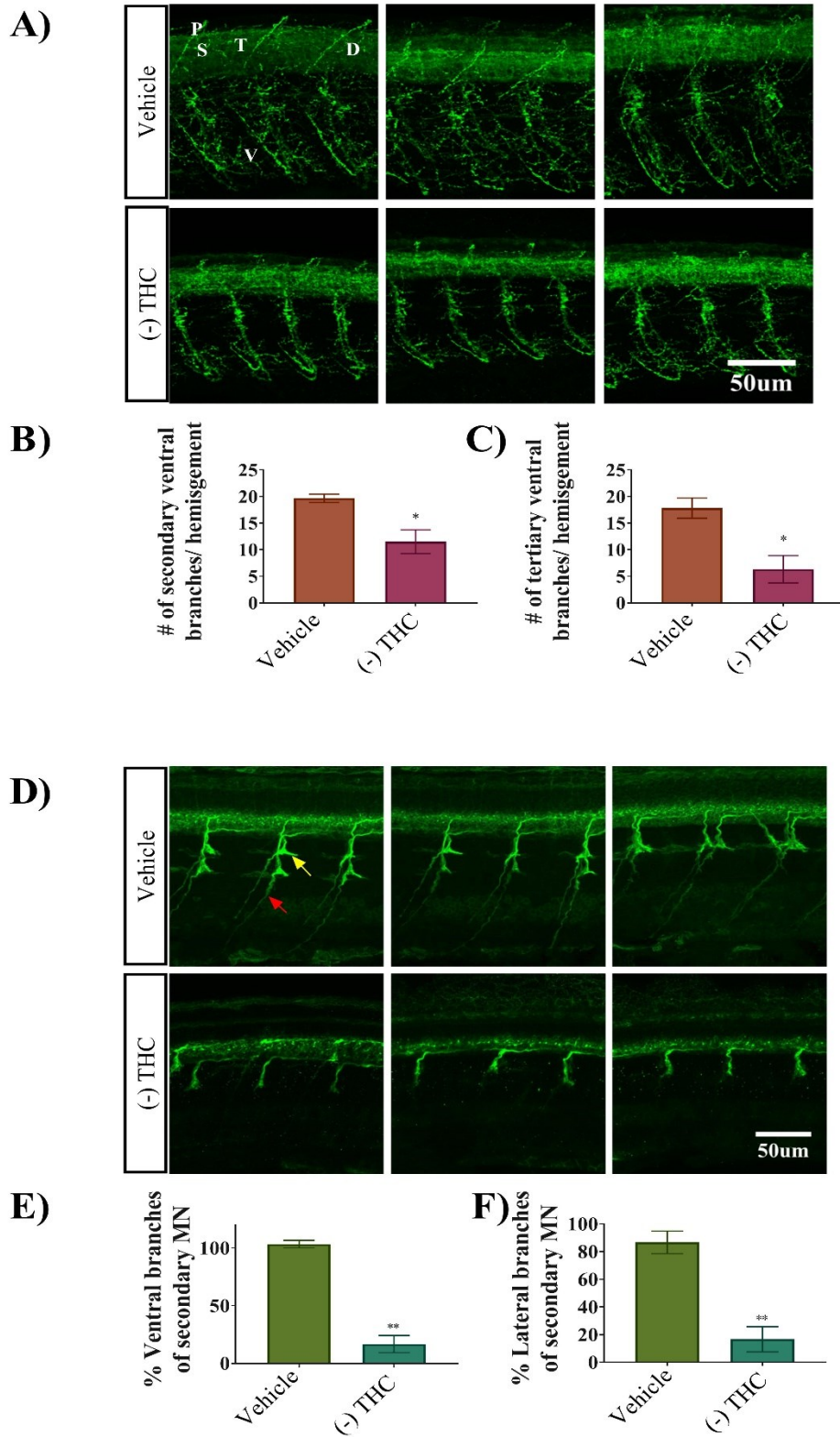


Figure 7.4 Transient exposure to (-) THC during gastrulation severely impacted the primary and secondary MN development in F0 embryos. (A) Example images of antibody labelling (anti-znp1) of axonal branches of primary motor neurons in 2 dpf embryos in vehicle controls, (-) THC (10 mg/L)-treated embryos. Primary, secondary and tertiary branches represented by the white letters P, S, and T, respectively; similarly, dorsal and ventral branches are shown by the white letters D and V, respectively. (B) Bar graphs showing the number of secondary ventral branches emanating from primary motor axons in vehicle control (n = 7) and (-) THC-treated embryos (n=8), counted using image J plugin neurite tracer. (C) Bar graphs showing the number of tertiary ventral branches emanating from primary motor axons in vehicle control (n = 7) and (-) THC treated embryos (n = 8), counted using image J plugin neurite tracer. (D) Example images of antibody labelling (anti-zn8) of axonal branches of secondary motor neurons in 2 dpf embryos in vehicle control, (-) THC (10 mg/L)-treated embryos. Ventral and lateral branches emanating from secondary motor neurons are indicated by red and yellow, respectively. (E-F) Bar graphs comparing percentage of ventral branches (E), and lateral branches (F) emanating from secondary motor neurons in vehicle control (n = 11) and (-) THC-treated embryos (n = 11). ** Significantly different from vehicle, $p < 0.01$, * $p < 0.05$.

Figure 7. 5 Exposure of (-) THC altered the muscle morphology of F0 embryos

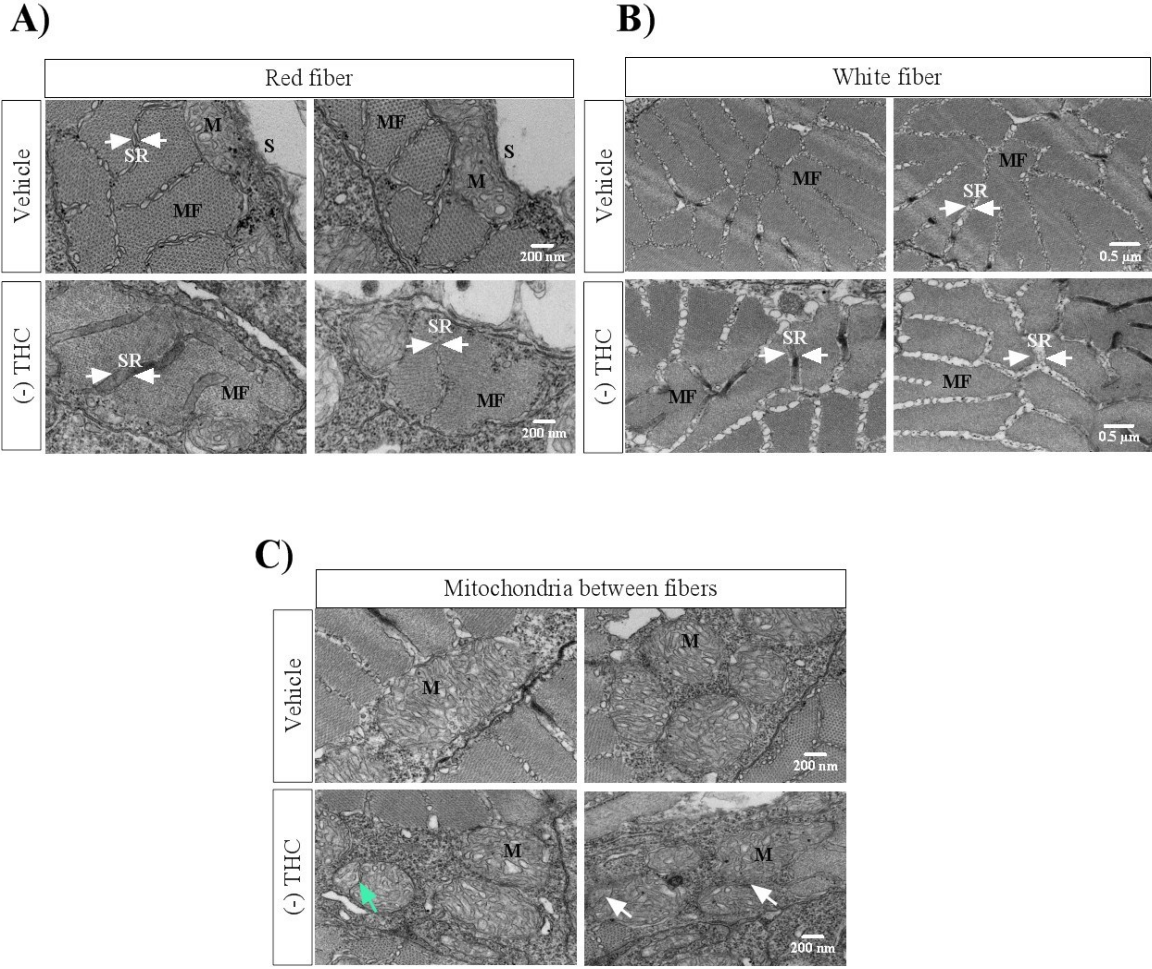


Figure 7.5 Transient exposure to (-) THC at gastrulation altered the muscle morphology of F0 embryos at 5dpf. (A) Representative transmission electron microscopy (TEM) images of red fiber from vehicle and 10 mg/L (-) THC-treated embryos. (B) Representative TEM images of white fiber from vehicle and (-) THC treated embryos. (C) Representative TEM images showing altered mitochondrial structure from vehicle and (-) THC treated embryos. A total of six vehicle- and five (-) THC-treated embryos were examined. The letter(s) of the alphabet S, M, MF and SR denotes skin, mitochondria, myofibrils and sarcoplasmic reticulum, respectively.

Figure 7. 6 Co-exposure of (-) THC with CB₁R antagonist prevented (-) THC-mediated effects

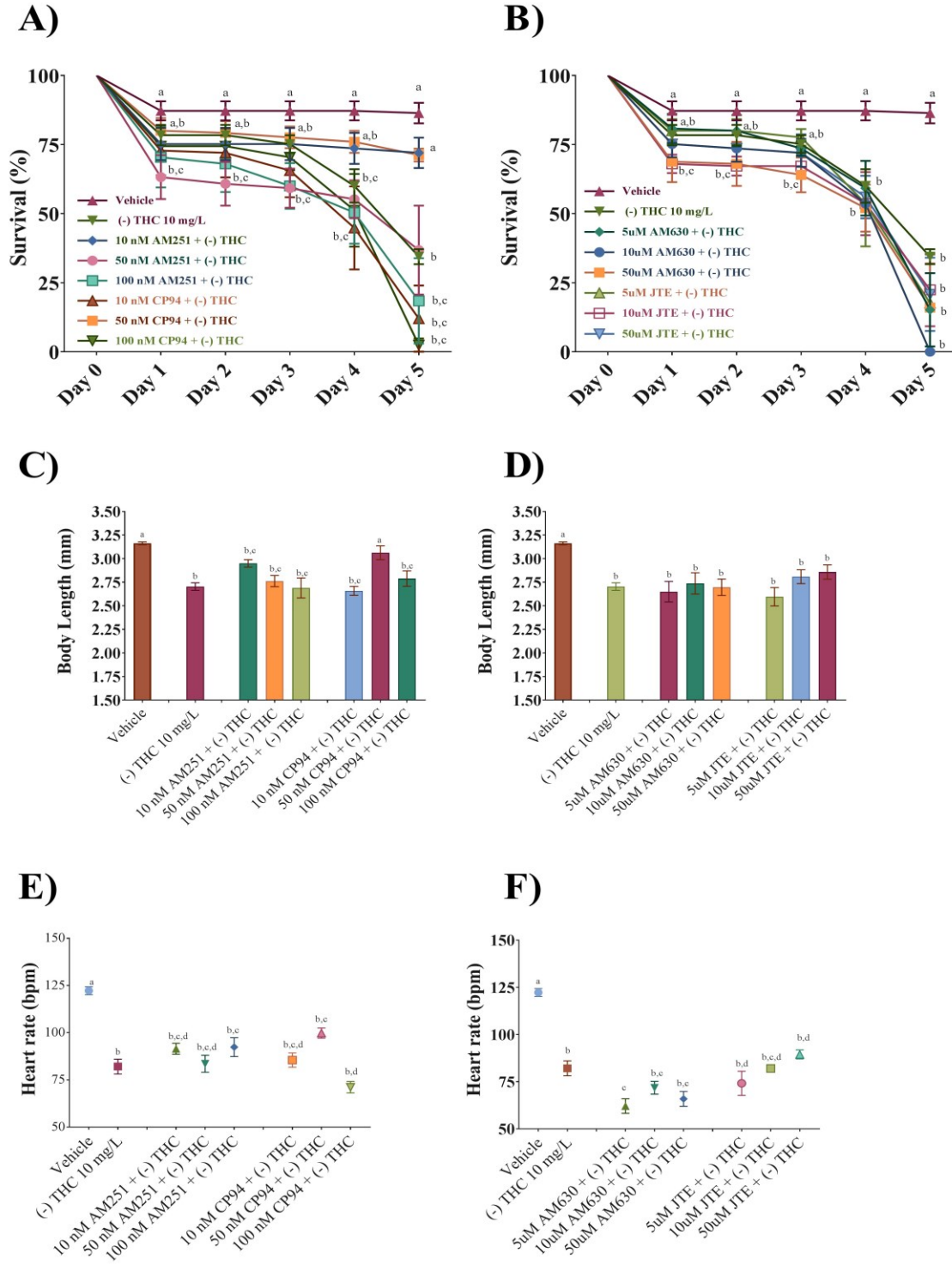


Figure 7.6 Co-exposure of (-) THC with CB₁R antagonist during gastrulation prevented

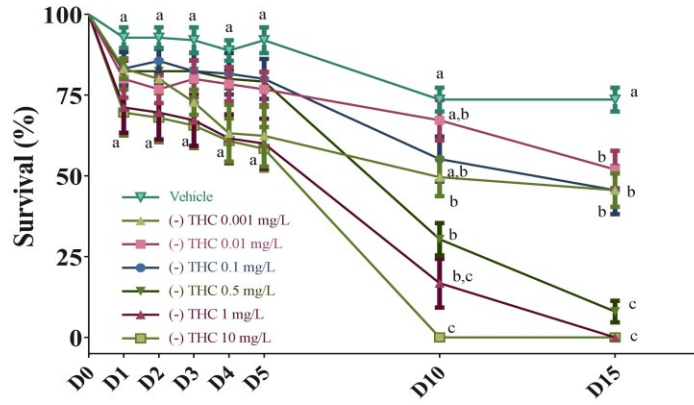
THC-mediated effects. (A) Line graphs showing the percentage of embryos that survived within the first 5 days of development following co-exposure of (-) THC (10 mg/L) and CB₁R antagonists (AM251 and CP-94, each at 10-100 nM) (N = 4 experiments and n = 25 embryos for each treatment). (B) Line graphs showing the percentage of embryos that survived within the first 5 days of development following co-exposure of (-) THC and CB₂R antagonists (AM630 and JTE907, each at 5-50 μM) (N = 4 experiments and n = 25 embryos for each treatment).

Significance was determined using two-way ANOVA followed by tukey's multiple comparison tests. Groups which share the same letter(s) of the alphabet are not statistically different from one another. (C) Bar graphs showing the body length of embryos at 2 dpf following co-exposure of (-) THC and CB₁R antagonists (AM251 and CP-94) (N = 4 experiments and n = 25 embryos for each treatment). (D) Bar graphs showing the body length of embryos at 2 dpf following co-exposure of (-) THC and CB₂R antagonists (AM630 and JTE907) (N = 4 experiments and n = 25 embryos for each treatment). (E) The graph showing the heart rate (beats per minutes, bpm) of embryos at 2 dpf following co-exposure of (-) THC and CB₁R antagonists (AM251 and CP-94) (N = 4 experiments and n = 25 embryos for each treatment). (F) The graph showing the heart rate (beats per minutes, bpm) of embryos at 2 dpf following co-exposure of (-) THC and CB₂R antagonists (AM630 and JTE907) (N = 4 experiments and n = 25 embryos for each treatment).

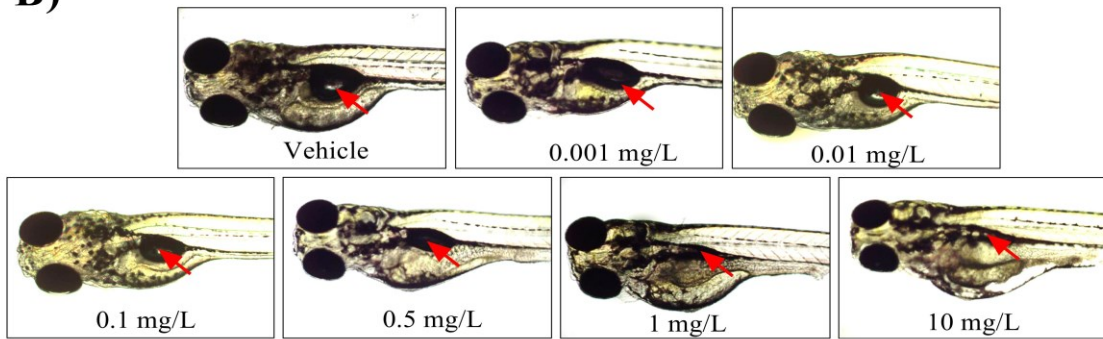
Groups which share the same letter(s) of the alphabet are not statistically different from one another. Significance was determined using Kruskal-Wallis tests followed by Dunn's multiple comparison test.

Figure 7. 7 (-) THC exposure is lethal to zebrafish development and alteration of swim bladder development might contribute towards the (-) THC-induced lethality

A)



B)



C)

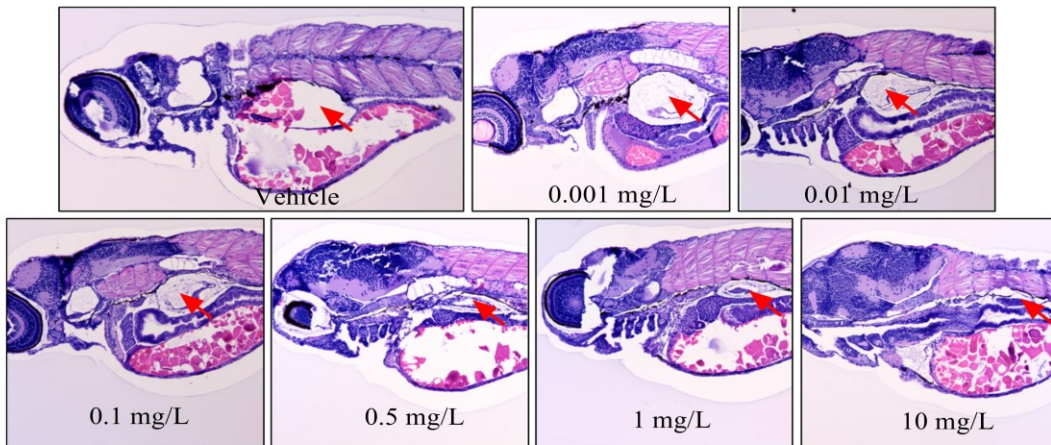
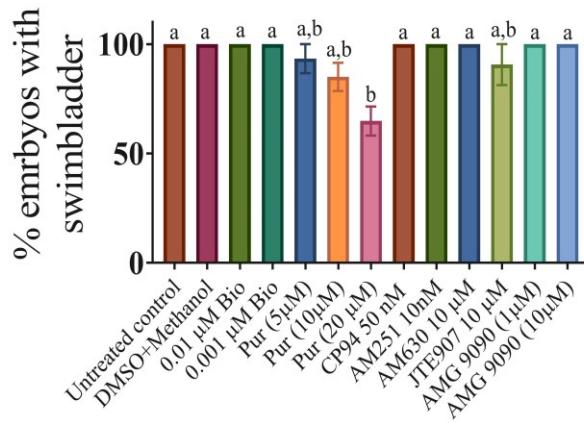


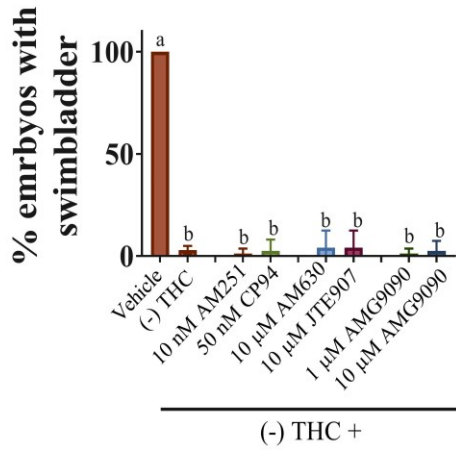
Figure 7.7 (-) THC exposure is lethal to zebrafish development and alteration of swim bladder development might contribute towards the THC-induced lethality. (A) Line graph showing the percentage of embryos that survived within the first 15 days of development following 0.01 to 10 mg/L (-) THC exposure during gastrulation (N=4 experiments and n=25 embryos for each treatment). Significance was determined using two-way ANOVA followed by tukey's multiple comparison tests. Groups which share the same letter(s) of the alphabet are not statistically different from one another. (B) Representative whole-mount images showing dose-dependent effects on swimbladder development by treatments with 0.001 to 10 mg/L (-) THC during gastrulation. (C) Representative H& E staining images of zebrafish embryos; longitudinal sections are showing the presence or absence of inflated swimbladder in (-) THC treated fish.

Figure 7. 8 Activation of hedgehog pathway inhibited (-) THC-mediated alteration of swimbladder

A)



B)



C)

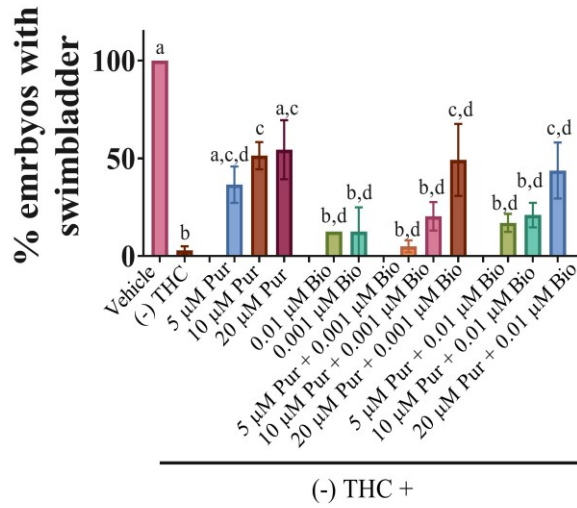


Figure 7.8 Activation of hedgehog pathway inhibited (-) THC-induced alteration of swimbladder. (A) Bar graphs showing percentage of embryos with inflated swimbladder for untreated control; vehicle control; Wnt activator BIO (0.01 and 0.001 μ M); hedgehog activator Purmorphamine (Pur; 5, 10 and 20 μ M); CB₁R antagonists (AM251, 10 nM; and CP94, 50 nM); CB₂R antagonists (AM630 and JTE907; each at 10 μ M); and TRPV1, TRPA and TRPM8 antagonist (AMG9090; 1 and 10 μ M). (B) Bar graphs showing the percentage of embryos with inflated swimbladder for co-exposure of 10 mg/L (-) THC with CB₁R, CB₂R and TRP channel antagonists. (C) Bar graphs showing the percentage of embryos with inflated swimbladder for co-exposure of 10 mg/L (-) THC with hedgehog (Pur) and Wnt activator (BIO). N = 4 experiments and n = 25 embryos for each treatment. Significance was determined using Kruskal-Wallis followed by Dunn's multiple comparison tests. Groups which share the same letter(s) of the alphabet are not statistically different from one another.

Figure 7. 9 RNaseq analysis of (-) THC treated embryos

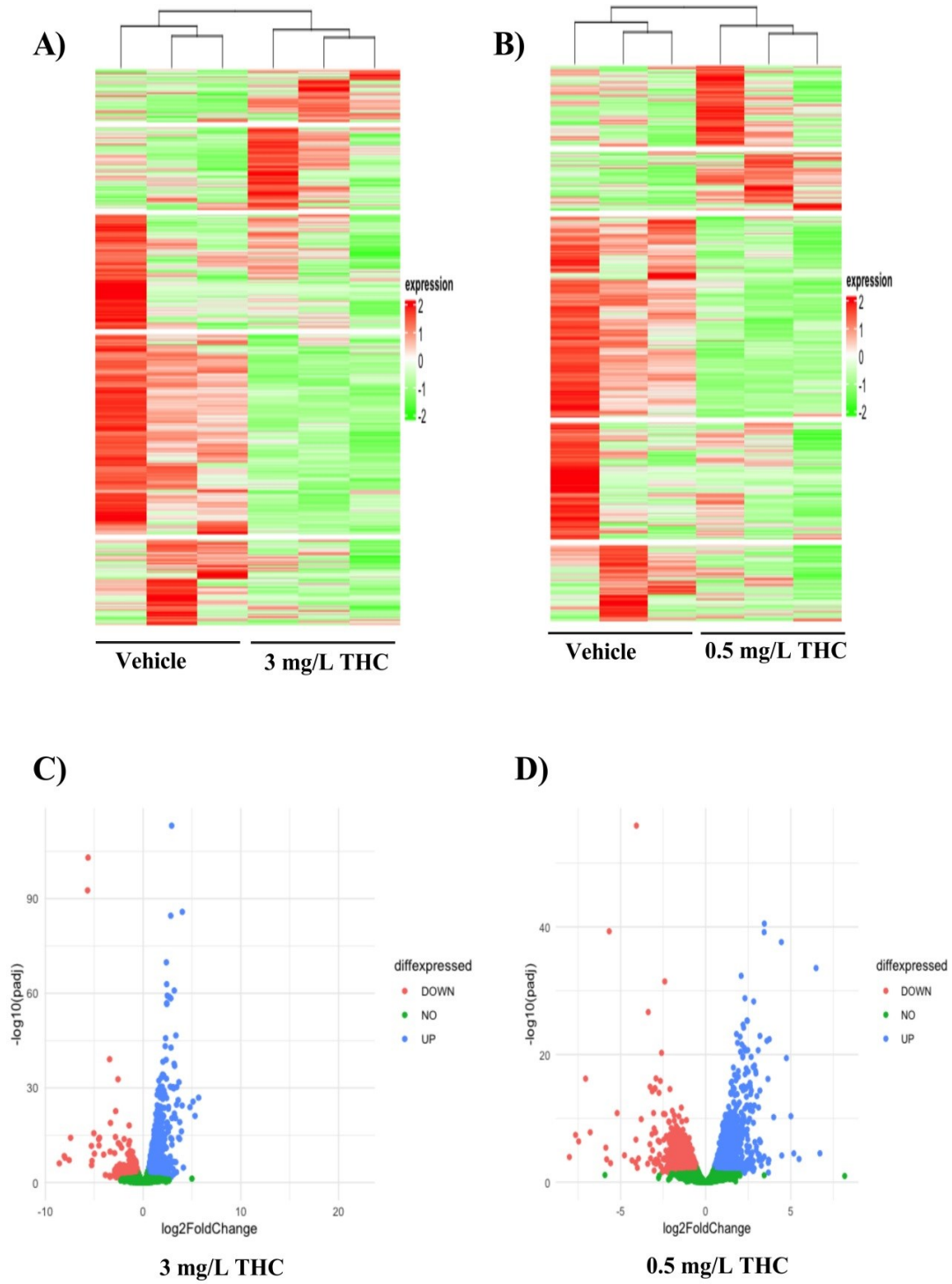
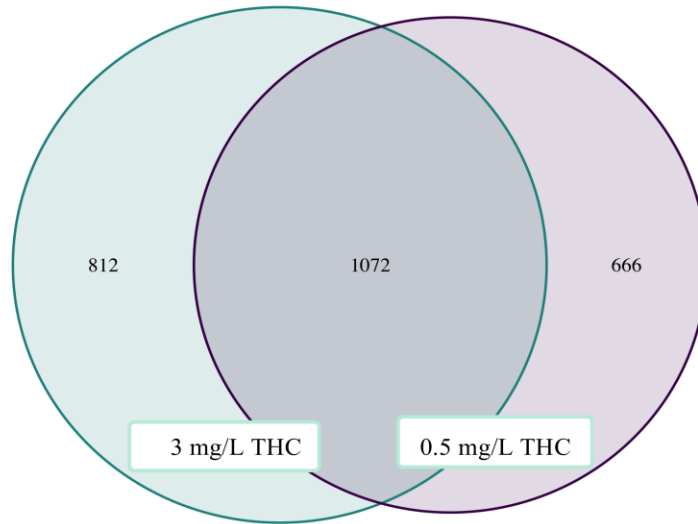


Figure 7.9 RNAseq analysis of (-) THC treated embryos. A) Heatmap of vehicle-treated and 3 mg/L (-) THC treated embryos. B) Heatmap of vehicle-treated and 0.5 mg/L (-) THC-treated embryos. Heatmaps show that C) Volcano plot showing the number of genes downregulated and upregulated in 3 mg/L (-) THC-treated embryos. D) Volcano plot showing the number of genes downregulated and upregulated in 0.5 mg/L treated-embryos.

Figure 7. 10 (-) THC mediated altered gene expression is linked to various biological process (BP)

A)



B)

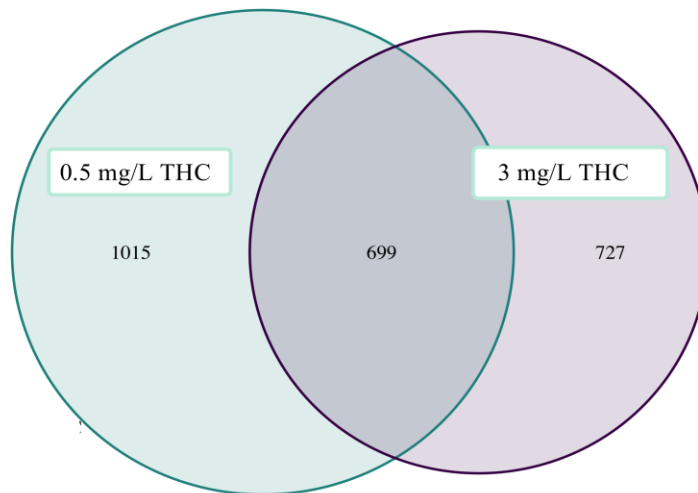


Figure 7.10 Ven diagram of 3 mg/L THC and 0.5 mg/L (-) THC treatment. A) Ven diagram showing the number of overlapping genes that were upregulated between the 3 mg/L and 0.5 mg/L (-) THC treatment groups. B) Ven diagram showing the number of overlapping genes that were downregulated between the 3 mg/L and 0.5 mg/L (-) THC treatment groups.

Figure 7. 11 (-) THC mediated altered gene expression is linked to various biological process (BP)

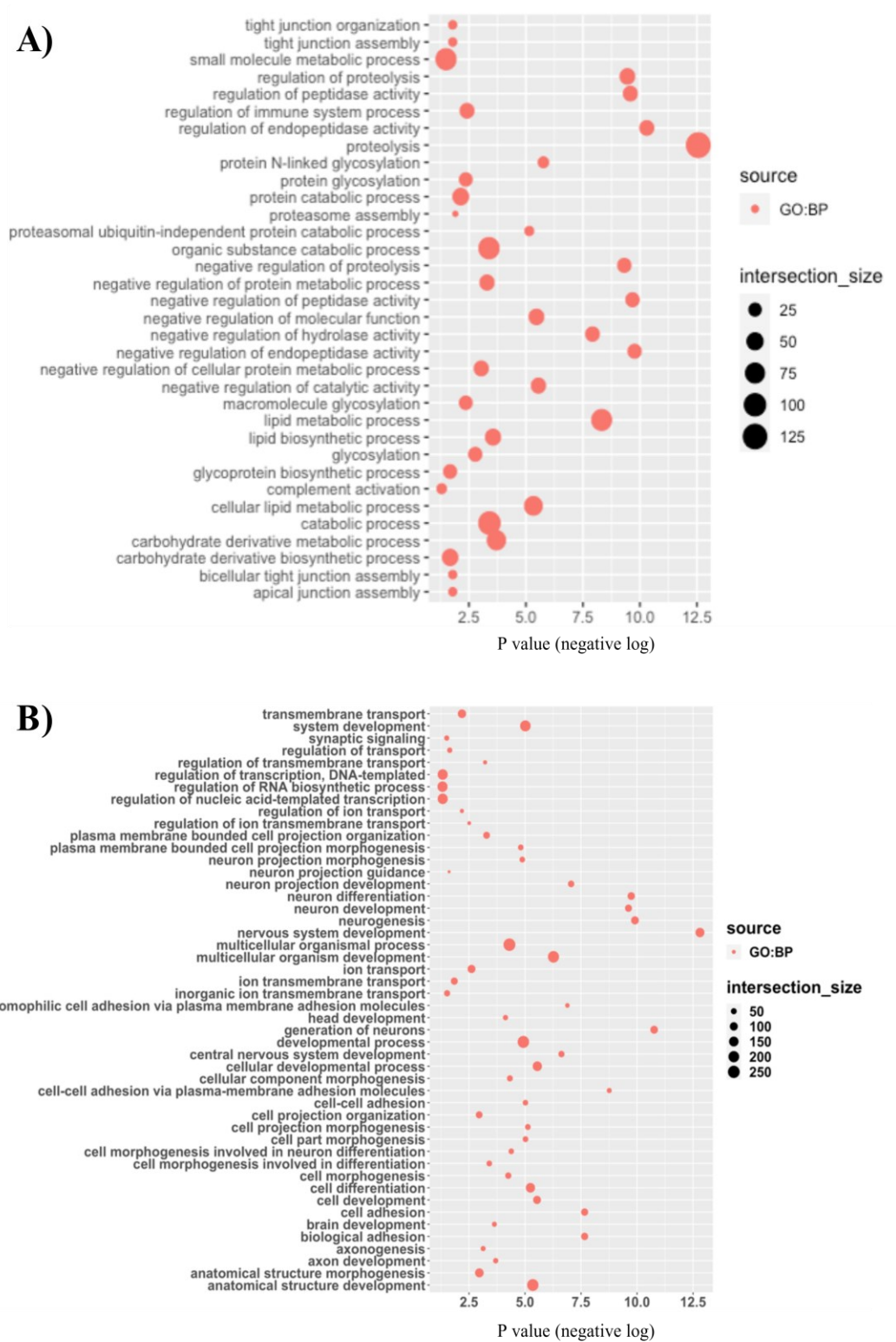
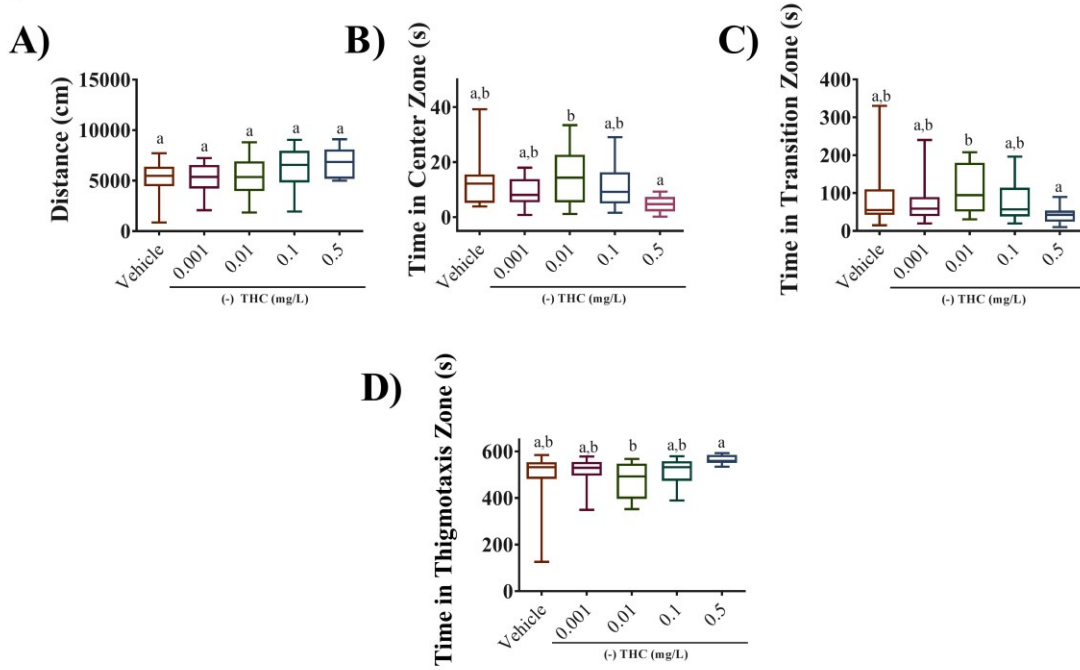


Figure 7.11 Gene expression those were altered following (-) THC exposure are linked to various biological processes (BP). (A) The graph shows major biological processes related to upregulated genes affected by 3 mg/L (-) THC treatment as predicted by the differentially expressed genes. B) The graph shows major biological processes related to downregulated genes affected by 3 mg/L (-) THC treatment as predicted by the differentially expressed genes.

Figure 7. 12 Adult zebrafish exhibited alteration in their behavior following a brief exposure of (-) THC in F0 embryos

i) Open Field Test



ii) Novel object approach test

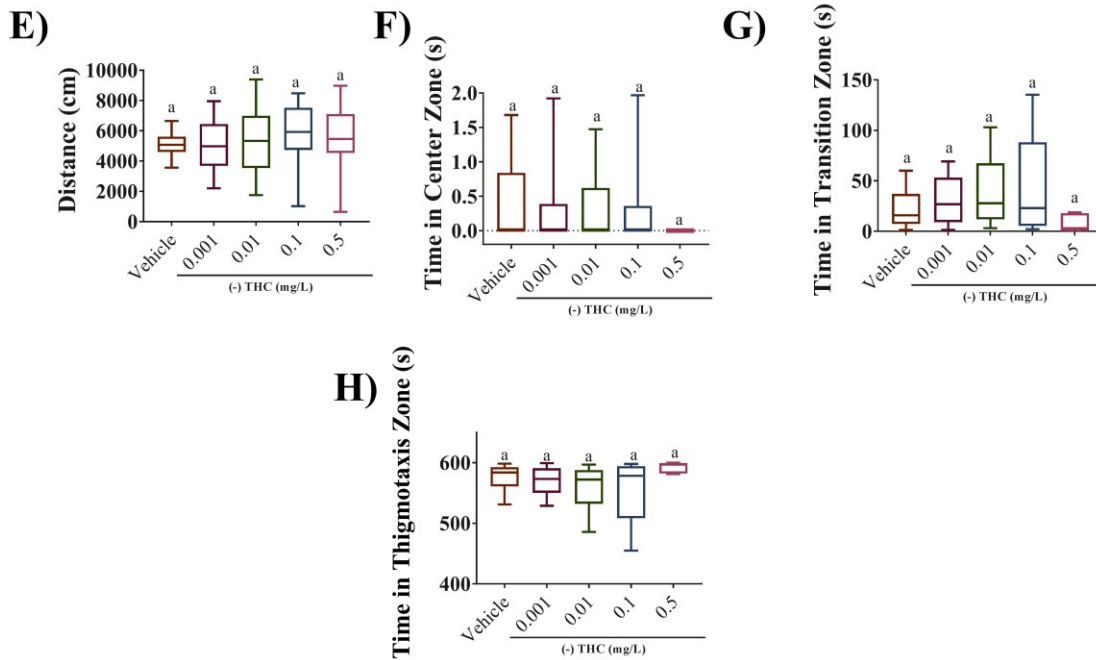
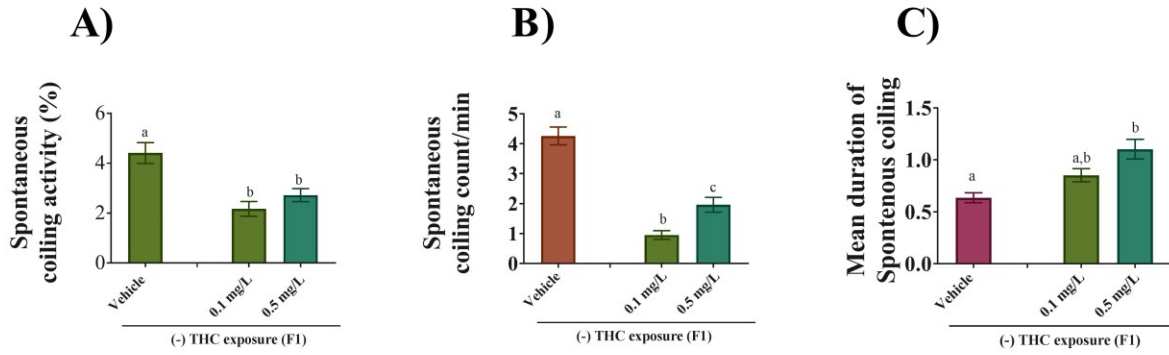


Figure 7.12 Adult zebrafish exhibited altered behavior following a brief exposure to (-) THC as F0 embryos. Open field tests in individual adults (panels A–E). The open field test was carried out on unexposed adult fish following an exposure of vehicle (n = 25), 0.001 (n = 20), 0.01(n = 25), 0.1 (n = 25), or 0.5 (n = 10) mg/L (-) THC during gastrulation in the F0 generation. Here, the data is presented in box whiskers plots (A-D); the line shows the median, the box extends from the 25th to the 75th percentile, and the range indicates the minimum to maximum values. Box plot showing (A) mean distance travelled, (B) time spent in center zone, (C) time spent in the transition zone, and (D) time spent in the thigmotaxis zone. Results from novel object approach tests in individual adults are shown in panels E-H. Adult fish had been transiently exposed to either vehicle (n = 25), 0.001 (n = 20), 0.01 (n = 25), 0.1 (n = 25), or 0.5 (n = 10) mg/L (-) THC during gastrulation as F0 embryos. Here, the data presented in box whiskers plot (A-H); line shows the median, box extends from the 25th to the 75th percentile, and range indicate minimum to maximum. Box plot showing (E) mean distance travelled, (F) time spent in center zone, (G) time spent in the transition zone, and (H) spent in the thigmotaxis zone. Significance was determined using Kruskal-Wallis followed by Dunn’s multiple comparison tests. Groups which share the same letter(s) of the alphabet are not statistically different from one another.

Figure 7. 13 Untreated F1 embryos showed a persistent alteration in their locomotion following an exposure in F0 generation

Spontaneous coiling activity at 1 dpf



Touch response at 2 dpf

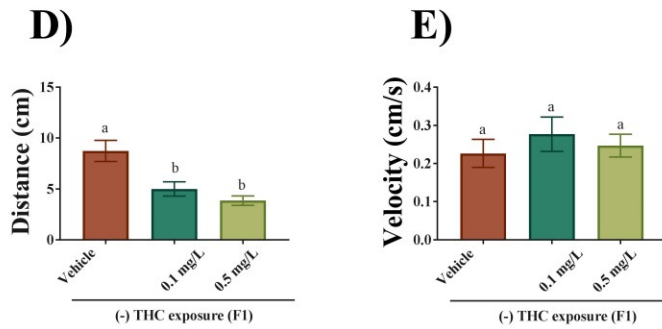


Figure 7.13 Untreated F1 embryos showed a persistent alteration in their locomotion following an exposure to (-) THC during gastrulation as F0 embryos. (A-C) Spontaneous coiling was recorded from F1 embryos at 1 dpf (within the chorion) collected from vehicle-treated (n = 22), 0.1 mg/L (-) THC (n = 42), and 0.5 mg/L (-) THC (n = 27)-treated parents. Mean spontaneous coiling activity (A), mean spontaneous coiling count/minute, and mean duration of spontaneous coiling activity (C) are presented. (D, E) Escape locomotion in response to touch of unexposed F1 embryos at 2 dpf collected from vehicle-treated (n = 33), 0.1 mg/L (-) THC (n = 48), and 0.5 mg/L (-) THC (n = 43) -treated parents. (D) Mean distance travelled by embryos in response to touch (E) and the mean velocity during escape response are presented. N=5 experiments. Significance was determined using Kruskal-Wallis followed by Dunn's multiple comparison tests. Groups which share the same letter(s) of the alphabet are not statistically different from one another.

Chapter 8

Discussion and conclusion

8.1 Overview of the findings

The focus of this thesis was to investigate the effects of brief cannabinoid exposure on zebrafish development. To do this, I exposed zebrafish embryos to different concentrations of cannabinoids (for example, THC, CBD and CBN) during gastrulation, allowed them to develop and then examined them during various developmental periods. My preliminary study (Chapter 3) revealed that THC and CBD exposure during gastrulation altered gross embryonic morphology, survival, hatching, heart rate, MN development, synaptic activity, muscle development, and responses to sound. In the following study (Chapter 4), I examined whether THC exposure altered M-cell development because these cells are born during the brief exposure period of gastrulation. I found that THC exposure slightly altered the morphology of M-cells and escape responses due to touch stimuli. The alterations in escape responses are well supported by the changes in M-cell morphology. Further, I asked whether muscle structure, and nicotinic receptor expression and organization were impacted by the brief exposure to cannabinoids. My results showed that THC exposure altered the organization of white and red fibers, and the expression of nicotinic receptors. Additionally, I wanted to determine if locomotion in more mature animals (e.g., 5 dpf larva) was affected by the early, brief exposure to THC. Hence, I examined free swimming in 5 dpf animals and found that the THC exposure significantly altered their locomotion. Together, these findings suggest that THC-induced altered locomotion occurred due to changes in MN branching, M-cell morphology, muscle fiber organization, and

synaptic activity. In Chapter 6, I studied the effects of CBN exposure on zebrafish development. Similar to the effects of THC and CBD, I found that CBN exposure affected gross embryonic morphology, survival, hatching, heart rate, MN development, and responses to sound. To better understand the altered responses to sound, I examined hair cell development associated with the otoliths and found that CBN exposure altered the growth of hair cells; this provides one possible explanation for the decreased responses to sound at 5 dpf. An initial examination into the pathways mediating these effects indicated that the effects of CBN on zebrafish development were largely mediated by CB₂Rs rather than CB₁Rs. In Chapter 7, I investigated the effect of the negative isoform of THC ((-) THC) on zebrafish development because i) (-) THC is a stereoisomer of THC and is the predominant form present in the cannabis plant, *Cannabis sativa*, and ii) the stereoselectivity of a compound can play an essential role in its pharmacological activity. My findings show that (-) THC impacts zebrafish development and that concentrations of (-) THC greater than 0.5 mg/L are lethal to zebrafish (likely) due to altered swimbladder development. In addition, my studies support a role for hedgehog signalling in the mechanism of action of cannabinoids, and RNAseq analysis showed that a number of hedgehog genes (*ptch2*, *smo*, *gli1* and *gli2b*) and cholesterol biosynthesis pathways are downregulated. Since cholesterol biosynthesis is linked to Shh signalling, alterations to cholesterol biosynthesis could be detrimental to zebrafish development. My findings clearly indicate that THC, CBD and CBN exposure alter the development of zebrafish embryos from a sub-cellular level (gene expression) to a behavioral level.

Furthermore, I also studied the long-term effects of brief cannabinoid exposure on zebrafish development. To do this, I raised vehicle-treated F0 embryos and cannabinoid (either CBD or (-) THC)-exposed F0 embryos to adulthood (afterwards abbreviated as F0-veh and F0-

CBD or F0-(-)THC adults, respectively) and examined their locomotor activity and behavior (open field, novel object approach and shoaling tests). I found that F0-CBD adult zebrafish had altered behaviors. F0-CBD adults exhibited a boldness in their character in the open field (OF) and novel object approach (NOA) tests (Chapter 5). In the OF tests, F0-CBD adults spent more time in the center and transition zone than F0-veh adults; and in the NOA test, F0-CBD fish spent more time in the center and transition zones exploring novel objects compared with F0-veh adults. Similarly, F0-CBD fish also showed reduced anxiety-like behavior in the shoaling test. In contrast, F0-(-)THC adults showed an indication of anxiety-like behavior in OF and NOA test, which was evident by the decreased time spent in the center zone and increased time spent in the thigmotaxis zone compared to F0-veh adults (Chapter 7).

Finally, to elucidate a possible transgenerational effect of cannabinoid exposure, I performed embryonic locomotion, immunohistochemical and gene expression (RT-qPCR) experiments on unexposed F1 embryos where the parents (in F0 generation) were treated with cannabinoids (ie., F0-CBD embryos). I showed that F1(F0-CBD) embryos exhibit altered primary MN branching, changes in locomotor activity, and downregulation of neuronal marker genes (such as *c-fos* and *bdnf*) (Chapter 5). In addition, expression of the 2-Ag degrading enzyme, *abhd6a*, was significantly decreased in F1(F0-CBD) embryos. Similarly, I found that F1 (F0- (-) THC) embryos exhibited altered locomotion. These results suggest that brief cannabinoid treatment during gastrulation, a critical stage of development, can have an effect on the next generation of animals. Taken together, my studies present convincing evidence that brief cannabinoid exposure of only 5.5 hours during gastrulation is detrimental for zebrafish development and has long-term and transgenerational effects.

8.2 Exposure to cannabinoids (THC, CBD, CBN and (-) THC) alters gross morphology, survival, hatching, heart rate, neuronal development (MN and M-cell), muscle development and synaptic activity

In my studies, I showed that zebrafish embryos exposed to THC, CBD, CBN and (-) THC for 5.5 hours during gastrulation exhibited physical abnormalities by the time of hatching, as well as alterations in heart rate, motor neuron branching, M-cell morphology, and synaptic activity, when compared with untreated and vehicle-treated embryos. My most significant findings can be summarized as follows: embryos treated with cannabinoids (THC, CBD, CBN and (-) THC) exhibited 1) shorter body lengths and mild deformities (Chapter 3, 6 and 7), 2) reduced survival (Chapter 3, 6 and 7), 3) reduced heart rates (Chapter 3, 6 and 7), 4) decreased frequency of mEPC activity at the NMJ (Chapter 3, 6 and 7), 5) alterations in branching patterns of secondary MNs and M-cell morphology (Chapter 4), 6) changes in the expression of postsynaptic nAChRs associated with skeletal musculature (Chapter 4), and 7) altered muscle fiber development (Chapter 4 and 7). Thus, my results suggest that exposure to cannabinoids very early in life alters embryonic development.

As indicated in the Introduction (Chapter 1), THC is the main psychoactive ingredient in the plant, *Cannabis sativa*. An increase in the potency and content of THC in cannabis has been reported in the last 25 years (ElSohly et al., 2000). Cannabis is used by pregnant women to reduce morning sickness, while CBD has been used to treat patients with nausea and loss of appetite during cancer therapies (Parker et al., 2011; Roberson et al., 2014). Cannabinol (CBN) is an oxidative product of THC and is non-psychoactive in nature. It is predominantly present in significant quantities in stored, dried and aged cannabis products (Harvey, 1990). (-) THC is a stereoisomer of THC and is the predominant form present in the plant cannabis, *Cannabis sativa*.

The stereoselectivity of a compound plays an essential role in pharmacological activity and stereoisomers may have opposing effects where one form is as an agonist while the other is an antagonist at the same receptor. In addition, some receptors may discriminate among the stereoisomers by favoring one form over the other (Weiskopf et al., 2002). With the recent legalization of cannabis use in various parts of the world, including several jurisdictions in Canada and the United States, the paucity of information on the potential effects of cannabinoids during very early embryonic development is troublesome given that pregnancy in humans may remain undetected in the first few weeks. Thus, it is important to understand the effects of cannabinoid exposure on developing embryos.

I chose to study cannabinoid exposure at a key time point in development, specifically during gastrulation, which occurs very early in embryogenesis. An important aspect of my study is that I focused on a brief period of exposure, for only ~5 hours, rather than chronic exposure over long term. Under these conditions, I found that exposure to cannabinoids altered embryonic development. For some of my experiments I chose to use concentrations of THC, CBD and CBN (6 mg/L, 3 mg/L and 3 mg/L, respectively) that are at the high end of the physiological range of cannabis use in humans. Human blood plasma concentrations of THC can peak as high as 0.25 mg/L during the smoking of a single cigarette (Huestis, 2007). In my study, I exposed embryos to concentrations ranging from 2 to 10 mg/L (6.6-33.3 μ M) THC while the newly fertilized eggs were still in the chorion, or egg casing. Under these conditions, approximately 0.1–10% of toxicants typically cross the chorion (Brox et al., 2014; Zhang et al., 2015), suggesting that approximately 0.006–0.6 mg/L THC was directly exposed to the embryo. Moreover, the THC content of cannabis has increased several-fold over the last 10–15 years. The CBD content in cannabis also varies tremendously, but when used for medicinal purposes is often used in

concentrations that range from 5 mg/kg (0.12 μ M or 0.04 mg/L) to as high of 100 mg/kg (2.4 μ M or 0.8 mg/L) (Carty et al., 2019; Rohleder et al., 2016), administered intra-peritoneally, with a maximum daily dose of ~1500 mg/day (or 14-23 mg/kg/day, equivalent to 0.6 μ M) (Iffland & Grotenhermen, 2017; McGregor et al., 2020).

My findings indicate that a bath concentration of THC equal to or higher than 6 mg/L affected zebrafish survival and hatching; however, the survival and hatching rates were altered at 3 mg/L or higher CBD concentration. Similarly, CBN concentrations \geq 1 mg/L significantly reduced survival and hatching of embryos. In contrast, the exposure of (-) THC with the concentration of 10 mg/L and 20 mg/L greatly affected survival, hatching.

I found a significant reduction in heart rate following exposure to cannabinoids (THC, CBD and CBN) at almost all concentrations used in my dose response studies. Acute cannabis smoking in humans leads to an increase in heart rate, while chronic cannabis use elicits long-lasting decreases in heart rate and blood pressure (Perez-Reyez et al., 1991). Studies on rodents show that administration of THC leads to decreases in heart rate as well (Graham & Li, 1973). Several lines of evidence suggest that the effects of cannabinoids on the cardiac system in vivo can be complex since cannabinoids might affect the autonomic outflow of nervous system (both central and peripheral) and morphology of cardiac system (Chousidis et al., 2020). The acute effects of cannabinoids on the resting heart rate of adult organisms are known to be inconsistent and may lead to little or no change in activity, or an increase or a decrease in heart rate (Benowitz et al., 1979; Niederhoffer & Szabo, 2000; Vidrio et al., 1996). Studying heart conditions in zebrafish has become increasingly important because both zebrafish and humans have atrium and ventricle chambers in the heart. The zebrafish heart is formed during early development and becomes fully functional around 3 dpf, thus abnormalities in cardiac function

may be due to effects of cannabinoid exposure during very early developmental stages. In my study, I exposed embryos during gastrulation and then examined the developmental effects at later stages. Zebrafish cardiac progenitor cells are present as early as the 512-cell stage in the early blastula (Stainier et al., 1993), and during gastrulation these precardiac cells involute, turn towards the animal pole and reach the embryonic axis around the 8-somite stage, where they combine to form two myocardial tubes (Stainier et al., 1993). Therefore, at the time of exposure, cardiac progenitor cells are present and may be impacted by cannabinoid treatment. A similar negative impact of cannabinoids on zebrafish embryonic development such as cardiac malformation and alteration in heart rate has been reported by other researchers (Chousidis et al., 2020; Graham & Li, 1973).

In addition to general morphological studies, I examined activity at the NMJ by recording mEPCs from fast twitch skeletal muscle of 2-day old embryos. The primary effect of cannabinoids (THC, CBD, CBN, or (-) THC treatment) was a reduction in mEPC frequency (Chapters 3, 5, 6, and 7) which typically signifies the presence of fewer synaptic sites, or a change in the release characteristics from MNs. Next, I focused my attention on presynaptic effects such as the morphology and branching patterns of MNs. Immunolabelling showed that exposure to THC, CBD, CBN and (-) THC significantly altered the branching of spinal MNs (Chapters 3, 5, 6, and 7), whereas the effect of THC was less severe at the concentrations that I tested. In general, a single primary MN and multiple secondary MNs innervate zebrafish white skeletal muscle fibers during development. Primary MNs are born around 9–11 hpf and their axons pioneer a path out to skeletal muscle (Westerfield et al., 1986). In each hemi-segment there are 3 (sometimes 4) primary MNs and up to 20–24 secondary MNs. The primary MNs have undergone their final round of DNA synthesis starting at 9 hpf, while the secondary MN first

appear about 5–6 hours later (Myers et al., 1986). Therefore, primary MN cell bodies are present at the time of exposure and may be directly impacted by cannabinoids. Secondary MNs would not have been born until at least 5–6 hours following exposure and yet were significantly affected by THC, CBD, CBN and (-) THC. Cannabinoids are highly lipophilic substances and may actually remain associated with cell membranes long after the exposure timeframe has elapsed. Thus, the slow release of cannabinoids from lipids after termination of the treatment may explain the effects of cannabinoids on secondary MNs.

I asked whether the reticulospinal neurons (M-cells, Mid2 and Mid3) involved in escape responses, would experience deficits in axonal projections when exposed to THC at the time of their birth. Multiple reports provide convincing data to show that the ECS, particularly the CB₁Rs, play a role in the differentiation of neural progenitor cells (Palazuelos et al., 2012; Xapelli et al., 2013), the proper development of axonal projections, and in neurite outgrowth (Bernard et al., 2005; Díaz-Alonso et al., 2012; Galve-Roperh et al., 2013; Harkany et al., 2007; Watson et al., 2008; Williams, Walsh, & Doherty, 2003). My findings in this part of the study (Chapter 4) suggest that brief exposure to THC subtly alters some aspects of M-cell morphology such as size and shape, although their axonal projections appear to be largely intact and project normally. The immunolabelling of muscle showed that exposure to THC resulted in smaller red and white fibers that appeared disorganized compared with vehicle controls. Exposure to (-) THC also resulted in altered muscle development, including disorganized mitochondrial structure. Zebrafish red and white trunk muscles arise from two completely separate precursor cell populations (Devoto et al., 1996; Westerfield et al., 1986). The red fibers are pioneer cells that migrate to the surface of the trunk where they form a single layer of muscle that becomes innervated by secondary motor neurons (Westerfield et al., 1986). The white fibers develop from

lateral pre-somatic cells and constitute a separate population of cells that can be identified via distinct morphological and genetic features (Devoto et al., 1996). CB₂R_s are known to be associated with embryonic stem cells but it is unclear if cannabinoid receptors are found on muscle precursors. Thus, whether cannabinoids directly affect muscle cell development cannot be ascertained at present. However, consistent with findings in this thesis, a recent study demonstrated that aspects of skeletal muscle cell differentiation are CB₁R-dependent, suggesting involvement of the ECS in muscle development (Iannotti et al., 2014).

Furthermore, my results showed that a 5.5 hr treatment of (-) THC at concentrations higher than 0.5 mg/L were lethal to zebrafish embryos and larva. Embryos treated with these concentrations did not survive past 15 dpf (Chapter 7). This study is the first to show exposure to (-) THC is deadly to an organism at such low concentrations; this lethality could be due to a lack of proper organ development, such as swimbladder development. This finding is important because (-) THC has not been shown to be deadly in humans or other organisms previously. In contrast, studies using the positive isoform, or a combination of positive and negative isoforms showed that THC treatments have a low to moderate effect on the development of an organism. For instance, our first couple of reports on cannabinoids (Chapters 3 and 4) showed that a racemic mixture of THC moderately affected different aspects of development, and the treated embryos survived to adulthood.

8.3 Exposure to THC, CBD, CBN and (-) THC resulted in locomotion defects

In this thesis, I investigated whether cannabinoid exposure affects the locomotion of zebrafish embryos. To do this, I examined a range of locomotor activities such as spontaneous

activity at 1 dpf, escape responses at 2 dpf, free swimming at 5 dpf, and locomotion in response to sound at 5 dpf. While the escape response is mediated by reticulospinal neuronal activity (M-cell, Mid2cm, Mid3cm neurons), swimming is generated by networks of neurons in the spinal cord, including excitatory and inhibitory interneurons, and primary and secondary MNs, as well as MN actions on muscle fibers. Escape responses and free swimming activity can be categorized as fast (>30 Hz) and slow frequency (<30 Hz) swimming (Naganawa & Hirata, 2011). Fast frequency escape responses involve the relay of sensory information to M-cells, which in turn excites a CPG network of neurons in the spinal cord that activates muscle fibers (Berg et al, 2018). During fast swimming, more dorsal MNs (both primary and secondary) become recruited and activated than ventral MNs. White fibers are active during fast swimming but not in slow swimming. In contrast, only the most ventral MNs are active during slow swimming. The red fibers are active during slow swimming and become deactivated during faster swimming. Slow free swimming, which only lasts few seconds, begins to appear at 3 dpf. By 4 dpf, embryos exhibit beat and glide locomotion and by 5 dpf they swim more frequently. Beat-and-glide locomotion consists of swim bouts, i.e., periods of rhythmic tail movement, and alternate period of rest (Sternberg & Wyart, 2015).

THC and (-) THC

In Chapter 3, I set out to examine whether the escape response to touch and sound (at 2 dpf and 5 dpf, respectively) was altered due to THC and CBD exposure. Despite small changes to the development of MN innervation patterns and the control of trunk muscle fibers, zebrafish embryos and larvae were still capable of responding to mechanical stimuli with robust C-starts. However, they were largely incapable of responding to sound. Moreover, the effects were more

pronounced following THC treatment compared with CBD treatment. I then asked if zebrafish embryos exhibit changes in escape response properties due to THC exposure (Chapter 4). Indeed there were minor changes in the escape response to touch, such as the angle of the C-bend. I also investigated locomotion in older, 5 dpf larvae, i.e. free swimming in zebrafish larvae, and found that the THC exposure altered their swimming activity. For (-) THC treatment (Chapter 7), I examined spontaneous activity at 1 dpf, escape response at 2 dpf, and free swimming at 5 dpf. The spontaneous activity was significantly reduced even at a low concentration of (-) THC treatment (0.001 mg/L). Significantly altered escape responses were also observed when the concentrations of (-) THC were ≥ 1 mg/L. Interestingly, I observed a biphasic response in free-swimming activity following exposure to (-) THC, where swimming activity was reduced when the concentration is below or above 1 mg/L (-) THC.

CBD and CBN

In addition, I examined if CBD exposure altered a range of locomotor activities, such as spontaneous activity at 1 dpf, escape response to touch at 2 dpf, and free swimming at 3-6 dpf (Chapter 5). My findings showed that exposure to CBD during gastrulation reduced various types of locomotor activities in the F0 generations. CBD exposed embryos exhibited significantly diminished spontaneous activity at 0.01 mg/L CBD, an increase in activity at intermediate concentrations and then a decrease at concentrations higher than 2 mg/L CBD, indicating the presence of a biphasic response. Regarding escape activity, CBD-treated embryos exhibited a decrease in travelling distance and velocity in response to a head touch when the concentration was ≥ 0.5 mg/L. Measurement of free-swimming activity showed that there were no significant changes in swimming activity at 3 and 4 dpf when free swimming starts to occur.

However, I observed a biphasic response in free swimming activity in larva aged 5 dpf and 6 dpf. Exposure to CBD at 0.1 mg/L and concentrations ≥ 2 mg/L resulted in decreased swimming activities, whereas 1 mg/L CBD treatment exhibited a similar swimming response as controls. Embryos exposed to concentrations of CBN higher than 1 mg/L exhibited a significant reduction in locomotor activity at 5 dpf (Chapter 6). The escape response rate to sound at 5 dpf was also decreased with the highest concentration of CBN (4 mg/L) tested. Exposure to these cannabinoids (THC, CBD, CBN and (-) THC) impacted zebrafish locomotion slightly differently from one another. This could be due to differences in their selectivity for the cannabinoid receptors. For instance, THC binds preferentially to CB₁R over CB₂R, while CBN has greater affinity for CB₂R than CB₁R. CB₁Rs and CB₂Rs may activate dissimilar suites of signalling cascades leading to the regulation of different genes and cellular responses. As a result, differential activation of CB₁R and CB₂Rs by the various cannabinoids may explain some of the differences in response observed.

Alterations in morphology and MN branching patterns may contribute to the reduced locomotor activity of cannabinoid-treated animals. Alternatively, a decreased level of activity could be linked to anxiolytic effects of cannabinoids that have been shown to occur in several animal models including zebrafish (Campos et al., 2013; Campos et al., 2012; Casarotto et al., 2010; Maximino et al., 2014). A ¹H NMR-based metabolomics study detected many new metabolites in CBN exposed (24 - 96 hpf) embryos, while several other metabolites were absent compared to controls (Chousidis et al., 2020). For instance, chronic exposure to 1 mg/L CBN resulted in the presence of seven new metabolites (glutamic acid, glutamine, homoserine, isoleucine, methionine, proline, and O-succinyl-L-homoserine), while several other metabolites were absent, such as glucose, mannose, xylose, fructose 6-phosphate, glucosamine, glucosamine

6-phosphate, hydroxyproline, cystathionine, serine, and uridine. Hence, it was suggested that CBN exposure resulted in an alteration in energy-related processes, such as hepatocyte function and glucose metabolism. Glucose metabolism is one of the major biochemical functions that appear to be affected by CBN exposure since neither glucose nor uridine diphosphate (involved in glucose-sensing mechanism) was detected following CBN exposure. There is likely to be an increase in the breakdown of glycogen to compensate for decreased glucose concentrations (Wang et al., 2013), which leads to glycogen depletion. This leads to a decreased rate of ATP regeneration which in turn results in muscle fatigue; this may account for the decreased activity exhibited by fish exposed to cannabinoids (THC, CBD, and CBN).

The fact that escape responses to sound were greatly diminished even though the fish were capable of swimming may implicate an impairment in hair cell function in cannabinoid-treated animals. Both inner and outer hair cells express CB₂Rs, but the level of CB₂Rs on outer hair cells is lower than that of the inner hair cells (Martín-Saldaña et al., 2016; Oka et al., 2005). Thus, precocious activation of CB₂Rs on precursor hair cells may impact or even delay normal development, leading to impaired sound detection. TEM analysis further showed that CBN treatment caused abnormal development of hair cells along the lateral line. Many studies showed that abnormal development of the lateral line is linked to swimming performance since the organism uses the lateral line to sense water flow (Orger & De Polavieja, 2017). Furthermore, previous studies on zebrafish have shown that downregulation of the eCB 2-AG induces weaker swimming performances (Martella et al., 2016) while a 96-hour exposure to THC and CBD induces hypo-locomotor activity (Carty et al., 2018). However, more work needs to be done to understand these effects.

Further, to explain the alteration of locomotion of CBD-treated animals, I showed that expression of neuronal activity marker genes such as *c-fos*, *bdnf* and *sox2* was decreased significantly in the F0 generation following transient exposure to CBD (Chapter 5). Interestingly, an upregulation of *c-fos* has been linked to behavioral hyperactivity (seizure) (Baraban et al., 2005) and anxiety-like behaviors in zebrafish (Baraban et al., 2005; Jesuthasan, 2012). Indeed, *c-fos* is typically documented as a marker of neuronal activity (Baraban et al., 2005; Chung, 2015; Jesuthasan, 2012; Reichert et al., 2019). For example, *c-fos* expression in zebrafish increased significantly in large neuronal populations in the forebrain, midbrain, and hindbrain shortly after exposure to drugs such as caffeine, 4-AP, and PTZ (Reichert et al., 2019). Moreover, chronic exposure (up to 96 hrs) to lower doses of THC significantly reduced *c-fos* expression in zebrafish, whereas CBD treatment increased *c-fos* expression in a concentration-dependent manner (Carty et al., 2019). My findings are a direct opposite of these results, but the exposure paradigm in my study (5.5 hrs) and the CBD concentration that I used (3 mg/L) are different. Hence, I believe that the shorter period of exposure and the higher CBD concentration used in the F0 embryos of my experiment might result in a different expression response of *c-fos*. The activity of the *c-fos* gene can be regulated by cAMP, Ras/MAP kinase, Ca²⁺ elevation and nerve growth factor (Howard, 2013). Different exposure paradigms or the higher concentration of CBD (used in this study) may interfere with one or more of these signalling components and influence the gene expression. Importantly, the reduced locomotor activity I observed is consistent with reduced *c-fos* expression, which is supported by existing literature.

8.4 CBN exposure during gastrulation affect zebrafish cilia development

The fourth study in my work focuses on the effects of CBN exposure on zebrafish development (Chapter 6). One of my most provocative findings is the effect of CBN exposure on hair cell development. My result suggests that exposure to CBN affects the development of hair cells associated with the inner ear and the lateral line system, even when at very low concentrations of CBN (0.01 mg/L). When exposed to the higher concentrations of CBN (4 mg/L), the development of hair cells was severely impacted. The structure, development, and functions of hair cells are conserved between fish and humans. Cadherin23 has been shown to be important for tip link formation in Zebrafish hair cells. The gene *starmaker* (*stm*) is responsible for the proper morphology of otolith (Söllner et al., 2004). The scaffolding protein *myo7a* is required for bundle integrity and the *mariner* mutant, in which functional *myo7a* is absent, lacks acoustic and vibrational sensitivity and displays a splayed hair bundle phenotype (Blanco-Sánchez et al., 2014; Nicolson et al., 1998). Exposure to lower concentrations of CBN (0.01 mg/L) in my thesis research resulted in similar splayed hair cells, indicative of the downregulation of some structural proteins. Co-exposure of embryos to CBN and the CB₂R antagonist (AM630) significantly improved the response rate of CBN-treated embryos to sound. Similarly, blocking CB₂R activity also prevented the abnormalities in the morphology of hair cells associated with the otoliths and the lateral line (pLL). Interestingly, a recent study showed that CB₂R is highly expressed in hair cells which is consistent with my findings that CB₂R might be involved in hair cell development (Deida et al., 2019). Studies showed that hair cells are highly sensitive to damage by ototoxic drugs (aminoglycoside antibiotics and chemotherapeutics) which can lead to complete loss of hair cells and hearing loss (Dror & Avraham, 2009; Rybak et al., 2007; Sliwinska-Kowalska & Davis, 2012).

Arguably, my most critical finding is that concentrations of CBN as low as 0.01 mg/L (and probably even lower if one takes into account diffusion through the chorion and concentration at receptor sites), have a measurable impact on cilia development. A number of signalling pathways such as those involving shh, wnt and notch are involved in hair cell proliferation, development, and regeneration (Lee & Tumber, 2012). Shh in particular plays an important role during hair cell development, partly via activation of smoothed (Smo), a G-protein coupled receptor (Chen et al., 2017; Fish et al., 2019). In fact, several studies report a role of CB₂R activation in hair cell development in rodents and zebrafish (Deida et al., 2019; Ghosh, 2017; Ghosh et al., 2018), and recent reports point to a potential heterodimerization of smo and cannabinoid receptors (Fish et al., 2019). In these models, Smo acts as a co-receptor with CB₂R to activate the shh pathway through G α _i, which inhibits adenylate cyclase (AC), leading to reduced cAMP production and PKA activity. Inhibition of PKA maintains Gli transcription factors in their activator forms (Gli A), thereby facilitating gene transcription for normal development of hair cells (Anvarian, et al., 2019; Carballo, et al., 2018). Early exposure to CBN may impact this pathway by either inhibiting smo activity, resulting in an upregulation of PKA and accumulation of a Gli repressor (Gli R) (Fish et al., 2019; Khaliullina, et al., 2015), or by binding to CB₂R, thereby stimulating PKA activity and increasing the Gli repressor, Gli R. In either case, the potentially harmful effect of CBN exposure to developing hair cells is of major importance precisely because cilia play critical developmental roles in brain, retinal phototransduction, hearing, and kidney functions.

While many of the more obvious effects in my study were obtained at the higher exposure concentrations, the effects of very low doses of CBN on kinocilia development are concerning. It is clear that more research needs to be done, to fully understand the impact of

CBN exposure on developing organisms as even brief exposure may have an impact on embryonic health and development.

8.5 (-) THC exposure during gastrulation affects swimbladder development and induce transcriptional changes

Following exposure to (-) THC, one of the most noticeable effects was a lack of movement (Chapter 7). I noticed that larvae that were not surviving were also not moving or swimming, and remained stationary at the bottom of the holding tanks. It was likely that they were not surviving because they were not swimming to feed. To investigate the reason for the lack of movement and their location at the bottom of the water column, I examined swimbladder development since it is required for buoyancy and is essential for survival (in most teleost species) (Yue et al., 2015). My results showed that the swimbladder was not fully developed in fish treated with (-) THC and was consistent with previous findings from the Ali lab that implicated deficits in endocannabinoid signalling with improper swimbladder development (Sufian et al., 2019). In addition, drug treatments that caused abnormal growth and development of the swimbladder (Jönsson et al., 2012; Yue et al., 2015) are linked to larval death in zebrafish (Goolish & Okutake, 1999). To understand how (-) THC treatment caused the swimbladder's abnormal development, I attempted to identify the receptor(s) that might mediate the effects of (-) THC pharmacologically. However, inhibition of CB₁R, CB₂R, TRPA1, and TRPV1 activity with antagonists did not prevent the (-) THC-mediated swimbladder alterations. This result led me to think that (-) THC may affect an essential pathway that is important for swimbladder development but that is unrelated to cannabinoid receptors and TRP channel activities. Studies have shown that Shh and Wnt are two critical pathways for zebrafish swimbladder development.

My findings suggested that overactivation of the Shh pathway using purmorphamine, but not Wnt activation using BIO, prevented the (-) THC-mediated abnormal swimbladder development. When taken together, these results suggest that (-) THC treatment might cause a change in the activity of the Shh pathway, which ultimately leads to the abnormal swimbladder development. My RNAseq results confirmed that components of the Shh pathway are downregulated. For instance, 0.5 mg/L (-) THC treatment significantly downregulated genes encoding Shh receptors (*ptch1*, *ptch2* and *smo*), the Shh ligand (*shhb*), and transcription factors associated with the Shh pathway (*gli1* and *gli2b*). It also significantly downregulated wnt signalling genes such as *wnt4a*, *wnt9b*, *wnt10a*, and *wnt11r*, as well as the noggin genes *nog1*, *nog2*, and *nog3*. Studies have shown that gli can modulate the wnt- and noggin-signalling pathways; therefore, downregulation of wnt signalling genes is not surprising (Carballo et al., 2018; Dahmane & Ruiz, 1999; Rimkus et al., 2016).

Interestingly, RNAseq analysis also indicated that the cholesterol biosynthesis pathway is severely compromised in (-) THC treated embryos. For example, relative expression of *hmgcra*, *sqle*, *lss*, *cyp51*, *nsdhl*, *hsd17b7*, *hsd17b12a*, *hsd17b12b*, *ebp*, *sc5d*, were downregulated following (-) THC treatment. Cholesterol plays an important role in the stability and architecture of the plasma membrane, which is essential for cell-to-cell interactions. In particular, high cholesterol is needed for myelin membrane growth (Saher et al., 2005). Further, the disturbance of cholesterol homeostasis has been associated with cardiovascular diseases and alterations in cholesterol metabolism has been linked with carcinogenesis (Cruz et al., 2013). Thus, cholesterol is required for normal embryonic development, and defects in cholesterol synthesis are associated with Smith-Lemli-Opitz syndrome (SLOS, a genetic disorder that is characterized by slow growth before and after birth) (Roux et al., 2000). SLOS is caused by the deficiency in the

enzyme 7-dehydrocholesterol reductase, which results in the abnormality of cholesterol metabolism. Cholesterol also plays a crucial role in the function of Shh, by acting as a posttranslational adduct (Porter et al., 1996). The amino terminal of the Shh protein is linked to cholesterol, which gives the Shh protein a strong affinity for the cell membrane. In addition to the Shh receptor, the Patched (ptch) receptor also has characteristics of cholesterol dependency (Roux et al., 2000) and perturbing cholesterol pathways can impact ptch function and activity. Thus, alterations in the cholesterol biosynthesis pathway can lead to defective Shh signalling, which in turn inhibits transcription of necessary genes that are crucial for normal cell proliferation and development. Together, these results indicate that impaired Shh signalling contributes to the (-) THC-induced lethality and transgenerational effects seen in zebrafish.

8.6 CBD and (-) THC exposure during gastrulation affect the behavior in the adult zebrafish

In the third (Chapter 5) and final (Chapter 7) study, I focused primarily on the long-term effects of CBD and (-) THC on zebrafish development. Here, I exposed F0 generation embryos for 5.5 hr during gastrulation to CBD and (-) THC and studied the effects on adults. My findings show that the exposure of CBD and (-) THC during gastrulation negatively impacted the behavior of the adult zebrafish.

In open field tests, adult zebrafish previously exposed to 3 mg/L CBD showed an indication of anxiety in their character by spending more time near the wall of the tank (Chapter 5). It would be interesting to see whether lower concentrations of CBD treatment (0.001-1 mg/L) resulted in similar findings. Accordingly, I tested a broader range (0.001- 10 mg/L) of (-) THC concentrations in a subsequent study (Chapter 7) for studying the effect of exposure to (-) THC

during gastrulation on adult behavior. The lower concentration range (0.001-0.1 mg/L) of (-) THC did not affect adult behavior significantly (Chapter 7). However, adult zebrafish that had been treated with 0.5 mg/L (-) THC as embryos spent more time near the tank wall and less time in the center zone, which indicates heightened levels of anxiety.

Similarly, adults previously treated with CBD at gastrulation showed an increased level of anxiety in NOA tests. However, adult zebrafish exposed previously to (-) THC (0.001-0.1 mg/L) at gastrulation did not show significant differences in the NOA test relative to controls. Similarly, Carty et al., 2019 showed that F0 embryos treated with low concentrations of THC and CBD (less than 2 mg/L) did not affect F0 adult behavior. However, another recent study in mice showed that the acute exposure to THC produced robust anxiety-like behavior in open field tests and novel object recognition (Kasten et al., 2019). Taken together, the findings from my thesis showed that the brief (-) THC and CBD exposure during early developmental periods can result in anxiety like behavior in adults, as reported by others.

8.7 CBD and (-) THC exposure during gastrulation affect the locomotion of zebrafish offspring in the F1 generation

In addition to examining the short-term and long-term effects of transient exposure to cannabinoids at gastrulation in the F0 animals, I have studied the transgeneration effects of cannabinoid treatments in F0 embryos on F1 embryos and adults from parents that had received either vehicle or cannabinoids during their gastrulation period (Chapters 5 and 7). My findings showed that exposure to CBD and (-) THC impacted locomotion, gene expression and motor neuron morphology of the F1 embryos. The impacted genes included ones involved in

neurogenesis and genes of the ECS. The F1(F0-CBD) embryos (3 mg/L CBD) exhibited altered spontaneous activity (biphasic) and significant changes in escape response characteristics relative to the F1(F0-veh) controls (Chapter 5). In Chapter 7, F1(F0-(-) THC) embryos (0.1 and 0.5 mg/L (-) THC) exhibited decreased spontaneous activity and travelled a reduced distance to touch relative to F1(F0-veh) controls. Carty et al, 2019 showed similar findings; CBD and (-) THC treatment caused altered movement in the unexposed F1 embryos.

To determine the factors that might underlie changes in locomotion in the F1 generation, I examined the morphology and branch patterns of MNs in F1(F0-CBD) embryos (Chapter 5). My findings showed that MNs of F1(F0-CBD) embryos were morphologically different from F1(F0-veh) controls and exhibited an increase in branching in the dorsal region. In addition, gene expression analysis through RT-qPCR showed that expression of neurotoxicity marker genes such as *c-fos* and *bdnf* was significantly reduced in F1(F0-CBD) embryos, but the expression of *sox2* remains unchanged. The gene encoding *sox2*, a neuronal stem cell marker, plays an important role in many biological processes including neuronal differentiation, proliferation and development. A recent study showed that a deficiency in *sox2* resulted in abnormal primary MN development such as truncated axonal branching, loss of MiP and an increase in the number of undifferentiated neuronal cells in the spinal cord of zebrafish embryo (Gong et al., 2020). Carty et al. (2019) showed that 0.15 mg/L CBD treatment in the F0 generation had a long-lasting impact on the gene expression of *c-fos*, i.e. increased *c-fos* expression in the unexposed F1 generation, which is in contrast to our findings. However, the authors used chronic exposure (up to 96 hrs) of cannabinoids. Thus, I believe that the different exposure paradigm and applied concentration of cannabinoid may impact the gene expression outcome differently.

The observation that *bdnf* expression is altered in F1(F0-CBD) embryos has important implications. Bdnf is important for neuronal survival, synapse formation and the guidance of axon growth cones (Colucci-D'amato et al., 2020). It plays multiple roles in CNS growth, development and the maintenance of synaptic plasticity. The gene encoding bdnf promotes axon outgrowth through the activation of signalling pathways involving ADF/cofilin, an actin binding protein which regulates the dynamics of actin. Thus, the formation and development of motor neurons has been linked to a series of genes which are downstream of bdnf (Gong et al., 2020). For instance, the level of Bdnf has been shown to increase the protein levels of a gene known as Down syndrome candidate region 1.4 (*dscr1.4*), which is an important factor in axon guidance. The increased activity of *dscr1.4* is further regulated by product(s) encoded by the *dap5* gene. Knockdown of *dap5* downregulates the activity of *dscr1.4*, thus, alleviated axonal outgrowth (Kim & Kim, 2020). Furthermore, findings in zebrafish show that methyl-CpG binding protein 2 (*mecp2*) and *bdnf* gene activity (target of *mecp2*) are required for proper axonal elongation of MN and synapse formation (Nozawa et al., 2017). Accumulating evidence indicates that bdnf signalling occurs through TrkB receptors and can influence morphological development of neurons and synapse formation (Cohen-Cory et al., 2010). In *Xenopus*, alterations in TrkB signalling caused significant abnormalities in the growth and branching of axon terminals (Marshak et al., 2007). More recently, TrkB signalling has been linked to the locomotion and development of zebrafish and the maintenance of neuronal populations (Sahu et al., 2019). The binding of Bdnf proteins to TrkB receptors leads to dimerization and autophosphorylation of tyrosine residue of Trk receptors. These phosphorylated residues serve as docking sites for adapter proteins and leads to the recruitment of protein kinases that trigger the activation of signalling pathways such as phosphatidylinositol-3 (PI3) kinase, mitogen-activated protein

(MAP) kinase and phospholipase C- γ (PLC γ). The recruitment of PI3K allows the phosphorylation of membrane lipid PIP2 to form PIP3, which leads to downstream phosphorylation of the serine-threonine kinase Akt. Activation of Akt stimulates activation of pro-survival proteins and suppression of pro-apoptotic proteins, thus promoting neuronal survival (Friedman, 2012). In addition, the recruitment of ras (GTPase) activates MAPK cascade leading to activation of ERK, which phosphorylates and activates CREB that ultimately regulates numerous genes expression involved in neuronal differentiation and survival (Friedman, 2012). Thus, *bdnf* influences gene expression and plays a role in neuronal development and neurite outgrowth (Cohen-Cory et al., 2010; Huang & Reichardt, 2003; Huber et al., 2003). My findings showed that *bdnf* expression was reduced in F1(F0-CBD) embryos, which supports the potential neurodevelopmental defects in these animals.

8.8 Mechanism of action of cannabinoid-induced developmental defects

8.8.1 Cannabinoid receptors mediated second messenger system

What is the mechanism of action of THC, CBD and CBN exposure during gastrulation in zebrafish? THC, CBD and CBN may act on a number of different receptors including, but not limited to, CB₁R, CB₂R, GPCR55, GPCR18, 5HT1Rs, and vanilloid TRPV1 receptors (Ibeas Bih et al., 2015; Pertwee, 2008). Importantly, CBD may act as an inverse agonist at CB₁R and CB₂Rs, thereby complicating an understanding of the downstream effects of a combination of these compounds. The typical/conventional cannabinoid receptors (CB₁R and CB₂R) are present from the early stages of neuronal life; and in the developing chick, the CB₁Rs first appear in the

CNS as early as the birth of the first neurons (Begbie et al., 2004). In zebrafish, cannabinoid receptors are present from the very initial stages of development. Quantification of mRNA showed that both CB₁R and CB₂Rs are present as early as 1 hpf, well before gastrulation begins, but the expression patterns are different such that the expression of CB₂R is high in the first day of development and then declines, whereas the expression of CB₁R is initially low but then increases after 24 hours (Oltrabella et al., 2017). The spatial profile of these receptors in zebrafish has not been fully mapped out but in the adult mammalian nervous system, CB₁R is abundant in the hippocampus, cortex, basal ganglia, and cerebellum (Mackie, 2005). These receptors are mainly localized to axon terminals and astrocytes (Navarrete & Araque, 2010). Knockout of CB₁R in mice shows alterations in axon development and disruptions in neuronal pathfinding during pre and postnatal brain development (Mulder et al., 2008; Wu et al., 2010). Moreover, perturbation of CB₁R signalling in zebrafish results in abnormal axonal growth and fasciculation in the anterior and posterior commissures of the forebrain, as well as changes in the trajectory of reticulospinal axons (Watson et al., 2008). In contrast, CB₂R is predominantly found in the digestive system, the reproductive system, the immune system, the peripheral nervous system, and to a lesser degree in the central nervous system (Atwood & MacKie, 2010). In fact, studies have shown that CB₂Rs contribute to the excitability and synaptic plasticity of neurons (Kano et al., 2009; Katona & Freund, 2012; Stempel et al., 2016). Both receptors (CB₁R and CB₂R) elicit their cellular activity through G-protein-dependent (G_s, G_{i/o}, G_{q/11} and G_{12/13}) and G-protein-independent pathways (G-protein receptor kinases and ion channels) (Dascal, 2001; Hamm, 1998; Ribas et al., 2007). Traditionally, they are coupled to G_{i/o} proteins which typically lead to inhibition of multiple downstream events such as inhibition of adenylyl cyclase, a reduction in voltage-gated Ca²⁺ channel activity, and activation of G-

protein-gated inwardly rectifying potassium channels (GIRK) and mitogen-activated protein kinases (MAPK) (Amin & Ali, 2019; Howlett, 2005).

What is the mode of action of the THC-, CBD- and CBN-mediated developmental effects in zebrafish embryos? My findings showed that blocking CB₁R activity prevented CBD-induced (appendices) and (-) THC-elicited effects (Chapter 7) on zebrafish embryonic morphology, body length, and survival. In contrast, blocking CB₂R prevented the CBN-induced effects on embryonic morphology, body length, survival, neuronal morphology, and cilia development, as well as some aspects of cardiac development. (Chapter 6). Blocking CB₂R activity inhibited some of the effects on cardiac morphology but did not prevent the effects on heart rate, suggesting that the CBN-mediated reduction in heart rate is facilitated by multiple pathways that do not involve CB₂Rs. Blocking CB₁Rs partially prevented the alterations in primary MN branching, whereas blocking CB₂Rs almost completely prevented the changes in MN branching. Block of CB₁R and CB₂R together resulted in similar findings obtained when blocking only CB₂R, which implied that the main receptor mediating the effects of CBN is CB₂R. These findings are consistent with a) the higher (relative) expression of CB₂R in the first 24 hours of development compared with CB₁R, and b) the relative higher affinity of CBN for CB₂Rs compared with CB₁R (Oltrabella et al., 2017). My studies on locomotion showed that inhibiting CB₂R activity prevented the reduction in swimming activity of CBN-treated embryos. I only observed a slight improvement in the swimming performance of embryos in the presence of CB₁R blockers, and combined blocking of CB₁R and CB₂R did not produce additive or synergistic effects. Taken together, my results suggest that during gastrulation CBN preferentially interacts with CB₂Rs to alter MN growth and locomotion.

The Ali lab and others showed previously that CB₁R and CB₂R activity is essential for embryonic development and plays a role in axonal growth (Sufian et al., 2019; Tapia et al., 2017). In addition, CB₁R agonists and antagonists are capable of altering axonal growth in embryonic organisms (Williams et al., 2003). These suggest that the over-activation/inhibition of CB₁R or CB₂R impaired normal embryonic development and neuronal maturation. In my study, embryonic exposure to cannabinoids (THC, CBD, and CBN) may lead to the over-activation of CB₁R or CB₂R. Since these receptors are coupled to G_{i/o}, their overactivation may lead to inhibition of adenylate cyclase and a reduction in cAMP and PKA activity. Tight regulation of cAMP levels is necessary for proper neuronal development and functioning. cAMP levels are highly regulated by phosphodiesterases (PDEs), which break down cAMP to limit the concentration and time course of cAMP signalling. For instance, cAMP levels are often high during development and then decline during maturation in rat DRG neurons. In these neurons, a high level of cAMP during development is associated with axonal growth; however, low levels during maturation are thought to occur with loss of the ability to regenerate (Cai et al., 2001). In addition, PKA phosphorylates and alters the activity of various target proteins (Nguyen & Woo, 2003). PKA is also involved in neurite outgrowth of rat motor neurons and is necessary for increasing neuronal length and branching point. In addition, decreased PKA expression is linked to reduced dendrite length in the hippocampus and cortical neurons (Harada et al., 2002). Hence, the exposure of zebrafish embryos to cannabinoids may inhibit adenylate cyclase, which in turn downregulates cAMP and PKA expression and ultimately influences embryonic development, including neuronal development and functioning.

Findings from RNAseq indicated that exposure to (-) THC altered the expression of genes encoding adenylate cyclase, protein kinases and PDE. For instance, although these

changes are not specifically mentioned in Chapter 7, the adenylylase genes *adcy7*, *adcyap1r1a*, and *adcy3a* are downregulated, while *adcyap1a* is upregulated. Similarly, expression of the PKA gene *prkar1aa* is downregulated, whereas *prkabb*, *prkacbb*, *prkcsh*, *prkcda*, and *prkab1b* are upregulated. In addition, PDE gene expression was also altered; i.e. *pde6c*, *pde6d*, and *pde5ab* expression were downregulated, which are responsible for regulating cAMP level inside the cell. Among other downstream events, MAP kinases (p38 MAP kinase, ERKs and JNK), and especially p38 MAP kinases, are involved in neurotoxicity and neurodegeneration (Asih et al., 2020). Exposure to (-) THC also changed the expression of *mapk* genes; *mapk12a* and *mapkapk2a* are upregulated, and *mapk10* is downregulated. Further research is needed to determine whether (-) THC exposure alters the protein expression of these genes. Together, these findings indicate cannabinoid exposure potentially negatively affected the downstream signalling of cannabinoid receptors activation, i.e., downregulates adenylylase, PDE, and protein kinase gene expression, resulting in interruptions in the normal development of zebrafish embryos.

My results also provide insights into the possible targets through which alterations of cAMP and kinase signalling cascades affect developmental processes. Interestingly, interactions between the cAMP second messenger system and the hedgehog signalling pathway are associated with many developmental processes. For example, an increased level of PKA activity is necessary for preventing the proteolytic processing of Gli transcription factor into its repressor form (GliR), which in turn facilitates the gene transcription required for normal development. In addition to demonstrating an interference with cAMP signalling, my RNAseq results also showed an alteration of hedgehog genes such as *ihha*, *smo*, *ptch2*, *gli1* and *gli2b* following cannabinoid treatments. Taken together, these results suggest that exposure to cannabinoids may

interfere with the expression of cAMP and hedgehog signalling, thereby influencing the transcription of genes required for embryonic development.

8.8.2 Reactive oxygen species (ROS)-mediated mechanism

Studies reported that chemical exposure (i.e., tetracycline) to zebrafish embryos results in the generation of reactive oxygen species (ROS) (Zhang et al., 2015). Embryonic development is sensitive to ROS, which results in oxidative stress-induced cell apoptosis that might contribute to abnormal embryonic development (Shi & Zhou, 2010; Yamashita, 2003). I observed blebbing of the tail and severe embryonic malformations when examining the effects of high concentrations of cannabinoids, which suggests an increase in apoptotic events. Indeed my preliminary findings showed an aberrant expression of ROS signalling genes, which supports the notion of ROS-mediated developmental defects of zebrafish. Two main signalling pathways involved in chemical drug-induced apoptosis are the p53 and caspase pathways (Li et al., 2011). The p53 pathway regulates apoptosis by upregulating pro-apoptotic genes (such as *p53* and *bax*) and downregulating anti-apoptotic genes, such as *bcl-2*. Thus, an up-regulation of genes encoding p53 leads to apoptosis by upregulating *bax* and downregulating the expression of *bcl* (Li et al., 2011). Although not reported in Chapter 7, my RNAseq results showed that the expression of *tp53inp1*, *baxa*, and *baxb* were upregulated whereas anti-apoptotic Bcl-2 genes (*bcl2a*, *bcl2l1*, *bcl2l10* and *bcl2l13*) were not downregulated. Thus, it seems like p53-bax-bcl2 is not the pathway for (-) THC-induced apoptosis. Regarding the caspase pathway, *caspase3* is an important player to be activated in the apoptotic pathway. Cytochrome c (*cyc*) from mitochondria promotes the activation of *caspase3* by forming cytochrome c/Apaf-1/caspase9

containing an apoptosome complex, which leads to apoptosis (Zhang et al., 2015). Results from my RNAseq experiments reveals that the expression of mRNA encoding for cytochrome c (cytochrome c oxidase subunit 7A1, *cox7a1*), apaf-1 (*apaf1*) and caspae 9 (*casp9*) is upregulated. My findings also showed an increase in the expression of other caspase genes such as *casp3b*, *caspb*, *caspa*, *casp6*, and *casp8*. Taken together, the caspase-dependent apoptotic pathway, but not the p53-bax-bcl2 pathway, might contribute towards the (-) THC-induced (or cannabinoid-induced) developmental toxicity in zebrafish larvae.

8.8.3 Endocannabinoid-mediated mechanisms

Endocannabinoids play essential roles in nervous system development and have been shown to contribute to axonal growth, fasciculation, elongation, proliferation, and differentiation of neuronal progenitor cells (Aguado et al., 2005; Rodrigues et al., 2019; Watson et al., 2008). Endocannabinoids have also been shown to play chemo-attractive and chemo-repulsive roles in the developing cortex (Berghuis et al., 2005, 2007). In that study, the authors found that activation of CB₁R with the agonist WIN55,212 resulted in growth cone repulsion, collapse and neurite retraction of GABAergic neurons. However, pretreatment of cultured interneurons with Rho-kinase reversed the neurite retraction and repulsion, indicating a role of Rho-kinase in axon guidance (Berghuis et al., 2007). Co-expression of CB₁R and DAGL α/β was reported in glutamatergic axons (excitatory axons), indicating a role of DAGLs in axonal growth. In comparison, GABAergic axons (inhibitory axons) did not express DAGLs but possessed RhoA kinase activity that would contribute to neurite repulsion (Harkany et al., 2008). In other studies, Tapia et al. (2017) showed that an increase in 2-AG levels potentiated axonal growth of

hippocampal neurons in a CB₁R-dependent manner. Similarly, the application of AEA to the cultured neurons caused the activation of CB₁R downstream signalling, including ERK (Berghuis et al., 2007). Several reports provide strong evidence for an interaction between the endocannabinoid system and growth factors during early development. For instance, CB₁R activation linked to FGF receptor activity influences neurite outgrowth in cerebellar neurons, while CB₁R interaction with TrKB receptors in cortical interneurons is required for interneuron migration and specification (Berghuis et al., 2005). Thus, the endocannabinoid system has the ability to control neuronal migration and differentiation by regulating growth factor activity. The endocannabinoid system has also been shown to modulate the expression of neurotransmitters in the basal ganglia that are involved in movement, such as GABA and glutamate (Benarroch, 2007). Hence, my results of altered neuronal branching and changes in locomotion (Chapters 3-7) are consistent with these previous findings. My RT-qPCR analysis of CBD treatment of F0 embryos in Chapter 5 showed an alteration in the expression of genes encoding for cannabinoid receptors (*CB₁R*, *CB₂R*, *GPCR55*, and *cnrip1a*), as well as eCBs synthesizing and degrading enzymes (such as *Nape-pld*, *dagla*, *daglb*, *mgll*, *abhd6a* and *abhd6b*). In addition, RNAseq analysis from (-) THC-treated (F0) embryos showed an altered expression of eCBs genes including, *faah2a*, *faah2b*, *trpm1b*, *trpm2*, *trpm4a*, *trpm6*, *trpm7*, *abhd4*, and *abhd14b* (Chapter 7). Additional findings from RNAseq analysis (not directly reported in Chapter 7) also showed an upregulation of Rho-cdc42-Rac pathway signalling, which suggests the involvement of Rho GTPases in mediating neuronal survival and death. In general, Rho and its downstream effector induce neuronal apoptosis, while Rac and its downstream effector promote neuronal survival (Huang & Reichardt, 2003; Huber et al., 2003). (-) THC-treated (F0) embryos exhibited upregulation of Rho genes (*rhogb*, *rhocb*, *rhoab*, *rhoca*, *rhov* and *rhoub*), effector MAPK genes

(such as *mapk12a* and *mapkapk2a*) and pro-apoptotic Bax genes (*baxa* and *baxb*). Additionally, *cdc42* gene (*cdc42l*) and Rac genes (*rac1a*, *rac1b* and *rac2*) were upregulated in (-) THC-treated embryos. Thus, (-) THC-induced neuronal alteration and developmental defect might be Rho-cdc42-Rac pathway-mediated. Taken together, THC, CBD, and CBN exposure might modulate the endocannabinoid synthesis/breakdown and disrupts the regular balance of the ECS, which ultimately affects the normal development of zebrafish embryos.

8.8.4 Epigenetic mechanism

RT-qPCR findings showed that CBD only significantly reduced the expression of the gene encoding for *abhd6a*, which is a 2-AG degrading enzyme, in the F1 generation while the expression of other ECS genes remained unchanged (Chapter 5). In addition, the expression of neuronal marker genes such as *c-fos* and *bdnf* were significantly reduced, whereas the expression of *sox2* and *nrf2* remain unchanged. Taken together, these results indicated that CBD treatment of zebrafish embryos might lead to changes in gene expression that persist even into the next generation of animals. However, questions remain regarding the molecular mechanism of these transgenerational effects of CBD. Many human and animal studies suggest that cannabis exposure during development affects epigenetic processes such as DNA methylation and histone modification. For example, prenatal CBD exposure in mice caused behavioral deficits in offsprings and perturbation of brain epigenome, i.e., changes in the methylation in the brain through bisulfite sequencing (Wanner et al., 2021). The Kollins lab showed that DNA methylation of human cannabis users was differed by at least 10 % compared to non-cannabis users (Murphy et al., 2018). They reported differential DNA methylation marks at 6640 CpG

sites (cytosine-phosphate-guanine), including at 3979 CpG islands in the gene promoter region (Murphy et al., 2018). They also reported that several signalling pathways were affected: oncogenic pathway (i.e., genes encoding for BRAF, PRCACA, AKT1, and FGF), hippo pathways (critical in cancer and embryonic body patterning), MAP kinase pathway, and Wnt signalling pathway.

DNA methylation usually occurs at cytosine residues and is referred to as cytosine methylation. Cytosine methylation takes place predominantly at the CpG dinucleotide; regions rich in CpGs are called CpG islands, which are usually found in gene promoters (where gene expression is regulated by methylation). Typically, CpG methylation in the promoters of genes leads to gene silencing; the suppression of gene activity occurred through methylation itself, or the methylation status prevents the binding of transcription factors. Methyl CpG-binding protein 2 (MeCP2 protein) and methyl CpG binding domain protein-1, -2, and -4 (MBD1, 2, and 4) can recognize such methylated DNA, which in turn recruit histone methyltransferases (HMT) and histone deacetylases (HDAC) to trigger histone modifications and chromatin packing (Parry & Clarke, 2011; Rotondo et al., 2021).

Methylation can also have a permissive or repressive effect depending on the modification of lysine residue. For instance, H3K4me3 (methylation on lysine4) is permissive, while H3K9me3 is repressive. In humans, DNA methylation is coordinated by four types of DNA methyltransferase (DNMTs) enzymes, encoded by the following genes: *DNMT1*, *DNMT3A*, *DNMT3B*, and *DNMT3C*. DNMT1 is a maintenance methyltransferase that copies pre-existing methylation marks onto new strands of DNA following DNA replication. On the other hand, DNMT3A, 3B, and 3C are *de novo* methyltransferases; they can methylate previously unmethylated DNA sequences and are responsible for methylation of promotor

sequences (REF). Due to a genome duplication event in zebrafish, six paralogues have been reported for DNA methylation enzymes. For example, *dnmt3a* is represented by *dnmt6* and *dnmt8*, whereas *dnmt3b* is represented by *dnmt3* (*dnmt3b3*), *dnmt4* (*dnmt3b1*), *dnmt5* (*dnmt3b4*), and *dnmt7* (*dnmt3b* and *dnmt3b2*). Further, *dnmt6* has been reported as *dnmt3ab* and *dnmt3a2*, while *dnmt8* is cited as *dnmt3aa* (Boyle, 2017). RNAseq analysis results not directly reported in Chapter 7 showed that (-) THC treatment caused a significant downregulation of DNA methyltransferases (*dnmt3aa*, *dnmt3ab*, *dnmt3ba* and *dnmt3bb.1*) and methyl CpG-binding proteins (*mecp2*, *mbd1a*, and *mbd3b*), whereas the expression of *mbd2* was significantly upregulated. This finding indicates that (-) THC treatment potentially impacts the methylation mechanism in zebrafish, thus influencing gene expression.

What is the mechanism for such epigenomic alternation? In general, gene expression is regulated by a network of DNA elements (known as promoter regions) where multiple transcription factors (proteins that bind to DNA) physically interact to generate an appropriate level of mRNA transcripts from a given gene. The regulatory mechanisms include DNA methylation, post-translational modification of nucleosomes, and recruitment of transcription factors, RNA polymerase II and non-coding RNAs (Morris et al., 2011). Thus, the DNA-protein complex forms a three-dimensional structure, which influences (facilitates/inhibits) the expression of associated genes.

Although how cannabinoid treatments at gastrulation leads to alterations in zebrafish gene expression that can also be transgeneration has not been evaluated directly in my studies, potential mechanisms could be one or more of the following. 1) Exposure to cannabinoids might impact any level of the regulatory mechanism mentioned above and disrupt the balance of these processes, thereby influence gene expression (Szutorisz & Hurd, 2016). 2) Cannabinoid exposure

might affect the demethylation process. DNMTs generate 5-methylcytosine at CpG sites; however, ten-eleven translocation (TET) proteins oxidize 5-methylcytosine into 5-hydroxymethylcytosine that leads to demethylation of the DNA and affect the gene expression. So, cannabinoid exposure might modify the level of DNMTs and TET enzymes and influence gene expression. 3) Cannabinoid exposure might alter posttranslational modification marks of histone tails such as methylation and acetylation, which are catalyzed by histone methyltransferases (HMT) and histone acetyltransferases (HAT), respectively. Acetylation of DNA is permissive, whereas deacetylation is mediated by histone deacetylases (HDAC) that lead to repression of transcription. Hence, cannabinoids exposure might influence the methylation or acetylation marker of the histone by upregulating/downregulating HMT, HAT, and HDAC enzymes or related proteins. These actions would result in alterations in the expression of critical functional genes. 4) Cannabinoid exposure might also affect the level of non-coding microRNAs (miRNA), which are produced from specific genes and target protein-coding RNA (mRNA) for degradation; these processes would influence protein production (Szutorisz & Hurd, 2016). miRNAs can modify gene expression through complementary binding to the target sequence and prevent the binding of the transcriptional machinery, leading to restriction of gene expression of a particular gene (Boyle, 2017). Such miRNAs-mediated regulation of gene expression has been shown for *bdnf*, and other genes involved synaptic plasticity (Li & Van Der Vaart, 2011).

8.9 Conclusion and future directions

In summary, my findings suggest that even brief exposure to cannabinoids may have an impact on embryonic health and development. In particular, a brief period of cannabinoid

exposure, i.e., only 5.5 hr exposure during gastrulation, is harmful to zebrafish development. It impacts a wide range of developmental aspects including gross morphology, survival and hatching rates, neuronal development and branching, synaptic activity, gene expression and locomotion. Additionally, these cannabinoid-induced alterations persisted into adulthood, where the adults experienced hypolocomotion. Furthermore, the offspring of cannabinoid-treated animals exhibited altered locomotion, MN branching and gene expression. The findings of my study indicate that exposure to cannabis or cannabinoids during early periods of development has long lasting impacts on the animal. These results have implications towards the use of cannabis products during early pregnancy. While my results should be interpreted with care, more research clearly needs to be done to fully understand the impact of cannabinoid exposure on developing organisms. To further extend our knowledge, the following questions of research can be addressed.

1. I showed that the THC-, CBD-, and CBN-induced developmental defects of zebrafish are mediated by CB₁R and CB₂R. However, what is the exact mechanism(s) that underlies the action of THC, CBD, and CBN? The mode of actions can be further studied using i) morpholino knockdown of CB₁R or CB₂R, or ii) CRISPR knockout of CB₁R or CB₂R. Exposure of THC, CBD, and CBN to knockdown/knockout (CB₁R or CB₂R) embryos can easily confirm whether these receptors are involved in mediating cannabinoid-induced effects. In other words, cannabinoids exposure in CB₁R/CB₂R knockout embryos should not produce cannabinoid-induced developmental defects. Nevertheless, if exposure of THC, CBD, and CBN to knockdown/knockout (CB₁R or CB₂R) embryos still produces considerable developmental defects in those knockout animals then that

indicates other receptors (GPCR55, TRPV1, TRPA1) are probably mediating those effects.

2. The ligands THC, CBD, and CBN have differential affinities for cannabinoid receptors such as CB₁R, CB₂R, and GPCR55. Furthermore, these ligands may induce diverse conformations of a receptor, which may favor one of the possible signalling cascades over another. Taken together, it might be possible that cannabinoid-induced downstream signalling cascades are very different for each of these ligands. For instance, one can determine if the cAMP/PKA or PI3K/Akt or PI3K/ERK or PLC/IP3 pathway is activated in response to cannabinoid exposure. To examine the downstream signalling cascade for these cannabinoids (THC, CBD, and CBN), one can quantify the mRNA and protein expression of PKA, PI3K, Akt, ERK and PLC using RT-qPCR and western blot respectively. Further, activation of these signalling cascades regulates various biological processes by phosphorylating specific target molecules (such as transcription factor). To elucidate further details of these mechanisms, one can also examine specific transcription factors (of related pathways such as PKA/PI3K/Akt/ERK), which regulates a variety of cellular and developmental processes.
3. RNAseq results indicate that numerous signalling pathways are altered in the (-) THC-treated embryos, but details are yet to be determined. For instance, one can determine how hedgehog signalling affects embryonic development or the exact signal transduction elements that are involved for the apoptotic pathway. Therefore, one could focus on individual pathways, to study the detail mechanisms that contribute to the (-) THC-

mediated lethality. For this purpose, someone can use pharmacological blocker/activator targeting candidate gene function or use knockdown/knockout of individual gene (such as *ptch1*, *ptch2*, and *smo*) to elucidate their roles.

4. I found that exposure to cannabinoids affects the morphology and branching of neurons (MN and M-cell). However, it remains unknown if the physiology of these neurons is altered by exposure to cannabinoids. To determine this, one can record the production of action potentials (APs) from the MN or M-cells of the cannabinoid-treated animals to see if cannabinoid exposure alters the amplitude, the shape, the timing and the ease of production of the APs. One may also study the individual currents (voltage-gated Na⁺ and K⁺ currents) that underlie the APs to determine if their properties have been altered.

5. My findings using H&E staining showed that the eye morphology is altered following (-) THC treatment although these changes have not been quantified in the thesis. Impaired vision might affect locomotion and the finding of food sources in (-) THC-treated embryos. Additional experiments are required to test whether (-) THC causes impaired vision. This could possibly be done using behavioral experiments on young/adult zebrafish to test whether they can distinguish light/dark or different colors. Also, one could carry out immunostaining using antibody to stain rod (Ab7-rho) and cone (zpr1) and bipolar cells (PKC β1, Santa Cruz Biotechnology) to examine the retinal morphology of zebrafish in a combination of regular microscopic and confocal imaging techniques.

6. I found that THC and CBD exposure affected locomotion and gene expression in the next generation of animals. However, a detailed epigenetic mechanism is still unknown. Additional experiments can be designed and performed to elucidate the mechanism of the transgenerational effect, including methylation or other forms of post-translational modifications. In particular, bisulfite sequencing of RNA (Murphy et al., 2018), a powerful method to determine the methylation status of cytosine residue, can be performed to identify methylation status at CpG islands regarding epigenetic modifications.

7. A mixture of cannabinoids is often used for medicinal purposes such as a 2:1 ratio of THC to CBD (Kasten et al., 2019). It would be important to determine how different combinations of cannabinoids affects the development of zebrafish embryos. This will help us to understand how the pharmacological interaction of these cannabinoids affects the development and behavior of an organism.

Despite the presence of these further questions and directions to be examined or explored, my studies have already provided considerable evidence of cannabinoid toxicity on zebrafish development, i.e. a detrimental effect of cannabinoid exposure during the early stages of development. One of the most interesting aspects of my study is the time course of the actions of the cannabinoids, which were applied for only 5.5 hours during gastrulation. The effects that I have noted occurred well beyond the exposure time period and suggest that brief exposure may have far-reaching consequences. Hence, this thesis may act as a framework to provide

background information in determining the consequence of exposing embryonic organisms to cannabinoids during early developmental periods.

References

- Achenbach, J. C., Hill, J., Hui, J. P. M., Morash, M. G., Berrue, F., & Ellis, L. D. (2018). Analysis of the Uptake, Metabolism, and Behavioral Effects of Cannabinoids on Zebrafish Larvae. *Zebrafish*. <https://doi.org/10.1089/zeb.2017.1541>
- Aguado, T., Monory, K., Palazuelos, J., Stella, N., Cravatt, B., Lutz, B., ... Galve-Roperh, I. (2005). The endocannabinoid system drives neural progenitor proliferation. *The FASEB Journal*. <https://doi.org/10.1096/fj.05-3995fje>
- Ahluwalia, J., Urban, L., Capogna, M., Bevan, S., & Nagy, I. (2000). Cannabinoid 1 receptors are expressed in nociceptive primary sensory neurons. *Neuroscience*. [https://doi.org/10.1016/S0306-4522\(00\)00389-4](https://doi.org/10.1016/S0306-4522(00)00389-4)
- Ahmed, K.T., Amin, M. R., Shah, P., & Ali, D. W. (2018). Motor neuron development in zebrafish is altered by brief (5-hr) exposures to THC (Δ^9 -tetrahydrocannabinol) or CBD (cannabidiol) during gastrulation. *Scientific Reports*, 8(1). <https://doi.org/10.1038/s41598-018-28689-z>
- Ahmed, Kazi T., & Ali, D. W. (2016). Nicotinic acetylcholine receptors (nAChRs) at zebrafish red and white muscle show different properties during development. *Developmental Neurobiology*. <https://doi.org/10.1002/dneu.22366>
- Ahn, K. H., Bertalovitz, A. C., Mierke, D. F., & Kendall, D. A. (2009). Dual role of the second extracellular loop of the cannabinoid receptor 1: Ligand binding and receptor localization. *Molecular Pharmacology*. <https://doi.org/10.1124/mol.109.057356>
- Akhtar, M. T., Ali, S., Rashidi, H., Van Der Kooy, F., Verpoorte, R., & Richardson, M. K. (2013). Developmental effects of cannabinoids on zebrafish larvae. *Zebrafish*. <https://doi.org/10.1089/zeb.2012.0785>
- Akopian, A. N., Ruparel, N. B., Patwardhan, A., & Hargreaves, K. M. (2008). Cannabinoids desensitize capsaicin and mustard oil responses in sensory neurons via TRPA1 activation. *Journal of Neuroscience*. <https://doi.org/10.1523/JNEUROSCI.1565-06.2008>
- Alexander, R. M. (1972). The energetics of vertical migration by fishes. *Symposia of the Society for Experimental Biology*.
- Ali, D. W., Buss, R. R., & Drapeau, P. (2000). Properties of miniature glutamatergic EPSCs in neurons of the locomotor regions of the developing zebrafish. *Journal of Neurophysiology*. <https://doi.org/10.1152/jn.2000.83.1.181>
- Amal, H., Fridman-Rozevich, L., Senn, R., Strelnikov, A., Gafni, M., Keren, O., & Sarne, Y. (2010). Long-term consequences of a single treatment of mice with an ultra-low dose of Δ^9 -tetrahydrocannabinol (THC). *Behavioural Brain Research*. <https://doi.org/10.1016/j.bbr.2009.09.021>
- Amin, M. R., & Ali, D. W. (2019). *Pharmacology of Medical Cannabis. Advances in Experimental Medicine and Biology* (Vol. 1162). https://doi.org/10.1007/978-3-030-21737-2_8
- An, D., Peigneur, S., Hendrickx, L. A., & Tytgat, J. (2020). Targeting cannabinoid receptors: Current status and prospects of natural products. *International Journal of Molecular Sciences*. <https://doi.org/10.3390/ijms21145064>
- Andre, C. M., Hausman, J. F., & Guerriero, G. (2016). Cannabis sativa: The plant of the thousand and one molecules. *Frontiers in Plant Science*. <https://doi.org/10.3389/fpls.2016.00019>

- Anvarian, Z., Mykytyn, K., Mukhopadhyay, S., Pedersen, L. B., & Christensen, S. T. (2019). Cellular signalling by primary cilia in development, organ function and disease. *Nature Reviews Nephrology*. <https://doi.org/10.1038/s41581-019-0116-9>
- Asih, P. R., Prikas, E., Stefanoska, K., Tan, A. R. P., Ahel, H. I., & Ittner, A. (2020). Functions of p38 MAP Kinases in the Central Nervous System. *Frontiers in Molecular Neuroscience*. <https://doi.org/10.3389/fnmol.2020.570586>
- Atwood, B. K., & MacKie, K. (2010). CB 2: A cannabinoid receptor with an identity crisis. *British Journal of Pharmacology*. <https://doi.org/10.1111/j.1476-5381.2010.00729.x>
- Babin, P. J., Goizet, C., & Raldúa, D. (2014). Zebrafish models of human motor neuron diseases: Advantages and limitations. *Progress in Neurobiology*. <https://doi.org/10.1016/j.pneurobio.2014.03.001>
- Badowski, S., & Smith, G. (2020). Cannabis use during pregnancy and postpartum. *Canadian Family Physician*.
- Bangs, F. K., Schrode, N., Hadjantonakis, A. K., & Anderson, K. V. (2015). Lineage specificity of primary cilia in the mouse embryo. *Nature Cell Biology*. <https://doi.org/10.1038/ncb3091>
- Baraban, S. C., Taylor, M. R., Castro, P. A., & Baier, H. (2005). Pentylentetrazole induced changes in zebrafish behavior, neural activity and c-fos expression. *Neuroscience*. <https://doi.org/10.1016/j.neuroscience.2004.11.031>
- Barann, M., Molderings, G., Brüss, M., Bönisch, H., Urban, B. W., & Göthert, M. (2002). Direct inhibition by cannabinoids of human 5-HT_{3A} receptors: Probable involvement of an allosteric modulatory site. *British Journal of Pharmacology*. <https://doi.org/10.1038/sj.bjp.0704829>
- Barnett-Norris, J., Hurst, D. P., Lynch, D. L., Guarnieri, F., Makriyannis, A., & Reggio, P. H. (2002). Conformational memories and the endocannabinoid binding site at the cannabinoid CB₁ receptor. *Journal of Medicinal Chemistry*. <https://doi.org/10.1021/jm0200761>
- Basnet, R. M., Zizioli, D., Taweedet, S., Finazzi, D., & Memo, M. (2019). Zebrafish larvae as a behavioral model in neuropharmacology. *Biomedicines*. <https://doi.org/10.3390/BIOMEDICINES7010023>
- Bayewitch, M., Rhee, M., Avidor-reiss, T., Breuer, A., Mechoulam, R., & Vogel, Z. (1996). Delta-9-Tetrahydrocannabinol Antagonizes the Peripheral Inhibition of Adenylyl Cyclase *. *Journal of Biological Chemistry*.
- Beaulieu, J. M., Sotnikova, T. D., Marion, S., Lefkowitz, R. J., Gainetdinov, R. R., & Caron, M. G. (2005). An Akt/ β -arrestin 2/PP2A signaling complex mediates dopaminergic neurotransmission and behavior. *Cell*. <https://doi.org/10.1016/j.cell.2005.05.012>
- Begbie, J., Doherty, P., & Graham, A. (2004). Cannabinoid receptor, CB₁, expression follows neuronal differentiation in the early chick embryo. *Journal of Anatomy*. <https://doi.org/10.1111/j.0021-8782.2004.00325.x>
- Benarroch, E. (2007). Endocannabinoids in basal ganglia circuits. *Neurology*.
- Benowitz, N. L., Rosenberg, J., Rogers, W., Bachman, J., & Jones, R. T. (1979). Cardiovascular effects of intravenous delta-9-tetrahydrocannabinol: Autonomic nervous mechanisms. *Clinical Pharmacology and Therapeutics*. <https://doi.org/10.1002/cpt1979254440>
- Berg, E. M., Björnfors, E. R., Pallucchi, I., Picton, L. D., & El Manira, A. (2018). Principles Governing Locomotion in Vertebrates: Lessons From Zebrafish. *Frontiers in Neural Circuits*. <https://doi.org/10.3389/fncir.2018.00073>
- Berghuis, P., Dobszay, M. B., Wang, X., Spano, S., Ledda, F., Sousa, K. M., ... Harkany, T. (2005). Endocannabinoids regulate interneuron migration and morphogenesis by

- transactivating the TrkB receptor. *Proceedings of the National Academy of Sciences of the United States of America*. <https://doi.org/10.1073/pnas.0509494102>
- Berghuis, P., Rajnicek, A. M., Morozov, Y. M., Ross, R. A., Mulder, J., Urbán, G. M., ... Harkany, T. (2007). Hardwiring the brain: Endocannabinoids shape neuronal connectivity. *Science*. <https://doi.org/10.1126/science.1137406>
- Bernard, C., Milh, M., Morozov, Y. M., Ben-Ari, Y., Freund, T. F., & Gozlan, H. (2005). Altering cannabinoid signaling during development disrupts neuronal activity. *Proceedings of the National Academy of Sciences of the United States of America*. <https://doi.org/10.1073/pnas.0409641102>
- Bisogno, T., Howell, F., Williams, G., Minassi, A., Cascio, M. G., Ligresti, A., ... Doherty, P. (2003). Cloning of the first sn1-DAG lipases points to the spatial and temporal regulation of endocannabinoid signaling in the brain. *Journal of Cell Biology*. <https://doi.org/10.1083/jcb.200305129>
- Blanco-Sánchez, B., Clément, A., Fierro, J., Washbourne, P., & Westerfield, M. (2014). Complexes of Usher proteins preassemble at the endoplasmic reticulum and are required for trafficking and ER homeostasis. *DMM Disease Models and Mechanisms*. <https://doi.org/10.1242/dmm.014068>
- Blankman, J. L., Simon, G. M., & Cravatt, B. F. (2007). A Comprehensive Profile of Brain Enzymes that Hydrolyze the Endocannabinoid 2-Arachidonoylglycerol. *Chemistry and Biology*. <https://doi.org/10.1016/j.chembiol.2007.11.006>
- Bolognini, D., Cascio, M. G., Parolaro, D., & Pertwee, R. G. (2012). AM630 behaves as a protean ligand at the human cannabinoid CB2 receptor. *British Journal of Pharmacology*, 165(8), 2561–2574. <https://doi.org/10.1111/j.1476-5381.2011.01503.x>
- Boyle, C. A. (2017). Intergenerational Effects Of Embryonic Cocaine Exposure In Zebrafish, (January). Retrieved from <https://commons.und.edu/theses>
- Braida, D., Limonta, V., Pegorini, S., Zani, A., Guerini-Rocco, C., Gori, E., & Sala, M. (2007). Hallucinatory and rewarding effect of salvinorin A in zebrafish: κ -opioid and CB1-cannabinoid receptor involvement. *Psychopharmacology*. <https://doi.org/10.1007/s00213-006-0639-1>
- Breivogel, C. S., & Childers, S. R. (1998). The functional neuroanatomy of brain Cannabinoid receptors. *Neurobiology of Disease*. <https://doi.org/10.1006/nbdi.1998.0229>
- Brennan, D., Chen, X., Cheng, L., Mahoney, M., & Riobo, N. A. (2012). Noncanonical Hedgehog Signaling. In *Vitamins and Hormones*. <https://doi.org/10.1016/B978-0-12-394622-5.00003-1>
- Brox, S., Ritter, A. P., Küster, E., & Reemtsma, T. (2014). A quantitative HPLC-MS/MS method for studying internal concentrations and toxicokinetics of 34 polar analytes in zebrafish (*Danio rerio*) embryos. *Analytical and Bioanalytical Chemistry*. <https://doi.org/10.1007/s00216-014-7929-y>
- Cai, D., Qiu, J., Cao, Z., McAtee, M., Bregman, B. S., & Filbin, M. T. (2001). Neuronal cyclic AMP controls the developmental loss in ability of axons to regenerate. *Journal of Neuroscience*. <https://doi.org/10.1523/jneurosci.21-13-04731.2001>
- Campbell, J. I. D., & Clark, J. M. (1988). An Encoding-Complex View of Cognitive Number Processing: Comment on McCloskey, Sokol, and Goodman (1986). *Journal of Experimental Psychology: General*. <https://doi.org/10.1037/0096-3445.117.2.204>
- Campos, Alline C., Ortega, Z., Palazuelos, J., Fogaça, M. V., Aguiar, D. C., Díaz-Alonso, J., ... Guimarães, F. S. (2013). The anxiolytic effect of cannabidiol on chronically stressed mice

- depends on hippocampal neurogenesis: Involvement of the endocannabinoid system. *International Journal of Neuropsychopharmacology*.
<https://doi.org/10.1017/S1461145712001502>
- Campos, Alline Cristina, Ferreira, F. R., & Guimarães, F. S. (2012). Cannabidiol blocks long-lasting behavioral consequences of predator threat stress: Possible involvement of 5HT1A receptors. *Journal of Psychiatric Research*. <https://doi.org/10.1016/j.jpsychires.2012.08.012>
- Campos, Alline Cristina, & Guimarães, F. S. (2008). Involvement of 5HT1A receptors in the anxiolytic-like effects of cannabidiol injected into the dorsolateral periaqueductal gray of rats. *Psychopharmacology*. <https://doi.org/10.1007/s00213-008-1168-x>
- Canadian Tobacco Alcohol and Drugs. (2017). Canadian Tobacco Alcohol and Drugs (CTADS): 2015 summary. *Ctads 2015*.
- Carballo, G. B., Honorato, J. R., De Lopes, G. P. F., & Spohr, T. C. L. D. S. E. (2018). A highlight on Sonic hedgehog pathway. *Cell Communication and Signaling*.
<https://doi.org/10.1186/s12964-018-0220-7>
- Carty, D. R., Miller, Z. S., Thornton, C., Pandelides, Z., Kutchma, M. L., & Willett, K. L. (2019). Multigenerational consequences of early-life cannabinoid exposure in zebrafish. *Toxicology and Applied Pharmacology*. <https://doi.org/10.1016/j.taap.2018.12.021>
- Carty, D. R., Thornton, C., Gledhill, J. H., & Willett, K. L. (2018). Developmental Effects of Cannabidiol and Δ^9 -Tetrahydrocannabinol in Zebrafish. *Toxicological Sciences : An Official Journal of the Society of Toxicology*. <https://doi.org/10.1093/toxsci/kfx232>
- Casarotto, P. C., Gomes, F. V., Resstel, L. B. M., & Guimarães, F. S. (2010). Cannabidiol inhibitory effect on marble-burying behaviour: Involvement of CB1 receptors. *Behavioural Pharmacology*. <https://doi.org/10.1097/FBP.0b013e32833b33c5>
- Caspary, T., García-García, M. J., Huangfu, D., Eggenschwiler, J. T., Wyler, M. R., Rakeman, A. S., ... Anderson, K. V. (2002). Mouse Dispatched homolog1 is required for long-range, but not juxtacrine, Hh signaling. *Current Biology*. [https://doi.org/10.1016/S0960-9822\(02\)01147-8](https://doi.org/10.1016/S0960-9822(02)01147-8)
- Caterina, M. J., & Julius, D. (1999). Sense and specificity: A molecular identity for nociceptors. *Current Opinion in Neurobiology*. [https://doi.org/10.1016/S0959-4388\(99\)00009-4](https://doi.org/10.1016/S0959-4388(99)00009-4)
- Chen, Y., Lu, X., Guo, L., Ni, W., Zhang, Y., Zhao, L., ... Li, H. (2017). Hedgehog signaling promotes the proliferation and subsequent hair cell formation of progenitor cells in the neonatal mouse cochlea. *Frontiers in Molecular Neuroscience*.
<https://doi.org/10.3389/fnmol.2017.00426>
- Childers, S. R., Sexton, T., & Roy, M. B. (1994). Effects of anandamide on cannabinoid receptors in rat brain membranes. *Biochemical Pharmacology*.
[https://doi.org/10.1016/0006-2952\(94\)90134-1](https://doi.org/10.1016/0006-2952(94)90134-1)
- Chousidis, I., Chatzimitakos, T., Leonardos, D., Filiou, M. D., Stalikas, C. D., & Leonardos, I. D. (2020). Cannabinol in the spotlight: Toxicometabolomic study and behavioral analysis of zebrafish embryos exposed to the unknown cannabinoid. *Chemosphere*.
<https://doi.org/10.1016/j.chemosphere.2020.126417>
- Chung, L. (2015). A Brief Introduction to the Transduction of Neural Activity into Fos Signal. *Development & Reproduction*. <https://doi.org/10.12717/dr.2015.19.2.061>
- Churchwell, J. C., Lopez-Larson, M., & Yurgelun-Todd, D. A. (2010). Altered frontal cortical volume and decision making in adolescent cannabis users. *Frontiers in Psychology*.
<https://doi.org/10.3389/fpsyg.2010.00225>
- Coffman, C. B., & Gentner, W. A. (1974). Cannabis sativa L.: effect of drying time and

- temperature on cannabinoid profile of stored leaf tissue. *Bulletin on Narcotics*.
- Cohen-Cory, S., Kidane, A. H., Shirkey, N. J., & Marshak, S. (2010). Brain-derived neurotrophic factor and the development of structural neuronal connectivity. *Developmental Neurobiology*. <https://doi.org/10.1002/dneu.20774>
- Colucci-D'amato, L., Speranza, L., & Volpicelli, F. (2020). Neurotrophic factor bdnf, physiological functions and therapeutic potential in depression, neurodegeneration and brain cancer. *International Journal of Molecular Sciences*. <https://doi.org/10.3390/ijms21207777>
- Cravatt, B. F., Giang, D. K., Mayfield, S. P., Boger, D. L., Lerner, R. A., & Gilula, N. B. (1996). Molecular characterization of an enzyme that degrades neuromodulatory fatty-acid amides. *Nature*. <https://doi.org/10.1038/384083a0>
- Crippa, J. A., Zuardi, A. W., Martín-Santos, R., Bhattacharyya, S., Atakan, Z., McGuire, P., & Fusar-Poli, P. (2009). Cannabis and anxiety: A critical review of the evidence. *Human Psychopharmacology*. <https://doi.org/10.1002/hup.1048>
- Cristino, L., de Petrocellis, L., Pryce, G., Baker, D., Guglielmotti, V., & Di Marzo, V. (2006). Immunohistochemical localization of cannabinoid type 1 and vanilloid transient receptor potential vanilloid type 1 receptors in the mouse brain. *Neuroscience*. <https://doi.org/10.1016/j.neuroscience.2006.02.074>
- Cruz, P. M. R., Mo, H., McConathy, W. J., Sabnis, N., & Lacko, A. G. (2013). The role of cholesterol metabolism and cholesterol transport in carcinogenesis: A review of scientific findings, relevant to future cancer therapeutics. *Frontiers in Pharmacology*. <https://doi.org/10.3389/fphar.2013.00119>
- D'Souza, D. C., Pittman, B., Perry, E., & Simen, A. (2009). Preliminary evidence of cannabinoid effects on brain-derived neurotrophic factor (BDNF) levels in humans. *Psychopharmacology*. <https://doi.org/10.1007/s00213-008-1333-2>
- Dahmane, N., & Ruiz I Altaba, A. (1999). Sonic hedgehog regulates the growth and patterning of the cerebellum. *Development*. <https://doi.org/10.1242/dev.126.14.3089>
- Dascal, N. (2001). Ion-channel regulation by G proteins. *Trends in Endocrinology and Metabolism*. [https://doi.org/10.1016/S1043-2760\(01\)00475-1](https://doi.org/10.1016/S1043-2760(01)00475-1)
- De Petrocellis, L., Bisogno, T., Maccarrone, M., Davis, J. B., Finazzi-Agrò, A., & Di Marzo, V. (2001). The Activity of Anandamide at Vanilloid VR1 Receptors Requires Facilitated Transport across the Cell Membrane and Is Limited by Intracellular Metabolism. *Journal of Biological Chemistry*. <https://doi.org/10.1074/jbc.M008555200>
- De Petrocellis, L., Ligresti, A., Moriello, A. S., Allarà, M., Bisogno, T., Petrosino, S., ... Di Marzo, V. (2011). Effects of cannabinoids and cannabinoid-enriched Cannabis extracts on TRP channels and endocannabinoid metabolic enzymes. *British Journal of Pharmacology*. <https://doi.org/10.1111/j.1476-5381.2010.01166.x>
- Dean, R., Duperreault, E., Newton, D., Krook, J., Ingraham, E., Gallup, J., ... Hamilton, T. J. (2020). Opposing effects of acute and repeated nicotine exposure on boldness in zebrafish. *Scientific Reports*, 10(1), 1–11. <https://doi.org/10.1038/s41598-020-65382-6>
- Degenhardt, L., Hall, W., & Lynskey, M. (2003). Exploring the association between cannabis use and depression. *Addiction*. <https://doi.org/10.1046/j.1360-0443.2003.00437.x>
- Deida, T., Luis, C., Rodríguez, R., Santana, A., & Behra, M. (2019). Hair Cell Development and Regeneration in Zebrafish Lacking the Cannabinoid Receptor2. *FASEB Journal Conference: Experimental Biology, Volume33(IssueS1)*, lb141–lb141.
- Devane, W. A., Hanuš, L., Breuer, A., Pertwee, R. G., Stevenson, L. A., Griffin, G., ... Mechoulam, R. (1992). Isolation and structure of a brain constituent that binds to the

- cannabinoid receptor. *Science*. <https://doi.org/10.1126/science.1470919>
- Devoto, S. H., Melançon, E., Eisen, J. S., & Westerfield, M. (1996). Identification of separate slow and fast muscle precursor cells in vivo, prior to somite formation. *Development*. <https://doi.org/10.1242/dev.122.11.3371>
- Díaz-Alonso, J., Aguado, T., Wu, C. S., Palazuelos, J., Hofmann, C., Garcez, P., ... Galve-Roperh, I. (2012). The CB1 cannabinoid receptor drives corticospinal motor neuron differentiation through the Ctip2/Satb2 transcriptional regulation axis. *Journal of Neuroscience*. <https://doi.org/10.1523/JNEUROSCI.0681-12.2012>
- Diogenes, A., Akopian, A. N., & Hargreaves, K. M. (2007). NGF Up-regulates TRPA1: Implications for orofacial pain. *Journal of Dental Research*. <https://doi.org/10.1177/154405910708600612>
- Diógenes, M. J., Assaife-Lopes, N., Pinto-Duarte, A., Ribeiro, J. A., & Sebastião, A. M. (2007). Influence of age on BDNF modulation of hippocampal synaptic transmission: Interplay with adenosine A2A receptors. *Hippocampus*. <https://doi.org/10.1002/hipo.20294>
- Downer, E. J., & Campbell, V. A. (2010). Phytocannabinoids, CNS cells and development: A dead issue? *Drug and Alcohol Review*. <https://doi.org/10.1111/j.1465-3362.2009.00102.x>
- Downer, E. J., Gowran, A., & Campbell, V. A. (2007). A comparison of the apoptotic effect of Δ^9 -tetrahydrocannabinol in the neonatal and adult rat cerebral cortex. *Brain Research*. <https://doi.org/10.1016/j.brainres.2007.07.076>
- Dror, A. A., & Avraham, K. B. (2009). Hearing loss: Mechanisms revealed by genetics and cell biology. *Annual Review of Genetics*. <https://doi.org/10.1146/annurev-genet-102108-134135>
- Egerton, A., Allison, C., Brett, R. R., & Pratt, J. A. (2006). Cannabinoids and prefrontal cortical function: Insights from preclinical studies. *Neuroscience and Biobehavioral Reviews*. <https://doi.org/10.1016/j.neubiorev.2005.12.002>
- Eisen, J. S., Myers, P. Z., & Westerfield, M. (1986). Pathway selection by growth cones of identified motoneurons in live zebra fish embryos. *Nature*, 320(6059), 269–271. <https://doi.org/10.1038/320269a0>
- Eisen, J. S., Pike, S. H., & Romancier, B. (1990). An identified motoneuron with variable fates in embryonic zebrafish. *Journal of Neuroscience*. <https://doi.org/10.1523/jneurosci.10-01-00034.1990>
- Ellis, L. (2019). Zebrafish as a High-Throughput In Vivo Model for Testing the Bioactivity of Cannabinoids. In *Recent Advances in Cannabinoid Research*. <https://doi.org/10.5772/intechopen.79321>
- ElSohly, M. A., Mehmedic, Z., Foster, S., Gon, C., Chandra, S., & Church, J. C. (2016). Changes in cannabis potency over the last 2 decades (1995-2014): Analysis of current data in the United States. *Biological Psychiatry*. <https://doi.org/10.1016/j.biopsych.2016.01.004>
- ElSohly, M. A., Ross, S. A., Mehmedic, Z., Arafat, R., Yi, B., & Banahan, B. F. (2000). Potency Trends of Δ^9 -THC and Other Cannabinoids in Confiscated Marijuana from 1980–1997. *Journal of Forensic Sciences*. <https://doi.org/10.1520/jfs14636j>
- Fashena, D., & Westerfield, M. (1999). Secondary motoneuron axons localize DM-GRASP on their fasciculated segments. *Journal of Comparative Neurology*. [https://doi.org/10.1002/\(SICI\)1096-9861\(19990412\)406:3<415::AID-CNE9>3.0.CO;2-2](https://doi.org/10.1002/(SICI)1096-9861(19990412)406:3<415::AID-CNE9>3.0.CO;2-2)
- Fay, J. F., Dunham, T. D., & Farrens, D. L. (2005). Cysteine residues in the human cannabinoid receptor: Only C257 and C264 are required for a functional receptor, and steric bulk at C386 impairs antagonist SR141716A binding. *Biochemistry*. <https://doi.org/10.1021/bi0472651>

- Fish, E. W., Murdaugh, L. B., Zhang, C., Boschen, K. E., Boa-Amponsem, O., Mendoza-Romero, H. N., ... Parnell, S. E. (2019). Cannabinoids Exacerbate Alcohol Teratogenesis by a CB1-Hedgehog Interaction. *Scientific Reports*. <https://doi.org/10.1038/s41598-019-52336-w>
- Fox, M. A., & Sanes, J. R. (2007). Synaptotagmin I and II are present in distinct subsets of central synapses. *Journal of Comparative Neurology*. <https://doi.org/10.1002/cne.21381>
- Fried, P. A. (1995). the ottawa prenatal prospective study (OPPS): Methodological issues and findings - it's easy to throw the baby out with the bath water. *Life Sciences*. [https://doi.org/10.1016/0024-3205\(95\)00203-1](https://doi.org/10.1016/0024-3205(95)00203-1)
- Friedman, W. (2012). Chapter 29 – Growth Factors. In *Basic Neurochemistry*.
- Friedrich, T., Lambert, A. M., Masino, M. A., & Downes, G. B. (2012). Mutation of zebrafish dihydrolipoamide branched-chain transacylase E2 results in motor dysfunction and models maple syrup urine disease. *DMM Disease Models and Mechanisms*. <https://doi.org/10.1242/dmm.008383>
- Galve-Roperh, I., Aguado, T., Palazuelos, J., & Guzman, M. (2008). Mechanisms of Control of Neuron Survival by the Endocannabinoid System. *Current Pharmaceutical Design*. <https://doi.org/10.2174/138161208785740117>
- Galve-Roperh, I., Chiurchiù, V., Díaz-Alonso, J., Bari, M., Guzmán, M., & Maccarrone, M. (2013). Cannabinoid receptor signaling in progenitor/stem cell proliferation and differentiation. *Progress in Lipid Research*. <https://doi.org/10.1016/j.plipres.2013.05.004>
- Gaoni, Y., & Mechoulam, R. (1964). Isolation, Structure, and Partial Synthesis of an Active Constituent of Hashish. *Journal of the American Chemical Society*. <https://doi.org/10.1021/ja01062a046>
- George, T., & Vaccarino, F. (2015). *Substance Abuse in Canada: The Effects of Cannabis Use During Adolescence*. Canadian Centre on Substance Abuse.
- Gerard, C. M., Mollereau, C., Vassart, G., & Parmentier, M. (1991). Molecular cloning of a human cannabinoid receptor which is also expressed in testis. *Biochemical Journal*. <https://doi.org/10.1042/bj2790129>
- Gérard, C., Mollereau, C., Vassart, G., & Parmentier, M. (1990). Nucleotide sequence of a human cannabinoid receptor cDNA. *Nucleic Acids Research*. <https://doi.org/10.1093/nar/18.23.7142>
- Ghosh, S. (2017). *Cannabinoid Receptors (CB) in Cochlea: Characterization and Otoprotective Functions*. ProQuest Dissertations and Theses.
- Ghosh, S., Sheth, S., Sheehan, K., Mukherjea, D., Dhukhwa, A., Borse, V., ... Ramkumar, V. (2018). The endocannabinoid/cannabinoid receptor 2 system protects against cisplatin-induced hearing loss. *Frontiers in Cellular Neuroscience*. <https://doi.org/10.3389/fncel.2018.00271>
- Gong, J., Hu, S., Huang, Z., Hu, Y., Wang, X., Zhao, J., ... Liu, D. (2020). The Requirement of Sox2 for the Spinal Cord Motor Neuron Development of Zebrafish. *Frontiers in Molecular Neuroscience*. <https://doi.org/10.3389/fnmol.2020.00034>
- Gonsiorek, W., Lunn, C., Fan, X., Narula, S., Lundell, D., & Hipkin, R. W. (2000). Endocannabinoid 2-arachidonyl glycerol is a full agonist through human type 2 cannabinoid receptor: Antagonism by anandamide. *Molecular Pharmacology*.
- Goolish, E. M., & Okutake, K. (1999). Lack of gas bladder inflation by the larvae of zebrafish in the absence of an air-water interface. *Journal of Fish Biology*. <https://doi.org/10.1006/jfbi.1999.1110>

- Graham, J. D. P., & Li, D. M. F. (1973). Cardiovascular and respiratory effects of cannabis in cat and rat. *British Journal of Pharmacology*. <https://doi.org/10.1111/j.1476-5381.1973.tb08262.x>
- Griffin, G., Atkinson, P. J., Showalter, V. M., Martin, B. R., & Abood, M. E. (1998). Evaluation of cannabinoid receptor agonists and antagonists using the guanosine-5'-O-(3-[35S]thio)-triphosphate binding assay in rat cerebellar membranes. *Journal of Pharmacology and Experimental Therapeutics*.
- Gunes, S., Arslan, M. A., Hekim, G. N. T., & Asci, R. (2016). The role of epigenetics in idiopathic male infertility. *Journal of Assisted Reproduction and Genetics*. <https://doi.org/10.1007/s10815-016-0682-8>
- Gyombolai, P., Tóth, A. D., Tímár, D., Turu, G., & Hunyady, L. (2014). Mutations in the 'DRY' motif of the CB1 cannabinoid receptor result in biased receptor variants. *Journal of Molecular Endocrinology*. <https://doi.org/10.1530/JME-14-0219>
- Hamilton, T. J., Krook, J., Szaszkievicz, J., & Burggren, W. (2021). Shoaling, boldness, anxiety-like behavior and locomotion in zebrafish (*Danio rerio*) are altered by acute benzo[a]pyrene exposure. *Science of the Total Environment*, 774, 145702. <https://doi.org/10.1016/j.scitotenv.2021.145702>
- Hamilton, T. J., Morrill, A., Lucas, K., Gallup, J., Harris, M., Healey, M., ... Tresguerres, M. (2017). Establishing zebrafish as a model to study the anxiolytic effects of scopolamine. *Scientific Reports*. <https://doi.org/10.1038/s41598-017-15374-w>
- Hamm, H. E. (1998). The many faces of G protein signaling. *Journal of Biological Chemistry*. <https://doi.org/10.1074/jbc.273.2.669>
- Harada, A., Teng, J., Takei, Y., Oguchi, K., & Hirokawa, N. (2002). MAP2 is required for dendrite elongation, PKA anchoring in dendrites, and proper PKA signal transduction. *Journal of Cell Biology*. <https://doi.org/10.1083/jcb.200110134>
- Harkany, T., Guzmán, M., Galve-Roperh, I., Berghuis, P., Devi, L. A., & Mackie, K. (2007). The emerging functions of endocannabinoid signaling during CNS development. *Trends in Pharmacological Sciences*. <https://doi.org/10.1016/j.tips.2006.12.004>
- Harkany, T., Mackie, K., & Doherty, P. (2008). Wiring and firing neuronal networks: endocannabinoids take center stage. *Current Opinion in Neurobiology*. <https://doi.org/10.1016/j.conb.2008.08.007>
- Harper, J. W., Heath, R. G., & Myers, W. A. (1977). Effects of cannabis sativa on ultrastructure of the synapse in monkey brain. *Journal of Neuroscience Research*. <https://doi.org/10.1002/jnr.490030202>
- Harvey, D. J. (1990). Stability of cannabinoids in dried samples of cannabis dating from around 1896-1905. *Journal of Ethnopharmacology*. [https://doi.org/10.1016/0378-8741\(90\)90068-5](https://doi.org/10.1016/0378-8741(90)90068-5)
- Hatta, K. (1992). Role of the floor plate in axonal patterning in the zebrafish CNS. *Neuron*. [https://doi.org/10.1016/0896-6273\(92\)90027-B](https://doi.org/10.1016/0896-6273(92)90027-B)
- Heath, R. G., Fitzjarrell, A. T., Fontana, C. J., & Garey, R. E. (1980). Cannabis sativa: Effects on brain function and ultrastructure in rhesus monkeys. *Biological Psychiatry*.
- Hejazi, N., Zhou, C., Oz, M., Sun, H., Jiang, H. Y., & Zhang, L. (2006). Δ^9 -Tetrahydrocannabinol and endogenous cannabinoid anandamide directly potentiate the function of glycine receptors. *Molecular Pharmacology*. <https://doi.org/10.1124/mol.105.019174>
- Herkenham, M., Lynn, A. B., Little, M. D., Johnson, M. R., Melvin, L. S., De Costa, B. R., & Rice, K. C. (1990). Cannabinoid receptor localization in brain. *Proceedings of the National*

- Academy of Sciences of the United States of America.*
<https://doi.org/10.1073/pnas.87.5.1932>
- Hermanson, D. J., Gamble-George, J. C., Marnett, L. J., & Patel, S. (2014). Substrate-selective COX-2 inhibition as a novel strategy for therapeutic endocannabinoid augmentation. *Trends in Pharmacological Sciences*. <https://doi.org/10.1016/j.tips.2014.04.006>
- Hill, A. J., Teraoka, H., Heideman, W., & Peterson, R. E. (2005). Zebrafish as a model vertebrate for investigating chemical toxicity. *Toxicological Sciences*.
<https://doi.org/10.1093/toxsci/kfi110>
- Howard, S. (2013). *Intracellular Signaling in Fundamental Neuroscience (Fourth Edition)*.
<https://doi.org/https://doi.org/10.1016/B978-0-12-385870-2.00009-3>
- Howe, K., Clark, M. D., Torroja, C. F., Torrance, J., Berthelot, C., Muffato, M., ... Stemple, D. L. (2013). The zebrafish reference genome sequence and its relationship to the human genome. *Nature*. <https://doi.org/10.1038/nature12111>
- Howlett, A. C. (2005a). Cannabinoid receptor signaling. *Handbook of Experimental Pharmacology*. https://doi.org/10.1007/3-540-26573-2_2
- Howlett, A. C. (2005b). Cannabinoid receptor signaling. *Handbook of Experimental Pharmacology*. <https://doi.org/10.1007/3-540-26573-2-2>
- Howlett, A. C., Barth, F., Bonner, T. I., Cabral, G., Casellas, P., Devane, W. A., ... Pertwee, R. G. (2002). International Union of Pharmacology. XXVII. Classification of cannabinoid receptors. *Pharmacological Reviews*. <https://doi.org/10.1124/pr.54.2.161>
- Howlett, Allyn C., & Mukhopadhyay, S. (2000). Cellular signal transduction by anandamide and 2-arachidonoylglycerol. *Chemistry and Physics of Lipids*. [https://doi.org/10.1016/S0009-3084\(00\)00187-0](https://doi.org/10.1016/S0009-3084(00)00187-0)
- Howlett, Allyn C., & Shim, J. (2011). Cannabinoid Receptors and Signal Transduction. *Receptors And Signal Transduction*.
- Hryhorowicz, S., Kaczmarek-Ryś, M., Andrzejewska, A., Staszak, K., Hryhorowicz, M., Korcz, A., & Słomski, R. (2019). Allosteric modulation of cannabinoid receptor 1— current challenges and future opportunities. *International Journal of Molecular Sciences*.
<https://doi.org/10.3390/ijms20235874>
- Hua, T., Vemuri, K., Pu, M., Qu, L., Han, G. W., Wu, Y., ... Liu, Z. J. (2016). Crystal Structure of the Human Cannabinoid Receptor CB1. *Cell*. <https://doi.org/10.1016/j.cell.2016.10.004>
- Huang, E. J., & Reichardt, L. F. (2003). Trk receptors: Roles in neuronal signal transduction. *Annual Review of Biochemistry*.
<https://doi.org/10.1146/annurev.biochem.72.121801.161629>
- Huang, S., Xiao, P., & Sun, J. (2020). Structural basis of signaling of cannabinoids receptors: paving a way for rational drug design in controlling multiple neurological and immune diseases. *Signal Transduction and Targeted Therapy*. <https://doi.org/10.1038/s41392-020-00240-5>
- Huber, A. B., Kolodkin, A. L., Ginty, D. D., & Cloutier, J. F. (2003). Signaling at the growth cone: Ligand-receptor complexes and the control of axon growth and guidance. *Annual Review of Neuroscience*. <https://doi.org/10.1146/annurev.neuro.26.010302.081139>
- Huestis, M. A. (2007). Human cannabinoid pharmacokinetics. *Chemistry and Biodiversity*.
<https://doi.org/10.1002/cbdv.200790152>
- Huestis, M. A., Henningfield, J. E., & Cone, E. J. (1992). Blood cannabinoids. i. absorption of the and formation of 11-oh-thc and thcooh during and after smoking marijuana. *Journal of Analytical Toxicology*. <https://doi.org/10.1093/jat/16.5.276>

- Huestis, M. A., Mitchell, J. M., & Cone, E. J. (1996). Urinary excretion profiles of 11-nor-9-carboxy- Δ^9 - tetrahydrocannabinol in humans after single smoked doses of marijuana. *Journal of Analytical Toxicology*. <https://doi.org/10.1093/jat/20.6.441>
- Huestis, M. A., Sampson, A. H., Holicky, B. J., Henningfield, J. E., & Cone, E. J. (1992). Characterization of the absorption phase of marijuana smoking. *Clinical Pharmacology & Therapeutics*. <https://doi.org/10.1038/clpt.1992.100>
- Khan, M., A. Sobocińska, A., M. Czarnecka, A., Król, M., Botta, B., & Szczylik, C. (2016). The Therapeutic Aspects of the Endocannabinoid System (ECS) for Cancer and their Development: From Nature to Laboratory. *Current Pharmaceutical Design*. <https://doi.org/10.2174/1381612822666151211094901>
- Iannotti, F. A., Silvestri, C., Mazzarella, E., Martella, A., Calvigioni, D., Piscitelli, F., ... Di Marzo, V. (2014). The endocannabinoid 2-AG controls skeletal muscle cell differentiation via CB1 receptor-dependent inhibition of Kv7 channels. *Proceedings of the National Academy of Sciences of the United States of America*, 111(24). <https://doi.org/10.1073/pnas.1406728111>
- Ibeas Bih, C., Chen, T., Nunn, A. V. W., Bazelat, M., Dallas, M., & Whalley, B. J. (2015). Molecular Targets of Cannabidiol in Neurological Disorders. *Neurotherapeutics*. <https://doi.org/10.1007/s13311-015-0377-3>
- Iffland, K., & Grotenhermen, F. (2017). An Update on Safety and Side Effects of Cannabidiol: A Review of Clinical Data and Relevant Animal Studies. *Cannabis and Cannabinoid Research*. <https://doi.org/10.1089/can.2016.0034>
- Incardona, J. P., Collier, T. K., & Scholz, N. L. (2004). Defects in cardiac function precede morphological abnormalities in fish embryos exposed to polycyclic aromatic hydrocarbons. *Toxicology and Applied Pharmacology*. <https://doi.org/10.1016/j.taap.2003.11.026>
- Iwasaki, M., Le, A. X., & Helms, J. A. (1997). Expression of indian hedgehog, bone morphogenetic protein 6 and gli during skeletal morphogenesis. *Mechanisms of Development*. [https://doi.org/10.1016/S0925-4773\(97\)00145-7](https://doi.org/10.1016/S0925-4773(97)00145-7)
- Jesuthasan, S. (2012). Fear, anxiety, and control in the zebrafish. *Developmental Neurobiology*. <https://doi.org/10.1002/dneu.20873>
- Jönsson, M. E., Kubota, A., Timme-Laragy, A. R., Woodin, B., & Stegeman, J. J. (2012). Ahr2-dependence of PCB126 effects on the swim bladder in relation to expression of CYP1 and cox-2 genes in developing zebrafish. *Toxicology and Applied Pharmacology*. <https://doi.org/10.1016/j.taap.2012.09.023>
- Jordan, C. J., & Xi, Z. X. (2019). Progress in brain cannabinoid CB 2 receptor research: From genes to behavior. *Neuroscience and Biobehavioral Reviews*. <https://doi.org/10.1016/j.neubiorev.2018.12.026>
- Kalueff, A. V., Gebhardt, M., Stewart, A. M., Cachat, J. M., Brimmer, M., Chawla, J. S., ... Schneider, H. (2013). Towards a comprehensive catalog of zebrafish behavior 1.0 and beyond. *Zebrafish*. <https://doi.org/10.1089/zeb.2012.0861>
- Kalueff, A. V., Stewart, A. M., & Gerlai, R. (2014). Zebrafish as an emerging model for studying complex brain disorders. *Trends in Pharmacological Sciences*. <https://doi.org/10.1016/j.tips.2013.12.002>
- Kano, M., Ohno-Shosaku, T., Hashimoto, Y., Uchigashima, M., & Watanabe, M. (2009). Endocannabinoid-mediated control of synaptic transmission. *Physiological Reviews*. <https://doi.org/10.1152/physrev.00019.2008>
- Kasarskis, A., Manova, K., & Anderson, K. V. (1998). A phenotype-based screen for embryonic

- lethal mutations in the mouse. *Proceedings of the National Academy of Sciences of the United States of America*. <https://doi.org/10.1073/pnas.95.13.7485>
- Kasten, C. R., Zhang, Y., & Boehm, S. L. (2019). Acute cannabinoids produce robust anxiety-like and locomotor effects in mice, but long-term consequences are age- And sex-dependent. *Frontiers in Behavioral Neuroscience*. <https://doi.org/10.3389/fnbeh.2019.00032>
- Katona, I., & Freund, T. F. (2012). Multiple functions of endocannabinoid signaling in the brain. *Annual Review of Neuroscience*. <https://doi.org/10.1146/annurev-neuro-062111-150420>
- Kenakin, T. (1995). Agonist-receptor efficacy II: agonist trafficking of receptor signals. *Trends in Pharmacological Sciences*. [https://doi.org/10.1016/S0165-6147\(00\)89032-X](https://doi.org/10.1016/S0165-6147(00)89032-X)
- Khaliullina, H., Bilgin, M., Sampaio, J. L., Shevchenko, A., & Eaton, S. (2015). Endocannabinoids are conserved inhibitors of the hedgehog pathway. *Proceedings of the National Academy of Sciences of the United States of America*. <https://doi.org/10.1073/pnas.1416463112>
- Kim, D., Cavanaugh, E. J., & Simkin, D. (2008). Inhibition of transient receptor potential A1 channel by phosphatidylinositol-4,5-bisphosphate. *American Journal of Physiology - Cell Physiology*. <https://doi.org/10.1152/ajpcell.00023.2008>
- Kim, S. W., & Kim, K. T. (2020). Expression of genes involved in axon guidance: how much have we learned? *International Journal of Molecular Sciences*. <https://doi.org/10.3390/ijms21103566>
- Kimmel, C. B., Ballard, W. W., Kimmel, S. R., Ullmann, B., & Schilling, T. F. (1995). Stages of embryonic development of the zebrafish. *Developmental Dynamics*. <https://doi.org/10.1002/aja.1002030302>
- Kimmel, C. B., Hatta, K., & Metcalfe, W. K. (1990). Early axonal contacts during development of an identified dendrite in the brain of the zebrafish. *Neuron*. [https://doi.org/10.1016/0896-6273\(90\)90111-R](https://doi.org/10.1016/0896-6273(90)90111-R)
- Klein, T. W. (2005). Cannabinoid-based drugs as anti-inflammatory therapeutics. *Nature Reviews Immunology*. <https://doi.org/10.1038/nri1602>
- Kohashi, T., Nakata, N., & Oda, Y. (2012). Effective sensory modality activating an escape triggering neuron switches during early development in zebrafish. *Journal of Neuroscience*. <https://doi.org/10.1523/JNEUROSCI.6169-11.2012>
- Kok, F. O., Oster, E., Mentzer, L., Hsieh, J. C., Henry, C. A., & Sirotkin, H. I. (2007). The role of the SPT6 chromatin remodeling factor in zebrafish embryogenesis. *Developmental Biology*. <https://doi.org/10.1016/j.ydbio.2007.04.039>
- Koren, G., & Cohen, R. (2020). The use of cannabis for Hyperemesis Gravidarum (HG). *Journal of Cannabis Research*. <https://doi.org/10.1186/s42238-020-0017-6>
- Kovacs, J. J., Hara, M. R., Davenport, C. L., Kim, J., & Lefkowitz, R. J. (2009). Arrestin Development: Emerging Roles for β -arrestins in Developmental Signaling Pathways. *Developmental Cell*. <https://doi.org/10.1016/j.devcel.2009.09.011>
- Kovacs, J. J., Whalen, E. J., Liu, R., Xiao, K., Kim, J., Chen, M., ... Lefkowitz, R. J. (2008). β -arrestin-mediated localization of smoothened to the primary cilium. *Science*. <https://doi.org/10.1126/science.1157983>
- Kowase, T., Nakazato, Y., Yoko-o, H., Morikawa, A., & Kojima, I. (2002). Immunohistochemical localization of growth factor-regulated channel (GRC) in human tissues. *Endocrine Journal*. <https://doi.org/10.1507/endocrj.49.349>
- Krook, J. T., Duperreault, E., Newton, D., Ross, M. S., & Hamilton, T. J. (2019). Repeated

- ethanol exposure increases anxiety-like behaviour in zebrafish during withdrawal. *PeerJ*. <https://doi.org/10.7717/peerj.6551>
- Kumar, A. M., Haney, M., Becker, T., Thompson, M. L., Kream, R. M., & Miczek, K. (1990). Effect of early exposure to δ -9-tetrahydrocannabinol on the levels of opioid peptides, gonadotropin-releasing hormone and substance P in the adult male rat brain. *Brain Research*. [https://doi.org/10.1016/0006-8993\(90\)91322-8](https://doi.org/10.1016/0006-8993(90)91322-8)
- Lam, C. S., Rastegar, S., & Strähle, U. (2006). Distribution of cannabinoid receptor 1 in the CNS of zebrafish. *Neuroscience*. <https://doi.org/10.1016/j.neuroscience.2005.10.069>
- Landfield, P. W., Cadwallader, L. B., & Vinsant, S. (1988). Quantitative changes in hippocampal structure following long-term exposure to Δ 9-tetrahydrocannabinol: possible mediation by glucocorticoid systems. *Brain Research*. [https://doi.org/10.1016/0006-8993\(88\)91597-1](https://doi.org/10.1016/0006-8993(88)91597-1)
- Laprairie, R. B., Bagher, A. M., Kelly, M. E. M., & Denovan-Wright, E. M. (2015). Cannabidiol is a negative allosteric modulator of the cannabinoid CB1 receptor. *British Journal of Pharmacology*. <https://doi.org/10.1111/bph.13250>
- Lauckner, J. E., Jensen, J. B., Chen, H. Y., Lu, H. C., Hille, B., & Mackie, K. (2008). GPR55 is a cannabinoid receptor that increases intracellular calcium and inhibits M current. *Proceedings of the National Academy of Sciences of the United States of America*. <https://doi.org/10.1073/pnas.0711278105>
- Lawston, J., Borella, A., Robinson, J. K., & Whitaker-Azmitia, P. M. (2000). Changes in hippocampal morphology following chronic treatment with the synthetic cannabinoid WIN 55,212-2. *Brain Research*. [https://doi.org/10.1016/S0006-8993\(00\)02739-6](https://doi.org/10.1016/S0006-8993(00)02739-6)
- Lee, D. K., Nguyen, T., Lynch, K. R., Cheng, R., Vanti, W. B., Arkhitko, O., ... O'Dowd, B. F. (2001). Discovery and mapping of ten novel G protein-coupled receptor genes. *Gene*. [https://doi.org/10.1016/S0378-1119\(01\)00651-5](https://doi.org/10.1016/S0378-1119(01)00651-5)
- Lee, J., & Tumber, T. (2012). Hairy tale of signaling in hair follicle development and cycling. *Seminars in Cell and Developmental Biology*. <https://doi.org/10.1016/j.semcdb.2012.08.003>
- Lefebvre, J. L., Jing, L., Becaficco, S., Franzini-Armstrong, C., & Granato, M. (2007). Differential requirement for MuSK and dystroglycan in generating patterns of neuromuscular innervation. *Proceedings of the National Academy of Sciences of the United States of America*, 104(7), 2483–2488. <https://doi.org/10.1073/pnas.0610822104>
- Lefkowitz, R. J., & Shenoy, S. K. (2005). Transduction of receptor signals by β -arrestins. *Science*. <https://doi.org/10.1126/science.1109237>
- Lerner, M., & Zeffert, J. T. (1968). Determination of tetrahydrocannabinol isomers in marijuana and hashish. *Bulleting on Narcotics*, (2), 53–59. Retrieved from https://www.unodc.org/unodc/en/data-and-analysis/bulletin/bulletin_1968-01-01_2_page010.html
- Levitas-Djerbi, T., & Appelbaum, L. (2017). Modeling sleep and neuropsychiatric disorders in zebrafish. *Current Opinion in Neurobiology*. <https://doi.org/10.1016/j.conb.2017.02.017>
- Leyton, M. (2019). Cannabis legalization: Did we make a mistake? update 2019. *Journal of Psychiatry and Neuroscience*. <https://doi.org/10.1503/jpn.190136>
- Li, G., Chen, J., Xie, P., Jiang, Y., Wu, L., & Zhang, X. (2011). Protein expression profiling in the zebrafish (*Danio rerio*) embryos exposed to the microcystin-LR. *Proteomics*. <https://doi.org/10.1002/pmic.201000442>
- Li, J., Liang, Y., Zhang, X., Lu, J., Zhang, J., Ruan, T., ... Jiang, G. (2011). Impaired gas bladder inflation in zebrafish exposed to a novel heterocyclic brominated flame retardant tris(2,3-dibromopropyl) Isocyanurate. *Environmental Science and Technology*.

- <https://doi.org/10.1021/es202420g>
- Li, M. D., & Van Der Vaart, A. D. (2011). MicroRNAs in addiction: Adaptation's middlemen. *Molecular Psychiatry*, 16(12), 1159–1168. <https://doi.org/10.1038/mp.2011.58>
- Lichtman, A. H., Varvel, S. A., & Martin, B. R. (2002). Endocannabinoids in cognition and dependence. *Prostaglandins Leukotrienes and Essential Fatty Acids*. <https://doi.org/10.1054/plef.2001.0351>
- Lichtman, Aron H., Shelton, C. C., Advani, T., & Cravatt, B. F. (2004). Mice lacking fatty acid amide hydrolase exhibit a cannabinoid receptor-mediated phenotypic hypoalgesia. *Pain*. <https://doi.org/10.1016/j.pain.2004.01.022>
- Liu, Y. J., Fan, H. B., Jin, Y., Ren, C. G., Jia, X. E., Wang, L., ... Ren, R. (2013). Cannabinoid receptor 2 suppresses leukocyte inflammatory migration by modulating the JNK/c-Jun/Alox5 pathway. *Journal of Biological Chemistry*. <https://doi.org/10.1074/jbc.M113.453811>
- Lu, H. C., & MacKie, K. (2016). An introduction to the endogenous cannabinoid system. *Biological Psychiatry*. <https://doi.org/10.1016/j.biopsych.2015.07.028>
- Lubman, D. I., Cheetham, A., & Yücel, M. (2015). Cannabis and adolescent brain development. *Pharmacology and Therapeutics*. <https://doi.org/10.1016/j.pharmthera.2014.11.009>
- Luna, V. M., & Brehm, P. (2006). An electrically coupled network of skeletal muscle in zebrafish distributes synaptic current. *Journal of General Physiology*. <https://doi.org/10.1085/jgp.200609501>
- Lyons, E. L., Kabler, S., Howlett, A., Kovach, A. L., & Thomas, B. (2018). Cb1 But Not CB2 cannabinoid receptor increases neurite extension in human neuroblastoma . *FASEB Journal Conference: Experimental Biology* .
- Ma, P., Song, N. N., Li, Y., Zhang, Q., Zhang, L., Zhang, L., ... Mao, B. (2019). Fine-Tuning of Shh/Gli Signaling Gradient by Non-proteolytic Ubiquitination during Neural Patterning. *Cell Reports*. <https://doi.org/10.1016/j.celrep.2019.06.017>
- Mackie, K. (2005). Distribution of cannabinoid receptors in the central and peripheral nervous system. *Handbook of Experimental Pharmacology*. <https://doi.org/10.1007/3-540-26573-2-10>
- MacLennan, S. J., Reynen, P. H., Kwan, J., & Bonhaus, D. W. (1998). Evidence for inverse agonism of SR141716A at human recombinant cannabinoid CB1 and CB2 receptors. *British Journal of Pharmacology*. <https://doi.org/10.1038/sj.bjp.0701915>
- Maes, J., Verlooy, L., Buenafe, O. E., de Witte, P. A. M., Esguerra, C. V., & Crawford, A. D. (2012). Evaluation of 14 Organic Solvents and Carriers for Screening Applications in Zebrafish Embryos and Larvae. *PLoS ONE*. <https://doi.org/10.1371/journal.pone.0043850>
- Malone, D. T., & Taylor, D. A. (2006). The effect of Δ^9 -tetrahydrocannabinol on sensorimotor gating in socially isolated rats. *Behavioural Brain Research*. <https://doi.org/10.1016/j.bbr.2005.07.009>
- Marino, S. M., & Gladyshev, V. N. (2010). Cysteine Function Governs Its Conservation and Degeneration and Restricts Its Utilization on Protein Surfaces. *Journal of Molecular Biology*. <https://doi.org/10.1016/j.jmb.2010.09.027>
- Marshak, S., Nikolakopoulou, A. M., Dirks, R., Martens, G. J., & Cohen-Cory, S. (2007). Cell-autonomous TrkB signaling in presynaptic retinal ganglion cells mediates axon arbor growth and synapse maturation during the establishment of retinotectal synaptic connectivity. *Journal of Neuroscience*. <https://doi.org/10.1523/JNEUROSCI.4434-06.2007>
- Martella, A., Sepe, R. M., Silvestri, C., Zang, J., Fasano, G., Carnevali, O., ... Di Marzo, V.

- (2016). Important role of endocannabinoid signaling in the development of functional vision and locomotion in zebrafish. *FASEB Journal*. <https://doi.org/10.1096/fj.201600602R>
- Martín-Saldaña, S., Trinidad, A., Ramil, E., Sánchez-López, A. J., Coronado, M. J., Martínez-Martínez, E., ... Ramírez-Camacho, R. (2016). Spontaneous Cannabinoid Receptor 2 (CB2) expression in the cochlea of adult albino rat and its up-regulation after cisplatin treatment. *PLoS ONE*. <https://doi.org/10.1371/journal.pone.0161954>
- Martin, B. R., Compton, D. R., Thomas, B. F., Prescott, W. R., Little, P. J., Razdan, R. K., ... Susan J., W. (1991). Behavioral, biochemical, and molecular modeling evaluations of cannabinoid analogs. *Pharmacology, Biochemistry and Behavior*. [https://doi.org/10.1016/0091-3057\(91\)90349-7](https://doi.org/10.1016/0091-3057(91)90349-7)
- Matsuda, L. A., Lolait, S. J., Brownstein, M. J., Young, A. C., & Bonner, T. I. (1990). Structure of a cannabinoid receptor and functional expression of the cloned cDNA. *Nature*. <https://doi.org/10.1038/346561a0>
- Maurya, N., & Velmurugan, B. K. (2018). Therapeutic applications of cannabinoids. *Chemico-Biological Interactions*. <https://doi.org/10.1016/j.cbi.2018.07.018>
- Maximino, C., Da Silva, A. W. B., Araújo, J., Lima, M. G., Miranda, V., Puty, B., ... Herculano, A. M. (2014). Fingerprinting of psychoactive drugs in zebrafish anxiety-like behaviors. *PLoS ONE*. <https://doi.org/10.1371/journal.pone.0103943>
- May, Z., Morrill, A., Holcombe, A., Johnston, T., Gallup, J., Fouad, K., ... Hamilton, T. J. (2016). Object recognition memory in zebrafish. *Behavioural Brain Research*. <https://doi.org/10.1016/j.bbr.2015.09.016>
- McGilveray, I. J. (2005). Pharmacokinetics of cannabinoids. *Pain Research and Management*. <https://doi.org/10.1155/2005/242516>
- McGregor, I. S., Cairns, E. A., Abelev, S., Cohen, R., Henderson, M., Couch, D., ... Gauld, N. (2020). Access to cannabidiol without a prescription: A cross-country comparison and analysis. *International Journal of Drug Policy*. <https://doi.org/10.1016/j.drugpo.2020.102935>
- McHugh, D., Page, J., Dunn, E., & Bradshaw, H. B. (2012). Δ 9-tetrahydrocannabinol and N-arachidonyl glycine are full agonists at GPR18 receptors and induce migration in human endometrial HEC-1B cells. *British Journal of Pharmacology*. <https://doi.org/10.1111/j.1476-5381.2011.01497.x>
- Mechoulam, R., & Shvo, Y. (1963). Hashish-I. The structure of Cannabidiol. *Tetrahedron*. [https://doi.org/10.1016/0040-4020\(63\)85022-X](https://doi.org/10.1016/0040-4020(63)85022-X)
- Mechoulam, Raphael, Ben-Shabat, S., Hanus, L., Ligumsky, M., Kaminski, N. E., Schatz, A. R., ... Vogel, Z. (1995). Identification of an endogenous 2-monoglyceride, present in canine gut, that binds to cannabinoid receptors. *Biochemical Pharmacology*. [https://doi.org/10.1016/0006-2952\(95\)00109-D](https://doi.org/10.1016/0006-2952(95)00109-D)
- Menelaou, E., & McLean, D. L. (2012). A Gradient in Endogenous Rhythmicity and Oscillatory Drive Matches Recruitment Order in an Axial Motor Pool. *Journal of Neuroscience*, 32(32), 10925–10939. <https://doi.org/10.1523/JNEUROSCI.1809-12.2012>
- Migliarini, B., & Carnevali, O. (2008). Anandamide modulates growth and lipid metabolism in the zebrafish *Danio rerio*. *Molecular and Cellular Endocrinology*. <https://doi.org/10.1016/j.mce.2008.01.021>
- Migliarini, B., & Carnevali, O. (2009). A novel role for the endocannabinoid system during zebrafish development. *Molecular and Cellular Endocrinology*. <https://doi.org/10.1016/j.mce.2008.11.014>

- Miller, J. B., Crow, M. T., & Stockdale, F. E. (1985). Slow and fast myosin heavy chain content defines three types of myotubes in early muscle cell cultures. *Journal of Cell Biology*. <https://doi.org/10.1083/jcb.101.5.1643>
- Mizoguchi, T., Togawa, S., Kawakami, K., & Itoh, M. (2011). Neuron and sensory epithelial cell fate is sequentially determined by notch signaling in zebrafish lateral line development. *Journal of Neuroscience*. <https://doi.org/10.1523/JNEUROSCI.3948-11.2011>
- Mokrysz, C., Freeman, T. P., Korkki, S., Griffiths, K., & Curran, H. V. (2016). Are adolescents more vulnerable to the harmful effects of cannabis than adults? A placebo-controlled study in human males. *Translational Psychiatry*. <https://doi.org/10.1038/tp.2016.225>
- Molina-Holgado, F., Amaro, A., González, M. I., Alvarez, F. J., & Leret, M. L. (1996). Effect of maternal Δ^9 -tetrahydrocannabinol on developing serotonergic system. *European Journal of Pharmacology*. [https://doi.org/10.1016/S0014-2999\(96\)00753-4](https://doi.org/10.1016/S0014-2999(96)00753-4)
- Mongeon, R., Walogorsky, M., Urban, J., Mandel, G., Ono, F., & Brehm, P. (2011). An acetylcholine receptor lacking both γ and ϵ subunits mediates transmission in zebrafish slow muscle synapses. *Journal of General Physiology*. <https://doi.org/10.1085/jgp.201110649>
- Moore, T. H., Zammit, S., Lingford-Hughes, A., Barnes, T. R., Jones, P. B., Burke, M., & Lewis, G. (2007). Cannabis use and risk of psychotic or affective mental health outcomes: a systematic review. *Lancet*. [https://doi.org/10.1016/S0140-6736\(07\)61162-3](https://doi.org/10.1016/S0140-6736(07)61162-3)
- Moreira, F. A., Aguiar, D. C., & Guimarães, F. S. (2006). Anxiolytic-like effect of cannabidiol in the rat Vogel conflict test. *Progress in Neuro-Psychopharmacology and Biological Psychiatry*. <https://doi.org/10.1016/j.pnpbp.2006.06.004>
- Moreira, F. A., & Guimarães, F. S. (2005). Cannabidiol inhibits the hyperlocomotion induced by psychotomimetic drugs in mice. *European Journal of Pharmacology*. <https://doi.org/10.1016/j.ejphar.2005.02.040>
- Morris, J. A. (2009). Zebrafish: A model system to examine the neurodevelopmental basis of schizophrenia. *Progress in Brain Research*. [https://doi.org/10.1016/S0079-6123\(09\)17911-6](https://doi.org/10.1016/S0079-6123(09)17911-6)
- Morris, C. V., Dinieri, J. A., Szutorisz, H., & Hurd, Y. L. (2011). Molecular mechanisms of maternal cannabis and cigarette use on human neurodevelopment. *European Journal of Neuroscience*. <https://doi.org/10.1111/j.1460-9568.2011.07884.x>
- Mulder, J., Aguado, T., Keimpema, E., Barabás, K., Rosado, C. J. B., Nguyen, L., ... Harkany, T. (2008). Endocannabinoid signaling controls pyramidal cell specification and long-range axon patterning. *Proceedings of the National Academy of Sciences of the United States of America*. <https://doi.org/10.1073/pnas.0803545105>
- Murataeva, N., Straiker, A., & MacKie, K. (2014). Parsing the players: 2-arachidonoylglycerol synthesis and degradation in the CNS. *British Journal of Pharmacology*. <https://doi.org/10.1111/bph.12411>
- Murphy, S. K., Itchon-Ramos, N., Visco, Z., Huang, Z., Grenier, C., Schrott, R., ... Kollins, S. H. (2018). Cannabinoid exposure and altered DNA methylation in rat and human sperm. *Epigenetics*. <https://doi.org/10.1080/15592294.2018.1554521>
- Myers, P. Z., Eisen, J. S., & Westerfield, M. (1986). Development and axonal outgrowth of identified motoneurons in the zebrafish. *Journal of Neuroscience*. <https://doi.org/10.1523/jneurosci.06-08-02278.1986>
- Naganawa, Y., & Hirata, H. (2011). Developmental transition of touch response from slow muscle-mediated coilings to fast muscle-mediated burst swimming in zebrafish. *Developmental Biology*. <https://doi.org/10.1016/j.ydbio.2011.04.027>

- Nahas, G. G., Frick, H. C., Lattimer, J. K., Latour, C., & Harvey, D. (2002). Pharmacokinetics of THC in brain and testis, male gametotoxicity and premature apoptosis of spermatozoa. *Human Psychopharmacology*. <https://doi.org/10.1002/hup.369>
- Navarrete, M., & Araque, A. (2010). Endocannabinoids potentiate synaptic transmission through stimulation of astrocytes. *Neuron*. <https://doi.org/10.1016/j.neuron.2010.08.043>
- Nguyen-Chi, M. E., Bryson-Richardson, R., Sonntag, C., Hall, T. E., Gibson, A., Sztal, T., ... Currie, P. D. (2012). Morphogenesis and Cell Fate Determination within the Adaxial Cell Equivalence Group of the Zebrafish Myotome. *PLoS Genetics*. <https://doi.org/10.1371/journal.pgen.1003014>
- Nguyen, P. V., & Woo, N. H. (2003). Regulation of hippocampal synaptic plasticity by cyclic AMP-dependent protein kinases. *Progress in Neurobiology*. <https://doi.org/10.1016/j.pneurobio.2003.12.003>
- Nicolson, T., Rüsç, A., Friedrich, R. W., Granato, M., Ruppertsberg, J. P., & Nüsslein-Volhard, C. (1998). Genetic analysis of vertebrate sensory hair cell mechanosensation: The zebrafish circler mutants. *Neuron*. [https://doi.org/10.1016/S0896-6273\(00\)80455-9](https://doi.org/10.1016/S0896-6273(00)80455-9)
- Niederhoffer, N., & Szabo, B. (2000). Cannabinoids cause central sympathoexcitation and bradycardia in rabbits. *Journal of Pharmacology and Experimental Therapeutics*.
- Nishimura, H., Tanimura, T., Semba, R., & Uwabe, C. (1974). Normal development of early human embryos: Observation of 90 specimens at Carnegie stages 7 to 13. *Teratology*. <https://doi.org/10.1002/tera.1420100102>
- Nozawa, K., Lin, Y., Kubodera, R., Shimizu, Y., Tanaka, H., & Ohshima, T. (2017). Zebrafish *Mecp2* is required for proper axonal elongation of motor neurons and synapse formation. *Developmental Neurobiology*. <https://doi.org/10.1002/dneu.22498>
- O'Shea, M., Singh, M. E., McGregor, I. S., & Mallet, P. E. (2004). Chronic cannabinoid exposure produces lasting memory impairment and increased anxiety in adolescent but not adult rats. *Journal of Psychopharmacology*. <https://doi.org/10.1177/026988110401800407>
- Ochi, H., & Westerfield, M. (2007). Signaling networks that regulate muscle development: Lessons from zebrafish. *Development Growth and Differentiation*. <https://doi.org/10.1111/j.1440-169X.2007.00905.x>
- Oka, S., Yanagimoto, S., Ikeda, S., Gokoh, M., Kishimoto, S., Waku, K., ... Sugiura, T. (2005). Evidence for the involvement of the cannabinoid CB2 receptor and its endogenous ligand 2-arachidonoylglycerol in 12-O-tetradecanoylphorbol-13-acetate-induced acute inflammation in mouse ear. *Journal of Biological Chemistry*. <https://doi.org/10.1074/jbc.M413260200>
- Oltrabella, F., Melgoza, A., Nguyen, B., & Guo, S. (2017). Role of the endocannabinoid system in vertebrates: Emphasis on the zebrafish model. *Development Growth and Differentiation*. <https://doi.org/10.1111/dgd.12351>
- Orger, M. B., & De Polavieja, G. G. (2017). Zebrafish Behavior: Opportunities and Challenges. *Annual Review of Neuroscience*, 40, 125–147. <https://doi.org/10.1146/annurev-neuro-071714-033857>
- Pai, W. Y., Hsu, C. C., Lai, C. Y., Chang, T. Z., Tsai, Y. L., & Her, G. M. (2013). Cannabinoid receptor 1 promotes hepatic lipid accumulation and lipotoxicity through the induction of SREBP-1c expression in zebrafish. *Transgenic Research*. <https://doi.org/10.1007/s11248-012-9685-0>
- Palazuelos, J., Ortega, Z., Díaz-Alonso, J., Guzmán, M., & Galve-Roperh, I. (2012). CB 2 cannabinoid receptors promote neural progenitor cell proliferation via mTORC1 signaling. *Journal of Biological Chemistry*. <https://doi.org/10.1074/jbc.M111.291294>

- Park, J. Y., Mott, M., Williams, T., Ikeda, H., Wen, H., Linhoff, M., & Ono, F. (2014). A single mutation in the acetylcholine receptor δ -subunit causes distinct effects in two types of neuromuscular synapses. *Journal of Neuroscience*, *34*(31), 10211–10218. <https://doi.org/10.1523/JNEUROSCI.0426-14.2014>
- Parker, L. A., Rock, E. M., & Limebeer, C. L. (2011). Regulation of nausea and vomiting by cannabinoids. *British Journal of Pharmacology*. <https://doi.org/10.1111/j.1476-5381.2010.01176.x>
- Parry, L., & Clarke, A. R. (2011). The roles of the methyl-CpG binding proteins in cancer. *Genes and Cancer*. <https://doi.org/10.1177/1947601911418499>
- Patten, I., & Placzek, M. (2000). The role of sonic hedgehog in neural tube patterning. *Cellular and Molecular Life Sciences*. <https://doi.org/10.1007/PL00000652>
- Pazour, G. J., Baker, S. A., Deane, J. A., Cole, D. G., Dickert, B. L., Rosenbaum, J. L., ... Besharse, J. C. (2002). The intraflagellar transport protein, IFT88, is essential for vertebrate photoreceptor assembly and maintenance. *Journal of Cell Biology*. <https://doi.org/10.1083/jcb.200107108>
- Pazour, G. J., Dickert, B. L., Vucica, Y., Seeley, E. S., Rosenbaum, J. L., Witman, G. B., & Cole, D. G. (2000). Chlamydomonas IFT88 and its mouse homologue, polycystic kidney disease gene Tg737, are required for assembly of cilia and flagella. *Journal of Cell Biology*. <https://doi.org/10.1083/jcb.151.3.709>
- Perez-Reyes, M. (1990). Marijuana smoking: Factors that influence the bioavailability of tetrahydrocannabinol. *NIDA Research Monograph Series*.
- Perez-Reyes, Mario, Timmons, M. C., Lipton, M. A., Davis, K. H., & Wall, M. E. (1972). Intravenous injection in man of Δ^9 -tetrahydrocannabinol and 11-OH- Δ^9 -tetrahydrocannabinol. *Science*. <https://doi.org/10.1126/science.177.4049.633>
- Perez-Reyez, M., Reid White, W., McDonald, S. A., Hicks, R. E., Robert Jeffcoat, A., & Edgar Cook, C. (1991). The pharmacologic effects of daily marijuana smoking in humans. *Pharmacology, Biochemistry and Behavior*. [https://doi.org/10.1016/0091-3057\(91\)90384-E](https://doi.org/10.1016/0091-3057(91)90384-E)
- Pertwee, R. G. (2008). The diverse CB1 and CB2 receptor pharmacology of three plant cannabinoids: delta9-tetrahydrocannabinol, cannabidiol and delta9-tetrahydrocannabivarin. *British Journal of Pharmacology*.
- Pertwee, Roger G. (2006). Cannabinoid pharmacology: The first 66 years. *British Journal of Pharmacology*. <https://doi.org/10.1038/sj.bjp.0706406>
- Pertwee, Roger G. (2008). Ligands that target cannabinoid receptors in the brain: From THC to anandamide and beyond. *Addiction Biology*. <https://doi.org/10.1111/j.1369-1600.2008.00108.x>
- Porter, J. A., Young, K. E., & Beachy, P. A. (1996). Cholesterol modification of hedgehog signaling proteins in animal development. *Science*. <https://doi.org/10.1126/science.274.5285.255>
- Price, E. R., & Mager, E. M. (2020). The effects of exposure to crude oil or PAHs on fish swim bladder development and function. *Comparative Biochemistry and Physiology Part - C: Toxicology and Pharmacology*. <https://doi.org/10.1016/j.cbpc.2020.108853>
- Price, M. R., Baillie, G. L., Thomas, A., Stevenson, L. A., Easson, M., Goodwin, R., ... Ross, R. A. (2005). Allosteric modulation of the Cannabinoid CB1 receptor. *Molecular Pharmacology*. <https://doi.org/10.1124/mol.105.016162>
- Qin, N., Neepner, M. P., Liu, Y., Hutchinson, T. L., Lubin, M. Lou, & Flores, C. M. (2008). TRPV2 is activated by cannabidiol and mediates CGRP release in cultured rat dorsal root

- ganglion neurons. *Journal of Neuroscience*. <https://doi.org/10.1523/JNEUROSCI.0504-08.2008>
- Quinn, H. R., Matsumoto, I., Callaghan, P. D., Long, L. E., Arnold, J. C., Gunasekaran, N., ... McGregor, I. S. (2008). Adolescent rats find repeated Δ 9-THC less aversive than adult rats but display greater residual cognitive deficits and changes in hippocampal protein expression following exposure. *Neuropsychopharmacology*. <https://doi.org/10.1038/sj.npp.1301475>
- Ramo, D. E., Liu, H., & Prochaska, J. J. (2012). Tobacco and marijuana use among adolescents and young adults: A systematic review of their co-use. *Clinical Psychology Review*. <https://doi.org/10.1016/j.cpr.2011.12.002>
- Ranganathan, M., & D'Souza, D. C. (2006). The acute effects of cannabinoids on memory in humans: A review. *Psychopharmacology*. <https://doi.org/10.1007/s00213-006-0508-y>
- Reichert, S., Pavón Arocas, O., & Rihel, J. (2019). The Neuropeptide Galanin Is Required for Homeostatic Rebound Sleep following Increased Neuronal Activity. *Neuron*. <https://doi.org/10.1016/j.neuron.2019.08.010>
- Renard, J., Krebs, M. O., Le Pen, G., & Jay, T. M. (2014). Long-term consequences of adolescent cannabinoid exposure in adult psychopathology. *Frontiers in Neuroscience*. <https://doi.org/10.3389/fnins.2014.00361>
- Repka, M. A., Elsohly, M. A., Munjal, M., & Ross, S. A. (2006). Temperature stability and bioadhesive properties of Δ 9- tetrahydrocannabinol incorporated hydroxypropylcellulose polymer matrix systems. *Drug Development and Industrial Pharmacy*. <https://doi.org/10.1080/03639040500387914>
- Resstel, L. B. M., Tavares, R. F., Lisboa, S. F. S., Joca, S. R. L., Corrêa, F. M. A., & Guimarães, F. S. (2009). 5-HT 1A receptors are involved in the cannabidiol-induced attenuation of behavioural and cardiovascular responses to acute restraint stress in rats. *British Journal of Pharmacology*. <https://doi.org/10.1111/j.1476-5381.2008.00046.x>
- Rhee, M. H., Bayewitch, M., Avidor-Reiss, T., Levy, R., & Vogel, Z. (1998). Cannabinoid receptor activation differentially regulates the various adenylyl cyclase isozymes. *Journal of Neurochemistry*. <https://doi.org/10.1046/j.1471-4159.1998.71041525.x>
- Rhee, M. H., Vogel, Z., Barg, J., Bayewitch, M., Levy, R., Hanuš, L., ... Mechoulam, R. (1997). Cannabinol derivatives: Binding to cannabinoid receptors and inhibition of adenylylcyclase. *Journal of Medicinal Chemistry*. <https://doi.org/10.1021/jm970126f>
- Ribas, C., Penela, P., Murga, C., Salcedo, A., García-Hoz, C., Jurado-Pueyo, M., ... Mayor, F. (2007). The G protein-coupled receptor kinase (GRK) interactome: Role of GRKs in GPCR regulation and signaling. *Biochimica et Biophysica Acta - Biomembranes*. <https://doi.org/10.1016/j.bbamem.2006.09.019>
- Rimkus, T. K., Carpenter, R. L., Qasem, S., Chan, M., & Lo, H. W. (2016). Targeting the sonic hedgehog signaling pathway: Review of smoothed and GLI inhibitors. *Cancers*. <https://doi.org/10.3390/cancers8020022>
- Roberson, E. K., Patrick, W. K., & Hurwitz, E. L. (2014). Marijuana use and maternal experiences of severe nausea during pregnancy in Hawai'i. *Hawai'i Journal of Medicine & Public Health : A Journal of Asia Pacific Medicine & Public Health*.
- Roberts, A. C., Pearce, K. C., Choe, R. C., Alzagatiti, J. B., Yeung, A. K., Bill, B. R., & Glanzman, D. L. (2016). Long-term habituation of the C-start escape response in zebrafish larvae. *Neurobiology of Learning and Memory*. <https://doi.org/10.1016/j.nlm.2016.08.014>
- Roberts, A. C., Reichl, J., Song, M. Y., Dearing, A. D., Moridzadeh, N., Lu, E. D., ...

- Glanzman, D. L. (2011). Habituation of the C-start response in larval zebrafish exhibits several distinct phases and sensitivity to NMDA receptor Blockade. *PLoS ONE*. <https://doi.org/10.1371/journal.pone.0029132>
- Rodrigues, R. S., Lourenço, D. M., Paulo, S. L., Mateus, J. M., Ferreira, M. F., Mouro, F. M., ... Xapelli, S. (2019). Cannabinoid actions on neural stem cells: Implications for pathophysiology. *Molecules*. <https://doi.org/10.3390/molecules24071350>
- Rodriguez-Martin, I., Herrero-Turrion, M. J., Marron Fdez de Velasco, E., Gonzalez-Sarmiento, R., & Rodriguez, R. E. (2007). Characterization of two duplicate zebrafish Cb2-like cannabinoid receptors. *Gene*. <https://doi.org/10.1016/j.gene.2006.09.016>
- Rohleder, C., Müller, J. K., Lange, B., & Leweke, F. M. (2016). Cannabidiol as a potential new type of an antipsychotic. A critical review of the evidence. *Frontiers in Pharmacology*. <https://doi.org/10.3389/fphar.2016.00422>
- Roncero, C., Valriberas-Herrero, I., Mezzatesta-Gava, M., Villegas, J. L., Aguilar, L., & Grau-López, L. (2020). Cannabis use during pregnancy and its relationship with fetal developmental outcomes and psychiatric disorders. A systematic review. *Reproductive Health*. <https://doi.org/10.1186/s12978-020-0880-9>
- Ross, S. A., & Elsohly, M. A. (1998). CBN and Δ^9 -THC concentration ratio as an indicator of the age of stored marijuana samples. *Bulletin on Narcotics*.
- Rotermann, M. (2021). Looking back from 2020, how cannabis use and related behaviours changed in Canada. *Health Reports*. <https://doi.org/10.25318/82-003-x202100400001-eng>
- Rotondo, J. C., Lanzillotti, C., Mazziotta, C., Tognon, M., & Martini, F. (2021). Epigenetics of Male Infertility: The Role of DNA Methylation. *Frontiers in Cell and Developmental Biology*, 9. <https://doi.org/10.3389/fcell.2021.689624/FULL>
- Roux, C., Wolf, C., Mulliez, N., Gaoua, W., Cormier, V., Chevy, F., & Citadelle, D. (2000). Role of cholesterol in embryonic development. In *American Journal of Clinical Nutrition*. <https://doi.org/10.1093/ajcn/71.5.1270s>
- Roy, B., & Ali, D. W. (2013). Patch clamp recordings from embryonic zebrafish mauthner cells. *Journal of Visualized Experiments*. <https://doi.org/10.3791/50551>
- Roy, B., Ferdous, J., & Ali, D. W. (2015). NMDA receptors on zebrafish Mauthner cells require CaMKII- α for normal development. *Developmental Neurobiology*. <https://doi.org/10.1002/dneu.22214>
- Ruhl, T., Prinz, N., Oellers, N., Seidel, N. I., Jonas, A., Albayram, Ö., ... Von Der Emde, G. (2014). Acute administration of THC impairs spatial but not associative memory function in zebrafish. *Psychopharmacology*. <https://doi.org/10.1007/s00213-014-3522-5>
- Runco, J., Aubin, A., & Layton, C. (2016). The Separation of Δ^8 -THC, Δ^9 -THC, and Their Enantiomers by UPC2 Using Trefoil Chiral Columns, 6.
- Rybak, L. P., Whitworth, C. A., Mukherjea, D., & Ramkumar, V. (2007). Mechanisms of cisplatin-induced ototoxicity and prevention. *Hearing Research*. <https://doi.org/10.1016/j.heares.2006.09.015>
- Ryberg, E., Larsson, N., Sjögren, S., Hjorth, S., Hermansson, N. O., Leonova, J., ... Greasley, P. J. (2007). The orphan receptor GPR55 is a novel cannabinoid receptor. *British Journal of Pharmacology*. <https://doi.org/10.1038/sj.bjp.0707460>
- Saera-Vila, A., Kish, P. E., & Kahana, A. (2016). Fgf regulates dedifferentiation during skeletal muscle regeneration in adult zebrafish. *Cellular Signalling*. <https://doi.org/10.1016/j.cellsig.2016.06.001>
- Saher, G., Brügger, B., Lappe-Siefke, C., Möbius, W., Tozawa, R. I., Wehr, M. C., ... Nave, K.

- A. (2005). High cholesterol level is essential for myelin membrane growth. *Nature Neuroscience*, 8(4), 468–475. <https://doi.org/10.1038/nn1426>
- Sahu, M. P., Pazos-Boubeta, Y., Pajanoja, C., Rozov, S., Panula, P., & Castrén, E. (2019). Neurotrophin receptor Ntrk2b function in the maintenance of dopamine and serotonin neurons in zebrafish. *Scientific Reports*. <https://doi.org/10.1038/s41598-019-39347-3>
- Saint-Amant, L., & Drapeau, P. (1998). Time course of the development of motor behaviors in the zebrafish embryo. *Journal of Neurobiology*. [https://doi.org/10.1002/\(SICI\)1097-4695\(199812\)37:4<622::AID-NEU10>3.0.CO;2-S](https://doi.org/10.1002/(SICI)1097-4695(199812)37:4<622::AID-NEU10>3.0.CO;2-S)
- Saint-Amant, L., & Drapeau, P. (2000). Motoneuron activity patterns related to the earliest behavior of the zebrafish embryo. *Journal of Neuroscience*. <https://doi.org/10.1523/jneurosci.20-11-03964.2000>
- Saint-Amant, L., & Drapeau, P. (2003). Whole-cell patch-clamp recordings from identified spinal neurons in the zebrafish embryo. *Methods in Cell Science*. <https://doi.org/10.1023/B:MICS.0000006896.02938.49>
- Sarne, Y., Asaf, F., Fishbein, M., Gafni, M., & Keren, O. (2011). The dual neuroprotective-neurotoxic profile of cannabinoid drugs. *British Journal of Pharmacology*. <https://doi.org/10.1111/j.1476-5381.2011.01280.x>
- Sarne, Y., & Mechoulam, R. (2005). Cannabinoids: Between neuroprotection and neurotoxicity. *Current Drug Targets: CNS and Neurological Disorders*. <https://doi.org/10.2174/156800705774933005>
- Savinainen, J. R., Järvinen, T., Laine, K., & Laitinen, J. T. (2001). Despite substantial degradation, 2-arachidonoylglycerol is a potent full efficacy agonist mediating CB1 receptor-dependent g-protein activation in rat cerebellar membranes. *British Journal of Pharmacology*, 134(3), 664–672. <https://doi.org/10.1038/sj.bjp.0704297>
- Savinainen, J. R., Saario, S. M., Niemi, R., Järvinen, T., & Laitinen, J. T. (2003). An optimized approach to study endocannabinoid signaling: Evidence against constitutive activity of rat brain adenosine A 1 and cannabinoid CB 1 receptors. *British Journal of Pharmacology*, 140(8), 1451–1459. <https://doi.org/10.1038/sj.bjp.0705577>
- Scallet, A. C., Uemura, E., Andrews, A., Ali, S. F., McMillan, D. E., Paule, M. G., ... Slikker, W. (1987). Morphometric studies of the rat hippocampus following chronic delta-9-tetrahydrocannabinol (THC). *Brain Research*. [https://doi.org/10.1016/0006-8993\(87\)91576-9](https://doi.org/10.1016/0006-8993(87)91576-9)
- Schneider, M. (2008). Puberty as a highly vulnerable developmental period for the consequences of cannabis exposure. *Addiction Biology*. <https://doi.org/10.1111/j.1369-1600.2008.00110.x>
- Schramm-Sapyta, N. L., Cha, Y. M., Chaudhry, S., Wilson, W. A., Swartzwelder, H. S., & Kuhn, C. M. (2007). Differential anxiogenic, aversive, and locomotor effects of THC in adolescent and adult rats. *Psychopharmacology*. <https://doi.org/10.1007/s00213-006-0676-9>
- Shan, S. D., Boutin, S., Ferdous, J., & Ali, D. W. (2015). Ethanol exposure during gastrulation alters neuronal morphology and behavior in zebrafish. *Neurotoxicology and Teratology*. <https://doi.org/10.1016/j.ntt.2015.01.004>
- Shao, Z., Yin, J., Chapman, K., Grzemska, M., Clark, L., Wang, J., & Rosenbaum, D. M. (2016). High-resolution crystal structure of the human CB1 cannabinoid receptor. *Nature*. <https://doi.org/10.1038/nature20613>
- Sharir, H., & Abood, M. E. (2010). Pharmacological characterization of GPR55, a putative cannabinoid receptor. *Pharmacology and Therapeutics*. <https://doi.org/10.1016/j.pharmthera.2010.02.004>

- Shi, X., & Zhou, B. (2010). The role of Nrf2 and MAPK pathways in PFOS-induced oxidative stress in zebrafish embryos. *Toxicological Sciences*. <https://doi.org/10.1093/toxsci/kfq066>
- Shim, J.-Y. (2010). Understanding Functional Residues of the Cannabinoid CB1 Receptor for Drug Discovery. *Current Topics in Medicinal Chemistry*. <https://doi.org/10.2174/156802610791164210>
- Sliwinska-Kowalska, M., & Davis, A. (2012). Noise-induced hearing loss. *Noise and Health*. <https://doi.org/10.4103/1463-1741.104893>
- Söllner, C., Nicolson, T., Rauch, G. J., Geisler, R., Schuster, S. C., Siemens, J., ... Weiler, C. (2004). Mutations in cadherin 23 affect tip links in zebrafish sensory hair cells. *Nature*. <https://doi.org/10.1038/nature02484>
- Solowij, N., & Pesa, N. (2011). Cannabis and cognition: Short-and long-term effects. In *Marijuana and Madness: Second Edition*. <https://doi.org/10.1017/CBO9780511706080.009>
- Solowij, N., Stephens, R. S., Roffman, R. A., Babor, T., Kadden, R., Miller, M., ... Vendetti, J. (2002). Cognitive functioning of long-term heavy cannabis users seeking treatment. *Journal of the American Medical Association*. <https://doi.org/10.1001/jama.287.9.1123>
- Spicer, L. (2002). Historical and Cultural Uses of Cannabis and the Canadian “Marijuana Clash.” *Library of Parliament*.
- Stainier, D. Y. R., Lee, R. K., & Fishman, M. C. (1993). Cardiovascular development in the zebrafish: I. Myocardial fate map and heart tube formation. *Development*. <https://doi.org/10.1242/dev.119.1.31>
- Stella, N., Schweitzer, P., & Plomelli, D. (1997). A second endogenous' cannabinoid that modulates long-term potentiation. *Nature*. <https://doi.org/10.1038/42015>
- Stempel, A. V., Stumpf, A., Zhang, H. Y., Özdoğan, T., Pannasch, U., Theis, A. K., ... Schmitz, D. (2016). Cannabinoid Type 2 Receptors Mediate a Cell Type-Specific Plasticity in the Hippocampus. *Neuron*. <https://doi.org/10.1016/j.neuron.2016.03.034>
- Sternberg, J. R., & Wyart, C. (2015). Neuronal wiring: Linking dendrite placement to synapse formation. *Current Biology*. <https://doi.org/10.1016/j.cub.2015.01.006>
- Stewart, A., Gaikwad, S., Kyzar, E., Green, J., Roth, A., & Kalueff, A. V. (2012). Modeling anxiety using adult zebrafish: A conceptual review. *Neuropharmacology*, 62(1), 135–143. <https://doi.org/10.1016/j.neuropharm.2011.07.037>
- Stewart, A. M., & Kalueff, A. V. (2014). The behavioral effects of acute Δ^9 -tetrahydrocannabinol and heroin (diacetylmorphine) exposure in adult zebrafish. *Brain Research*. <https://doi.org/10.1016/j.brainres.2013.11.002>
- Stiglick, A., & Kalant, H. (1985). Residual effects of chronic cannabis treatment on behavior in mature rats. *Psychopharmacology*. <https://doi.org/10.1007/BF00429660>
- Stooke-Vaughan, G. A., Huang, P., Hammond, K. L., Schier, A. F., & Whitfield, T. T. (2012). The role of hair cells, cilia and ciliary motility in otolith formation in the zebrafish otic vesicle. *Development*. <https://doi.org/10.1242/dev.079947>
- Story, G. M., Peier, A. M., Reeve, A. J., Eid, S. R., Mosbacher, J., Hricik, T. R., ... Patapoutian, A. (2003). ANKTM1, a TRP-like channel expressed in nociceptive neurons, is activated by cold temperatures. *Cell*. [https://doi.org/10.1016/S0092-8674\(03\)00158-2](https://doi.org/10.1016/S0092-8674(03)00158-2)
- Sufian, M. S., Amin, M. R., Kanyo, R., Ted Allison, W., & Ali, D. W. (2019). CB₁ and CB₂ receptors play differential roles in early zebrafish locomotor development. *Journal of Experimental Biology*, 222(16). <https://doi.org/10.1242/jeb.206680>
- Sullivan, J. M. (2000). Cellular and molecular mechanisms underlying learning and memory impairments produced by cannabinoids. *Learning and Memory*.

- <https://doi.org/10.1101/lm.7.3.132>
- Sylantsev, S., Jensen, T. P., Ross, R. A., & Rusakov, D. A. (2013). Cannabinoid- and lysophosphatidylinositol-sensitive receptor GPR55 boosts neurotransmitter release at central synapses. *Proceedings of the National Academy of Sciences of the United States of America*. <https://doi.org/10.1073/pnas.1211204110>
- Sylvain, N. J., Brewster, D. L., & Ali, D. W. (2010). Zebrafish embryos exposed to alcohol undergo abnormal development of motor neurons and muscle fibers. *Neurotoxicology and Teratology*. <https://doi.org/10.1016/j.ntt.2010.03.001>
- Szczepny, A., Hime, G. R., & Loveland, K. L. (2006). Expression of hedgehog signalling components in adult mouse testis. *Developmental Dynamics*. <https://doi.org/10.1002/dvdy.20931>
- Szutorisz, H., & Hurd, Y. L. (2016). Epigenetic effects of cannabis exposure. *Biological Psychiatry*. <https://doi.org/10.1016/j.biopsych.2015.09.014>
- Tanimura, A., Yamazaki, M., Hashimoto, Y., Uchigashima, M., Kawata, S., Abe, M., ... Kano, M. (2010). The Endocannabinoid 2-Arachidonoylglycerol Produced by Diacylglycerol Lipase α Mediates Retrograde Suppression of Synaptic Transmission. *Neuron*. <https://doi.org/10.1016/j.neuron.2010.01.021>
- Tapia, M., Dominguez, A., Zhang, W., Puerto, A. Del, Ciorraga, M., Benitez, M. J., ... Garrido, J. J. (2017). Cannabinoid receptors modulate neuronal morphology and ankyring density at the axon initial segment. *Frontiers in Cellular Neuroscience*. <https://doi.org/10.3389/fncel.2017.00005>
- Thisse, B., Pflumio, S., Furthauer, M., Loppin, B., Heyer, V., Degraeve, A., ... Thisse, C. (2001). Expression of the zebrafish genome during embryogenesis (NIH R01 RR15402-01). *ZFIN Direct Data Submission*.
- Thomas, A., Baillie, G. L., Phillips, A. M., Razdan, R. K., Ross, R. A., & Pertwee, R. G. (2007). Cannabidiol displays unexpectedly high potency as an antagonist of CB 1 and CB 2 receptor agonists in vitro. *British Journal of Pharmacology*, 150(5), 613–623. <https://doi.org/10.1038/sj.bjp.0707133>
- Trevarrow, B., Marks, D. L., & Kimmel, C. B. (1990). Organization of hindbrain segments in the zebrafish embryo. *Neuron*. [https://doi.org/10.1016/0896-6273\(90\)90194-K](https://doi.org/10.1016/0896-6273(90)90194-K)
- Trofin, I. G., Vlad, C. C., Dabija, G., & Filipescu, L. (2011). Influence of storage conditions on the chemical potency of herbal cannabis. *Revista de Chimie*.
- Tselnicker, I., Keren, O., Hefetz, A., Pick, C. G., & Sarne, Y. (2007). A single low dose of tetrahydrocannabinol induces long-term cognitive deficits. *Neuroscience Letters*. <https://doi.org/10.1016/j.neulet.2006.10.033>
- Turner, C. E., & Elsohly, M. A. (1979). Constituents of cannabis sativa L. XVI. A possible decomposition pathway of Δ^9 -tetrahydrocannabinol to cannabinol. *Journal of Heterocyclic Chemistry*. <https://doi.org/10.1002/jhet.5570160834>
- Turner, S. E., Williams, C. M., Iversen, L., & Whalley, B. J. (2017). Molecular Pharmacology of Phytocannabinoids. *Progress in the Chemistry of Organic Natural Products*. https://doi.org/10.1007/978-3-319-45541-9_3
- Turu, G., & Hunyady, L. (2010). Signal transduction of the CB1 cannabinoid receptor. *Journal of Molecular Endocrinology*. <https://doi.org/10.1677/JME-08-0190>
- United Nations Office on Drugs and Crime. (2020). *World drug report 2020: Drug use and health consequences*. United Nations publication.
- Varvel, S. A., Anum, E. A., & Lichtman, A. H. (2005). Disruption of CB1 receptor signaling

- impairs extinction of spatial memory in mice. *Psychopharmacology*.
<https://doi.org/10.1007/s00213-004-2121-2>
- Vidrio, H., Sánchez-Salvatori, M. A., & Medina, M. (1996). Cardiovascular effects of (-)-11-OH- Δ 8-tetrahydrocannabinol- dimethylheptyl in rats. *Journal of Cardiovascular Pharmacology*. <https://doi.org/10.1097/00005344-199608000-00022>
- Volkow, N. D., Han, B., Compton, W. M., & McCance-Katz, E. F. (2019). Self-reported Medical and Nonmedical Cannabis Use among Pregnant Women in the United States. *JAMA - Journal of the American Medical Association*.
<https://doi.org/10.1001/jama.2019.7982>
- Vortkamp, A., Lee, K., Lanske, B., Segre, G. V., Kronenberg, H. M., & Tabin, C. J. (1996). Regulation of rate of cartilage differentiation by Indian Hedgehog and PTH-related protein. *Science*. <https://doi.org/10.1126/science.273.5275.613>
- Walter, L., & Stella, N. (2004). Cannabinoids and neuroinflammation. *British Journal of Pharmacology*. <https://doi.org/10.1038/sj.bjp.0705667>
- Walters, R. W., Shukla, A. K., Kovacs, J. J., Violin, J. D., DeWire, S. M., Lam, C. M., ... Lefkowitz, R. J. (2009). β -Arrestin1 mediates nicotinic acid-induced flushing, but not its antilipolytic effect, in mice. *Journal of Clinical Investigation*.
<https://doi.org/10.1172/JCI36806>
- Wang, W., Wu, Z., Dai, Z., Yang, Y., Wang, J., & Wu, G. (2013). Glycine metabolism in animals and humans: Implications for nutrition and health. *Amino Acids*.
<https://doi.org/10.1007/s00726-013-1493-1>
- Wanner, N. M., Colwell, M., Drown, C., & Faulk, C. (2021). Developmental cannabidiol exposure increases anxiety and modifies genome-wide brain DNA methylation in adult female mice. *Clinical Epigenetics*, 13(1), 1–16. <https://doi.org/10.1186/s13148-020-00993-4>
- Waterman, R. E. (1969). Development of the lateral musculature in the teleost, *Brachydanio rerio*: A fine structural study. *American Journal of Anatomy*.
<https://doi.org/10.1002/aja.1001250406>
- Watson, S., Chambers, D., Hobbs, C., Doherty, P., & Graham, A. (2008). The endocannabinoid receptor, CB1, is required for normal axonal growth and fasciculation. *Molecular and Cellular Neuroscience*. <https://doi.org/10.1016/j.mcn.2008.02.001>
- Webb, J. (2011). Hearing and lateral line | Lateral Line Structure. In *Encyclopedia of Fish Physiology*. <https://doi.org/10.1016/B978-0-12-374553-8.00010-1>
- Weiskopf, R. B., Nau, C., & Strichartz, G. R. (2002). Drug chirality in anesthesia. *Anesthesiology*. <https://doi.org/10.1097/00000542-200208000-00029>
- Westerfield, M., McMurray, J. V., & Eisen, J. S. (1986). Identified motoneurons and their innervation of axial muscles in the zebrafish. *Journal of Neuroscience*.
<https://doi.org/10.1523/jneurosci.06-08-02267.1986>
- Wheatley, M., Wootten, D., Conner, M. T., Simms, J., Kendrick, R., Logan, R. T., ... Barwell, J. (2012). Lifting the lid on GPCRs: The role of extracellular loops. *British Journal of Pharmacology*. <https://doi.org/10.1111/j.1476-5381.2011.01629.x>
- Whyte, L. S., Ryberg, E., Sims, N. A., Ridge, S. A., Mackie, K., Greasley, P. J., ... Rogers, M. J. (2009). The putative cannabinoid receptor GPR55 affects osteoclast function in vitro and bone mass in vivo. *Proceedings of the National Academy of Sciences of the United States of America*. <https://doi.org/10.1073/pnas.0902743106>
- Williams, E. J., Walsh, F. S., & Doherty, P. (2003). The FGF receptor uses the endocannabinoid

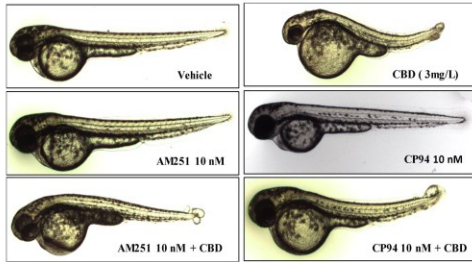
- signaling system to couple to an axonal growth response. *Journal of Cell Biology*.
<https://doi.org/10.1083/jcb.200210164>
- Winata, C. L., Korzh, S., Kondrychyn, I., Zheng, W., Korzh, V., & Gong, Z. (2009). Development of zebrafish swimbladder: The requirement of Hedgehog signaling in specification and organization of the three tissue layers. *Developmental Biology*.
<https://doi.org/10.1016/j.ydbio.2009.04.035>
- Witherow, D. S., Garrison, T. R., Miller, W. E., & Lefkowitz, R. J. (2004). beta-Arrestin inhibits NF-kappaB activity by means of its interaction with the NF-kappaB inhibitor IkappaBalpha. *Proc Natl Acad Sci U S A*.
- Wollner, H. J., Hatchett, J. R., Levine, J., & Loewe, S. (1942). Isolation of a Physiologically Active Tetrahydrocannabinol from Cannabis Sativa Resin. *Journal of the American Chemical Society*. <https://doi.org/10.1021/ja01253a008>
- Woolley, M. J., & Conner, A. C. (2017). Understanding the common themes and diverse roles of the second extracellular loop (ECL2) of the GPCR super-family. *Molecular and Cellular Endocrinology*. <https://doi.org/10.1016/j.mce.2016.11.023>
- Wu, C. S., Zhu, J., Wager-Miller, J., Wang, S., O'Leary, D., Monory, K., ... Lu, H. C. (2010). Requirement of cannabinoid CB1 receptors in cortical pyramidal neurons for appropriate development of corticothalamic and thalamocortical projections. *European Journal of Neuroscience*. <https://doi.org/10.1111/j.1460-9568.2010.07337.x>
- Xapelli, S., Agasse, F., Sardà-Arroyo, L., Bernardino, L., Santos, T., Ribeiro, F. F., ... Malva, J. O. (2013). Activation of Type 1 Cannabinoid Receptor (CB1R) Promotes Neurogenesis in Murine Subventricular Zone Cell Cultures. *PLoS ONE*.
<https://doi.org/10.1371/journal.pone.0063529>
- Yamashita, M. (2003). Apoptosis in zebrafish development. In *Comparative Biochemistry and Physiology - B Biochemistry and Molecular Biology*.
<https://doi.org/10.1016/j.cbpc.2003.08.013>
- Yazulla, S., & Studholme, K. M. (2001). Neurochemical anatomy of the zebrafish retina as determined by immunocytochemistry. *Journal of Neurocytology*.
<https://doi.org/10.1023/A:1016512617484>
- Youn, Y. H., & Han, Y. G. (2018). Primary Cilia in Brain Development and Diseases. *American Journal of Pathology*. <https://doi.org/10.1016/j.ajpath.2017.08.031>
- Yue, M. S., Peterson, R. E., & Heideman, W. (2015). Dioxin inhibition of swim bladder development in zebrafish: Is it secondary to heart failure? *Aquatic Toxicology*.
<https://doi.org/10.1016/j.aquatox.2015.02.016>
- Zamengo, L., Bettin, C., Badocco, D., Di Marco, V., Miolo, G., & Frison, G. (2019). The role of time and storage conditions on the composition of hashish and marijuana samples: A four-year study. *Forensic Science International*. <https://doi.org/10.1016/j.forsciint.2019.02.058>
- Zhang, F., Qin, W., Zhang, J. P., & Hu, C. Q. (2015). Antibiotic toxicity and absorption in zebrafish using liquid chromatography-tandem mass spectrometry. *PLoS ONE*.
<https://doi.org/10.1371/journal.pone.0124805>
- Zhang, Q., Cheng, J., & Xin, Q. (2015). Effects of tetracycline on developmental toxicity and molecular responses in zebrafish (*Danio rerio*) embryos. *Ecotoxicology*.
<https://doi.org/10.1007/s10646-015-1417-9>
- Zhang, X. C., Zhou, Y., & Cao, C. (2018). Proton transfer during class-A GPCR activation: do the CWxP motif and the membrane potential act in concert? *Biophysics Reports*.
<https://doi.org/10.1007/s41048-018-0056-0>

- Zhang, X. M., Ramalho-Santos, M., & McMahon, A. P. (2001). Smoothed mutants reveal redundant roles for Shh and Ihh signaling including regulation of L/R asymmetry by the mouse node. *Cell*. [https://doi.org/10.1016/S0092-8674\(01\)00385-3](https://doi.org/10.1016/S0092-8674(01)00385-3)
- Zheng, J. (2013). Molecular mechanism of TRP channels. *Comprehensive Physiology*. <https://doi.org/10.1002/cphy.c120001>
- Zindler, F., Beedgen, F., Brandt, D., Steiner, M., Stengel, D., Baumann, L., & Braunbeck, T. (2019). Analysis of tail coiling activity of zebrafish (*Danio rerio*) embryos allows for the differentiation of neurotoxicants with different modes of action. *Ecotoxicology and Environmental Safety*. <https://doi.org/10.1016/j.ecoenv.2019.109754>
- Zou, S., & Kumar, U. (2018). Cannabinoid receptors and the endocannabinoid system: Signaling and function in the central nervous system. *International Journal of Molecular Sciences*. <https://doi.org/10.3390/ijms19030833>
- Zuardi, A. W., Antunes Rodrigues, J., & Cunha, J. M. (1991). Effects of cannabidiol in animal models predictive of antipsychotic activity. *Psychopharmacology*. <https://doi.org/10.1007/BF02244189>
- Zygmunt, P. M., Petersson, J., Andersson, D. A., Chuang, H. H., Sørgård, M., Di Marzo, V., ... Högestätt, E. D. (1999). Vanilloid receptors on sensory nerves mediate the vasodilator action of anandamide. *Nature*. <https://doi.org/10.1038/22761>

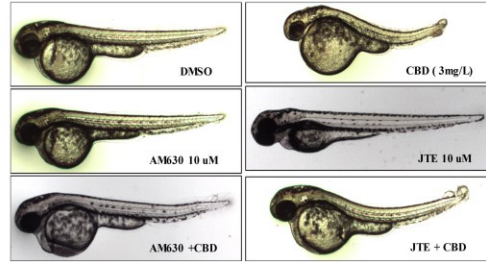
Appendices

Appendix Figure 1 Blocking CB₂R activity inhibited CBD-induced defects in gross morphology of zebrafish embryos.

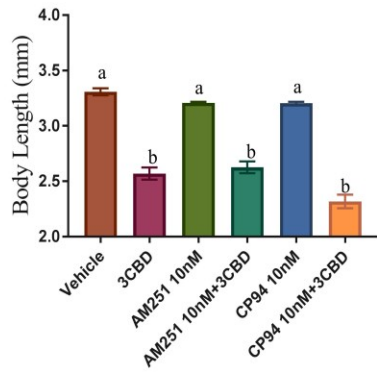
A)



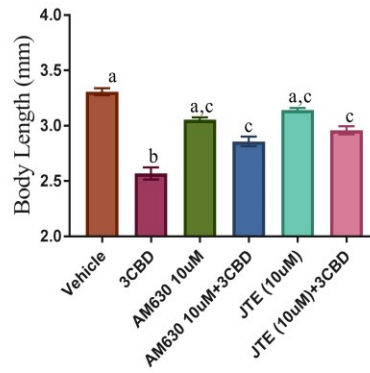
B)



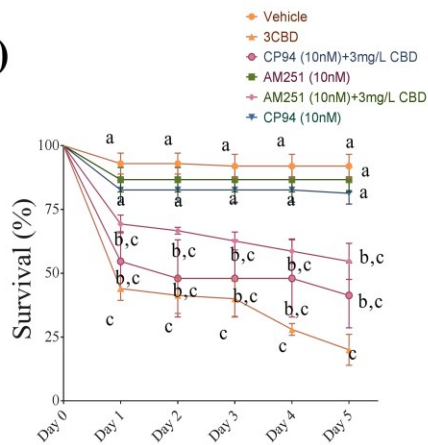
C)



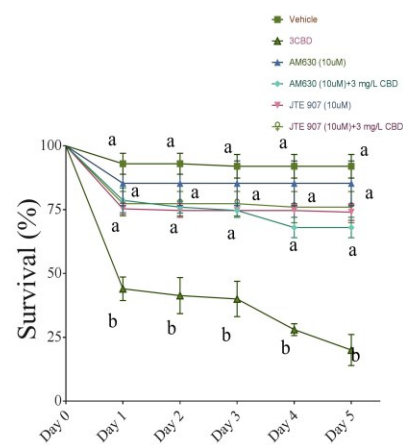
D)



E)



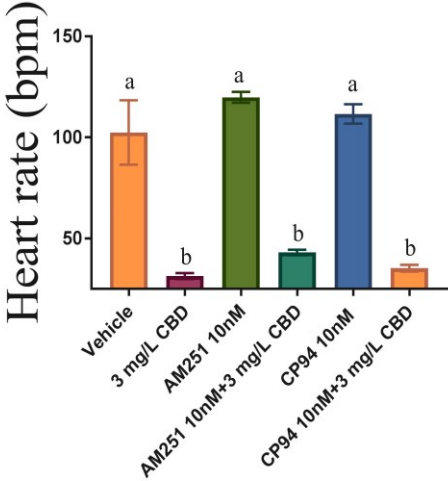
F)



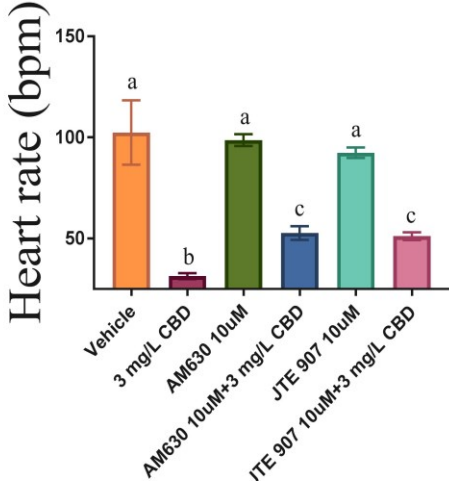
Appendix Figure 1 Blocking CB₂R activity inhibited CBD-induced defects in gross morphology of zebrafish embryos. (A, B) Embryos were treated with vehicle or DMSO, or exposed to 3 mg/L CBD, 10 nM AM251, 10 nM CP94, 10 nM AM251 + 3 mg/L CBD, 10 nM CP94 + 3 mg/L CBD, 10 μM AM630 + 3 mg/L CBD or 10 μM JTE907 + 3 mg/L CBD (from 5.25 hpf to 10.75 hpf) and then allowed to develop in normal embryo media. Images were taken at 48–52 hpf. Representative images are shown. (C) Bar graph showing the body lengths of fish in the vehicle control (n = 41), 10 nM AM251 (n = 30), 10 nM CP94 (n = 40), 10 nM AM251 + 3 mg/L CBD (n = 51), and 10 nM CP94 + 3 mg/L CBD (n = 45) groups. (D) Bar graph showing the body lengths of fish in the vehicle control (n = 41), 10 μM AM630 (n = 35), 10 μM JTE907 (n = 42), 10 μM AM630 + 3 mg/L CBD (n = 45), and 10 μM JTE907 + 3 mg/L CBD (n = 45) groups. (E) Line graph showing the percentage of embryos that survived within the first 5 days of development following CBD exposure or combined exposure of CBD with CB₁R antagonists during gastrulation (N=4 experiments and n = 20 embryos for each treatment). (F) Line graph showing the percentage of embryos that survived within the first 5 days of development following CBD exposure or combined exposure of CBD with CB₂R antagonists during gastrulation (N=4 experiments and n = 20 embryos for each treatment). For survival, significance was determined using two-way ANOVA followed by tukey's multiple comparison tests. For body length, significance was determined using Kruskal-Wallis tests followed by Dunn's multiple comparison test. Groups which share the same letter(s) of the alphabet are not statistically different from one another.

Appendix Figure 2 Blocking CB₂R activity inhibited CBD-induced reduction in heart rate of zebrafish embryos

A)

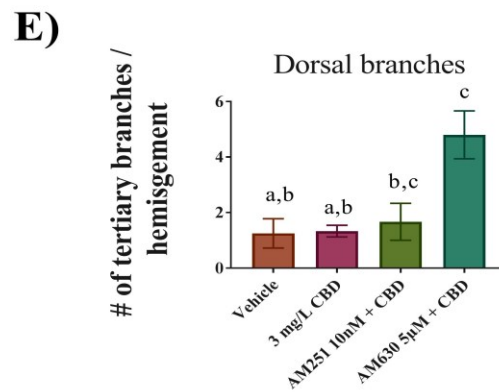
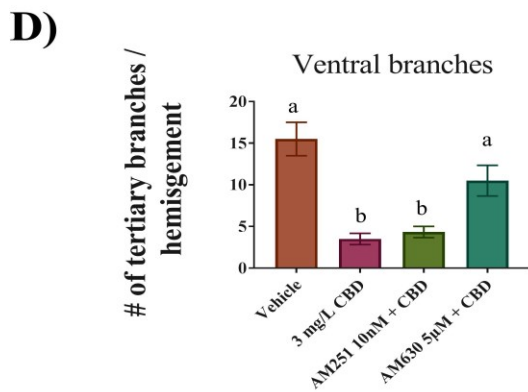
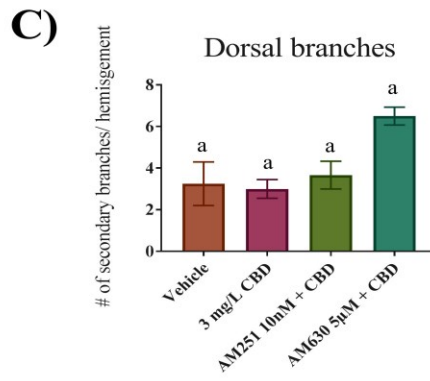
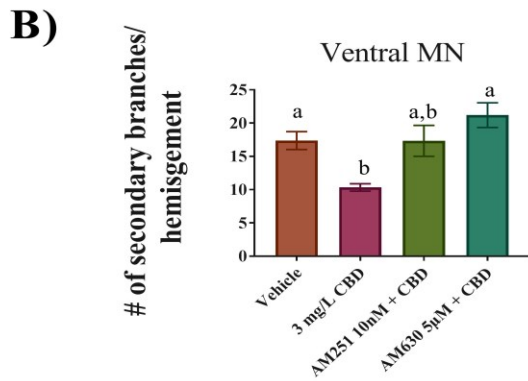
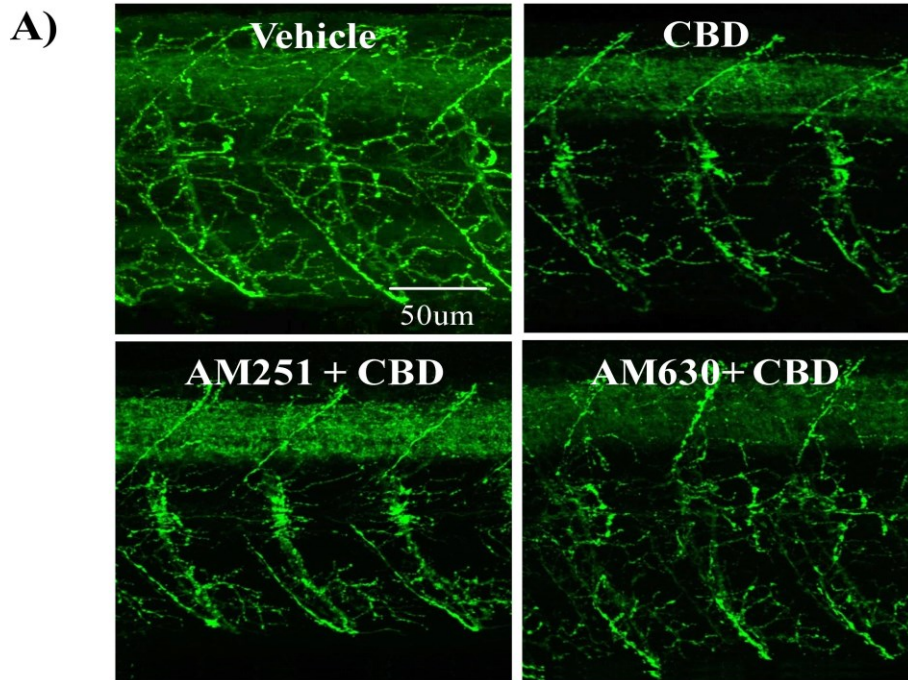


B)



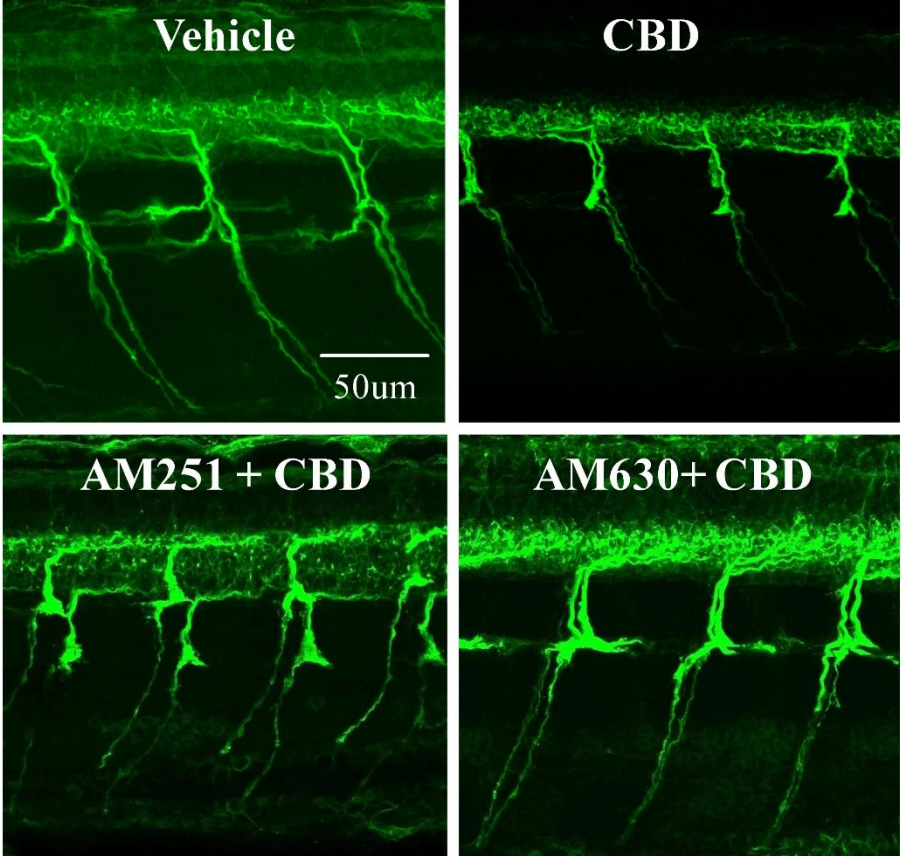
Appendix Figure 2 Blocking CB₂R activity inhibited CBD-induced reduction in heart rate of zebrafish embryos. (A) Bar graph showing the heart rate of embryos treated with 10 nM AM251 (n = 40), 10 nM CP94 (n = 40), 10 nM AM251 + 3 mg/L CBD (n= 50), 10 nM CP94 + 3 mg/L CBD (n = 45). (B) Bar graph showing the heart rate of embryos treated with 10 μ M AM630 (n = 35), 10 μ M JTE907 (n = 40), 10 μ M AM630 + 3 mg/L CBD (n= 45), 10 μ M JTE907 + 3 mg/L CBD (n = 45). For heart rates, significance was determined using Kruskal-Wallis tests followed by Dunn's multiple comparison test. Groups which share the same letter(s) of the alphabet are not statistically different from one another.

Appendix Figure 3 Combined exposure of CB₂R and CBD inhibits CBD-induced alteration of primary MN branching



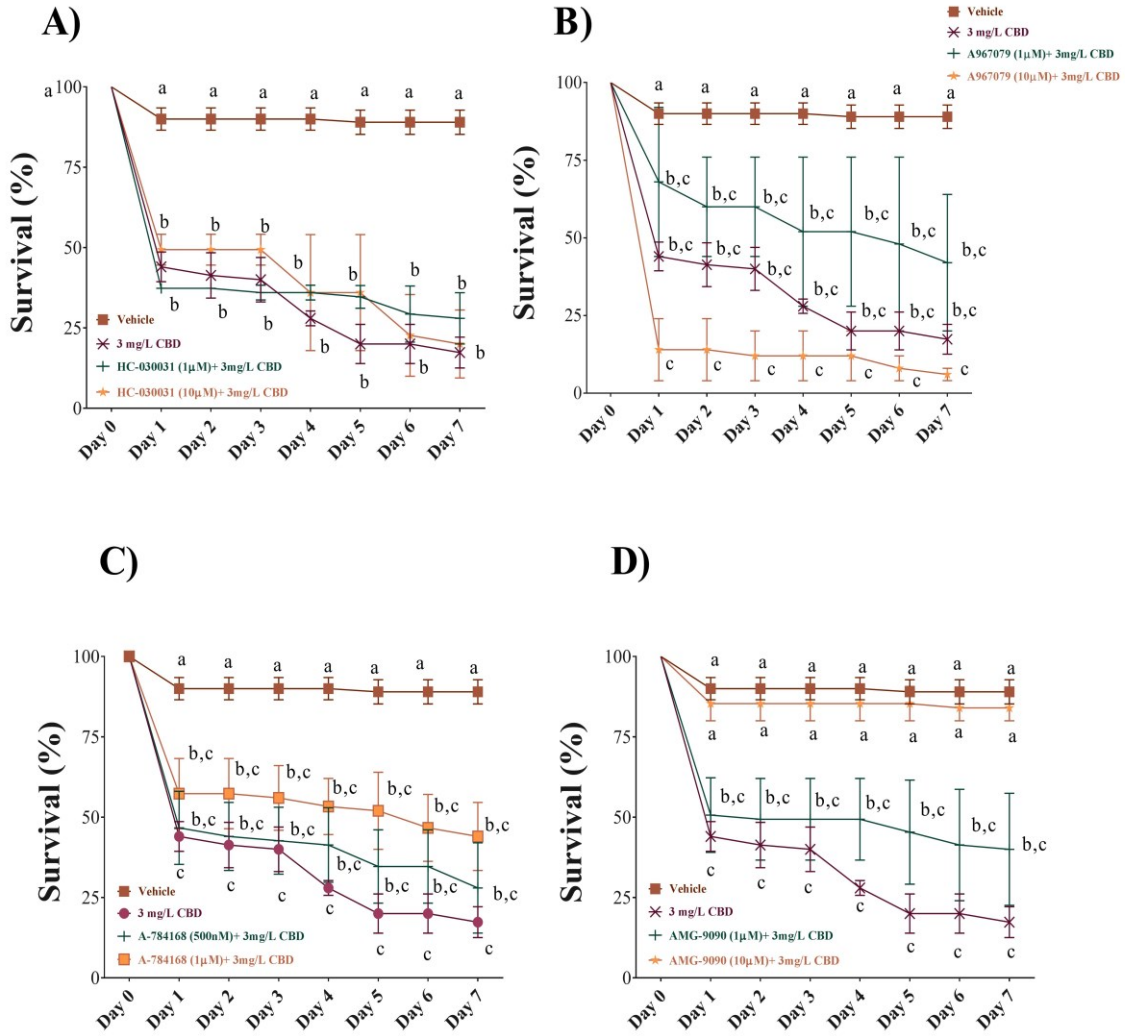
Appendix Figure 3 Combined exposure of CB₂R antagonists and CBD inhibits CBD-induced alteration of primary MN branching. (A) Znp-1 (green) antibody was used to label primary motor neuronal axons and their branches in vehicle control (n=6), 3 mg/L CBD (n=6), AM251 10 nm + 3 mg/L CBD (n=6), AM630 10 μ m + 3 mg/L CBD (n = 6), respectively. Representative images are shown. (B-E) Quantification of the secondary and tertiary branches in the presence of AM251 and AM630. (B, C) Bar graphs showing the number of secondary ventral and dorsal branches emanating from the main axon. (D, E) Bar graphs showing the number of tertiary dorsal and ventral branches emanating from the main axon. Scale bar represents 50 μ m. Significance was determined using Kruskal-Wallis tests followed by Dunn's multiple comparison test. Groups which share the same letter(s) of the alphabet are not statistically different from one another.

Appendix Figure 4 Combined exposure of CB₂R antagonists and CBD inhibits CBD-induced alteration of secondary MN branching.



Appendix Figure 4 Combined exposure of CB₂R antagonists and CBD inhibits CBD-induced alteration of secondary MN branching. Zn-8 (green) antibody was used to label primary motor neuronal axons and their branches in vehicle control (n=6), 3 mg/L CBD (n=6), AM251 10 nm + 3 mg/L CBD (n=6), AM630 10 μM + 3 mg/L CBD (n = 6) treated groups. Representative images are shown.

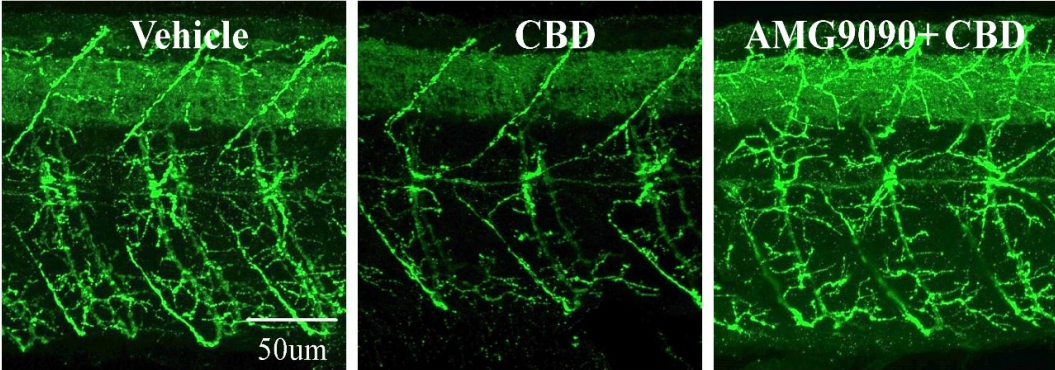
Appendix Figure 5 Blocking TRPV1 activity inhibited CBD-induced mortality of zebrafish embryos.



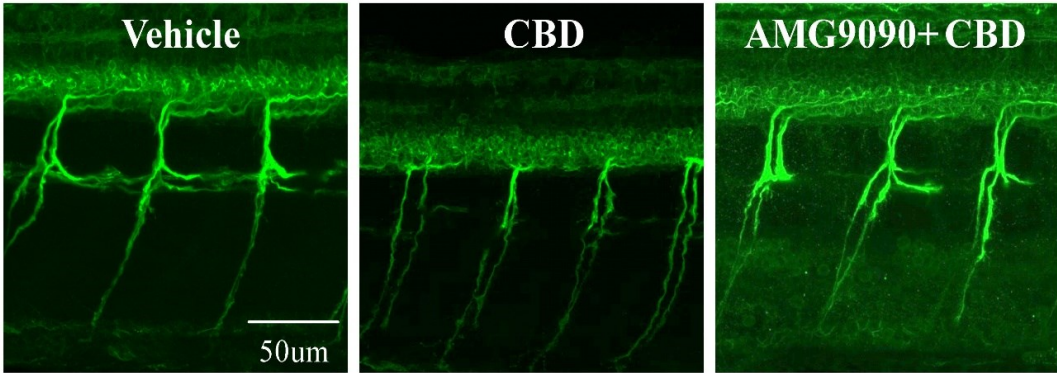
Appendix Figure 5 Blocking TRPV1 activity inhibited CBD-induced mortality of zebrafish embryos. (A) Line graphs showing the percentage of embryos that survived within the first 5 days of development following 3 mg/L CBD exposure or combined exposure of CBD with two different concentrations of the TRPA1 antagonist HC-0300331 during gastrulation (N=4 experiments and n = 20 embryos for each treatment). (B) Line graphs showing the percentage of embryos that survived within the first 5 days of development following 3 mg/L CBD exposure or combined exposure of CBD with two different concentrations of the TRPA1 antagonist A967079 during gastrulation (N=4 experiments and n = 20 embryos for each treatment). (C) Line graphs showing the percentage of embryos that survived within the first 5 days of development following 3 mg/L CBD exposure or combined exposure of CBD with two different concentrations of the TRPV1 antagonist A784168 during gastrulation (N=4 experiments and n = 20 embryos for each treatment). (D) Line graphs showing the percentage of embryos that survived within the first 5 days of development following 3 mg/L CBD exposure or combined exposure of CBD with two concentration of the TRPV1, TRPA1, and TRPM8 antagonist AMG9090 during gastrulation (N=4 experiments and n = 20 embryos for each treatment). Significance was determined using two-way ANOVA followed by tukey's multiple comparison tests. Groups which share the same letter(s) of the alphabet are not statistically different from one another.

Appendix Figure 6 Combined exposure of TRPV1 antagonists and CBD inhibits CBD-induced alteration of primary and secondary MN branching

A)



B)



Appendix Figure 6 Co-treatment with a TRPV1 antagonist inhibits 3 mg/L CBD-induced alteration of primary and secondary MN branching. (A) Znp-1 (green) antibody was used to label primary motor neuronal axons and their branches in vehicle control (n=6), 3 mg/L CBD (n=6), and μ M concentration AMG9090 + 3 mg/L CBD (n=6) treatment groups. Representative images are presented. (B) Zn-8 (green) antibody was used to label secondary motor neuronal axons and their branches in vehicle control (n=6), 3 mg/L CBD (n=6), 10 μ M concentration AMG9090 + 3 mg/L CBD (n=6) treatment groups. Representative images are shown.